

**Arginine-rich Tat- and (R-X-R)-motif Peptidomimetics for
DNA/RNA Binding, Antimicrobial Action and Cell Penetration**

Thesis Submitted to AcSIR
For the Award of the Degree of
DOCTOR OF PHILOSOPHY

In Chemical Sciences



By
Govind Sudhakar Bhosle
Registration Number : 10CC12A26013

Research Supervisor
Dr. Moneesha Fernandes
Division of Organic Chemistry
CSIR-National Chemical Laboratory
Pune, India.

Research Co-supervisor
Dr. Souvik Maiti
CSIR-IGIB, New Delhi
May, 2018

Certificate

This is to certify that work incorporated in this Ph. D. thesis entitled “**Arginine-rich Tat- and (R-X-R)-motif Peptidomimetics for DNA/RNA Binding, Antimicrobial Action and Cell Penetration**” submitted by **Mr. Govind Sudhakar Bhosle** to the **Academy of Scientific and Innovative Research (AcSIR)** in the fulfillment of their requirements for the award of the *Degree of Doctor of Philosophy in Chemical Sciences* embodies original research work under my supervision. I further certify that this work has not been submitted to any other university or institution in part or full for the award of any degree or diploma. Research material obtained from other sources has been duly acknowledged in thesis. Any text, illustration, table etc. used in the thesis is from other sources, have been duly cited and acknowledged.

Research Student

Govind Sudhakar Bhosle

Dr. Moneesha Fernandes

Research Supervisor

Organic Chemistry Division,
CSIR-National Chemical Laboratory,
Pune – 411008

Declaration

I hereby declare that the thesis entitled **Arginine-rich Tat- and (R-X-R)-motif Peptidomimetics for DNA/RNA Binding, Antimicrobial Action and Cell Penetration.**” submitted for the degree of Doctor of Philosophy to the **Academy of Scientific and Innovative Research (AcSIR)** has been carried out by me at the Organic Chemistry Division, National Chemical Laboratory, Pune – 411 008, India, under the supervision of **Dr. Moneesha Fernandes**. Any material as has been obtained by other sources has been duly acknowledged in this thesis. I declare that the present work or any part thereof has not been submitted to any other University for the award of any other degree or diploma.

Date :

CSIR - National Chemical Laboratory

Pune - 411008

Research Student

Govind Sudhakar Bhosle

Dedicated to My Parents



Acknowledgement

It has been said that you learn more from your failures than your successes – if that is true, I must have learned a lot. Scientific research is a lot like gambling: intermittent reward is a powerful motivator. Although the six years I've spent here have been filled with much frustration (and some successes too), I do feel it has been worth it for I have learned not only about science, but about who I am. There have been many people who have helped me be who I am today, and they deserve my thanks.

First and foremost, I would like to express my heartfelt and sincere gratitude to my research supervisor Dr. Moneesha Fernandes who introduced me to an fascinating area of the peptide chemistry and taught me the importance of good practices in the lab. Her motivation, inspiration, encouragement and persistent guidance have helped me realize my dream to reality. I am thankful for her patience, motivation, timely advice and the continuous support provided during every stage of my research work.

I am thankful to my research co-supervisor Dr. Souvik Maiti for his constant support and help in biophysical studies and during my stay at IGIB New Delhi. Dr. Souvik taught me ITC and various biophysical methods for which I am thankful to him.

I would equally like to offer my sincere thanks to Dr. Vaijayanti Kumar, It is from her that I learnt how to understand and tackle basic research problems in chemistry and biology of drug delivery. She provided me with constant encouragement, guidance and support at every difficult phase during my research work.

I take this opportunity to offer my sincere appreciation to Dr. G. J. Sanjayan, Dr.K. Krishnamoorthy, for their valuable suggestions and advice.

I extend my sincere thanks to the current Director of CSIR-NCL Dr. Ashwini Kumar Nangia., Dr. Sourav Pal (former director), Head of Organic Chemistry Division, Dr. Anil Kumar for their kind help and encouragement during the course of this work. I am also very much thankful to Dr. Mahesh Kulkarni, Dr. Dhanshekharan and their group members for allowing me to use cell culture facility. A special thanks to Shakuntala for training me in basics of cell culture. The help from Dr. Shanta Kumari for the MALDI-TOF, HRMS and LC-MS analysis is highly appreciated. The kind support from NMR group is greatly acknowledged.

Acknowledgement

I wish to sincerely thank our research collaborators from combichem bioresource centre CSIR-NCL Dr. Dhiman Sarkar, Laxman Navle, Amar Yeware, and their lab-mates for in vitro studies of our oligomers. I am also thankful to Dr. Durba sengupta and Shalmali Kharche for simulation and docking studies.

I have had the privilege to work in a lab of very nice people. My deepest gratitude to Amit, Manisha, Harsha, Ragini, Aniket, Komal, Atish, for their help, support and keeping a constant joyful atmosphere in lab. I wish all my labmates high success in their life. I thank Mr. Bhumkar and Mr. Gurav for the laboratory assistance.

I would like to specially thank Kundan, Mubarak and Amol for their constant help, suggestions and for unconditional support during thick and thin.

The help provided for biophysical studies by Dr. Souvik's group at CSIR-IGIB New Delhi. Specially Santy, Smita, Hemant, Prachi, Gopal, Soundhar is greatly acknowledged. I wish to extend my sincere thanks to them also.

I have high regards for my seniors and colleagues who have provided me with unconditional support and help during my Ph D. course. My lab seniors Dr. Madhuri, Dr. Seema, Dr. Namrata, Dr. Kiran, Dr. Venu, Dr. Manoj, Dr. Anjan, Dr. Tanaya and Dr. Harshit trained and helped me in lab work which I greatly acknowledge. Also I would like to thank my seniors Dr. Ravi, Dr. Kishore, Dr. Rahul, Dr. Ankush Bhise, Dr. Nagesh, Dr. Deepak, Dr. Majid, Dr. Atul, Dr. Chinmay, Dr. Bhausahab, Dr. Pradip.

I would like to thank my loving parents for giving unconditional love, constant support and encouragement without which I never would have been able to achieve my goals.

I also thank my beloved friends Umrao, Jagdish, Vaijinath, shyam, Balasaheb, Sakha, Ulhas, Pradnya, Archana, Rohini for their individual support and encouragement during my carrier. Also my thanks to the Golden Jubilee Hostelites and friends from NCL and outside Prakash, Bhausahab, Atul, Milind, Dhyaneswar, Hemendra, Shrikant, Vijay, Nilesh, shahaji, satej, and Dyaneshwar for their constant help and support.

I would also like to thank my family members Usha, Sheetal, Pratibha, Nikita, Kedar, Om and Arti for their love and encouragement provided and without whose support my ambition can hardly be realized. I would also like to thank my uncle Mr. Vyankat, Mr.

Acknowledgement

Madhukar, Mr.Padmakar, Mr. Bharat and their family for love, kindness and support. The help from my cousin's Vinod, Rahul, Nitin, Pramod, Vinod, Santosh is also highly appreciable.

I thank my better half Gitanjali and son Ayush for brining joy and love during Ph.D tenure.

I offer my sincere regards to Dr. Govind Burse, Mr. Vitthal Thorat who directed me throughout my carrer. The help and support from Jayaprabha family (Pawar sir, yadav sir, Ghadge sir, Burge sir, Mhaske sir) is highly acknowledged. Thanks to Dr. Gill Sir, Dr. Shingte Sir, Dr. Sathe Sir, for inspiring me directly or indirectly in research carrier.

I am grateful to UGC, New Delhi, for awarding the research fellowship and , I am also thankful to the Academy of Scientific and Innovative Research (AcSIR).

My greatest regards to the Almighty for bestowing upon me the courage to face the complexities of life and complete this dissertation successfully and for inculcating in me the dedication and discipline.

Govind S. Bhosle

Contents		
Abbreviations		i
Synopsis		iii
Chapter 1		
1	Introduction to Peptidomimetics	
1.1	Introduction	1
1.1.1	Peptides and their role in drug discovery	1
1.1.1.1	Natural Peptides	1
1.1.1.2	Synthetic peptides	3
1.1.2	Peptides as Drugs	5
1.1.3	Limitations of Peptides as Drugs	6
1.1.4	Advantages of peptides as drugs	7
1.2	The importance of peptidomimetics	7
1.3	Applications of Peptidomimetics	8
1.3.1	DNA Condensing Peptides	8
1.3.1.1	Application of DNA Condensations	9
1.3.1.2	Cationic peptides	11
1.3.2	RNA as a therapeutic target and RNA-binding peptides	12
1.3.3	Cell Penetrating peptides	13
1.3.3.1	Proposed mechanisms for cellular uptake of CPPs	15
1.3.3.2	Structure-activity studies of CPPs	18
1.3.3.3	Cell-Penetrating Oligomers other than peptides	19
1.3.4	Antimicrobial Peptides	20
1.3.4.1	Mechanism of action of antimicrobial peptides	21
1.3.4.2	Factors affecting antimicrobial activity of peptides	23
1.3.4.3	Morphology and Structure of Bacterial Cell Membranes	24
1.3.5	Summary	26
1.3.6	Present work	27
1.3.7	References	29

Chapter 2		
2	Tat peptide analogues : Synthesis and DNA, RNA interactions.	
	SECTION A	
A	Modulation of Tat peptide-DNA interaction by arginine substitution in HIV-1 (48-57) Tat peptide.	
2A.1	Introduction	38
2A.2	Rationale, design and objectives of the present work	39
2A.3	Work done	39
2A.4	Results and Discussion	40
2A.4.1	Synthesis of amino acid surrogate X, precursor to amino acid r	40
2A.4.2	Synthesis of Tat peptide oligomers	41
2A.4.3	UV-Melting Studies	45
2A.4.4	Agarose Gel Electrophoresis Mobility Shift Assay	47
2A.4.5	Circular Dichroism Spectroscopic Studies	49
2A.4.6	Cell uptake and Cytotoxicity studies	50
2A.4.6.1	Cellular uptake studies	50
2A.4.6.2	Confocal Microscopy studies	51
2A.4.6.3	Cytotoxicity studies	53
2A.4.7	Stability to enzymatic hydrolysis	53
2A.5	Summary and Conclusions	56
2A.6	Experimental Section	57
2A.7	Appendix A	64
2A.8	References	76
	SECTION B	
B	Superior HIV-1 TAR-Binders with Conformationally Constrained R52 Arginine Mimics in Tat (48-57) Peptide.	
2B.1	Introduction	78
2B.2	Rationale, design and objectives of the present work	80
2B.3	Results and Discussion	82

2B.3.1	Synthesis of arginine surrogates	82
2B.3.2	Synthesis of Tat peptide oligomers	83
2B.3.3	UV-Melting Studies	86
2B.3.4	Isothermal Titration Calorimetric evaluation of the Tat-TAR binding	87
2B.3.5	Electrophoretic Gel Mobility Shift Assay	88
2B.3.6	Circular Dichroism Spectroscopic Studies	90
2B.3.7	Computational analysis of Tat peptides binding to TAR RNA	91
2B.3.8	Cell uptake studies and Cytotoxicity	95
2B.4	Summary and Conclusions	98
2B.5	Experimental Section	99
2B.6	Appendix B	106
2B.7	References	116
Chapter 3		
3	(R-X-R)₄-motif peptides containing conformationally constrained cyclohexane-derived spacers: Effect on cellular uptake.	
3.1	Introduction	120
3.2	Rationale, design and objectives of the present work	121
3.3	Results and discussion	122
3.3.1	Solid phase peptide synthesis of (R-X-R)-motif CPPs	122
3.3.2	Circular Dichroism analysis of synthesized peptides	126
3.3.3	Flow Cytometry analysis	127
3.3.3.1	General principle of Flow Cytometry analysis	127
3.3.3.2	Flow cytometry analysis of cf-labeled (R-X-R)-motif peptides	129
3.3.4	Confocal microscopy analysis	130
3.3.4.1	Principle of confocal microscopy	130
3.3.4.2	Confocal microscopic analysis of synthesized peptides	131
3.3.5	Cytotoxicity studies by MTT assay and Hemolysis assay	132
3.3.6	Protease stability of Peptides	134
3.4	Summary and conclusion	137
3.5	Experimental procedure and spectral data	137

3.6	Appendix C	139
3.7	References	146
Chapter 4		
4	Antibacterial and anti-TB Tat-peptidomimetics with improved efficacy.	
4.1	Introduction	148
4.2	Rationale, design and objectives of the present work	149
4.3	Results	150
4.3.1	Synthesis of Tat peptide analogues	150
4.3.2	Antibacterial activity of the Tat peptide analogues of the study	154
4.3.3	Activity against <i>Mycobacterium tuberculosis</i>	156
4.3.4	Circular Dichroism studies	159
4.3.5	Fluorescence- and transmission electron microscopy analysis	160
4.3.6	Cytotoxicity studies	163
4.4	Discussion	165
4.5	Summary and Conclusion	168
4.6	Experimental Section	169
4.7	Appendix D	172
4.8	References	178


Abbreviations

Ac	Acetate
Ac ₂ O	Acetic anhydride
Ahx	6-Amino hexanoic acid
Boc	Di-tert butyl carbonate
CD	Circular Dichroism
CPOs	Cell-penetrating oligomers
CPPs	Cell-penetrating peptides
<i>cf</i>	5, (6)-carboxyfluorescein
DEPT	Distortionless Enhancement by Polarization Transfer
DI	Deionized
DMF	N,N- Dimethylformamide
DIPCDI	N,N'Diisopropylcarbodiimide
DIPEA/DIEA	Diisopropylethylamine
DMAP	4,4- Dimethylaminopyridine
DMSO	N,N-Dimethyl sulfoxide
DNA	2'-deoxyribonucleic acid
EDTA	Ethylenediaminetetraacetic acid
Et ₃ N	Triethylamine
EtOH	Ethanol
Fmoc	Fluorenylmethyloxycarbonyl
HeLa cell	Henrita Lacks cell
h	Hours
HOBt	Hydroxy benztriazole
HRMS	High Resolution Mass Spectrometry
M	Molar
MALDI-TOF	Matrix Assisted Laser Desorption Ionisation-Time of Flight
MBHA	4-(methyl)benzhydrylamine-resin
MeOH	Methanol
mg	milligram
MHz	Megahertz
min	Minutes

Abbreviations

mL	Millilitre
mM	Millimolar
mmol	Millimoles
MS	Mass spectrometry
MW	Molecular weight
μL	Microliter
μM	Micromolar
nm	Nanometer
NMR	Nuclear Magnetic Resonance
pDNA	Plasmid deoxyribonucleic acid
Pet-ether	Petroleum ether
PNA	Peptide Nucleic Acid
R	Arginine
RNA	Ribose Nucleic Acid
RP-HPLC	Reversed Phase-High Performance Liquid Chromatography
siRNA	Small interfering RNA
Tat	Trans-activating transcriptional activator
TBTU	O-(Benzotriazol-1-yl)-N,N,N',N'-tetramethyluronium tetrafluoroborate
TFMSA	Trifluoromethanesulfonic acid
THF	Tetrahydrofuran
TLC	Thin layer chromatography
T _m	Melting temperature
UV-Vis	Ultraviolet-Visible

Synopsis

	Synopsis of the Thesis to be submitted to the Academy of Scientific and Innovative Research for the Award of the Degree of Doctor of Philosophy in Chemical science.
Name of the Candidate	Mr. Govind Sudhakar Bhosle
Degree Enrolment No. & Date	Ph. D. in Chemical Sciences (10CC12A26013); August 2012
Title of the Thesis	Arginine-rich Tat- and (R-X-R)-motif Peptidomimetics for DNA/RNA Binding, Antimicrobial Action and Cell Penetration.
Research Supervisor	Dr. Moneesha Fernandes (AcSIR, CSIR-NCL, Pune)

Statement of purpose: Although there are many natural and non-natural biologically active peptides, they have severe drawback of proteolytic degradation. This proteolytic degradation of peptides results into a poor bioavailability so that they are usually administered as intravenous or intramuscular injections. There are various different strategies have been developed in order to discover new compounds with improved binding ability with DNA and RNA, bioavailability and cell penetrating abilities. We emphasize the application of peptidomimetics for interactions of peptides with DNA/RNA, cell penetration abilities and antibacterial, antitubercular activity. The work presented in the thesis can be divided into four chapters:

Chapter 1: Introduction to Peptidomimetics

There is a growing number of biologically active peptides which have potential for the development of new therapeutics. However, native peptides are only rarely directly usable as drugs, due to inherent limitations which include rapid proteolysis and metabolism, poor transport properties, rapid excretion through liver and kidneys, and low oral availability. Furthermore, peptides are often aselective in their actions owing to their flexible structure. In efforts to address these limitations, peptides are modified into mimetics with specific physical, chemical and biological characteristics. These so-called peptidomimetics are derived from peptides by partly or completely removing the amide bonds while retaining essential amino acid side chains in a defined, spatial relationship. This chapter deals with the application of the peptidomimetic design in medicinal chemistry. In the search modified peptides with improved stability and pharmacokinetic properties leading to extensive research effort in this field. To design and develop novel synthetic approaches many structural modifications of peptides were investigated

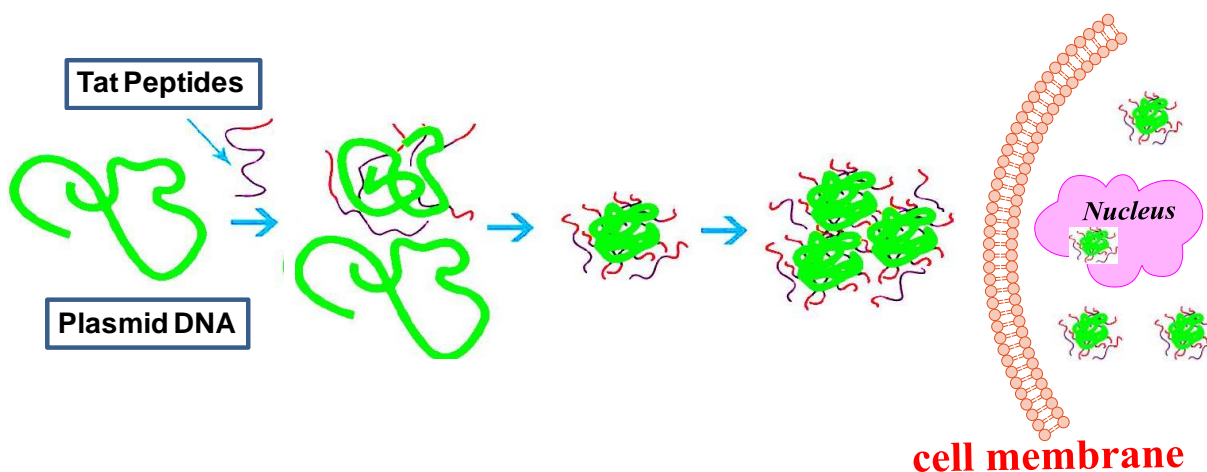
Synopsis

by rational design and molecular modeling methods. In this chapter recent advances in the synthesis of conformationally restricted building blocks and peptide bond isosteres are discussed.

Chapter 2: Tat peptide analogues : Synthesis and DNA, RNA interactions.

Section A: Modulation of Tat peptide-DNA interaction by arginine substitution in HIV-1 (48-57) Tat peptide.

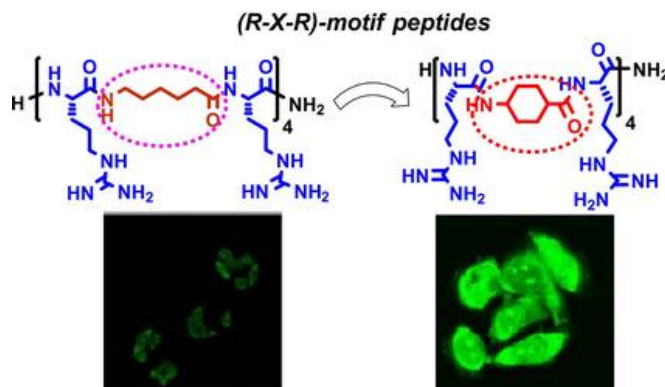
This section deals with understanding the interactions of cationic peptides with possible target and off-target biomolecules, that can prove useful in the rational development of drugs. In this chapter, we have attempted to modulate the Tat peptide-calf thymus DNA interaction through arginine substitution by non-proteogenic, conformationally constrained arginine mimics in HIV-1 Tat peptide. The mimics were found to enhance the protease resistance properties of the derived peptides. Various biophysical techniques were used to investigate the effect of introduction of non-natural arginine analogue into the Tat peptide. Tat peptide analogues effectively induced complete plasmid DNA condensation, which is important for gene transfection. Results from flow cytometry and confocal microscopy experiments proved that peptides can be successfully further explored as non-viral gene delivery vectors.



Section B: Superior HIV-1 TAR-Binders with Conformationally Constrained R52 Arginine Mimics in Tat (48-57) Peptide.

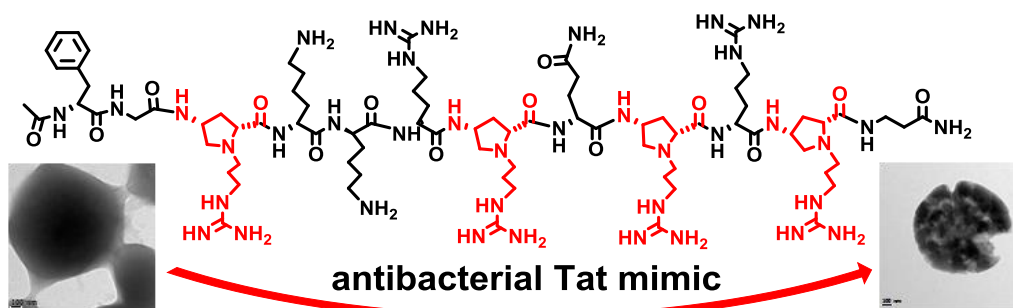
In this section we have reported modulation in binding affinity of the Tat(48-57) peptide analogues to HIV-1 TAR RNA by replacing R52, an essential and critical residue for Tat's

Synopsis



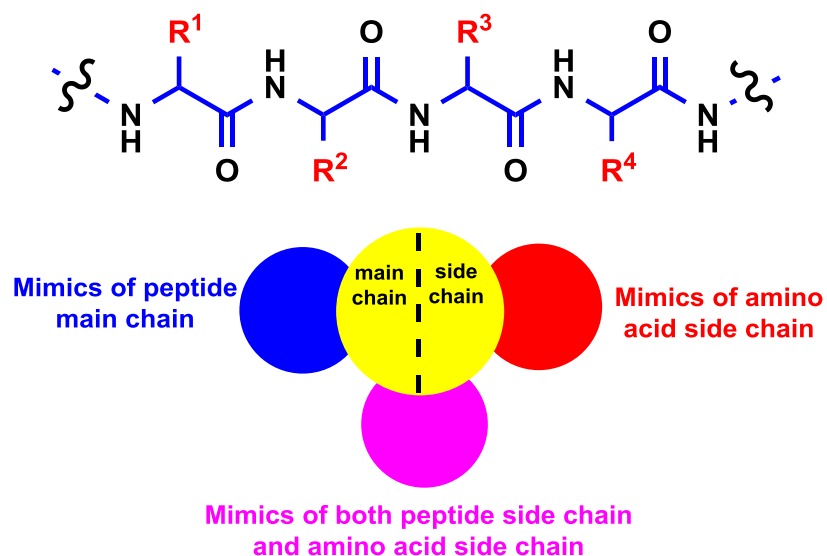
Chapter 4: Antibacterial and anti-TB Tat-peptidomimetics with improved efficacy.

In this chapter we have explored Tat peptide analogues as non-natural antimicrobial peptides, that are ideal as next generation antibiotics because of their ability to circumvent the problems of drug resistance and *in vivo* instability. We reported novel all- α - and α,γ -mixed Tat peptide analogues as potential antibacterial and anti-TB agents. These peptides have broad spectrum antibacterial activities against Gram-positive and Gram-negative bacteria and are also effective against active and dormant forms of *Mycobacterium tuberculosis*, including strains that are resistant to rifampicin and isoniazid. The introduction of the non-natural amino acids of the study in the Tat peptide analogues results in increased resistance to degradation by proteolysis, significantly increasing their half-life. The peptides appear to inhibit bacteria by a membrane disruption mechanism, and have only a low cytotoxic effect on mammalian cells.



CHAPTER 1

Introduction to Peptidomimetics



Structural studies and chemical modifications in naturally occurring peptides could enhance the efficacy of these peptidomimetics. Numerous types of peptidomimetics have been reported such as Cell-Penetrating Peptides (CPPs), Antimicrobial peptides, inhibitors of protein-protein-, DNA-protein-, RNA-protein interactions, etc. The cell uptake mechanism of these peptidomimetics is not understood completely, but it is known that it may vary and depend on their structural backbone, amphipathicity, associated cargo, etc. Along with peptidomimetics, liposomes and dendrimers have also been studied for drug delivery applications. Many peptidomimetics were found to have enhanced uptake properties with good biocompatibility. Many of them are currently being evaluated in various clinical trials. A concise review of the literature is discussed in this chapter.

1.1 Introduction

Peptidomimetics are molecules that possess identifiable similarities to a peptide, and that can act as a ligand of a biological receptor, can imitate or inhibit the effect of a natural peptide. Peptidomimetics can arise either from modifications of existing peptides or by designing similar systems that mimic peptides such as peptoids, β -peptides, etc. These altered chemical structures are designed to tune molecular properties such as stability or biological activity.

Peptides play vital roles in many biological and physiological processes. Life without peptides would be impossible since they function as hormones, enzyme inhibitors or substrates, growth promoters or inhibitors and neurotransmitters.¹

1.1.1 Role of Peptides in Drug Discovery

1.1.1.1 Natural Peptides

A peptide is a polymeric chain of amino acid residues which are joined together by amide bond. Structure of an amide bond is shown in Figure 1.1. A dipeptide consists of two amino acid residues, while a tripeptide is made up of three amino acid residues etc. A chain of 50 amino acid residues is called an oligopeptide, while proteins are made up of >50-100 residues.

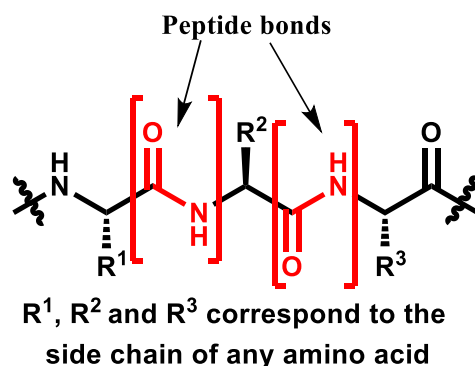


Figure 1.1 Representative structure of the backbone of a peptide

There are 20 natural amino acids found in peptides and proteins in human. It has been discovered that two more amino acids namely selenocysteine and pyrrolysine have been involved in the biosynthesis of peptides.² One of the common characteristics of all the natural amino acids is that the side chain is attached to a chiral α -carbon except glycine. The L-configuration is found to be

common in most of the naturally occurring proteins and peptides but there are some which are found in archaea and bacteria.

The formation of disulphide bond is one of the important feature of proteins and peptides. The two cysteine residues joined together by covalent bond is called as disulphide bond. The disulphide bridges offers stability and correct folding to proteins. The disulphide stabilizes the structure by connecting separate peptide chains or cross-linking different parts of one peptide chain. This stabilization has important function in proteins because they are excreted into the extracellular medium which results into faster degradation of disulphide linkages.

As the chain of peptide increases the number of intramolecular interactions increases which results into formation of number of secondary structures such as helices, turns and sheets. The occurrence of β -turn structure is common in shorter peptides while larger peptide contains higher order structures due to large number of secondary interactions. The large varieties of side chain present in amino acids, proteins or peptides interact with target in number of ways. The types of interactions involved are electrostatic interactions such as van der Waals interactions, ionic, hydrogen bonding, and π - π -interactions.

Peptides possess many different types of biological activities. In humans peptides like orexin,³ somatostatin,⁴ substance P⁵ and the family of opioid peptides⁶ functions as neurotransmitters or hormones. Commonly occurring peptide hormones in human are prolactin,⁷ vasopressin⁸ and oxytocin.⁹ There are many toxins present in venomous snakes and other animals which consist of peptide components. Conotoxins, melittin and apamine are the neurotoxins that are useful in cancer treatment.¹⁰ The venom of some species of cobra has made up of nicotinic receptor antagonist cobratoxin.¹¹ Peptides have also some biological applications such as flavoring agents. The aspartame is an artificial sweetener and the taste of meat also originates from beefy meaty peptide.¹² Vasoactive peptides are peptides with significant actions on vascular smooth muscle as well as other tissues. They include vasoconstrictors, vasodilators, and peptides with mixed effects. Antagonists of these peptides or the enzymes that produce them have useful clinical properties. In addition to their actions on smooth muscle, vasoactive peptides function as neurotransmitters and local systemic hormones. The well-known vasoactive peptides include angiotensin, bradykinin, natriuretic peptides, calcitonin gene-related peptide (CGRP), endothelin, neuropeptide Y (NPY), substance P and vasoactive intestinal peptide (VIP), and vasopressin .¹³

1.1.1.2 Synthetic Peptides

The synthesis of the dipeptide glycylglycine (Gly-Gly) from 3,5-diketopiperazine has started the field of peptide chemistry by Emil Fischer.¹⁴ There were many developments resulted in modern peptide synthesis which involves Curtius rearrangement of acyl azides resulted into formation of peptide bonds,¹⁵ First synthesis of the octadecapeptide Leu-(Gly)-Leu-(Gly)₃-Leu-(Gly)₉ in 1907 by Fisher,¹⁶ Later the concept of cleavable protecting group has introduced by Bergmann and Zervas¹⁷ and Characterization and synthesis of the biologically active peptide oxytocin by du Vigneaud's.¹⁸

The formation of the amide bond is a key step in the synthesis of peptides. Routinely activation of the carboxylic acid moiety has been preferred before the reaction with amine. Classically carbodiimides were the immediate choice as activating agents¹⁹ but this method has major limitation that it forms cyclic intermediate which results in to racemisation of the amino acid,²⁰ There were attempts to solve the problem by use of HOBt or HOAt. The later on the combination of onium salts such as HATU, HBTU²¹, TBTU.²² and diisopropylethylamine as base are used. Later the use of BOP²³ and PyBOP²⁴ also came into effect to bypass the formation of byproduct HMPA which is potential carcinogen.

With the emergence of advances in peptide chemistry selective manipulation of number of different protecting groups has also been possible. The protecting groups are acid-cleavable, base- cleavable and those which can be cleaved by other methods. The discovery of benzyloxycarbonyl group (Cbz), protecting group is removed by catalytic hydrogenation.²⁵ The use of allyl ester can be done to achieve protection of acids and allyloxycarbonyl (Alloc-) used for amines, both of them can be deprotected with a Pd(0)-reagent. The protection of acids is achieved by *tert*-butyl ester.²⁶ The protecting groups like *tert*-butoxycarbonyl (Boc-)²⁷ and trityl (Tr-)²⁸ groups are used for the protection of amines. The fluorenylmethoxycarbonyl (Fmoc-)²⁹ and methyl/ethyl esters³⁰ are used for protection of amines and acids, respectively when deprotection by base is needed. Depending on the requirements of the specific group's large number of other protection and deprotection chemistry can be used.²⁵

Time consuming and difficult purification and identification of every step of solution phase peptide synthesis has led to the discovery of solid phase peptide synthesis. Robert Merrifield revolutionize the field of peptide synthesis.³¹ To improve the applicability of solid phase peptide synthesis large number of modifications occurred in original resins. Acid-labile Rink and Wang

resins are the typical resins used in SPPS. Discovery of Rink amide resin further revolutionize the field. When rink amide undergoes acidic cleavage, the resulting peptide forms with a C-terminal amide instead of a free carboxylic acid. With the introduction of automated peptide synthesizer in the field of peptide synthesis drastic reduction in the time required for the synthesis of longer peptides has been made possible.³²

The schematic representation for SPPS can be summarized in Figure 1.2. Initially the carboxyl terminus of the amino acid of target peptide is linked to the resin and N-terminus is then deprotected. The deprotected N-terminus is then linked to N-protected residue by using standard coupling agents and its N-terminal protection is removed to further increase the length of peptide. The same process is repeated until the desired length of peptide sequence is completed. The peptide is then cleaved from solid support by using suitable reagents to avoid side reactions.³³ The process of precipitation, followed by purification by HPLC can be done to get pure peptide.

Recently heating by microwave irradiation has emerged as a new direction in peptide synthesis to speed up the synthesis.³⁴ To shorten the reaction time required, heating of the reaction mixture up to a temperature of 60 °C at the coupling has significantly reduced the time and improved the yield of peptides.³⁵ Even if the use of microwave heating has fasten the peptide synthesis but there are amino acids such as histidine and cysteine which are known to show racemization.³⁶ Microwave technology has also later been implemented in automated peptide synthesis.³⁷

The SPPS strategy offers great advantages over the solution phase method. In this strategy, the carboxyl-terminus amino acid is linked to a solid support having reactive functional groups, (Figure 1.2). The next *N*-protected amino acid can couple to the resin-bound amino acid either by using an preactivated ester or by an *in situ* activation with available peptide coupling reagents.

All the reagents along with protected amino acids are used in excess so that reaction will drive to completion. The washing of resin can be done at each step to remove unreacted reagents. To synthesize desired length of the peptide all the steps i.e. deprotection, coupling reactions and washing cycles are repeated. So the need of purification step after every amino acid attachment step is avoided. In the last step, cleavage can be done to effect removal of side-chain protecting groups and solid support from peptide. Further, the crude peptide can be purified to get the desired peptide.

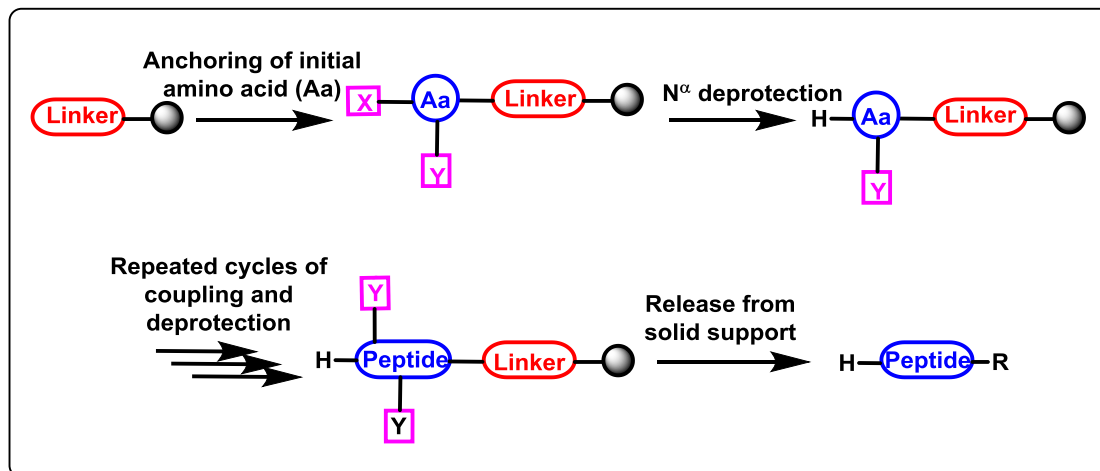


Figure 1.2 The schematic representation of SPPS.³⁶ X: Cleavable N^α -protecting group. Y: Side chain amino acid (Aa) protecting group. R: C-terminus functionality.

The advantages of solid phase synthesis are:

- (i) To avoid the loss due to transfer all the reactions are performed in a single vessel.
- (ii) To achieve high coupling efficiency, large excess of carboxylic acid monomer and coupling reagents can be used.
- (iii) SPPS offers reduction in purification cost as excess of reagents can be removed by simple filtration and washing steps.
- (iv) The method can be scaled up by automation and semi-micro manipulation.

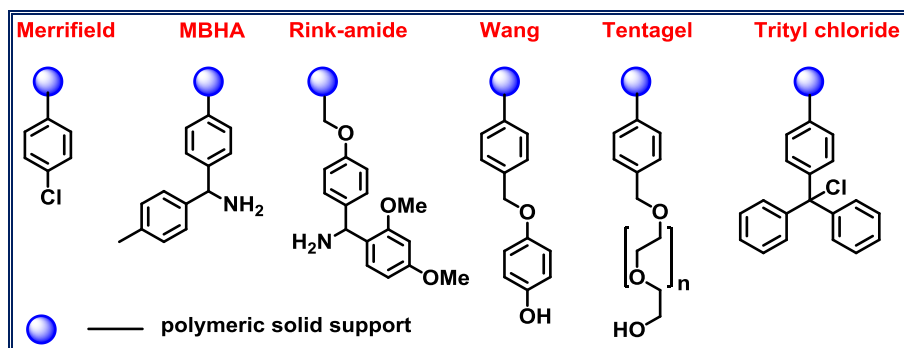


Figure 1.3 Few representative structures of functionalized resins used in SPPS.

1.1.2 Use of Peptides as Drugs

Despite the fact that there are many peptides which shows biological activity whose origin is from natural sources, but the relative percentage of peptides that are used as therapeutics is low.

Currently there are large number of natural and unnatural peptides are in clinical use; like antiretroviral peptide enfuvirtide used for the cure of HIV-1 infections, Leuprorelin for treatment of hormone-responsive cancers, Bivalirudin as anticoagulant, Insulin used in treatment of diabetes, Cyclosporine which is used as immunosuppressant, and Calcitonin for osteoporosis and hypercalcemia are used in therapy. Along with these there are number of synthetic peptides which are in commercial practice as therapeutics; like in the treatment of diabetes insipidus, bedwetting, or nocturia, gigantism and desmopressin is used. Eptifibatid which inhibits platelet aggregation, atosiban helps in prevention of premature labour, and octreotide which is used in the treatment of acromegaly.³⁸

1.1.3 Limitations of Peptides as Drugs

The peptides and proteins abundant in nature and they are important part of the nutrition. The utility of peptides as therapeutics has been significantly hampered by the existence of different routes and methods for their metabolism and elimination. Peptides get degraded immediately when they administered orally as soon as they reach to gastrointestinal tract.^{39,40}

To overcome the part of the problem, a parenteral route for the administration of peptides were used. Within a few minutes small peptides entering the circulation are typically metabolised by the peptidases in the plasma and elimination of larger peptides is done by the kidneys or liver.⁴¹ Once the peptide or protein has been eliminated from the blood stream it is also rapidly metabolised. The factors governing the elimination and metabolism peptides are hydrophobicity and overall charge of the compound.⁴¹ For bigger peptides, aggregation, denaturation also cause loss in biological activity.¹

The use of subcutaneous or intravenous injection for administering the peptide can bypass the limitations. The alternative ways of administering drug can enhance efficacy of drug. For the effective delivery of desmopressin and oxytocin, the use of a nasal spray has been reported earlier. The administration of drug by using injection leads to the repeated injections due to the rapid clearance of the peptides and discomfort to the patient.¹ Conformationally flexibility of linear peptides is also one of the problem associated with linear peptides. The offtarget effects of peptide therapeutics is another area of concern for linear natural peptides due to their inherent flexibility. This flexibility leads to non-selective binding to additional receptors leading to side-effects.⁴²

In the production large quantities of peptides, cost and complexity is another area of concern. There are variety of methods for production of peptides like, chemical synthesis, recombinant DNA technology, transgenic plants and animals and enzymatic synthesis. Most of these methods have limitations. Chemical synthesis yields small amounts of the product although it offers unlimited possibilities for the modification of peptides, the overall yield is very less for large peptides due to the large number of synthetic steps required. The use of biotechnological methods limits the possibilities for modifications of the natural peptides though it is used to produce larger amounts of peptides.

1.1.4. Advantages of peptides as drugs

Some of the distinct properties of peptides makes them ideal candidates in drug discovery, even if they have several limitation. To exploit the efficacy of a natural protein towards modulating the activity of some drug targets peptides can be used. The high efficacy and selectivity of peptides than small molecules offers extra advantage to use as therapeutic agent.⁴² The risk associated with toxic metabolites is also significantly reduced than for small molecules. The short half-life of the metabolites resulting from degradation of peptides offers low risk of accumulation in the tissues.⁴²

1.2. The importance of peptidomimetics

The therapeutic use of peptides is of great importance to diverse areas such as neurology, endocrinology and hematology. The use of peptides as drugs, is hampered by their bioavailability and biostability.¹ Peptides based active pharmaceutical ingredients suffers from major drawbacks like rapid degradation by proteases, poor oral availability, difficult transportation through cell membranes, non-selective receptor binding and challenging, multistep preparation etc.⁴³ To exhibit better pharmacological properties, small, protein-like chains called peptidomimetics have been designed to mimic natural analogs.

Peptidomimetics have been synthesized by cyclization of linear peptides⁴⁴ and/or coupling of stable unnatural amino acids.⁴⁵ Unnatural amino acids can be generated from their native analogs via modifications such as amine alkylation,⁴⁶ side chain substitution,⁴⁷ structural bond extension,⁴⁸ cyclization,⁴⁹ and isosteric replacements⁵⁰ (Figure 1.4) within the amino acid backbone. The important aspect of peptide chemistry is to achieve isosteric replacements within a peptide backbone. Such replacements can alter electrostatic properties and can form favorable

secondary conformations which resulting in improved pharmaco-kinetic properties. Backbone modifications of amino acids can be categorized as follows: (i) changing the amino functionality; (ii) replacement of α -CH; (iii) extension of the backbone by one or two atoms and (iv) atom modification of the carbonyl function (Figure 1.4).

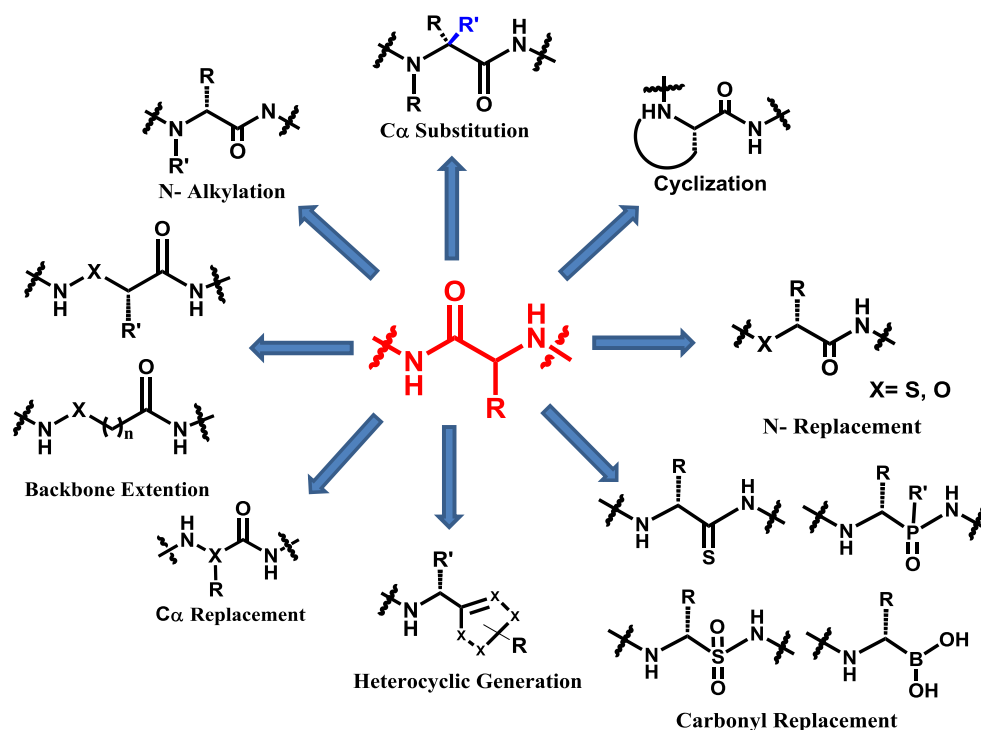


Figure 1.4 Structures of backbones used to synthesize a variety of peptidomimetics.

1.3. Applications of Peptidomimetics

1.3.1 DNA Condensing Peptides

Deoxyribonucleic acid is a molecule which encodes the genetic information used in the development and functioning of all known living organisms and many viruses. Nucleotides are the fundamental units of DNA molecules which are double stranded helices that consist of two long biopolymers. Each nucleotide is made of a nucleobase- guanine, adenine, thymine or cytosine (G, A, T and C respectively) and a backbone made of deoxyribose sugar and phosphate groups. The diameter of DNA is about 2 nm, while the length of a stretched single-molecule may be up to several dozens of centimeters depending on the organism. Genomic DNA is a very long molecule, which must fit into a very small space inside a cell or virus particle. DNA gets condensed in the nuclei of bacteria, eukaryotic nuclei, and viruses. DNA condensation and

decondensation are involved in gene expression, chromosomal changes during the cell cycle, and in the delivery of genes in gene therapy. DNA condensing into chromosomes is shown in Figure 1.5.

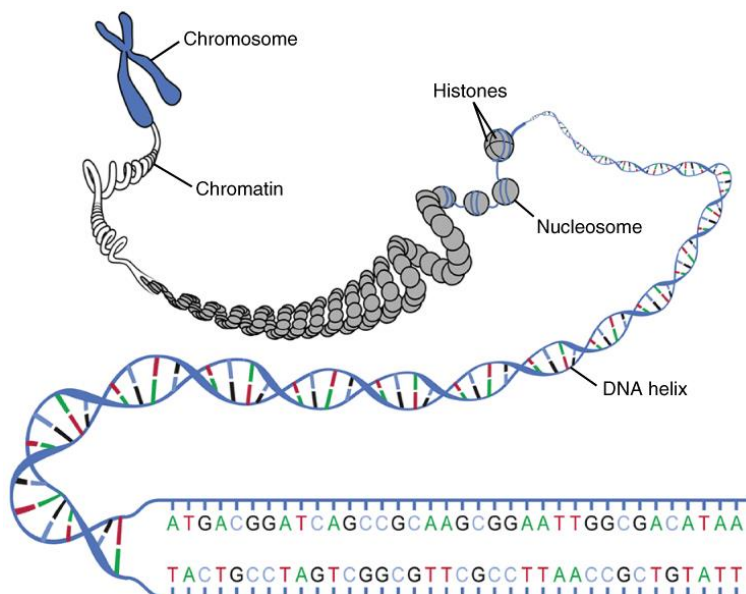


Figure 1.5. DNA condensing into a chromosome, shown schematically.⁵¹

If fully extended has 160,000 base pairs of T4 phage DNA which span around 54 μm , but when they are in condensed form, the T4 DNA molecule has to fit in a virus capsid about of about 100 nm in diameter. The space required for the DNA *in vivo* is much smaller than space required in free diffusion in the solution. In order to get rid of the volume constraints, DNA has a unique property to pack itself in the small space with the help of ions and other molecules. DNA condensation helps conserve space in cells. Condensation of DNA is the reason because of which the approximately two meters of human DNA accommodates into a cell that is only a few micrometers of size. DNA condensation is “the collapse of extended DNA chains into compact, orderly⁵² particles that contain only a few molecules”. DNA helices are separated by just one or two layers of water in the condensed state.

1.3.1.1 Application of DNA Condensations

The substitution of defective genes and disrupting their expression at transcription or translation level is called as gene therapy. Gene therapy involves the use of variety of cargoes such as

plasmids, antisense oligonucleotides, small/short interfering RNA, triplex DNA etc. in the cure of many deadly diseases.⁵³ Efficiency in transfection of DNA is very important to the success of gene therapy. The efficiency in the transfection of DNA depends upon delivery of DNA. The number of DNA molecules reaching the nucleus and the efficiency of DNA expression decides the success of gene therapy. The elongated random coil state and negative charge on DNA molecules under physiological conditions lead to a number of challenges such as stability upon exposure to enzymatic degradation and transporting DNAs through biological membranes. This leads to the discovery of viral and non-viral delivery vehicles.

Literature survey reveals that high efficiencies can be achieved by viral systems but they are associated with potential toxicity, immunogenicity, and other risks.⁵⁴ There are physical methods reported for delivery of drugs by non-viral gene delivery, such as electroporation, microinjection and gene guns, which are invasive and suffer from many other drawbacks.⁵⁵

Recently new methods of non-viral gene delivery have appeared in literature in which the use of DNA binding chemical agents and transfer of genes to cells occurs. In the process of DNA condensation the condensing agents induces different morphologies in to the relaxed DNA which then forms micro- or nano-particles. In literature there are large number of chemical entities reported as DNA condensing agents. (Figure 1.6), including small molecules^{56,57} polymeric materials⁵⁸ biomolecules^{59,60} and nanomaterials.⁶¹ Many of these are approved by regulatory agencies for gene therapy and several others are at various stages of clinical trials.⁶² However, transfection efficiency of these chemical entities *in vivo* is less than that of viral vectors. Improvement in the efficiency of transfection of non-viral vectors is one of the important area of research in gene therapy. New polymeric molecules, surfactants and nanomaterials are being investigated and applied in DNA condensation, transfection and gene therapy.

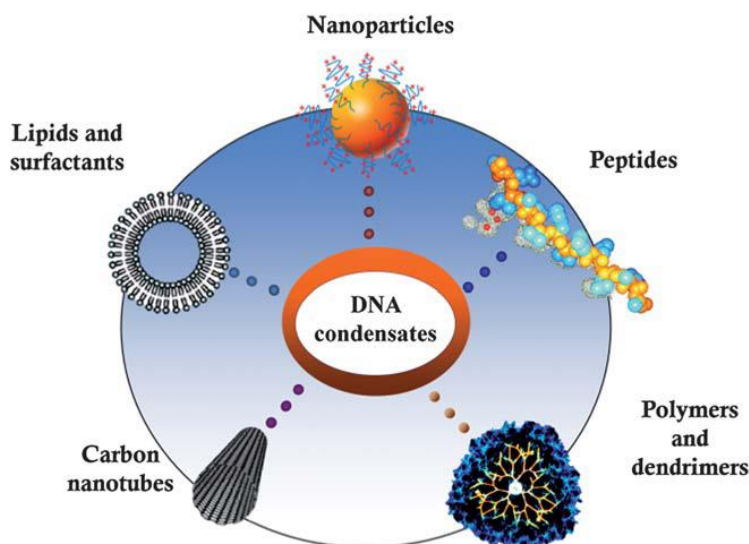


Figure 1.6 Different types of Chemical entities used as DNA condensing agents.⁶³

1.3.1.2 Cationic peptides

Peptides are one of the most promising candidates for DNA condensation on nonviral gene vectors. The biocompatibility of peptides and their easy and scalable solid-phase synthesis makes them ideal candidates.^{64,65} Cationic peptides has ability to condense DNA and avoid the peptides of getting degradation. The positive charge on condensed nanoparticles facilitate the interaction with the cell membrane and cell entry. The success of gene therapy depends on receptor targeting, nuclear localization, membrane fusion, and endosomal escape of DNA condensates. To achieve all these factors, peptide sequences can be engineered. Specific amino acid sequences with cationic residues or targeting motifs have been applied for efficient transport of DNA into the nucleus. Under physiological conditions lysine (K) and arginine (R) residues possesses positive charge. Peptide based condensing agents contain mostly, both amino acids. Protamines and Histones are the known DNA binding proteins and literature survey revealed that they are used in condensation of DNA *in vitro*.⁶⁶

Poly-L-lysines are also widely used as condensing agents in gene delivery. The high toxicity is associated with DNA condensing agents which contains large number of lysine residues, although it enhances the transfection efficiency.^{67,68} To avoid this toxicity, they have been complexed with other polymers such as PEG.^{69,70} Arginine-rich peptides, are known to enhance translocation through cell membranes besides their ability to condense DNA effectively. Most of the peptide sequences, presence of arginine determines the membrane translocation ability of

peptide sequence. The condensation behavior of both lysine and arginine containing peptides is different.⁷¹ The peptide KALA,⁷² offers , effective condensation and protects DNA against degradation, and also promotes cellular membrane permeation. There are many peptide-based vector which are capable of DNA-binding, cell-targeting and membrane-fusion motifs could condense DNA into nanoparticles for high transfection efficiency.⁷³

1.3.2 RNA as a therapeutic target and RNA-binding peptides

The major structural difference between DNA and RNA is that, minor groove of A form of RNA is shallower than B form of DNA and major groove of A-form RNA is deeper and narrower than the B-form of DNA. This structural difference allows selectivity to certain ligands to bind with RNA rather than DNA. This ability of RNA makes it an favoured therapeutic target⁷⁴. Until recently scientific community has achieved partial success in the development of small molecule therapeutics that can selectively target RNA. RNA targetting has become formidable challenge although there are exceptions to this like antibiotics⁷⁵ and antisense technology⁷⁶. There are several factors which affects RNA binding of small molecule ligands like large surface area, strong binding of endogenous ligands, cell permeability and stability. Conformational dynamics of RNA and crystallizing a particular structure of RNA in solution are the biggest challenges in targeting RNA.^{76,77}

Modeling studies have been used to screen ligands against various RNA motifs, and ligand-RNA dynamics have been studied using NMR and molecular dynamics simulation in order to address the above said challenges.⁷⁸

High-throughput screening of chemical libraries were also performed in which a large number of ligand libraries were screened against various RNAs.⁷⁹ Several RNAs have been well studied as therapeutic targets, including viral RNAs such as the HIV-1 TAR RNA, HCV internal ribosome entry site (IRES),⁸⁰ as well as expanded nucleotide repeats r(CCUG) involved with the development of myotonic dystrophy type 2.⁸¹

Rational drug design is difficult with RNA since it has the presence of the 2'-OH group, which leads to the formation of a different secondary structures such as hairpins, loops, bulges, turns and pseudoknots.⁸² Due to a inadequate structural information on RNAs and RNA-protein complexes, the area of specific recognition of RNA molecules by RNA binders was not explored well. Fortunately, in the past few years with the emergence of crystallography and NMR

techniques coupled with combinatorial tools, resulted in few cases of successfully designed peptide or small-molecule RNA binders. RNA is well known to play an increasing number of roles in the cell like transcription regulation⁸³, translation⁸³, and catalysis⁸⁴. Peptides that can bind RNA would be explored as biochemical tools and lead compound for therapeutics. An understanding of the structural dynamics of RNA molecules and its role in many biological processes has led to the design of sequence-specific RNA binding molecules. To understand the basic principles of nucleic acid recognition and the development of new RNA-targeting drugs, sequence-specific targeting of RNA is essential. Recently few reports appeared in literature where zinc finger protein were utilized to target sites in the major groove⁸⁵ whereas polyamides were used to target sites in minor groove⁸⁶.

In order to disrupt Tat–TAR interactions, Peptides and peptidomimetics have been used as medium-sized molecules. A linear arginine rich segment Tat, RKKRRQRRK, has been shown to compete with full length Tat for TAR-binding, by inhibiting the virus at the post-transcriptional level.⁸⁷ A combinatorial library of peptoids and D-amino acids inhibitors were generated with unique secondary structures by Hamy and coworkers.⁸⁸ In Literature nanomolar concentrations of the hybrid peptoid/peptide CGP64222 was shown to inhibit formation of the Tat–TAR complex. This inhibition involves conformational change of the RNA upon binding with hybrid peptoid/peptide CGP64222.⁸⁸ Cyclic peptides with an arginine-rich scaffold to generate ARM mimetics, were also reported by Friedler and co-workers to inhibit nuclear import and disrupt Tat-RNA binding.⁸⁹ The template of D-Pro-L-Pro residue were also utilized to induce β turn in cyclic peptides,⁹⁰ and were found to inhibit both reverse transcription and Tat-dependent transcription.⁹¹

1.3.3 Cell Penetrating peptides

Cell penetrating peptides are the peptides that contain less than 40 amino acids and are able to enter cells by various mechanisms and in most cases are able to facilitate the intracellular delivery of covalently- or noncovalently-conjugated bioactive cargo in a nontoxic manner.

The influx of exogenous molecules like peptides, proteins, and oligonucleotides are protected by cellular membranes due to their hydrophobic nature. (Figure 1.7) To deliver therapeutic agents across cellular membranes several strategies have been implemented. Those include electroporation, microinjection and liposome- and virus-based vectors. However, these methods

have serious drawbacks, including high toxicity, low efficiency, poor specificity and bioavailability.

The HIV-1 TAT transactivating factor^{92,93} and *Drosophila* Antennapedia transcription factor⁹⁴ proteins were among the first proteins shown to be translocate across cell membranes and enter cells. The discovery of the 16 mer Antennapedia peptide, penetratin, and 11 mer Tat(47-58) peptide further revealed that short sequences of these proteins could exhibit membrane permeation abilities. Tat and penetratin peptide has laid the foundation to progresses the delivery of a variety of cargos. In literature a number of studies have reported the numerous applications of CPPs in the delivery of various cargos such as polymers, liposomes, nanoparticles.⁹⁵ The ability to be taken up by a variety of cell types, no restriction with respect to the size or type of cargo dose- dependent efficiency and low cytotoxicity are advantageous factors for the use of CPPs.⁹⁶

Besides the natural peptides like Tat and penetratin, protein chimera and purely synthetic sequences were found to be able to cross cell membranes. In some cases, these were proved to be even more effective delivery agents then protein-derived CPPs.

The synthetic peptides were designed by using rational design strategies, prediction programs or even trial and error. These efforts include introduction of unnatural amino acids⁹⁸ and other modifications. The sequences of amino acids in CPPs are known to vary considerably. Numerous CPP sequence made up of positively charged amino acids. Oligoarginines are among the most widely used CPPs.⁹⁹ Certain structural attributes such as a helical component has been shown, in some reports, to be beneficial for cell penetration.¹⁰⁰ Efficiency of cargo delivery could also be improved through the use of dendrimers,^{101,102} cyclic peptides,¹⁰³ and non-natural amino acids. Despite the discovery of large number of delivery vehicles, the need for further modifications arises when CPPs are used to deliver larger biomolecules (nucleic acids, proteins) inside cells. For example, *in vivo* delivery requires a longer drug circulation time, which in turn requires a more stable complex to form between the CPP and its cargo. This can be achieved by adding different hydrophilic groups to an already cell permeable peptide.¹⁰⁴

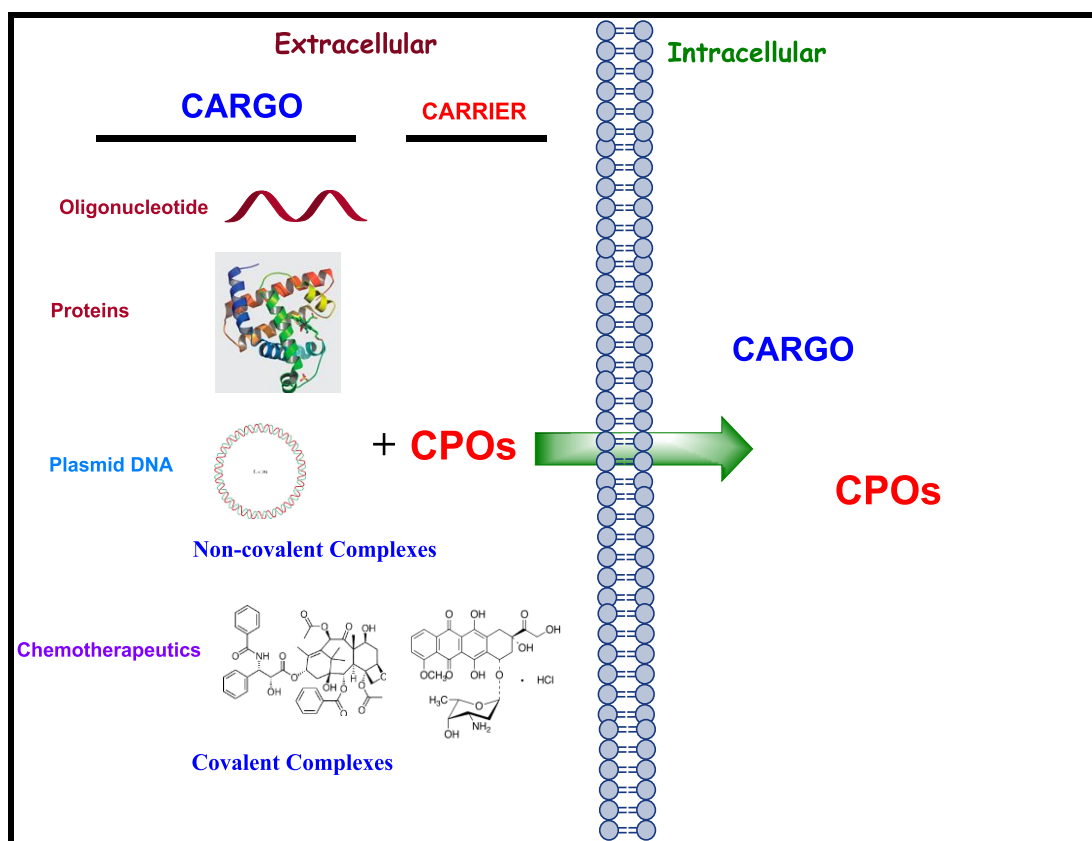


Figure 1.7 Strategies to attach cargo molecules to CPOs (Cell Penetrating Oligomers) and their release inside the cell from the associated CPO.⁹⁷

1.3.3.1 Proposed mechanisms for cellular uptake of CPPs

The mechanism of how CPPs enter into cells is not yet fully understood and it is now accepted that each CPP can enter cells via one or simultaneously more than one mechanisms, which may differ in the presence of cargo, and even in the case of different cargos or their mode of attachment to the CPP. The suggested mechanisms that apply to majority of the CPPs in delivering associated cargo to cells (Figure 1.8) are

- a) Energy-dependent or endocytotic penetration
- b) Energy-independent or non-endocytotic or direct penetration
- c) Receptor-mediated cell penetration

1.3.3.1a Energy-dependent or endocytotic penetration

Endocytosis is one of the major mechanisms of cell entry that have been reported for CPPs, and can be divided into two main categories:

- I) Phagocytosis: a process which occurs in specialized cells e.g. macrophages
- II) Pinocytosis: a process which is active in most of the cells. Pinocytosis is the set of pathways that include macropinocytosis,¹⁰⁵ clathrin-mediated endocytosis,¹⁰⁶ caveolae-mediated endocytosis¹⁰⁷ and other less well-characterized pathways.¹⁰⁸

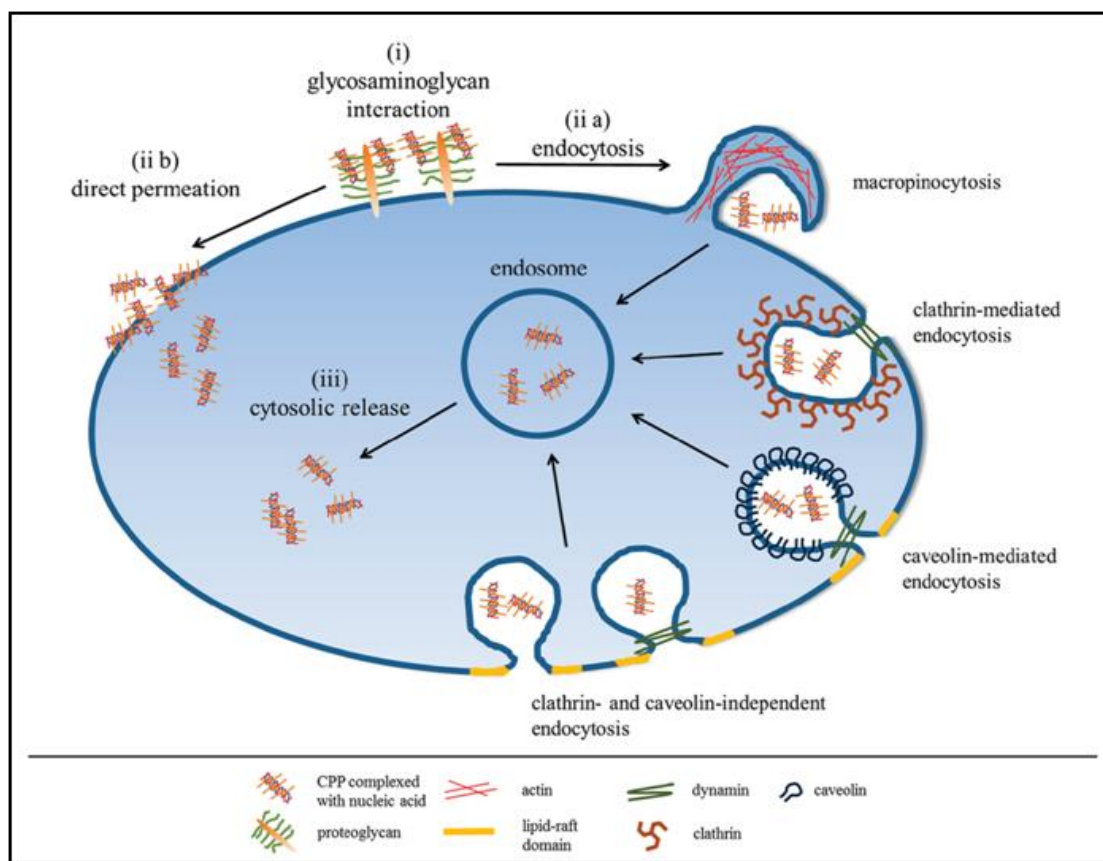


Figure 1.8 Various mechanisms of cellular uptake of CPOs complexed with cargo.¹⁰³

Energy-dependent mechanisms of CPPs translocation across biological membranes may be demonstrated through: (i) Cellular uptake studies carried out at low temperature (usually at 4°C) or in energy/ATP depleted condition; (ii) cell uptake studies in the presence of drug which will specifically arrest a known internalization pathway; (iii) incubation with molecular markers of known internalisation pathways (e.g., Caveolin-1, early endosome antigen-1 - EEA1) or evaluation of peptide or peptide conjugate co-localization with their specific endocytosis internalization pathways ; (iv) overexpression of dominant negative mutants of proteins involved

in the internalization process (e.g., Dynamin). (v) use of endosomal release agents. Thus, cell uptake mechanisms of many CPPs have been demonstrated; for Tat peptide, pinocytosis, along with endocytosis-independent mechanisms were the suggested pathways.¹⁰⁹

1.3.3.1b Energy-independent or non-endocytotic or direct penetration

Initial experimental results showed cellular uptake which was carried out at low temperature (usually at 4°C) did not significantly affect the entry of some CPPs. These results suggested the presence of energy-independent (non-endocytosis or direct penetration) mechanism in addition to the known energy-dependent endocytosis as a mechanism involved in cell entry of CPPs.¹¹⁰ Many physical models¹⁰⁹ such as inverted micelle formation,¹¹⁰ pore formation,¹¹¹ the carpet-like model¹¹² and the membrane thinning model¹¹³ have been therefore proposed to show the direct penetration of CPPs. The work of Lundberg et al. for viral derived protein VP22 and of Richard et al. for tat (48-60) and nonarginine CPPs was published in 2000. These reports suggested that step of trypsin digestion of the cell membrane-adsorbed peptide is included in the protocol in flow cytometry analysis. Similarly the use of methanol or formaldehyde in cell fixation, in mild conditions, leads to the artifactual uptake of some CPPs.¹¹⁴

1.3.3.1c Receptor-mediated cell penetration

Binding of CPPs to cell surface proteoglycans prior to internalization of cells is still the subject of debate.¹¹⁵ Boisguerin and co-workers¹¹⁶ compared 22 different but known CPPs, and demonstrated that the 22 CPPs could be classified by their behaviour into three main groups showing high, medium and low cellular uptake, even after trypsinization. Moreover, they showed additional agents (e.g. chloroquine as endosome rupture reagent), which should increase cellular uptake or spread out endosomal/entrapped CPPs in cytoplasm, only have low effects.

Cell uptake of cargoes such as negatively charged oligonucleotides (ONs) with CPPs:

The group of Divita and Heitz¹¹⁷ introduced the idea of noncovalent association of nucleic acids with a carrier CPP for cellular delivery in 1997. Now, it has been well documented that when negatively charged oligonucleotides are mixed with positively charged CPPs they form nanoparticles via electrostatic and/or hydrophobic interactions. Both endocytotic and non-endocytotic pathways are proposed for cellular uptake of non-covalent CPP-ON complexes. siRNA and antisense oligonucleotides (asONs) need to reach the cytoplasm for exerting activity, and the splice switching ONs function in the nucleus of the cell. Therefore, the endocytic

mechanism may not seem effective at the first glance because the internalized material remains entrapped in the endosomes. In living cells, however, the non-endocytic uptake is not the prevailing mechanism for majority of CPPs, especially if coupled to cargo molecules¹¹⁸ and currently, most of the published data points to endocytic internalization of noncovalent ON-CPP complexes. Similar to the cellular uptake of CPPs themselves,¹¹⁹ ON-CPP complexes initially interact with the negatively charged glycosaminoglycans of the extracellular matrix. This interaction triggers the activation of Rho GTPase Rac1 and actin network remodelling, which favours macropinocytosis and increases membrane fluidity.¹¹⁹ The endocytic uptake of positively charged CPP-ON complexes is typically of oligoarginine-based delivery.¹²⁰

1.3.3.2 Structure-activity studies of CPPs

Systematic structure-activity studies¹²¹ showed that guanidine groups on cationic CPPs were essential for cellular uptake. To address the then unknown relative contributions of lysines and arginines to the cell-penetrating function, homooligomers of L- and D-arginine were synthesized and compared with homooligomers of lysine, ornithine and histidines for cell uptake.¹²² This study showed that homooligomers of lysine were less effective than tat (49-57) in cell-penetrating function, but homooligomers of arginine were dramatically better than tat (49-57). Thus, it was concluded that the cationic charge of lysines alone was not sufficient for cell uptake while cationic guanidinium groups of arginines and their number were critical (5-20 arginines, with 7-9 being the best compromise of cost and performance).

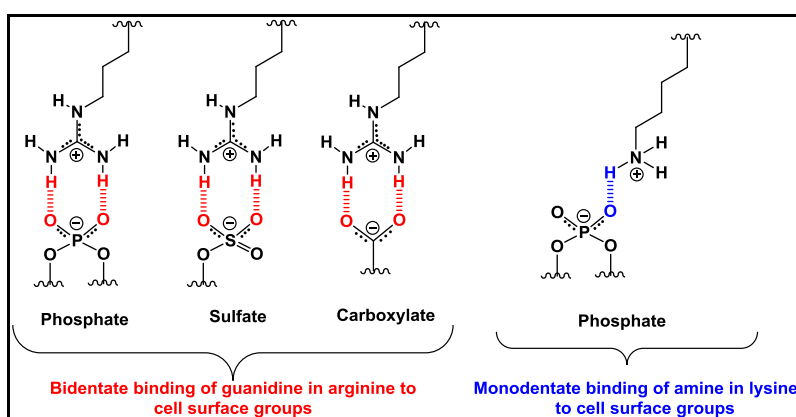


Figure 1.9 Representative interactions between guanidine and amine present in arginine and lysine respectively with cell surface functional groups.¹²²

It was hypothesized that the guanidine group in arginine has the capability to form a bidentate hydrogen bond with anionic cell surface phosphates, carboxylates and/or sulphates, whereas the interaction of lysine residues is through monodentate binding of ammonium groups. This hydrogen bonding is crucial in initial binding of guanidine-rich CPPs to the cell surface prior to internalisation (Figure 1.9).¹²²

1.3.3.3 Cell-Penetrating Oligomers other than peptides

A variety of scaffolds, including beta-peptides, carbohydrates, heterocycles, and peptide nucleic acids, upon preguanidinylation, exhibit cell-penetrating activity. Similarly, the peptide backbone of CPPs has been replaced by carbamates, carbonates, peptoids, etc. and these changes showed variations in cell uptake property for these CPOs. Some of these CPOs are discussed herein and shown in Figure 1.10.

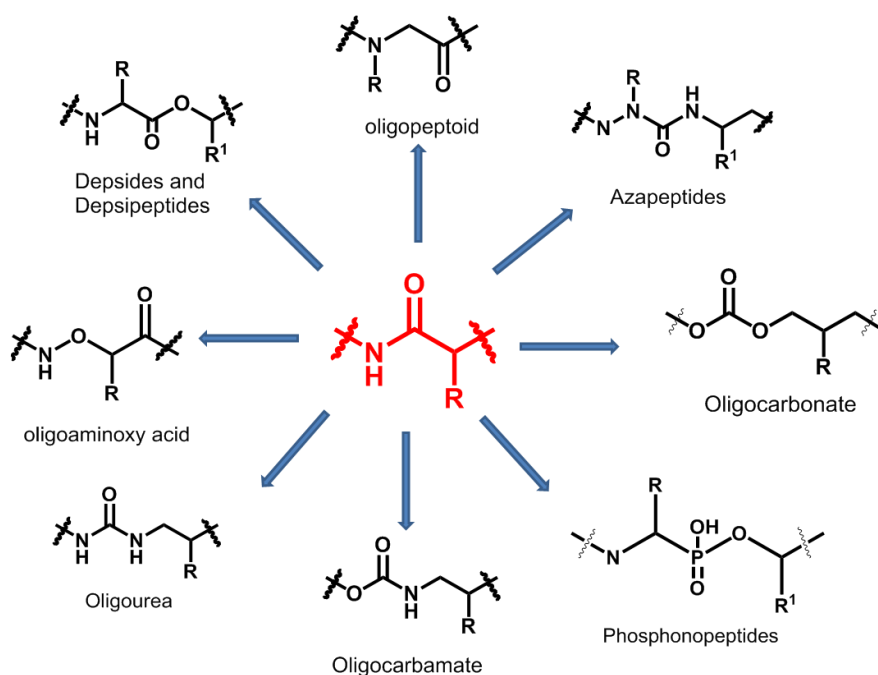


Figure 1.10 Representative backbone structures of various CPOs other than polyamides.

Rana and co-workers¹²³ synthesized the oligocarbamate and oligourea mimics of tat (47-57) peptide and demonstrated inhibition of transcriptional activity of tat protein in human cells. Covalently conjugated siRNA-tat (47-57) oligocarbamate and tat (47-57) peptide could effectively induce RNAi activity.¹²⁴ Wender and co-workers reported guanidylated oligocarbamates as a new class of molecular transporters. The 9-mer oligocarbamate was shown to be the most efficient transporters, entering cells faster than nonamer of D-Arg and HIV-1 tat

(49-57) peptide.¹²⁵ Wender and co-workers¹²⁶ reported polyguanidine molecular transporters linked through carbonate linkages (Figure 1.10). They were demonstrated to transport covalently conjugated luciferin cargo into cells efficiently.

Zhang et al.¹²⁷ used D- and L- α -aminoxy acids to synthesize CPPs that were internalized and showed diffuse cytosolic distribution. These peptides also showed serum stability and low cytotoxicity. Zuckermann and co-workers demonstrated that N-substituted glycine peptoid oligomers could condense plasmid DNA and deliver it efficiently into cells.¹²⁸ Cell penetrating abilities of a series of peptoids bearing amino or guanidino functions has also been demonstrated.^{129,130}

1.3.4 Antimicrobial Peptides

The protection of most animals against invading pathogens is done by innate immune system. The host-defence system produces chemical molecules along with skin and the mucous membrane to avoid micro organisms of getting entry and thereby infection.

The problem of multidrug resistance is worsening day by day with the use of conventional antibiotics. Antibiotic resistance arises in different strains of bacteria and fungi due to indiscriminate use of antibiotics.¹³¹ *S.aureus* have developed resistance as gentamicin resistant *S. aureus*, streptomycin resistant *S.aureus*, methicillin resistant *Staphylococcus aureus* (MRSA) etc. Recently resistance has been observed for vancomycin as well which was last hope against drug resistance bacteria. There are alternatives like linezolid can replace vancomycin against resistant bacteria.¹³² The unique characteristic of bacteria is their rapid multiplication, due to which quick spread of mutation occurs through the population which leads to the acceleration in the process of development of resistance. The killing of bacteria can be achieved by targeting specific bacterial target in appropriate concentration. Bacteria possess their own defense mechanisms. In some cases bacteria pump out the antibiotic before its action, so the concentration inside the bacteria will not be sufficient enough to kill the bacterial cells.¹³³ Destruction of the attacking molecule of the antibiotic is another strategy adopted by bacteria. In the case of penicillins, the first antibiotic discovered cleavage of the β -lactam ring takes place by β -lactamase enzyme produced by resistant bacteria¹³³. Hiding or reprogramming of the target is also one of the strategy of resistant bacteria to nullify the effect of antibiotics. To overcome the resistance machinery of these pathogens, new drug resistant antibiotics can be tailored and

designed by circumventing these mechanisms. Hence, it is the need of the hour to develop new strategies for inhibiting the growth of drug resistant bacteria. The action of antimicrobial peptides through disruption of bacterial membranes made them attractive candidates in antibiotic drug discovery programs.

The two main types of natural AMPs are the cationic and anionic peptides. The cationic peptides are short peptides capable of forming an α -helical structure. The bacterial membrane allows the entry of peptide by forming α -helical structure. The use of cationic peptides helps in bringing peptides and negatively charged bacterial membrane together. The peptides cecropins, magainin, dermaseptin, etc. belongs to this class. These peptides exert their action against majority of Gram negative bacteria and a some Gram positive bacteria. The anionic AMPs are also amphiphilic in nature.¹³⁴ Their mechanism of action is not yet clearly understood. Another class of peptides namely defensins made up of cysteine residues, forms disulphide bonds.¹³⁵

1.3.4.1 Mechanism of action

Even with the large number of literature reports, the mechanism of action of AMPs is not fully understood. Initially it was thought that membrane is the only target of AMPs, but many research groups reported that multiple cell targets are exist. Cell membrane of the pathogen is the primary target for majority of AMPs. Initially the attachment of bacterial membrane with cationic or anionic AMPs by electrostatic attraction between AMPs with the bacterial surface occurs. This attachment is stronger if the peptide possesses a greater number of cationic residues like lysine and arginine. After this initial binding, further modes of action can be described by three different mechanisms through which the Antimicrobial peptides target the bacterial membrane.

1.3.4.1a The Carpet model

When the ratio of peptide to lipid is low, peptide gets oriented parallel to the surface of bacterial membrane by forming a 'carpet'. This carpet is formed due to multiple electrostatic interactions with head groups of phospholipid present on bacterial membrane. The dense layer of peptide is formed due to presence of lipids which helps in reducing the repulsion in between peptide molecules. As the repulsive forces decreases the membrane disruption occurs due to unfavorable energetic of membrane. Due to this it does not involve pore formation and membrane penetration. Cecropins are known to attack bacterial membranes by this mechanism¹³⁶.

1.3.4.1b The Barrel-Stave model

In this model arrangement of peptides is considered like peptide helices are placed in the form of a barrel inside the lipid bilayer. The hydrophilic residues of the peptide are act interior of the barrel while the hydrophobic region of the peptide is aligned with that of the lipids of the bilayer. The insertion of the hydrophobic part of the peptide into the membrane occurs when it gets bind to bacterial membrane which leads to phase conformational transition of peptide takes place. This mechanism is not widely found among AMPs. This mechanism is known to found in almathecine and ceratotoxin A.^{137,138}

1.3.4.1c The toroid pore model

This is one of the most studied and commonly occurring mechanisms of action. As the AMPs insert into the membrane, the lipid monolayers twist and bend continuously to make the water core lined by both the peptides and the lipids. The polar heads of the lipid interact with their counterpart polar groups in the peptide. Strain in the membrane is caused by orientation of alpha helices on the surface of the membrane and displacement of the hydrophobic residues of the polar heads. The peptides like magainin act by this mechanism.¹³⁹

1.3.4.1d Alternate methods of action

Not all AMPs has ability to penetrate in to the bacterial membrane, but still they can cause harm to the cell. This is because they cause harm to the bacterial cell by targeting some other cellular processes and pathways. There are many reports that multiple targets of action exist for AMPs. Cecropin A, which acts through mechanism of membrane disruption, but it has also been reported to disturb gene transcription process in *E. coli*.¹⁴⁰ This is one of the reason why the bacteria finds a difficulty in developing resistance against AMPs. As AMPs possess unique modes of action and multiple targets. Alternate targets might involve disruption of protein folding, interaction with proteins, nucleic acids etc. For example, indolicidin, inhibit DNA synthesis in *E. coli* without causing lysis of the bacterial membrane.¹⁴¹ Similarly pyrrocoricin diminish the activity of ATPase of recombinant DnaK by interfering with protein folding.¹⁴² Some peptides have also been found to target lipid II crucial in the biosynthesis of cell wall of bacteria leading to disrupt cell wall synthesis.¹⁴³

1.3.4.2 Factors affecting antimicrobial activity of peptides

There are several factors which affects antimicrobial activity of peptides. These properties have direct correlation with the structure and composition of the cell membrane of bacteria and fungi. Some properties and their effects are discussed as follows.

1.3.4.2a Cationic nature

As discussed previously, due to the presence of anionic phospholipids bacterial membrane is negatively charged. Initial attachment of cationic peptides occurs through these membranes by electrostatic interactions. Cationic AMPs with α -helical structure are amphiphatic in nature and possess a net positive charge of at least +2. Higher hemolytic activity could be attributed with an increase in cationic charge. There is no straight relationship between peptide charge and its antibacterial activity. It reported that up to a threshold limit of net charge of +8, increasing the positive charge did not affect the hemolysis.¹⁴⁴

1.3.4.2b Secondary structure

There are variety of interactions between the amino acids, AMPs can form different secondary structures like alpha helices, beta sheets or random coils. Contributions of the ability to form a secondary structure in solution and self-associate are important criteria in determining the antimicrobial activity of AMPs.¹⁴⁵ There are some peptides which do not form alpha helical structure in solution but when they come in contact with phospholipid bilayer of bacteria forms an helical structure making entry of peptide easy. Amphipathicity of peptide could be the driving force of this transition into a helix in presence of lipid membrane. The α -helix further helps in neutralizing the excess positive charge and reduce peptide-peptide repulsion by interactions of hydrophilic chains electrostatically with negatively charged lipids. The peptides made up of parallel sheets linked by disulphide bridges are called β -sheet peptides. The role of disulphide bonds is to provide stability to the molecule. The disulphide bond also helps in bending of the molecule to penetrate in the membranes. To achieve the deep penetration of antimicrobial peptides in the bacterial membrane the formation of a secondary structure is of prime importance.

1.3.4.2c Hydrophobicity

Hydrophobicity of peptides is one of deciding factor for antimicrobial activity. The final entry of AMPs facilitated through membranes through hydrophobic interactions between the peptide and the membrane. The solubility of peptide should be fair enough in water. At the same time, it should also be able to interact with the hydrophobic region of the bilayer. Due to the self association property of peptides there is threshold value of hydrophobicity beyond which the antimicrobial activity of AMPs decreases and hemolytic activity increases.¹⁴⁶ Therefore maintaining the balance of hydrophilicity and hydrophobicity of peptides is most important for antimicrobial activity.

1.3.4.2d Fatty acid conjugation

As stated in previous paragraph hydrophobicity has been found to be detrimental factor on activity of an AMP. There are many proteins such as myelin in eukaryotes¹⁴⁷ and murein in *E. Coli*¹⁴⁸ has been found to be covalently linked to fatty acids. Similarly there are several fatty acid conjugated AMPs like daptomycin¹⁴⁹ and polymyxin have also been discovered in nature. Hence, there has been various attempts in improving the activity of AMPs by conjugating them with fatty acids of varying chain length. This helps in improving the hydrophobicity of the peptide besides maintaining the hydrophobicity/hydrophilicity balance.

1.3.4.3 Morphology and Structure of Bacterial Cell Membranes

The composition of bacterial membranes is important in understanding the mode of action of antimicrobial agents. Compared to eukaryotic cells, bacterial membranes contains high proportions of proteins as they large number of functions to perform. The amount of cholesterol in bacterial membranes is also less. Bacteria also lacks nucleus and all the genetic material is enclosed inside an irregular shaped region called the nucleoid.

Bacteria can be divided into Gram-positive and Gram-negative according to the ability to retain the Gram stain. Gram-negative bacteria turn red in colour due to washing out of crystal violet due to damage of its outer lipopolysaccharide membrane while Gram-positive bacteria turn purple in colour due to retention of crystal violet in the peptidoglycan layer on counterstaining with safranin. The Gram-negative cell envelope can be divided into the outer membrane, a peptidoglycan cell wall and the cytoplasmic or inner membrane. The outer membrane is found

only in the Gram-negative bacteria and is a lipid bilayer consisting mainly of glycolipids especially lipopolysaccharide (LPS). LPS is a negatively charged molecule made up of lipid A, eight to twelve variable sugar units and three to eight phosphate residues attached to O antigen. The peptidoglycan layer is a rigid layer giving a firm structure and shape to the bacteria (Figure 1.11). It is composed of repeating units of disaccharide N-acetyl glucosamine (NAG)- N-acetyl muramic acid (NAM) cross-linked by pentapeptide chains. The outer membrane is attached with the peptidoglycan layer by lipoprotein called Braun's protein. The inner membrane is a phospholipid bilayer which contains proteins necessary for most of the cellular processes like energy production, lipid synthesis, etc. Teichoic acids provide the anionic surface for the Gram positive bacteria as they are negatively charged and are of two types: wall teichoic acids which are attached to the peptidoglycan and lipoteichoic acids that are connected to the cell membrane (Figure 1.11). Selective targeting of specific bacteria can be made possible by considering these differences in composition of the cell membrane.

Mycobacterial species are Gram-positive, non spore-forming, aerobic bacteria, which made up of thick cell wall that offer them a unique impermeability to many molecules. The innermost is composed of peptidoglycan. External to the peptidoglycan is a covalently linked polymer of sugars, arabinogalactan, to which mycolic acids are esterified. Finally, a variable mixture of glycolipids and lipoglycans are thought to interact via their acyl groups with the mycolic acids through hydrophobic interactions. Figure 1.11 summarizes this unique cell wall and shows how it compares with the cell walls of Gram-negative and Gram-positive bacteria. A capsule composed of non-covalently linked loosely associated glycans, lipids and proteins has been shown to decorate the outer surface of the mycobacterial envelope. The prevalence of mycolic acid molecules covalently linked to arabinogalactan in the intermediate layer confers its high hydrophobicity and decreased permeability to external compounds. In addition to the intrinsic basis of antimicrobial resistance of mycobacteria related to their peculiar cell wall, both life-style and pathological consequences of infection dictate additional levels of difficulty in obtaining effective chemotherapeutical drugs. Mycobacteria are able to replicate inside the macrophage.

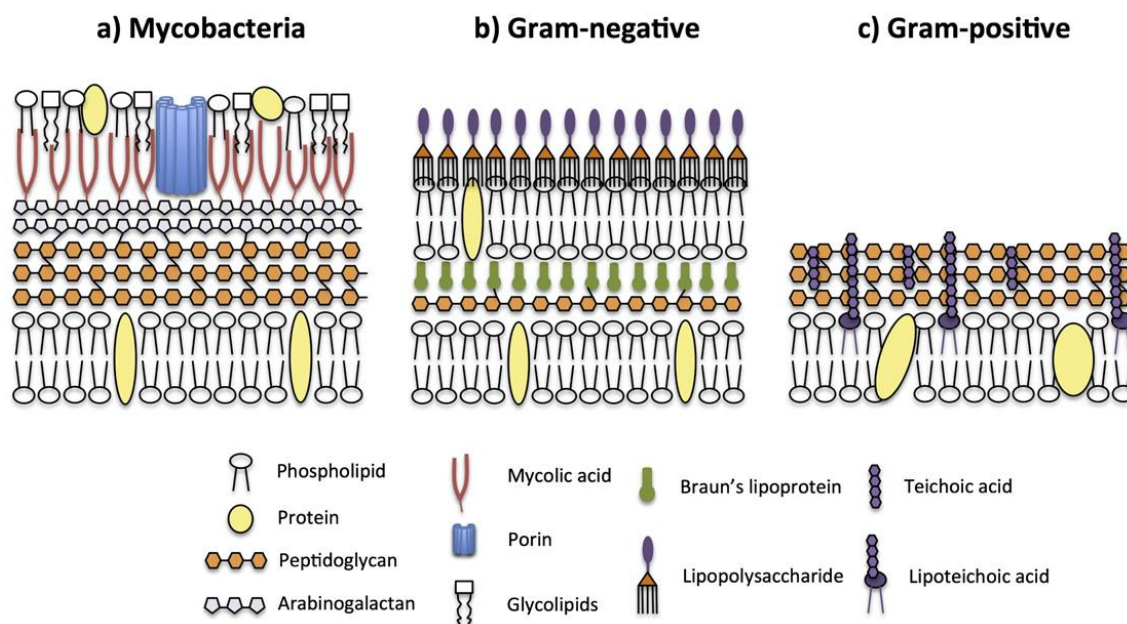


Figure 1.11 Comparison between cell envelopes of mycobacteria and other bacteria.¹⁵⁰

1.3.5 Summary

Natural peptides suffer from lack of bioavailability, low stability due to rapid protease degradation, difficulties during passage through the cell membrane and challenging multistep preparations, even though they provide high levels of biodiversity, biological activity, specificity and low toxicity in therapeutic uses. Peptidomimetics have evolved to bypass the limitations of native peptides in therapeutic use. Peptidomimetics can be evaluated by manipulations of the amino acid backbone of native peptides. Such manipulations enrich structural diversity and create novel peptidomimetics having defined secondary structures and pharmacological properties. In this chapter, we have outlined recent developments in peptidomimetics that were formed via hetero atom replacement or insertion into the amino acid backbone. Antimicrobial peptides are also described along with their possible modes of action and advantages over widely-used antibiotics.

1.3.6 Present work

The work described in this thesis illustrates the design and synthesis of different chemically modified peptides for their applications in DNA/RNA binding, antimicrobial action and cell penetration. It is described as per the following chapters:

Chapter 1: Introduction to Peptidomimetics

This chapter gives a background of literature and relevant studies that are important to the work carried out and described in this thesis. It deals with the application of peptidomimetic design in medicinal chemistry. The demand for peptides with improved stability profiles and pharmacokinetic properties is driving extensive research efforts in this field. Many structural modifications of peptides guided by rational design and molecular modeling have been established to develop novel synthetic approaches. Recent advances in the synthesis of conformationally restricted building blocks and peptide bond isosteres are discussed. The importance and advantages of synthetic antimicrobial peptides over conventional small molecule drugs are also elaborated.

Chapter 2: Tat peptide analogues : Synthesis and DNA, RNA interactions.

Section A: Modulation of Tat peptide-DNA interaction by arginine substitution in HIV-1 (48-57) Tat peptide.

This section deals with understanding the interactions of cationic peptides with possible target and off-target biomolecules, that can prove useful in the rational development of drugs. In this chapter, we have attempted to modulate the Tat(48-57) peptide- DNA interaction through arginine substitution by the arginine mimic, (2*S*,4*S*)-4-amino-N1-(3-guanidinopropyl)-proline (**r**). The Tat peptide mimics were found to possess enhanced protease resistance properties. Various biophysical techniques were used to investigate the effect of introduction of the non-natural arginine analogue into the Tat peptide. Tat peptide analogues effectively induced complete plasmid DNA condensation, which is important for gene transfection. Results from flow cytometry and confocal microscopy experiments proved that peptides can be successfully further explored as non-viral gene delivery vectors.

Section B: Superior HIV-1 TAR-Binders with Conformationally Constrained R52 Arginine Mimics in Tat (48-57) Peptide.

In this section we have reported modulation in binding affinity of the Tat(48-57) peptide analogues to HIV-1 TAR RNA by replacing R52, an essential and critical residue for Tat's specific binding, by the arginine mimics, (2*S*,4*S*)-4-guanidinoproline or (2*S*,4*S*)-4-amino-N-(3-guanidinopropyl)-proline. The resulting α Tat1M peptide containing (2*S*,4*S*)-4-guanidinoproline was found to be a far superior binder than γ Tat1M, a peptide containing another conformationally constrained arginine mimic, (2*S*,4*S*)-4-amino-N-(3-guanidinopropyl)-proline, or even the control Tat peptide itself. Several studies including CD, ITC, gel electrophoresis, UV spectroscopy and molecular dynamics simulations were carried out and suggest the compact nature of α Tat1M to be responsible for the increased interactions observed with TAR RNA for this peptide. The Tat mimetics further have better cell uptake properties in comparison to the control Tat peptide, thus increasing their application potential as specific TAR-binding molecules.

Chapter 3: (R-X-R)₄-motif peptides containing conformationally constrained cyclohexane-derived spacers: Effect on cellular uptake.

In this chapter we describe arginine-rich peptides having the (R-X-R)_n-motif, where X is replaced by constrained cyclic 1,4-cyclohexane-derived spacers. Here, several-fold increase in the cell penetrating abilities of such CPPs was observed, when the linear flexible spacer (-X-) in the (R-X-R) motif was replaced by conformationally constrained cyclohexanoic acid and cyclohexaneacetic acid. Internalization of these oligomers in mammalian cell lines was found to be an energy-dependent process. Incorporation of these constrained, non-proteinogenic amino acid spacers in the CPPs was also shown to enhance their proteolytic stability.

Chapter 4: Antibacterial and anti-TB Tat-peptidomimetics with improved efficacy and half-life.

In this chapter we have evaluated Tat peptide analogues as non-natural antimicrobial peptides, that are ideal as next generation antibiotics because of their ability to circumvent the problems of drug resistance and *in vivo* instability. We describe novel all- α - and α,γ -mixed Tat peptide analogues as potential antibacterial and anti-TB agents. These peptides have broad spectrum antibacterial activities against Gram-positive and Gram-negative bacteria and are also effective against active and dormant forms of *Mycobacterium tuberculosis*, including strains that are

resistant to rifampicin and isoniazid. The introduction of the non-natural amino acids of the study in the Tat peptide analogues results in increased resistance to degradation by proteolysis, significantly increasing their half-life. The peptides appear to inhibit bacteria by a membrane disruption mechanism, and have only a low cytotoxic effect on mammalian cells.

1.3.7 References

1. Antosova, Z.; Mackova, M.; Kral V.; Macek, T.; *Trends Biotechnol.*, **2009**, *27*, 628.
2. Ambrogelly, A.; Palioura, S.; Soll, D. *Nat. Chem. Biol.*, **2007**, *3*, 29-35.
3. Sakurai, T.; Amemiya, A.; Ishii, M.; Matsuzaki, I.; Chemelli, R. M.; Tanaka, H.; Williams, S. C.; Richardson, J. A.; Kozlowski, G. P.; Wilson, S.; Arch, J. R. S.; Buckingham, R. E.; Haynes, A. C.; Carr, S. A.; Annan, R. S.; McNulty, D. E.; Liu, W.; Terrett, J. A.; Elshourbagy, N. A.; Bergsma, D. J.; Yanagisawa, M.; *Cell*, **1998**, *924*, 573-585.
4. Liu, Y.; Lu, D.; Zhang, Y.; Li, S.; Liu, X.; Lin, H. *Gene*, **2010**, *463*, 21-28.
5. Harrison, S.; Geppetti, P. Substance P.; *Int. J. Biochem. Cell Biol.*, **2001**, *33*, 555-576.
6. Ling, N.; Burgus, R.; Guillemin, R.; *Proc. Natl. Acad. Sci. U.S.A.*, **1976**, *73*, 3942-3946.
7. Bole-Feysot, C.; Goffin, V.; Edery, M.; Binart, N.; Kelly, P. A.; *Endocr. Rev.*, **1998**, *19*, 225-268.
8. Nielsen, S.; Chou, C. L.; Marples, D.; Christensen, E. I.; Kishore, B. K.; Knepper, M. A.; *Proc. Natl. Acad. Sci. U.S.A.*, **1995**, *92*, 1013-1017.
9. Lee, H.; Macbeth, A. H.; Pagani, J. H.; Young 3rd, W. S.; *Prog. Neurobiol.* **2009**, *88*, 127-151.
10. Oršolić, N. *Cancer Metastasis Rev.*, **2012**, *31*, 173-194.
11. Whiteaker, P.; Christensen, S.; Yoshikami, D.; Dowell, C.; Watkins, M.; Gulyas, J.; Rivier, J.; Olivera, B. M.; McIntosh, J. M.; *Biochem.*, **2007**, *46*, 6628-6638.
12. Tamura, M.; Nakatsuka, T.; Tada, M.; Kawasaki, Y.; Kikuchi, E.; Okai, H.; *Agric. Biol. Chem.*, **1989**, *53*, 319-325.
13. Said, S.I., *Hypertension*, **1983**, *5*, 117.
14. Fischer, E.; Fourneau, E.; *Ber. dtsh. Chem. Ges.*, **1901**, *34*, 2868-2877.
15. Curtius, T.; *Ber. dtsh. Chem. Ges.*, **1902**, *35*, 3226-3228.
16. Fischer, E.; *Ber. dtsh. Chem. Ges.*, **1907**, *40*, 1754-1767.
17. Bergmann, M.; Zervas, L.; *Ber. dtsh. Chem. Ges. A/B*, **1932**, *65*, 1192-1201.

18. du Vigneaud, V.; Ressler, C.; Swan, C. J. M.; Roberts, C. W.; Katsoyannis, P. G.; Gordon, S.; *J. Am. Chem. Soc.*, **1953**, *75*, 4879-4880.
19. Khorana, H. G.; *Chem. Ind. (London, U. K.)*, **1955**, 1087-8.
20. Goodman, M.; McGahren, W. J.; *Tetrahedron*, **1967**, *23*, 2031-2050.
21. Carpino, L. A.; Imazumi, H.; El-Faham, A.; Ferrer, F. J.; Zhang, C.; Lee, Y.; Foxman, B. M.; Henklein, P.; Hanay, C.; Mügge, C.; Wenschuh, H.; Klose, J.; Beyermann, M.; Bienert, M.; *Angew. Chem. Int. Ed.*, **2002**, *41*, 441-445.
22. Abdelmoty, I.; Albericio, F.; Carpino, L. A.; Foxman, B. M.; Kates, S. A.; *Lett. Peptide Sci.*, **1994**, *1*, 57-67.
23. Castro, B.; Dormoy, J. R.; Evin, G.; Selve, C., *Tetrahedron Lett.*, **1975**, *16*, 1219-1222.
24. Coste, J.; Le-Nguyen, D.; Castro, B.; *Tetrahedron Lett.*, **1990**, *31*, 205-208.
25. Wuts, P. G. M.; Greene, T. W. In *Greene's protective groups in organic synthesis*; Wiley-Interscience: Hoboken, **2007**; pp 1082.
26. Anderson, G. W.; Callahan, F. M.; *J. Am. Chem. Soc.*, **1960**, *82*, 3359-3363.
27. Carpino, L. A.; *J. Am. Chem. Soc.*, **1957**, *79*, 4427-4431.
28. Applegate, H. E.; Cimarusti, C. M.; Dolfini, J. E.; Funke, P. T.; Koster, W. H.; Puar, M. S.; Slusarchyk, W. A.; Young, M. G. *J. Org. Chem.*; **1979**, *44*, 811-818.
29. Carpino, L. A.; Han, G. Y.; *J. Am. Chem. Soc.*, **1970**, *92*, 5748-5749.
30. Bodanszky, M.; *Int. J. Pept. Protein Res.*; **1984**, *23*, 111-111.
31. Merrifield, R. B.; *J. Am. Chem. Soc.*, **1963**, *85*, 2149-2154.
32. Merrifield, R. B.; *Science* **1965**, *150*, 178-185.
33. Bodanszky, M. In *Peptide synthesis*; Peptide Chemistry: A Practical Textbook; Springer Verlag: Berlin, **1988**; pp 55.
34. Erdélyi, M.; Gogoll, A.; *Synthesis*, **2002**, *2002*, 1592-1596.
35. Palasek, S. A.; Cox, Z. J.; Collins, J. M.; *J. Pept. Sci.*; **2007**, *13*, 143-148.
36. Pedersen, S. L.; Tofteng, A. P.; Malik, L.; Jensen, K. J.; *Chem. Soc. Rev.*, **2012**, *41*, 1826-1844.
37. Malik, L.; Tofteng, A. P.; Pedersen, S. L.; Sørensen, K. K.; Jensen, K. J.; *J. Pept. Sci.* **2010**, *16*, 506-512.
38. Stevenson, C. L.; *Curr. Pharm. Biotechnol.*; **2009**, *101*, 122-137.
39. Lemke, T. L.; Williams, D. A. In *Foye's principles of medicinal chemistry*; Wolters

Kluwer/Lippincott Williams & Wilkins: Philadelphia, **2008**, 1377.

40. Pauletti, G. M.; Gangwar, S.; Knipp, G. T.; Nerurkar, M. M.; Okumu, F. W.; Tamura, K.; Siahhaan, T. J.; Borchardt, R. T.; *J. Controlled Release*, **1996**, *41*, 3-17.

41. McMartin, C.; *Adv. Drug Res.*, **1992**, *22*, 39-106.

42. Sato, A. K.; Viswanathan, M.; Kent, R. B.; Wood, C. R.; *Curr. Opin. Biotechnol.*; **2006**, *17*, 638-642.

43. Vlieghe, P.; Lisowski, V.; Martinez, J. Khrestchatsky, M.; *Drug Discovery Today*, **2010**, *15*, 40.

44. Lambert, J. N.; Mitchell, J. P.; Roberts, K. D.; *J. Chem. Soc., Perkin Trans.*, **2001**, *1*, 471.

45. Giannis, A.; Ru'bsam, F.; Bernard, T.; Urs, A. M.; *Academic Press*, **1997**, *29*, 1.

46. Yoo, B.; Kirshenbaum, K.; *Curr. Opin. Chem. Biol.*, **2008**, *12*, 714.

47. Haskell-Luevano, C.; Toth, K.; Boteju, L.; Castrucci, C. A. M. d. L.; Hadley, M. E.; Hruby, V. J.; *J. Med. Chem.*, **1997**, *40*, 2740.

48. Sharma, G. V. M.; Babu, B. S.; Ramakrishna, K. V. S.; Nagendar, P.; Kunwar, A. C.; Schramm, P.; Baldauf, C.; Hofmann, H. J.; *Chem.–Eur. J.*, *2009*, *15*, 5552.

49. Su, T. H.; Yang, D.; Volkots, J.; Woolfrey, S.; Dam, P.; Wong, U.; Sinha, R. M.; Scarborough, B.; Zhu, Y.; *Bioorg. Med. Chem. Lett.*, **2003**, *13*, 729.

50. Ahn, J.-M.; Boyle, N. A.; MacDonald, M. T.; Janda, K. D.; *Mini-Rev. Med. Chem.*, **2002**, *2*, 463.

51. http://www.genome.gov/Images/EdKit/bio2b_large.gif

52. Bloomfield, V.A.; *Biopolymers*, **1997**, *44*, 269-282.

53. Lander, E. S.; Linton, L. M.; Birren, B.; Nusbaum, C.; Zody, M. C.; Baldwin, J.; Devon, K.; Dewar, K.; Doyle, M.; Fitzhugh, W.; *Nature*, **2001**, *409*, 860.

54. Itaka, K.; Kataoka, K.; *Eur. J. Pharm. Biopharm.*, **2009**, *71*, 475.

55. Gao, X.; Kim, K.-S.; Liu, D.; *AAPS J.*, **2007**, *9*, E92.

56. Gosule, L. C.; Schellman, J. A.; *J. Mol. Biol.*, **1978**, *121*, 311.

57. Est'avez-Torres, A.; Baigl, D.; *Soft Matter*, **2011**, *7*, 6746.

58. Martin, A.; Davies, M.; Rackstraw, B.; Roberts, C.; Stolnik, S.; Tendler, S.; Williams, P.; *FEBS Lett.*, **2000**, *480*, 106.

59. Itaka, K.; Kataoka, K.; *Eur. J. Pharm. Biopharm.*, **2009**, *71*, 475.

60. Lochmann, D.; Jauk, E.; Zimmer, A.; *Eur. J. Pharm. Biopharm.*, **2004**, *58*, 237.

61. Ganguli, M.; Babu, J. V.; Maiti, S.; *Langmuir*, **2004**, *20*, 5165.
62. Ginn, S. L.; Alexander, I. E.; Edelstein, M. L.; Abedi, M. R.; Wixon, J.; *J. Gene Med.*, **2013**, *15*, 65.
63. Zhou, T.; Llizo, A.; Wang, C.; Xu, G.; Yang, Y.; *Nanoscale*, **2013**, *5*, 8288.
64. Andersson, L.; Blomberg, L.; Flegel, M.; Lepsa, L.; Nilsson, B.; Verlander, M.; *Pept. Sci.*, **2000**, *55*, 227.
65. Houghten, R. A. *Proc. Natl. Acad. Sci. U. S. A.*, **1985**, *82*, 5131.
66. Hsiang, M. W.; Cole, R. D.; *Proc. Natl. Acad. Sci. U. S. A.*, **1977**, *74*, 4852.
67. Mann, A.; Richa, R.; Ganguli, M.; *J. Controlled Release*, **2008**, *125*, 252.
68. Plank, C.; Tang, M. X.; Wolfe, A. R.; Szoka, F. C.; *Hum. Gene Ther.*, **1999**, *10*, 319.
69. Rimann, M.; Luhmann, T.; Textor, M.; Guerino, B.; Ogier, J.; Hall, H.; *Bioconjugate Chem.*, **2008**, *19*, 548.
70. Martin, M.; Rice, K.; *AAPS J.*, **2007**, *9*, E18.
71. Mann, A.; Thakur, G.; Shukla, V.; Singh, A. K.; Khanduri, R.; Naik, R.; Jiang, Y.; Kalra, N.; Dwarakanath, B.; Langel, U.; *Mol. Pharmaceutics*, **2011**, *8*, 1729.
72. Wyman, T. B.; Nicol, F.; Zelphati, O.; Scaria, P. V.; Plank, C.; Szoka, F. C.; *Biochemistry*, **1997**, *36*, 3008.
73. Wang, Y.; Mangipudi, S. S.; Canine, B. F.; Hate, A.; *J. Controlled Release*, **2009**, *137*, 46.
74. (a) Schroeder, R.; Barta, A.; Semrad, K.; *Nat. Rev. Mol. Cell Biol.*, **2004**, *5*, 908–919; (b) Zaman, G. J. R.; Michiels, P. J. A.; van Boeckel, C. A. A.; *Drug Discovery Today*, **2003**, *8*, 297–306.
75. (a) Hermann, T.; *Curr. Opin. Struct. Biol.*, **2005**, *15*, 355–366; (b) Carter, A. P.; Clemons, W. M.; Brodersen, D. E.; Morgan-Warren, R. J.; Wimberly, B. T.; Ramakrishnan, V.; *Nature*, **2000**, *407*, 340–348.
76. Davidson, B. L.; McCray, P. B. Jr.; *Nat. Rev. Genet.*, **2011**, *12*, 329–340.
77. Lu, J.; Kadakkuzha, B. M.; Zhao, L. M.; X. Qi. Fan.; Xia, T.; *Biochemistry*, **2011**, *50*, 5042–5057.
78. (a) Seedhouse, S. J.; Labuda, L. P.; Disney, M. D.; *Bioorg. Med. Chem. Lett.*, **2010**, *20*, 1338–1343.
79. (a) Galicia-Vazquez, G.; Lindqvist, L.; Wang, X.; Harvey, I.; Liu J.; *J. Anal. Biochem.*, **2009**, *384*, 180–188.

80. (a) Lee, S. J.; Hyun, S.; Kieft, J. S.; Yu, J.; *J. Am. Chem. Soc.*, **2009**, *131*, 2224–2230; (b) Hyun, S.; Na, J.; Lee, S. J.; Park, S.; Yu, J.; *ChemBioChem*, **2010**, *11*, 767–770.
81. (a) Guan, L.; Disney, M. D.; *ACS Chem. Biol.*, **2011**, *7*, 73–86; (b) Sobczak, K.; Michlewski, G.; de Mezer, M.; Kierzek, E.; Krol, J.; Olejniczak, M.; Kierzek, R.; Krzyzosiak, W. J.; *J. Biol. Chem.*, **2010**, *285*, 12755–12764; (c) Rzuczek, S. G.; Gao, Y.; Tang, Z.-Z.; Thornton, C. A.; Kodadek, T.; Disney, M. D.; *ACS Chem. Biol.*, **2013**, *8*, 2312–2321.
82. Williamson, J.R.; *Nat Struct Biol.*; **2000**, *7*, 834–837.
83. Caprara, M.G.; Nilsen, T.W.; *Nat Struct Biol.*; **2000**, *7*, 831–833.
84. Derose, V.J.; *Chem. Biol.* **2002**, *9*, 961–969.
85. Klug, A.; *J Mol Biol.*; **1999**, *293*, 215–218.
86. White, S.; Szewczyk, J.W.; Turner, J.M.; Baird, E.E.; Dervan, P.B.; *Nature*, **1998**, *391*, 468.
87. Choudhury, I.; Wang, J.; Rabson, A. B.; Stein, S.; Pooyan, S.; Stein, S.; Leibowitz, M. J.; *J. Acquir. Immune Defic. Syndr. Hum. Retrovirol.*, **1998**, *17*, 104–111.
88. Hamy, F.; Felder, E. R.; Heizmann, G.; Lazdins, J.; Aboul-ela, F.; Varani, G.; Karn, J.; Klimkait, T.; *PNAS*, **1997**, *94*, 8, 3548–3553.
89. Friedler, F. D.; Luedtke, A, N.; Tor, W. Y.; Loyter, A.; Gilon, C.; *J. Biol. Chem.*, **2000**, *275*, 23783–23789.
90. Davidson, A.; Leeper, T. C.; Athanassiou, Z.; Patora-Komisarska, K.; Karn, J.; Robinson, J. A.; Varani, G.; *Proc. Natl. Acad. Sci. U. S. A.*, **2009**, *106*, 11931–11936.
91. M. S. Lalonde, M. A. Lobritz, A. Ratcliff, M. Chamanian, Z. Athanassiou, M. Tyagi, J. Wong, J. A. Robinson, J. Karn, Varani, G.; E. Arts, J.; *PLoS Pathog.*, **2011**, *7*, e1002038.
92. Frankel, A. D.; Pabo, C. O.; *Cell*, **1988**, *55*, 1189–1193.
93. Green, M.; Loewenstein, P. M.; *Cell*, 1988, *55*, 1179–1188.
94. Derossi, D.; Joliot, A. H.; Chassaing, G.; Prochiantz, A. *J. Biol. Chem.* **1994**, *269*, 10444–10450.
95. Langel, Ü. *Cell-Penetrating Peptides: Methods and Protocols*; Springer-Verlag GmbH: New York, **2011**.
96. Heitz, F.; Morris, M. C.; Divita, G.; *J. Pharmacol.* **2009**, *157*, 195–206.
97. Copolovici, D.M.; Langel, K.; Eriste, E.; Langel, U.L.; *ACS Nano*, **2014**, *8*, 1972–1994.
98. Akdag, I. O.; Ozkirimli, E.; *Journal of Chemistry*, **2013**, *2013*, 9.
99. (a) Sanders, W. S.; Johnston, C. I.; Bridges, S. M.; Burgess, S. C.; Willeford, K. O.; *PLoS*

- Comput Biol*, **2011**, 7, e1002101. (b) Gautam, A.; Chaudhary, K.; Kumar, R.; Sharma, A.; Kapoor, P.; Tyagi, A.; Raghava, G.; *Journal of Translational Medicine*, **2013**, 11, 74.
100. Tang, H.; Yin, L.; Kim, K.H.; Cheng, J.; *Chem. Sci.*, **2013**, 4, 3839.
101. Yadav, A. K.; Dey, N.; Chattopadhyay, S.; Ganguli, M.; Fernandes, M.; *Org. Biomol. Chem.*, **2017**, 15, 9579.
102. Abes, S.; Moulton, H. M.; Clair, P.; Prevot, P.; Youngblood, D. S.; Wu, R. P.; Iversen, P. L.; Lebleu, B.; *Journal of Controlled Release*, **2006**, 116, 304-313.
103. Nakase, I.; Akita, H.; Kogure, K.; Gräslund, A.; Langel, Ü.; Harashima, H.; Futaki, S.; *Accounts of Chemical Research*, **2011**, 45, 1132-1139.
104. Fittipaldi, A.; Ferrari, A.; Zoppé, M.; Arcangeli, C.; Pellegrini, V.; Beltram, F.; Giacca, M.; *Journal of Biological Chemistry*, **2003**, 278, 34141-34149.
105. (a) Wadia, J.; Stan, R.; Dowdy, S.; *Nature Medicine*, **2004**, 10, 310-315. (b) Kaplan, I.; Wadia, J.; Dowdy, S.; *Journal of Controlled Release*, **2005**, 102, 247-253.
106. Richard, J. P.; Melikov, K.; Brooks, H.; Prevot, P.; Lebleu, B.; Chernomordik, L. V.; *Journal of Biological Chemistry*, **2005**, 280, 15300-15306.
107. Fittipaldi, A.; Ferrari, A.; Zoppé, M.; Arcangeli, C.; Pellegrini, V.; Beltram, F.; Giacca, M.; *Journal of Biological Chemistry*, **2003**, 278, 34141-34149.
108. (a) Conner, S.; Schmid, S.; *Nature*, **2003**, 422, 37-44. (b) Mayor, S.; Pagano, R.; *Nature reviews. Molecular Cell Biology*, **2007**, 8, 603-612.
109. Sara, T.; Ana Luísa, C.; Miguel, M.; Maria, C. P. d. L.; *Pharmaceuticals*, **2010**, 3.
110. Derossi, D.; Joliot, A.; Chassaing, G.; Prochiantz, A. *The Journal of Biological Chemistry* **1994**, 269, 10444-10450.
111. Matsuzaki, K.; Yoneyama, S.; Murase, O.; Miyajima, K.; *Biochemistry*, **1996**, 35, 8450-8456.
112. Pouny, Y.; Rapaport, D.; Mor, A.; Nicolas, P.; Shai, Y.; *Biochemistry*, **1992**, 31, 12416-12423.
113. Lee, M.-T.; Hung, W.-C.; Chen, F.-Y.; Huang, H. W.; *Biophysical Journal*, **2005**, 89, 4006-4016.
114. (a) Lundberg, M.; Johansson, M.; *Nature Biotechnology*, **2001** 19, 713-4. (b) Richard, J. P.; Melikov, K.; Vives, E.; Ramos, C.; Verbeure, B.; Gait, M. J.; Chernomordik, L. V.; Lebleu, B.; *Journal of Biological Chemistry*, **2003**, 278, 585-590.

115. (a) Tyagi, M.; Rusnati, M.; Presta, M.; Giacca, M.; *Journal of Biological Chemistry*, **2001**, *276*, 3254-3261. (b) Nakase, I.; Tadokoro, A.; Kawabata, N.; Takeuchi, T.; Katoh, H.; Hiramoto, K.; Negishi, M.; Nomizu, M.; Sugiura, Y.; Futaki, S.; *Biochemistry*, **2006**, *46*, 492-501.
116. Mueller, J.; Kretschmar, I.; Volkmer, R.; Boisguerin, P.; *Bioconjugate Chemistry*, **2008**, *19*, 2363-2374.
117. Morris, M.; Vidal, P.; Chaloin, L.; Heitz, F.; Divita, G.; *Nucleic Acids Research*, **1997**, *25*, 2730-2736.
118. (a) Lundin, P.; Johansson, H.; Guterstam, P.; Holm, T.; Hansen, M.; Langel, U.; El Andaloussi, S.; *Bioconjugate Chemistry*, **2008**, *19*, 2535-2542. (b) Vives, E.; *Journal of Controlled Release*, **2005**, *109*, 77-85.
119. (a) Nakase, I.; Tadokoro, A.; Kawabata, N.; Takeuchi, T.; Katoh, H.; Hiramoto, K.; Negishi, M.; Nomizu, M.; Sugiura, Y.; Futaki, S.; *Biochemistry*, **2007**, *46*, 492-501. (b) Ziegler, A.; Seelig, J.; *Biophysical Journal*, **2008**, *94*, 2142-2149.
120. (a) Nakamura, Y.; Kogure, K.; Futaki, S.; Harashima, H. *Journal of Controlled Release* **2007**, *119*, 360-367. (b) Eguchi, A.; Meade, B.; Chang, Y.-C.; Fredrickson, C.; Willert, K.; Puri, N.; Dowdy, S. *Nature biotechnology* **2009**, *27*, 567-571. (c) Tönges, L.; Lingor, P.; Egle, R.; Dietz, G.; Fahr, A.; Bähr, M. *RNA (New York, N.Y.)* **2006**, *12*, 1431-1438.
121. Mitchell, D. J.; Steinman, L.; Kim, D. T.; Fathman, C. G.; Rothbard, J. B.; *The Journal of Peptide Research*, **2000**, *56*, 318-325.
122. Rothbard, J. B.; Jessop, T. C.; Lewis, R. S.; Murray, B. A.; Wender, P. A.; *Journal of the American Chemical Society*, **2004**, *126*, 9506-9507.
123. Xilu, W.; Ikramul, H.; Tariq, M. R.; *Journal of the American Chemical Society*, **1997**, *119*.
124. Chiu, Y.-L.; Ali, A.; Chu, C.-Y.; Cao, H.; Rana, T.; *Chemistry & Biology*, **2004**, *11*, 1165-1175.
125. Wender, P. A.; Rothbard, J. B.; Jessop, T. C.; Kreider, E. L.; Wylie, B. L.; *Journal of the American Chemical Society*, **2002**, *124*, 13382-13383.
126. Cooley, C.; Trantow, B.; Nederberg, F.; Kiesewetter, M.; Hedrick, J.; Waymouth, R.; Wender, P.; *Journal of the American Chemical Society*, **2009**, *131*, 16401-16403.
127. Ma, Y.; Yang, D.; Ma, Y.; Zhang, Y.-H.; *ChemBiochem*, **2012**, *13*, 73-79.
128. Murphy, J. E.; Uno, T.; Hamer, J. D.; Cohen, F. E.; Dwarki, V.; Zuckermann, R. N.; *Proceedings of the National Academy of Sciences*, **1998**, *95*, 1517-1522.

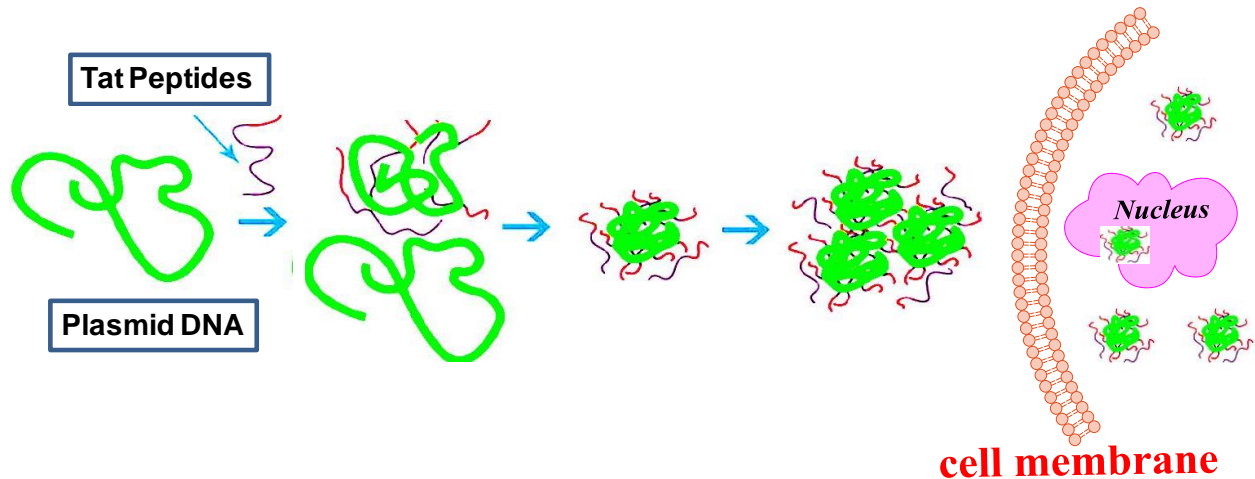
129. Wender, P.; Mitchell, D.; Pattabiraman, K.; Pelkey, E.; Steinman, L.; Rothbard, J.; *Proceedings of the National Academy of Sciences of the United States of America*, **2000**, *97*, 13003-13008.
130. Schröder, T.; Niemeier, N.; Afonin, S.; Ulrich, A. S.; Krug, H. F.; Bräse, S.; *Journal of Medicinal Chemistry*, **2008**, *51*, 376-379.
131. Klevens, M.; Morrison, M.; Nadle, J.; Petit, S.; Gershman, K.; Ray, S.; Harrison, L.; Lynfield, R.; Dumyati, G.; Townes, J.; Craig, A.; Zell, E.; Fosheim, G.; McDougal, L.; Carey, R.; Fridkin, S.; *JAMA*, *2007*, *298*, 15,1763-1771.
132. Chien, J.W.; Kucia, M.L.; Salata, R.A.; *Clin Infect Dis*, **2000**, *30*,1,146-151.
133. Walsh, C.; *Nature*, **2000**,*406*, 6797, 775-781.
134. Falla, T.; Karunaratne, D.; Hancock, R.; *J. Biol. Chem.*, **1996**, *271*, 32, 19298-19303.
135. Ganz, T.; Selsted, M.; Szklarek, D.; Harwig, S.; Daher, K.; Bainton, D.; Lehrer, R.; *J. Clin. Invest.*, **1985**, *76*, 4,1427-1435.
136. Gazit, E.; Boman, A.; Boman, H.G.; Shai, Y.; *Biochemistry*, **1995**, *34*, 11479-11488.
137. He, K.; Ludtke, S.; Heller, W.; Huang, H.; *Biophys J*, **1996**, *71*, 5, 2669-2679.
138. Saint, N.; *Peptides*, **2003**, *24*, 11, 1779-1784.
139. Ludtke, S.; He, K.; Heller, W.; Harroun, T.; Yang, L.; Huang, H.; *Biochemistry*, **1996**, *35*,43,13723-13728.
140. Hong, R.W.; Shchepetov, M.; Weiser, J.N.; Axelsen, P.H.; *Antimicrob Agents Chemother*, **2003**, *47*, 1, 1-6.
141. Subbalakshmi, C.; Sitaram, N.; *FEMS Microbiol Lett.*; **1998**, *160*, 1, 91-96.
142. Kragol, G.; Lovas, S.; Varadi, G.; Condie, B.A.; Hoffmann, R.; Otvos, L.; *Biochemistry* **2001**, *40*, 10, 3016-3026.
143. Breukink, E.; *Science*, **1999**, *286*, 5448, 2361-2364.
144. Jiang, Z.; Vasil, A.I.; Hale, J.D.; Hancock, R.E.W.; Vasil, M.L.; Hodges, R.S.; *Biopolymers*, **2008**, *90*, 3, 369-383.
145. Jin, Y.; Hammer, J.; Pate, M.; Zhang, Y.; Zhu, F.; Zmuda, E.; Blazyk, J.; *Antimicrob Agents Chemother*, **2005**, *49*, 12, 4957-4964.
146. Chen, Y.; Guarnieri, M.T.; Vasil, A.I.; Vasil, M.L.; Mant, C.T.; Hodges, R.S.; *Antimicrob Agents Chemother*, **2007**, *51*, 4, 1398-1406.
147. Braun, P.; Radin, N.; *Biochemistr*, **1969**, *8*, 11, 4310-4318.

148. Hantke, K.; Braun, V.; *European Journal of Biochemistry*, **1973**, *34*, 2, 284-296.
149. Straus, S.; Hancock, R.; *Biochimica et Biophysica Acta (BBA) – Biomembranes*, **2006**, *1758*, 9, 1215-1223.
150. Silva, J.P.; Appelberg, R.; Gama, F.M.; *Biotechnology Advances*, **2016**, *34*, 924–940.

CHAPTER 2

SECTION A

Modulation of Tat peptide-DNA interaction by arginine substitution in HIV-1 Tat (48-57) peptide



Understanding the interactions of cationic peptides with possible target and off-target biomolecules, that can prove useful in the rational development of drugs. In this chapter, we have attempted to modulate the Tat peptide- DNA interaction through arginine substitution by non-proteogenic, conformationally constrained arginine mimics in HIV-1 Tat(48-57) peptide. The mimics were found to enhance the protease resistance properties of the derived peptides. Various biophysical techniques were used to investigate the effect of introduction of non-natural arginine analogue into the Tat peptide. Tat peptide analogues effectively induced complete plasmid DNA condensation, which is important for gene transfection. Results from flow cytometry and confocal microscopy experiments proved that peptides can be successfully further explored as non-viral gene delivery vectors.

2A.1 Introduction

The safe and efficient delivery of foreign DNA into cells is the biggest hurdle in gene therapy. Delivery of naked gene molecules is a difficult task because of problems related to enzymatic degradation, site specificity and poor cellular uptake.¹ Efficient gene delivery vehicles have to fulfill some essential requirements such as highly stable transport of DNA, protection from nucleases, cell penetrating abilities, high and steady expression of the therapeutic DNA, low cellular toxicity,^{2,3} etc. Along with these properties gene delivery vehicles should force the extended DNA molecules into compact, ordered arrangements. Among the available DNA-condensing tools, cationic peptides are attractive. Cationic peptides and other basic polymers having overall positive charge interact with the phosphate backbone of DNA which is negatively charged by electrostatic interactions.⁴ Cationic and basic peptides as well as polymer-based vehicles are known to enhance the condensation of DNA to small particles. DNA-condensing peptides also prevent DNA from being degraded by cytosolic nucleases.⁵ Cationic lipids can also act as effective DNA delivering agents in vitro but their in vivo applications are limited by the presence of serum.⁶ Attempts to use the long poly-L-lysines (100–190 residues) commonly used as DNA-binding or condensing moieties showed these to be toxic.⁷ The ability of polyamido amine (PAMAM) dendrimers to condense DNA and penetrate cell membranes gives them great potential in gene therapy and drug delivery but their high positive surface charge makes them cytotoxic.⁸

The basic region of HIV-1 Tat (Transactivation of transcription) peptide contains several lysines and arginines in its sequence, and acts as both, a DNA-condensing- and potent membrane-active peptide, that improves the intracellular delivery of its complex with DNA.⁹ The positively charged lysine and arginine residues bind electrostatically to plasmid DNA, leading to internalisation into cells through an endocytosis-mediated mechanism.¹⁰ POLYTAT, a high molecular weight form of Tat, was shown to exhibit a reversible affinity for DNA, allowing controlled DNA release, endosomal escape and improving gene expression. The high-molecular weight of the POLYTAT improved the transfection efficiencies compared to the control Tat peptides by increasing binding to cell membrane, and reduced the particle size due to its improved ability to condense DNA.¹¹

Thus the successful use of peptide-DNA complexes for gene delivery still remains a challenge. In order to address this challenge detailed studies of peptide-DNA complexes are essential.

2A.2 Rationale, design and objectives of the present work

As the natural Tat(48-57) peptide sequence is rich in positively charged lysine and arginine residues, it is very susceptible to enzymatic degradation.¹² As shown in Figure 2A.1, the arginine and lysine residues are cleavage sites for a majority of proteases. The replacement of these residues by non-natural mimetics could lead to resistance from proteases. We envisaged an arginine mimic (r, Figure 2A.2) derived from proline and anticipated that replacement of arginine in the Tat(48-57) peptide by this mimic could lead to enhanced protease resistance and could also influence the conformation of the resulting Tat peptide, thus influencing its binding to DNA. The possibility of the pyrrolidine ring nitrogen being protonated, in addition to the guanidine group, would increase the electrostatic interactions with the negatively charged DNA.

Proteolytic degradation map of Tat protein		
Enzyme	No. of Cleavages	Positions of cleavage sites
Arg-C-Proteinase	6	48, 51, 52, 54, 55, 56
Chymotrypsin	1	46
Clostripain	6	48, 51, 52, 54, 55, 56
LysC	2	49, 50
LysN	2	48, 49
Pepsin	2	45, 46
Proteinase K	1	46
Trypsin	7	49, 50, 51, 52, 55, 56, 57

Natural Tat peptide
Gly-Arg-Lys-Lys-Arg-Arg-Gln-Arg-Arg-Arg
48 49 50 51 52 53 54 55 56 57

Figure 2A.1 Proteolytic degradation pattern of Tat (48-57) peptide¹²

2A.3 Work done

In this section, the synthesis of (2S,4S)-4-amino-N-(3-guanidinopropyl)proline (r) and its incorporation into the Tat(48-57) peptide (GRKKRRQRRR) at predefined positions is described. The positions of arginine replacement were defined by considering the proteolytic degradation susceptible sites in Tat peptide. The resultant Tat peptide oligomers were evaluated for their

ability to bind with DNA by using UV-melting studies and agarose gel electrophoresis. Circular dichroism studies of peptide:DNA complexes were done to see the effect of peptide binding on the overall structure of DNA. The cell penetrating ability of the Tat peptide analogues was evaluated by flow cytometry and confocal microscopy. The cell viability of the Tat peptide analogues was evaluated by the hemolysis and MTT cell viability assays. The effect of introduction of unnatural amino acid on its enzymatic stability was studied with the help of RP-HPLC.

2A.4 Results and Discussion

2A.4.1 Synthesis of amino acid surrogate **X**, precursor to amino acid **r**

Our laboratory has earlier reported the use of *N*-(aminoalkyl)proline-derived compounds towards the synthesis of peptide nucleic acids,¹⁴ cell-penetrating oligomers¹⁵ and as anti-glycation agents.¹⁶ The amino acid surrogate, (2*S*,4*S*)-4-amino-*N*1-(3-guanidinopropyl)-proline (**r**), was derived from (2*S*,4*R*)-4-hydroxyproline through the orthogonally protected precursors **X** (Figure 2A.2). The incorporation of precursor **X** in combination with α -amino acids during peptide synthesis leads to α,γ -peptides containing the residue **r**.

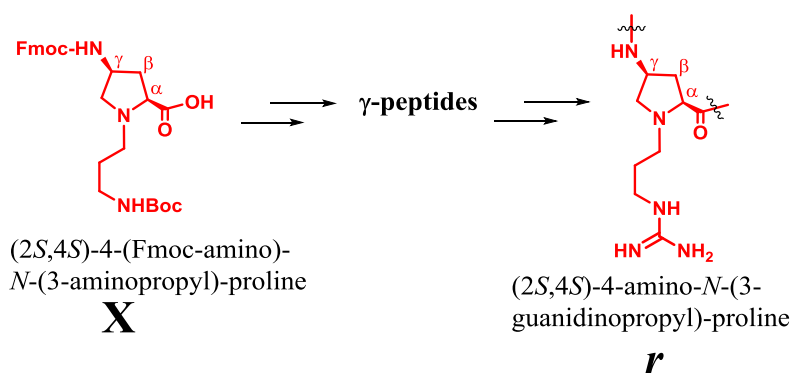
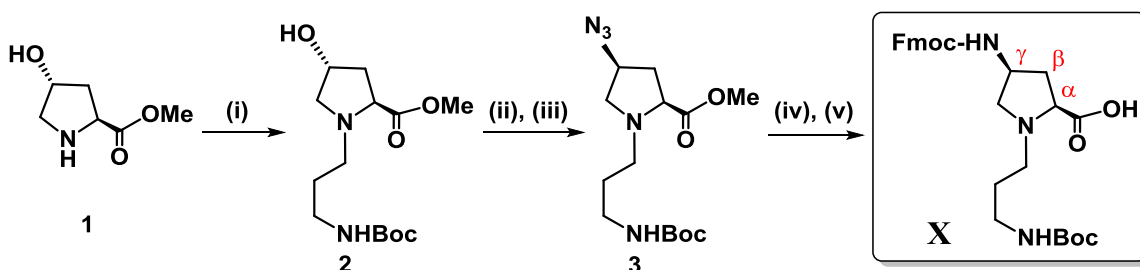


Figure 2A.2. Amino acid surrogate- **r** of the study.

Scheme 2A.1 summarises the synthesis of protected non-natural amino acid **X**. The monomer was synthesized from commercially available *trans*-L-4-hydroxyproline. The hydroxyproline methyl ester **1** was *N*-alkylated upon reaction with 3-((*tert*-butyloxycarbonyl)amino)propyl methylsulfonate in the presence of triethylamine and catalytic amount of DMAP in DMF.³⁸ The 4-hydroxyl group in compound **2** was then converted to the azide **3** by mesylation, followed by

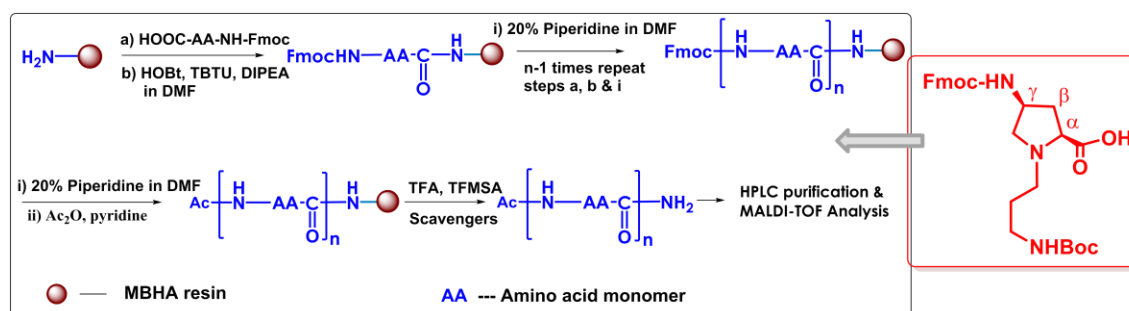
S_N2 displacement of the 4-*O*-mesyl group using NaN_3 in DMF. Catalytic hydrogenation of the azide group in **3** to the amine, followed by hydrolysis of the ester function and subsequent protection of the free amine using Fmoc-Cl and NaHCO_3 in dioxane: H_2O (1:1) yielded orthogonally protected non-natural amino acid **X**. (Scheme 2A.1).



Scheme 2A.1. Synthesis of orthogonally protected non-natural amino acid **X**. Reagents and conditions: (i) $\text{MsO}-(\text{CH}_2)_3\text{-NH-Boc}$, Et_3N , DMAP, DMF, 70°C , 62 % (ii) MsCl , Et_3N , CH_2Cl_2 , 73% (iii) NaN_3 , DMF, 65°C , 67 % (iv) (a) H_2 , Pd/C, MeOH, (b) LiOH, then HCl, 62 % for (a) and (b) (v) (a) Fmoc-Cl, NaHCO_3 , H_2O -dioxane, (b) Dowex H^+ resin, 58 % for (a) and (b).

2A.4.2 Synthesis of Tat peptide oligomers

The orthogonally protected monomer **X** described above was utilized in the solid phase synthesis of the peptides, along with other standard protected amino acids. The peptides were assembled on MBHA resin by Fmoc-chemistry protocols, as required (Scheme 2A.2). β -Alanine was coupled as the first spacer amino acid, followed by the coupling of other amino acids. All the coupling steps were done in dry DMF in presence of DIPEA, with HOBt and TBTU as coupling agents. Removal of the Boc-protecting group was achieved using 50% TFA in CH_2Cl_2 , while the Fmoc group was deprotected by using 20% piperidine in DMF. A phenylalanine residue was added at the N-termini of the peptides in order to facilitate concentration calculation from the absorbance. Guanidinylation of monomers **X** to arginine surrogates **r** was performed on the solid support after *N*-acetylation of the phenylalanine residue at *N*-terminus, and deprotection of the appropriate amino group, using 1*H*-pyrazole-1-carboxamide hydrochloride and DIPEA in dry DMF. The peptides are listed in Table 2A.1, and their chemical structures are illustrated in Figure 2A.3.



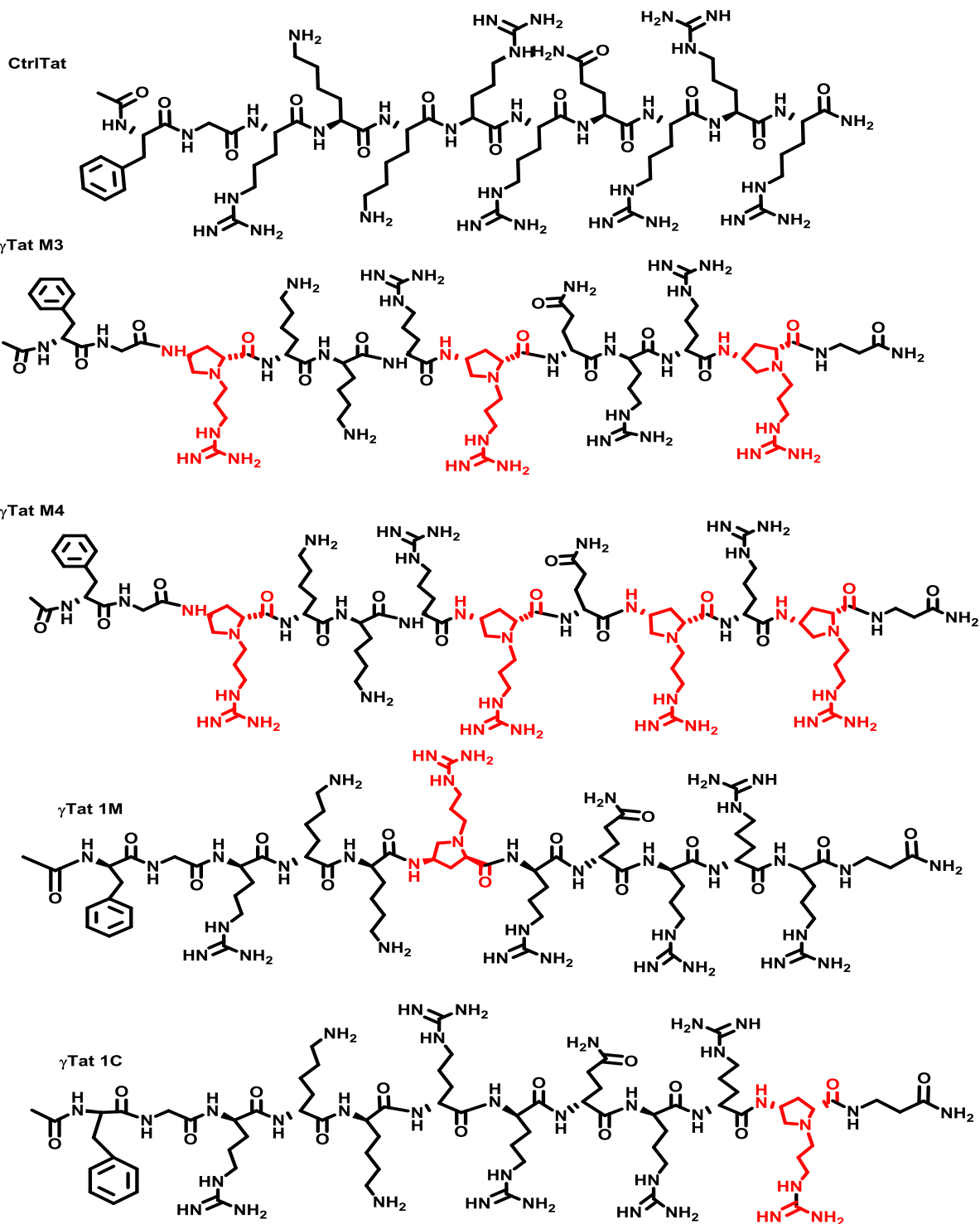
Scheme 2A.2 Schematic representation of solid phase peptide synthesis by Fmoc chemistry protocol

Table 2A.1 Oligomers of the study.

Sr. No.	Peptide name	No. of positive charges	Peptide Composition ^[a]	Mass (MALDI-TOF)	
				Calcd.	Obsd.
1	γTatM3	11	$\text{Ac-FGrKKRrQRRr-}\beta\text{Ala-NH}_2$	1821.23	1827.17
2	γTatM4	12	$\text{Ac-FGrKKRrQrRr-}\beta\text{Ala-NH}_2$	1876.31	1877.27
3	γTat1M	9	$\text{Ac-FGRKKrRQRRR-}\beta\text{Ala-NH}_2$	1710.06	1709.99
4	γTat1C	9	$\text{Ac-FGRKKRRQRRr-}\beta\text{Ala-NH}_2$	1711.07	1711.14
5	CtrlTat	8	$\text{Ac-FGRKKRRQRRR-NH}_2$	1583.98	1586.74
6	$\gamma\text{TatM3-cf}$	11	$\text{cf-GrKKRrQRRr-}\beta\text{Ala-NH}_2$	1991.13	1991.82
7	$\gamma\text{TatM4-cf}$	12	$\text{cf-GrKKRrQrRr-}\beta\text{Ala-NH}_2$	2046.17	2047.09
8	$\gamma\text{Tat1M-cf}$	9	$\text{cf-GRKKrRQRRR-}\beta\text{Ala-NH}_2$	1881.05	1881.43
9	$\gamma\text{Tat1C-cf}$	9	$\text{cf-GRKKRRQRRr-}\beta\text{Ala-NH}_2$	1881.05	1880.26
10	CtrlTat-cf	8	$\text{cf-GRKKRRQRRR-NH}_2$	1754.97	1756.00

^[a] *cf* = 5(6)-carboxyfluorescein; *r* = (2S,4S)-4-amino-N1-(3-guanidinopropyl)-proline; *Ac* = acetate; βAla = β -alanine.

The peptides thus contain *r* units at pre-defined positions (Table 2A.1). The peptide γTatM3 contains three *r* units that replace arginines at R49, R53 and R57 (Figure 2A.1) while γTatM4 contains four *r* units that replace arginines at positions R49, R53, R55 and R57. The γTat1M and γTat1C consist of one *r* unit each to replace R52 and R57 respectively. A control Tat peptide (CtrlTat) was also synthesized for comparison (Table 2A.1, entry 5). For cell uptake studies, the peptides were tagged with fluorescein at their N-termini by treating them with 5/6-carboxyfluorescein in the presence of HOBt and diisopropyl carbodiimide (DIPCDI) as coupling agents. This yielded fluorescein-tagged peptides Ctrl-*cf*, $\gamma\text{TatM3-cf}$, $\gamma\text{TatM4-cf}$, $\gamma\text{Tat1M-cf}$, $\gamma\text{Tat1C-cf}$ (Table 2A.1, entries 6-10).



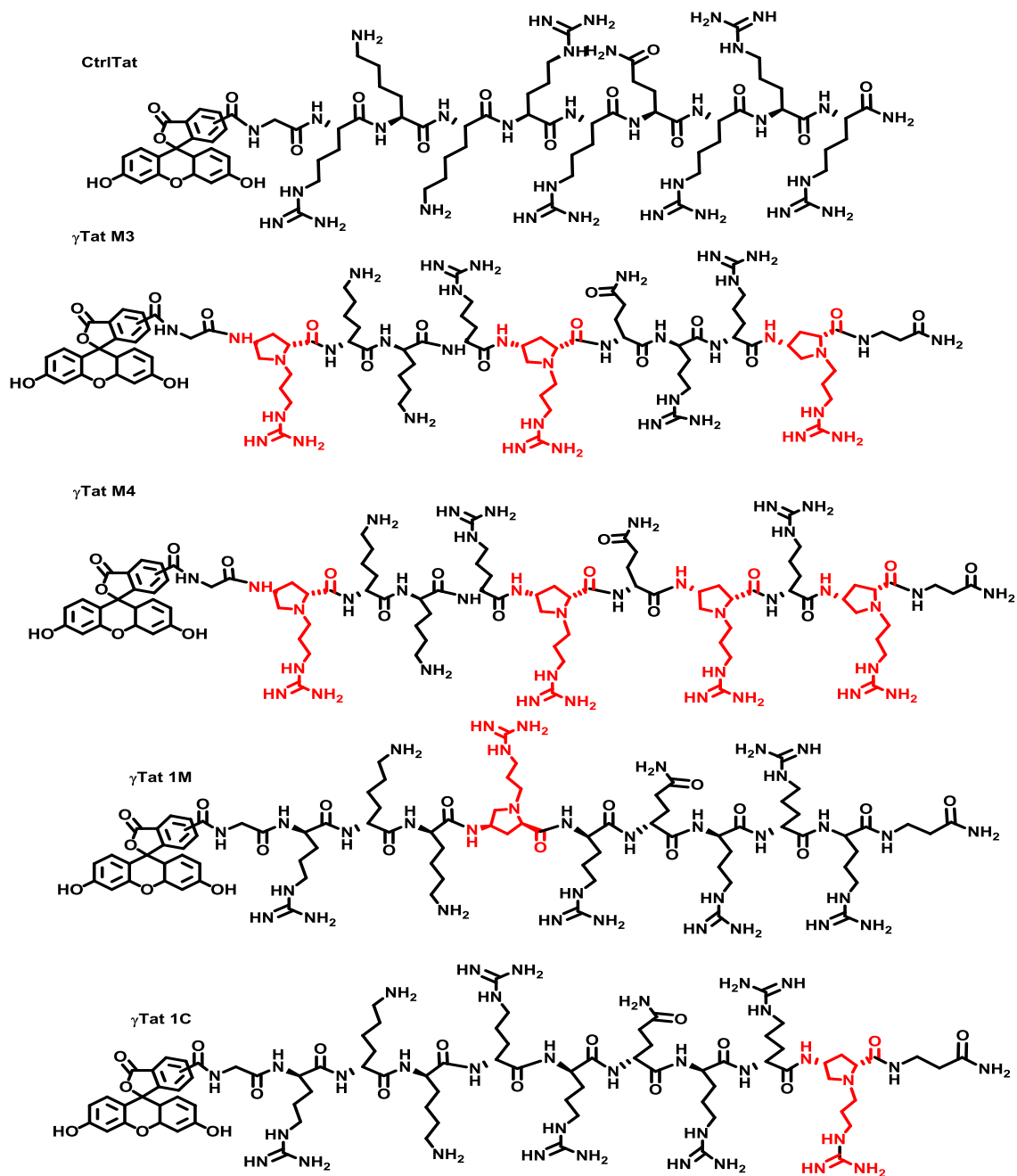


Figure 2A.3. Chemical structures of Tat peptide analogues.

The synthesized peptides were cleaved from the resin by the TFA-TFMSA cleavage protocol to yield C-terminal amides, while the N-terminals were either capped as acetates or labelled with carboxyfluorescein. All the peptides were purified by RP-HPLC on a C18 column, and their purity was re-checked by analytical HPLC. They were characterized by MALDI-TOF analysis; the data are listed in Table 2A.1.

2A.3.3 UV-Melting Studies

UV melting studies have been widely used for characterization of DNA - peptide complexations in the literature, as they can directly predict the stability of DNA-peptide complexes. The sum of the absorbance of the individual nucleotide and the effect of the interaction between the nucleotides gives total absorbance of polynucleotide. Due to the effect of the interaction between the nucleotides the absorbance of single strand is less than the sum of absorbance of its nucleotides and absorbance of double strand is less than that of absorbance of two individual single strands. This decrease in absorbance of polynucleotide due to coupling of transition dipoles of adjacent nucleotides is called as hypochromicity, whereas, hyperchromicity results in increase in absorption when a double-stranded nucleic acid is converted into single strands. This transition from double helix to single strand is associated with strong entropic component. This component is temperature-dependent. The temperature at which 50% of this transition occurs is known as the melting temperature (T_m). Such a thermal dissociation of nucleic acid helices in solution to give single-stranded DNA/RNA is a function of base composition, sequence, chain length as well as of temperature, salt concentration, and pH of the buffer. A graph of absorbance against temperature gives a standard sigmoidal curve in case of duplexes and at the midpoint of the sigmoidal curve the duplex and the single strands exist in equal proportions.

When a peptide molecule interacts with DNA and forms a peptide:DNA complex, it usually results in changes in absorbance. The magnitude of change may be correlated to the strength of interaction.

Calf thymus DNA (ctDNA) is a natural DNA widely used in studies of DNA binding anticancer agents and DNA binding agents that modulate DNA structure and function. Figure 2A.4 shows the UV-visible absorption spectrum of calf thymus DNA with and without addition of peptides. Differences observed in the DNA melting temperature (T_m) values at various compositions of DNA-Peptide complexes would directly suggest whether the presence of different peptides at various charge ratios would impart any stability to the ctDNA.

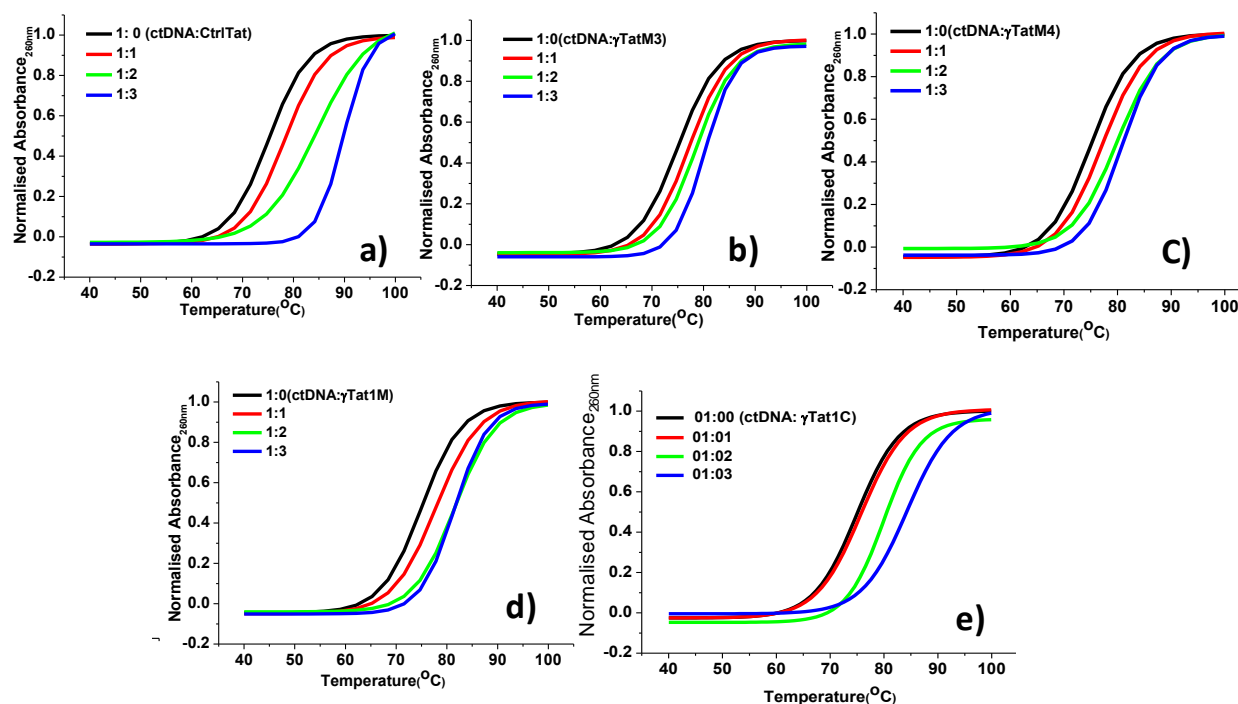


Figure 2A.4. UV-thermal melting profile of calf thymus DNA alone and in the presence of the Tat peptides of the study in increasing molar ratios. a) ctrlTat b) γ TatM3 c) γ TatM4 d) γ Tat1M e) γ Tat1C. ctDNA was taken at 50 μ M concentration and peptide concentration was increased from 1:0 to 1:3 molar ratio, in 10 mM potassium phosphate buffer, pH 7.0. Experiments were carried out in triplicates (± 1).

We investigated the effect of the introduction of arginine mimic r in the Tat(48-57) peptide on the binding of the peptides to ctDNA. The increase in the T_m indicates a stabilization of the DNA, while a decrease indicates destabilization. The melting temperature (T_m) of ctDNA in absence of peptides was observed to be 71.5 $^{\circ}$ C, which is characteristic of ctDNA melting. The UV-melting profiles of ctDNA complexes with ctrlTat peptide and its modifications, in increasing charge ratios are shown in Figure 2A.4 and the data are listed in Table 2A.2. The melting temperatures of ctDNA complexes with all the Tat peptide analogues were found to increase with increasing peptide concentration, similar to CtrlTat, indicating the stabilization effect of these peptides.

All the Tat peptide analogues are stabilising the peptide-ctDNA complex at 1:1 peptide :ctDNA molar ratio. The ctrlTat peptide stabilized the ctDNA complex the most with a melting temperature of 85.3 $^{\circ}$ C at the ctDNA:peptide molar ratio 1:3. Among the Tat peptide analogues,

the complex formed by γ Tat1C with ctDNA was the most stable ($T_m = 80.6$ °C) at the ratio 1:3. Increase in the relative concentration of peptides resulted in enhanced stabilisation of the complexes with ctDNA (Figure 2A.4). However, the degree of stabilization by the Tat peptide analogues was less than that observed with the ctrlTat peptide.

Table 2A.2. UV-thermal melting data of calf thymus DNA alone and in the presence of the Tat peptides.

Peptide	UV- T_m in °C (ΔT_m , °C)*		
	ctDNA: peptide ratio		
	1:1	1:2	1:3
CtrlTat	74.7(3.2)	84.1(12.6)	85.3(13.8)
γ TatM3	74.6(3.1)	74.7(3.2)	75.8(4.3)
γ TatM4	74.7(3.2)	77.8(6.3)	77.8(6.3)
γ Tat1M	74.6(3.1)	77.8(6.3)	77.8(6.3)
γ Tat1C	72.5(1.0)	76.5(5.0)	80.6(9.1)

*The values of ΔT_m in parentheses indicate the difference in T_m between the ctDNA:peptide complex and ctDNA alone. T_m of ctDNA alone = 71.5 °C. Experiments were carried out in triplicates (± 1).

2A.4.4 Agarose Gel Electrophoresis Mobility Shift Assay

The binding of peptides to DNA was further studied by a gel mobility shift assay. As ctDNA is highly polydisperse in nature, the rather low disperse plasmid DNA (pGLO) was used in this study instead of ctDNA for clarity of analysis on agarose gels. Assuming electrostatic interactions to be the main contributing factor in the binding of cationic peptides such as the Tat peptides of this study to DNA, using pDNA in this study as opposed to ctDNA, as used in the previous UV- T_m studies, would not be unreasonable, and would also serve to generalize the effect of the Tat peptides on binding to any DNA. Plasmid DNA typically shows three bands on an agarose gel that correspond to supercoiled, open-circular, and linear DNA. Upon binding of peptides such as those of the present study, the bands are retarded and can be visualised closer to the loading wells.

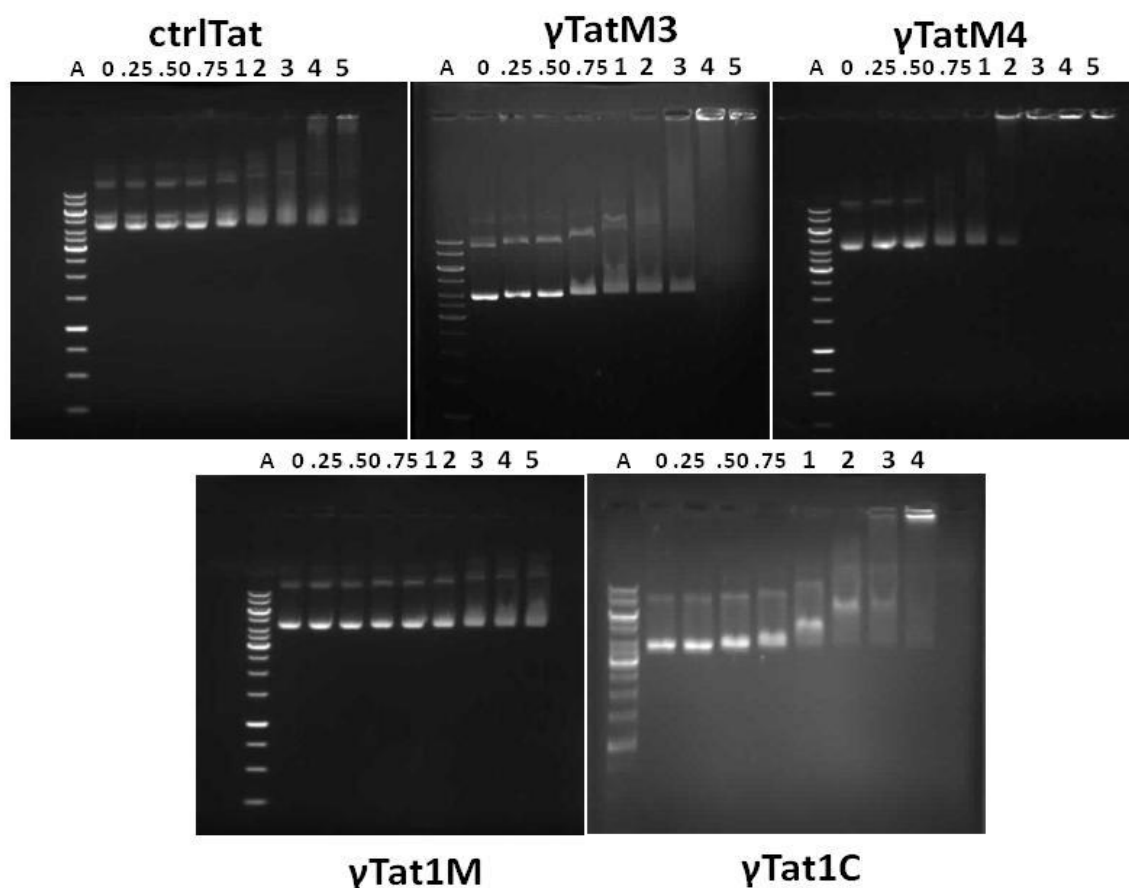


Figure 2A.5. Agarose gel electrophoresis study of different DNA–Peptide complexes at various charge ratios: Lane 1, standard ladder; lane 2, free DNA 20 ng/μL; lanes 3–10, Peptide-DNA complexes at various charge ratio: lane 3, $Z^{+/-} = 0.25$; lane 4, $Z^{+/-} = 0.50$; lane 5, $Z^{+/-} = 0.75$; lane 6, $Z^{+/-} = 1.0$; lane 7, $Z^{+/-} = 2.0$; lane 8, $Z^{+/-} = 3.0$; lane 9, $Z^{+/-} = 4.0$; lane 10, $Z^{+/-} = 5.0$.

Complexes of plasmid DNA were formed with the Tat peptides at different charge ratios ($Z^{+/-}$) ranging from 0:1 through 5:1 of peptide N (+):DNA phosphate (-), and subsequently analyzed by agarose gel electrophoresis (Figure 2A.5). The DNA condensing ability of γ TatM4 was seen to be highest among all the peptides, when complete condensation was observed at the ratio 3:1. In the case of γ TatM3 and γ Tat1C complete DNA condensation was observed at the charge ratio 4:1, whereas γ Tat1M showed little condensation of plasmid DNA even at the charge ratio 5:1, where significant of the pDNA was observed to be still uncondensed. Except for γ Tat1M, all the Tat peptides of the study showed either significant or complete condensation of DNA at this higher charge ratio ($Z^{+/-} = 5$). It is noteworthy that although the number of positive charges in γ Tat1M and γ Tat1C is the same, their DNA condensing abilities were found to be strikingly

different. These results imply that electrostatic interactions are not the only forces responsible for the binding of the Tat peptides to DNA, and that other interactions such as hydrogen-bonding, Van der Waal's forces, etc., might also play a significant role.

2A.4.5 Circular Dichroism Spectroscopic Studies

Conformational changes of DNA upon complexation with cationic peptides can be visualised by CD spectroscopy. The CD spectra of the Tat peptides of the study were recorded in water (Figure 1A.6), where the Tat₄₇₋₅₈ peptide is reported to display a random coil structure.²⁰ The CD spectra of the Tat peptides of the study displayed similar CD spectra, with only variations in the amplitude. Signature CD signals of defined secondary structures such as α -helix or β -sheet were not observed. Further, the contribution of the Tat peptides to the region between 240 to 320 nm, where characteristic signals of nucleic acids are observed, was negligible.

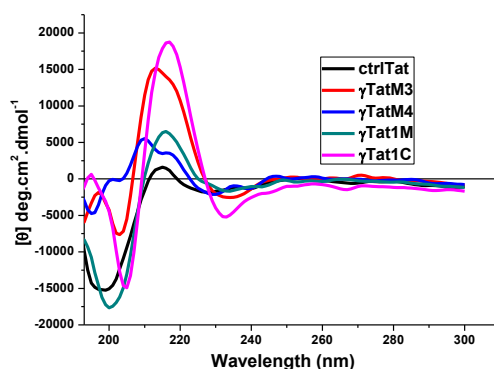


Figure 2A.6. CD spectra of Tat peptides (500 μ M) of the study in water.

Next, CD spectra of ctDNA were recorded in presence and absence of the Tat peptides. The CD spectrum of ctDNA alone shows a maximum at 270 nm and minimum at 240 nm, indicative of a B-DNA type of structure. Increasing molar ratio of peptides (from 1:0 through 1:5, ctDNA:peptide) resulted in a red shift of the spectra, with the final spectrum (1:5 ctDNA:peptide ratio) displaying maxima and minima at \sim 285 nm and \sim 250 nm respectively (Figure 2A.7). This shift (10 - 15 nm) was accompanied by a decrease in amplitude of the maximum at 270-285 nm, indicating destacking. A similar decrease in amplitude was also observed for the minimum at 240-250 nm. Similar changes were observed with all the Tat peptides of the study, as observed with CtrlTat. These results suggest that replacement of arginines from natural Tat peptide with

newly synthesized Tat peptide mimics does result in some structural changes in ctDNA upon binding of the peptides, including destacking.

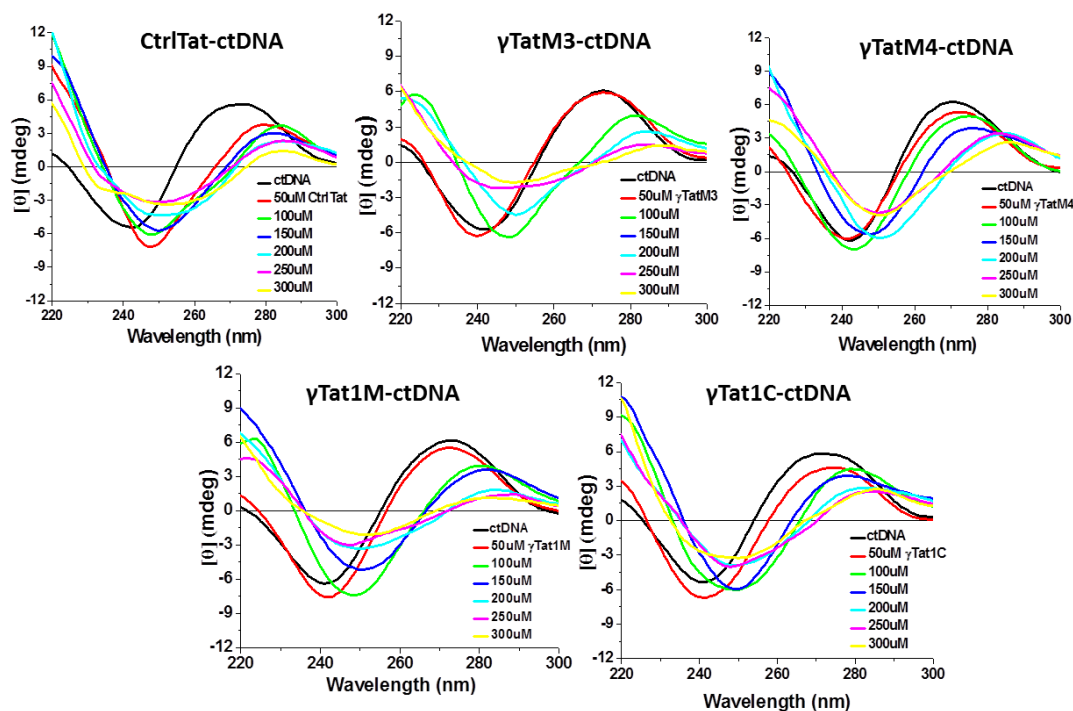


Figure 2A.7 Effect of Tat peptide and its analogues on the CD spectra of ctDNA at different molar concentrations. ctDNA was taken at 100 μM concentration and the studies were carried out in 10 mM potassium phosphate buffer at pH 7.

2A. 4.6 Cellular uptake and Cytotoxicity studies

2A. 4.6.1 Cellular uptake studies

An attractive advantage of developing Tat peptide analogues as DNA condensing molecules is their ability to penetrate into the cells. They could therefore, be used as non-viral vectors for gene delivery. We therefore, sought to evaluate the effect that the inclusion of *r* as arginine mimics would have on the cell-penetrating properties of the derived Tat peptides. Thus, the peptides were labeled with a fluorescent tag (Table 2A.1, entries 6-10) and their uptake in HeLa cells was studied by flow cytometry (Figure 2A.8). The effect of a similar pre-organized β -amino acid was recently reported to have a positive effect on the cell-permeation properties of the Tat peptide,²¹ although in this report, three β -amino acid residues were simultaneously included in the derived Tat peptide. HeLa cells were treated with the *cf*-labeled Tat peptides and subjected to

flow cytometry. The excess of the peptides bound to cell surface were washed with heparin before trypsinization to avoid misinterpretation of results in flow cytometric analysis.²² Thus, the fluorescence-positive cells that were obtained are indicative of internalized peptides alone and exclude those superficially and externally associated with the cell membrane.

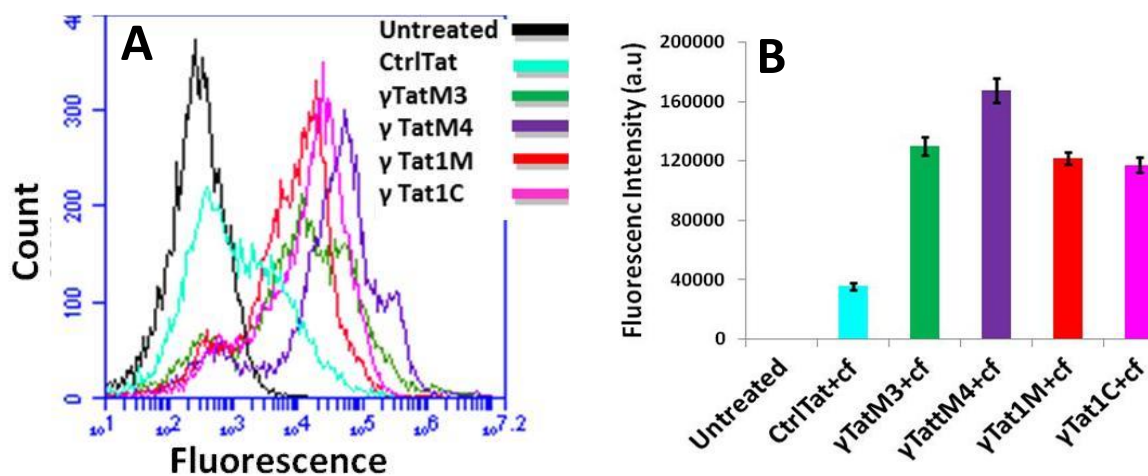


Figure 2A.8. Flow cytometry data for the uptake of Tat peptides in HeLa cells. (A) Number of positive cells and (B) Mean fluorescence. Cells were incubated for 4 h at 37 °C temp with peptides taken at 5 μ M conc.

All the Tat peptide analogues were internalized by >95% of the counted cells (Figure 2A.8.A), although the mean fluorescence of cells varied considerably (Figure 2A.8.B). Significantly, both γ TatM3 and γ TatM4 possessed better cell-penetrating ability than the CtrlTat peptide. The peptide γ TatM4 was shown to have the best cell permeability amongst all the Tat peptides. Thus, the flow cytometry experiments revealed that with increasing arginine substitution by the mimic **r**, the cellular uptake of peptide was found to increase, pointing to the favourable effect of this non-natural amino acid mimic on the cell penetrating properties of the derived peptides.

2A. 4.6.2 Confocal Microscopy studies

To determine the intracellular localization of the Tat peptides, confocal microscopy analysis was carried out after incubating the cells with fluorescein-labelled peptides. In order to understand the localization of green fluorescence-labeled peptides, HeLa cells were counter-stained with DAPI and lysotracker red after fixing the cells with paraformaldehyde. DAPI was used to stain the nucleus, while lysotracker red was used to stain the lysosomes.

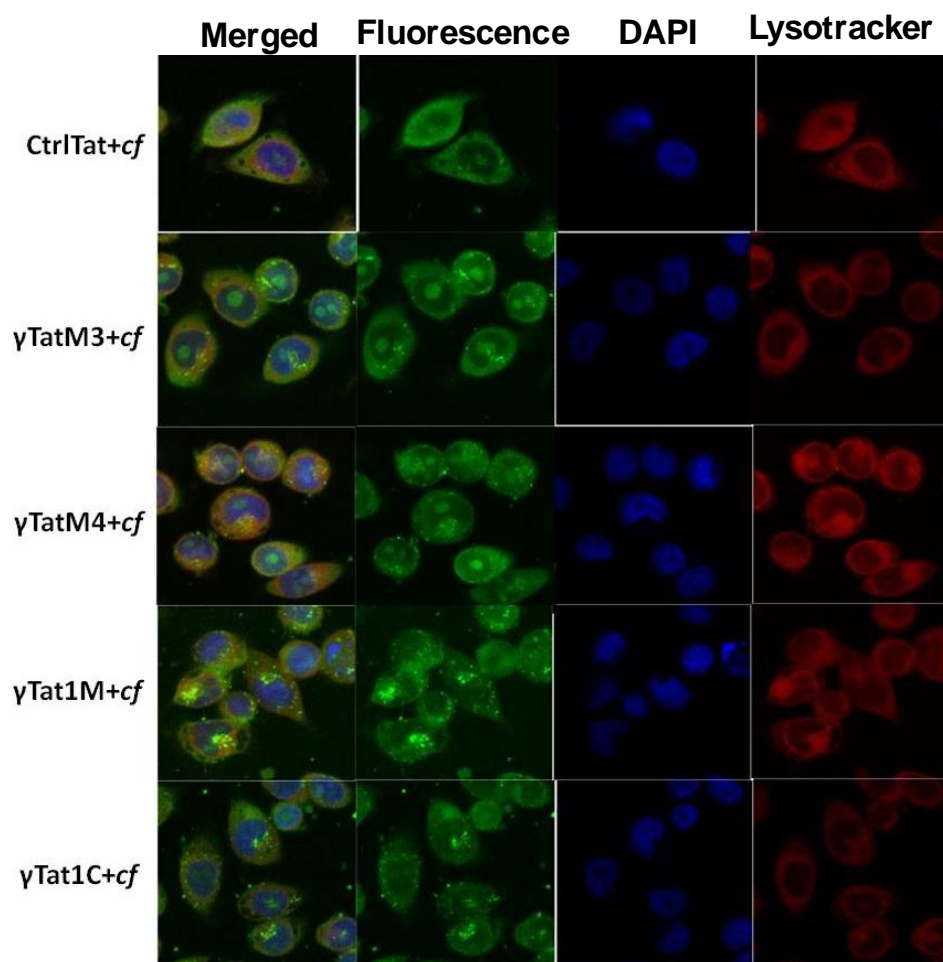


Figure 2A.9. Confocal microscopy of Tat peptide analogues with HeLa cells. Merge = merged image of peptide, DAPI and Lysotracker. Fluorescence = Carboxyfluorescein labeled peptides. DAPI = Nucleus stain, Lysotracker = Lysosome stain.

All the Tat peptide analogues showed significant presence in the cytoplasm and also inside the nuclei and nucleoli (Figure 2A.9), indicating their ability to traverse cell and nuclear membranes. Their distribution was punctate, rather than diffuse, suggesting the endocytosis mode of uptake.²³ Considering fluorescein as a model cargo molecule, it may be foreseen that a similar conjugation strategy be applied for covalently conjugating other cell-impermeable drugs to the Tat peptides to deliver them into cells for more effective therapeutic applications. This improves the prospects of these Tat peptide molecules as promising candidates for the development of drug delivery vehicles.

2A. 4.6.3 Cytotoxicity studies

We further evaluated the effect of the Tat peptides on cell viability. This was assessed by the standard MTT cell viability and hemolysis assays. MTT assay is a colorimetric assay, where enzymes present in viable cells effect the reduction of the tetrazolium dye, 3-(4,5-dimethylthiazol-2-yl)-2,5-diphenyltetrazolium bromide, leading to the formation of a purple formazan derivative. A decreased colour intensity indicates low cell viability as a result of increased cytotoxicity. Figure 2A.10A shows the cell viability profile in the MTT assay. HeLa cells were treated with increasing concentrations of the Tat peptides and the cell viability assayed after 12 h. Even at the higher concentration of 50 μM , only a slight drop in cell viability was observed, with $\sim 85\%$ cell viability for all the Tat peptides.

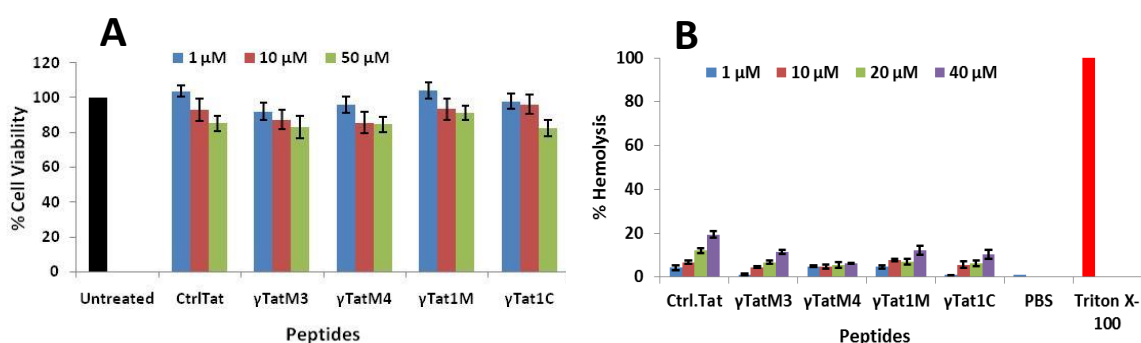


Figure 2A.10. (A) Cell viability assessed by the MTT assay. (B) Hemolysis assay.

The cytotoxicity of the Tat peptides was further evaluated by the hemolysis assay, when human RBCs were treated with the peptides for 1 h. The disruption of the red blood cell (RBC) membrane is an indication of toxicity, resulting in release of hemoglobin, that can be measured spectrophotometrically. An increase in absorbance is therefore, indicative of increased hemolysis and toxicity. RBCs treated with PBS and Triton X-100 were used as the negative and positive controls respectively. As evident from Figure 2A.10B, the Tat peptides had a very low hemolytic effect ($\leq 10\%$). Thus, the Tat peptides of the study were demonstrated to be relatively non-toxic to mammalian cells, while demonstrating good cell penetration properties.

2A.4.7 Stability to enzymatic hydrolysis

A major limitation of natural peptides is their inactivation by proteases. Poor protease stability severely limits the clinical use of potentially therapeutic peptides. The Tat-peptide contains

multiple arginine and lysine residues, which constitute proteolytic sites (at their C-termini) of trypsin,²⁴ thus making this enzyme ideal for a study of their protease resistance. The non-natural amino acids used in the present work confer the derived peptide with improved protease resistance properties, increasing their application potential in biological systems, by increasing their half-life significantly. MALDI-TOF analysis of the fragments obtained after trypsin digestion reaffirmed the protective effect the amino acid surrogates.

The stability of the Tat peptides of the study to hydrolytic digestion by enzymes was studied by treating the peptides with trypsin, a commercially available protease, and estimating the percent intact peptide remaining over time by HPLC analysis. The results of such a study with γ TatM4 as a representative example, in comparison to the control Tat peptide (ctrlTat) is shown in Figure 2A.11. It is evident that the introduction of the arginine surrogate *r* within the Tat peptide sequence conferred the derived peptide with significant resistance to digestion by trypsin. In particular, the $t_{1/2}$ of γ TatM4 was found to be 16 h in comparison to 4 h for the ctrlTat peptide. After 24 h, 30% of the γ TatM4 peptide still remained intact, while only 4% of the ctrlTat peptide was found to be intact at the same time point.

The fragments obtained after digestion with trypsin were analysed by MALDI-TOF in order to gain insight into the sites where enzymolysis had occurred. The results are (Table 2A.3). In the case of the ctrlTat peptide, cleavage was observed at the C-terminal sites of most of the lysine and arginine residues.

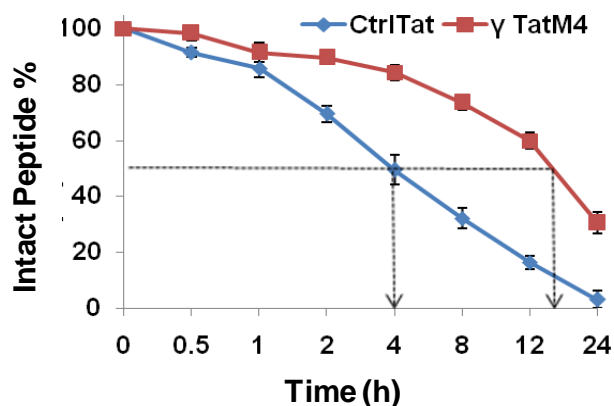


Figure 2A.11. Stability of the γ TatM4 and ctrlTat peptides to proteolytic digestion by trypsin. The values are expressed as the mean of triplicates. Standard deviation is calculated from three independent experiments.

Five fragments, in addition to the intact peptide, that included cleavage at the C-termini of residues K₅, R₆, R₇, R₉, R₁₀ were observed for the ctrlTat peptide even after 0.5 h. In contrast, the γ TatM4 peptide was observed to be completely intact at this time point, with no observed fragmentation.

The molecular ion of the intact γ TatM4 peptide was observed even after 24 h, and cleavage was observed to occur only at the C-termini of the K5 and R6 residues, while the other cleavage sites were blocked by the presence of the arginine analogues of the study. In comparison, the molecular ion peak of the ctrlTat peptide was completely absent after only 8 h.

Table 2A.3 Trypsin fragmentation analysis

Peptides \rightarrow	ctrlTat* <i>Ac-F₁-G₂-R₃-K₄-K₅-R₆-R₇-Q₈-R₉-R₁₀-R₁₁-NH₂</i>	γ TatM4# <i>Ac-F₁-G₂-M₃-K₄-K₅-R₆-M₇-Q₈-M₉-R₁₀-M₁₁-βAla-NH₂</i>
Time (h) \downarrow	Fragments(MALDI-TOF)	
0	1583	1874
0.5	673, 829, 986, 1272, 1428, 1582	1874
1	673, 829, 986, 1272, 1428, 1582	728, 885, 1874
2	673, 829, 986, 1272, 1428, 1582	728, 885, 1874
4	673, 829, 986, 1272, 1428, 1582	728, 885, 1874
8	673, 829, 986, 1272, 1428, 1582	728, 885, 1874
12	673, 829, 986, 1272, 1428, 1582	728, 885, 1874
24	673, 829, 986, 1272, 1428, 1582	728, 885, 1874

* 673 = (K5-R6), 829 = (R6-R7), 986 = (R7-Q8), 1272 = (R9-R10), 1428 = (R10-R11), 1582 = Intact

728 = (K5-R6), 885 = (R6-M7), 1874 = Intact

In order to assess the proteolytic stability of peptide with other endopeptidases Exposure to the enzymes chymotrypsin and pepsin also confirmed the superior stability of γ TatM4 to proteolytic digestion in comparison to ctrlTat (Figure 2A.12). The peptide γ TatM4 remained intact while ctrlTat showed 20 % degradation after 24 h in the presence of pepsin. Similarly, in the presence of Chymotrypsin, γ TatM4 remained intact after 24 h, while only 16 % of ctrlTat peptide was found to be intact at the same time point (Table 2A.4). This clearly illustrates that the introduction of unnatural amino acid residue *r* into the Tat peptide sequence significantly enhances the protease-resistance properties of the Tat peptides.

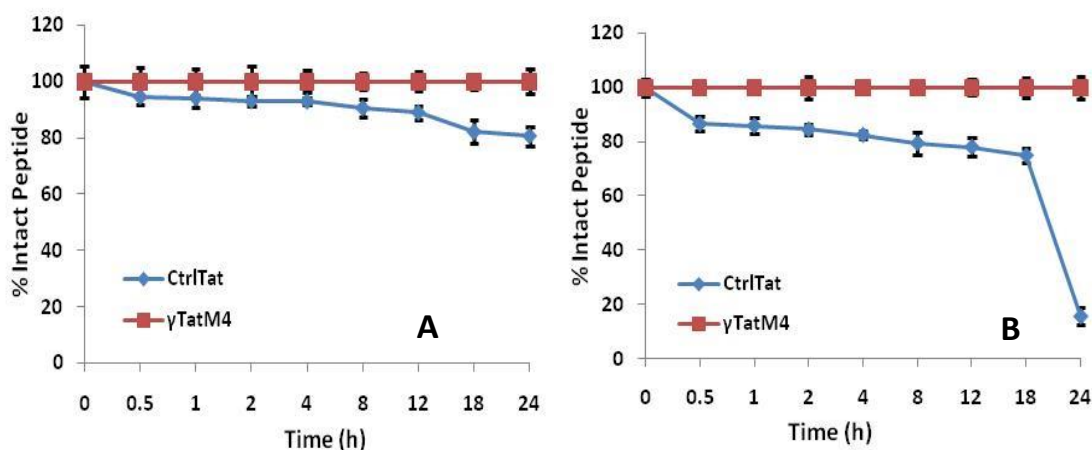


Figure 2A.12. Stability of the γ TatM4 and ctrlTat peptides to proteolytic digestion by A) Pepsin B) Chymotrypsin. The values are expressed as the mean of triplicates. Standard deviation is calculated from three independent experiments.

Table 2A.4 Stability of the γ TatM4 and ctrlTat peptides to proteolytic digestion by Pepsin and Chymotrypsin.

Time (h)	% Intact Peptide			
	Pepsin		Chymotrypsin	
	ctrlTat	γ TatM4	ctrlTat	γ TatM4
0	100 ± 2.6	100 ± 5.7	100 ± 3.0	100 ± 3.2
0.5	94.6 ± 2.8	100 ± 5.0	86.7 ± 2.6	100 ± 1.5
1	94.2 ± 3.4	100 ± 4.6	86.0 ± 2.9	100 ± 2.4
2	93.1 ± 1.8	100 ± 5.3	84.6 ± 1.8	100 ± 4.3
4	93.0 ± 1.3	100 ± 4.0	82.6 ± 1.3	100 ± 1.8
8	90.6 ± 3.0	100 ± 2.9	79.6 ± 4.1	100 ± 2.3
12	89.0 ± 2.4	100 ± 3.5	78.2 ± 3.5	100 ± 2.9
18	82.1 ± 4.2	100 ± 2.7	75.1 ± 2.6	100 ± 3.8
24	80.6 ± 3.5	100 ± 4.4	15.9 ± 3.3	100 ± 4.2

2A.5 Summary and Conclusions

In summary, conformationally constrained the non-natural arginine mimic, (2*S*,4*S*)-4-amino-N1-(3-guanidinopropyl)-proline, was designed and incorporated into Tat(48-57) at predefined positions in lieu of arginine. The resulting Tat peptide analogues were able to bind to ctDNA and effect stabilization. They were also able to induce complete pDNA condensation that is important for gene transfection. Increasing arginine substitutions by the mimic, **r**, resulted in increased cellular uptake of the peptides. The Tat peptides of the study were demonstrated to be relatively non-toxic to mammalian cells, while demonstrating good cell penetration properties.

They may therefore, be considered promising candidates for further development as drug delivery vehicles.

2A.6 Experimental Section

2A.6.1 General Information

All the reagents used were obtained commercially and were of ≥ 95 % purity and used without further purification. DMF, CH₂Cl₂, pyridine were dried over P₂O₅, CaH₂, KOH respectively. DMF, CH₂Cl₂ were stored by adding 4 Å molecular sieves and pyridine by adding KOH. Column chromatography was performed for purification of compounds on silica gel (100- 200 mesh or 60-120 mesh, Merck). TLCs were performed on pre-coated with silica gel 60 F254 (Merck) aluminium sheets. TLCs were performed using petroleum ether-ethyl acetate and ethyl acetate-methanol solvent systems. TLCs were visualised after spraying with ninhydrin reagent and heating. ¹H and ¹³C NMR spectra were recorded on a Bruker AV 200 or AV 400 or AV 500 spectrometer fitted with an Aspect 3000 computer and all the chemical shifts (ppm) are referred to internal TMS, chloroform-d for ¹H and/or ¹³C NMR. ¹H NMR data are reported in the order of chemical shift, multiplicity (s, singlet; d, doublet; t, triplet; q, quartet; br, broad; br s, broad singlet; m, multiplet and/ or multiple resonance), number of protons. HRMS mass spectra were recorded on a Thermo Scientific Q-Exactive, Accela 1250 pump MALDI-TOF spectra were obtained from a Voyager-De-STR (Applied Biosystems) and CHCA (α -Cyano-4-hydroxycinnamic acid) matrix was used to analyze MALDI-TOF samples. All final compounds and oligomers were $\geq 95\%$ pure, as determined by ¹H NMR, ¹³C NMR, HRMS, HPLC and/or MALDI-TOF analysis, as applicable. UV absorbance was performed on a Varian Cary 300 UV-VIS spectrophotometer.

2A.6.2 Experimental procedures and spectral data

(2*S*,4*R*)-methyl-1-(3-(*tert*-butyloxycarbonyl-amino)propyl)-4-hydroxypyrrolidine-2-carboxylate (**2**)

To a 250 mL round bottom flask containing *trans*-4-hydroxy-L-proline methyl ester **1** (5 g, 34.5 mmol) dissolved in dry DMF (15 mL), triethylamine (14.4 mL, 103.0 mmol) and catalytic amount of DMAP were added. The above reaction mixture was stirred for 30 min at room temperature and 2-((Boc)amino)propyl methanesulfonate (13.1 g, 51.5 mmol) dissolved in dry DMF was added drop-wise. The reaction was heated at 70 °C for 10 h and monitored by TLC.

The solvent was evaporated *in vacuo* and the crude reaction mixture was taken up in ethyl acetate and water. The layers were separated, and the aqueous phase extracted with ethyl acetate. The combined organic extracts were washed with brine, dried over Na₂SO₄ and evaporated under vacuum. The crude product was purified by silica gel column chromatography using a gradient of ethyl acetate in petroleum ether to give title compound **2** as a pale yellow gummy liquid (6.4 g, 62%). $[\alpha]_D^{20}$ -143.72 (*c* 0.1, CHCl₃).

¹H NMR (200 MHz, CDCl₃) δ : 5.38 (br s, 1H), 4.45 (m, 1H), 3.72 (s, 3H), 3.54 (m, 1H), 3.36 (m, 1H), 3.19 (m, 2H), 2.73 (m, 2H), 2.56 (m, 2H), 2.14 (m, 2H), 1.63 (m, 2H), 1.44 (s, 9H).

¹³C NMR (50 MHz, CDCl₃) δ : 174.4, 156.3, 77.1, 70.0, 64.4, 60.9, 51.8, 39.3, 38.5, 28.4, 28.0.

¹³C DEPT (50 MHz, CDCl₃) δ : 70.0, 64.4, 60.9, 51.9, 51.8, 39.3, 38.5, 28.4, 28.0.

HRMS (ESI): *m/z* calculated for C₁₄H₂₆N₂O₅: 302.1842, Observed [M⁺+H]: 303.1915, [M⁺+Na]: 325.1713.

(2*S*,4*S*)-methyl-4-azido-1-(3-(*tert*-butyloxycarbonyl amino)propyl)pyrrolidine-2 carboxylate (3)

Dry triethylamine (10 mL) was added to a solution of compound **2** (5 g, 16.5 mmol) in dry CH₂Cl₂. The reaction mixture was stirred for 30 min, mesyl chloride (3.8 mL, 49.6 mmol) was added drop-wise by syringe and stirring continued for another 30 min at 0-5 °C. The reaction was monitored by TLC. Upon completion, excess of CH₂Cl₂ and water (100 mL) were added. The layers were separated, and the aqueous phase was extracted with CH₂Cl₂ (3 x 100 mL). The combined organic extracts were washed with brine (100 mL), dried over Na₂SO₄. The solvents were evaporated *in vacuo* and the mesylate obtained was used in the further reaction. The mesyl compound was dissolved in dry DMF (10 mL) and sodium azide (2.56 g, 39.5mmol) was added portion-wise at room temperature with constant stirring. The reaction was heated at 65 °C for the next 6 h and monitored by TLC. Upon completion of reaction, solvent was evaporated *in vacuo*, followed by addition of ethyl acetate and water. The layers were separated, and the aqueous phase was extracted with ethyl acetate. The combined organic extracts were washed with brine, dried over Na₂SO₄ and evaporated. The crude residue was purified by silica gel column chromatography using a gradient of ethyl acetate in petroleum ether to give the title compound **3** as a pale yellow solid (1.72 g, 67%). $[\alpha]_D^{20}$ -137.92 (*c* 0.1, CHCl₃).

¹H NMR (200 MHz, CDCl₃) δ: 5.47 (br s, 1H, NH), 3.96 (m, 1H), 3.77 (s, 3H), 3.25 (m, 4H), 2.88 (m, 1H), 2.53 (m, 3H), 2.15 (m, 1H), 1.44 (s, 9H).

¹³C NMR (50 MHz, CDCl₃) δ: 173.3, 156.2, 78.6, 64.8, 58.7, 58.0, 52.1, 51.7, 38.5, 35.4, 28.4, 27.8.

¹³C DEPT (50 MHz, CDCl₃) δ: 64.8, 58.7, 58.0, 52.1, 51.7, 38.4, 35.4, 28.4, 27.7.

HRMS (ESI): m/z calculated for C₁₄H₂₅N₅O₄: 327.1907; observed [M⁺+H]: 328.1977; [M⁺+Na]: 342.2131.

(2S,4R)-4-(((9H-fluoren-9 yl)methoxy)carbonyl)amino)-1-(3-(tert-butyloxycarbonyl amino)propyl)pyrrolidine-2-carboxylic acid (X)

To a solution of azido compound **3** (1.5 g, 4.58 mmol) dissolved in dry MeOH (25 mL), 10% palladium on charcoal (300 mg, 20% w/w) was added and the resulting reaction mixture stirred under hydrogen gas at 50 psi for 3 h and the reaction was monitored by TLC. After completion of reaction, it was filtered through celite and water:methanol (1:1, 10 mL) were added. 2N LiOH (15 mL) was further added and the reaction was stirred for 30 min. Methanol was evaporated under reduced pressure and the resulting reaction mixture was neutralised with dil. HCl. The solvents were evaporated and the residue was suspended in methanol and filtered. The supernatant was evaporated *in vacuo* and dried in a desiccator to give the corresponding amino acid. To a solution of the amino acid, dissolved in 1, 4-dioxane:water (1:1, 5 ml), NaHCO₃ (3.0 g, 36 mmol) was added to maintain an alkaline pH. The resulting reaction mixture was stirred at room temperature for 30 min and Fmoc-Cl (2.69 g, 10.4 mmol) was added slowly. Stirring was further continued overnight at room temperature. The reaction was monitored by TLC. Upon completion of reaction, the reaction mixture was made slightly acidic by addition of Dowex H⁺ resin, which was subsequently filtered off. The dioxane was removed under vacuum and the crude compound extracted in ethyl acetate. The combined organic extracts were washed with brine and dried over sodium sulfate and evaporated *in vacuo*. The crude product was purified by silica gel column chromatography to give the title compound **X** (1.02 gm, 58 %) as a solid yellowish foam. $[\alpha]_D^{20}$ -27.36 (*c* 0.1, CHCl₃).

¹H NMR (200 MHz, CDCl₃) δ: 7.75 (m, 2H), 7.57 (m, 2H), 7.34 (m, 4H), 4.61 (m, 1H), 4.38 (m, 2H), 4.21 (m, 2H), 3.77 (m, 1H), 3.13 (m, 3H), 2.80 (m, 1H), 2.53 (m, 2H), 2.33 (m, 1H), 2.00 (m, 2H), 1.46 & 1.44 (s, 9H).

^{13}C NMR (50 MHz, CDCl_3) δ : 174.3, 155.9, 144.0, 141.3, 127.1, 120.0, 79.0, 66.6, 64.4, 52.2, 47.3, 36.8, 28.1.

^{13}C DEPT (50 MHz, CDCl_3) δ : 127.0, 124.7, 119.9, 66.6, 64.4, 52.2, 47.2, 36.8, 28.4.

HRMS (ESI): m/z calculated for $\text{C}_{28}\text{H}_{35}\text{N}_3\text{O}_6$: 509.2526; observed: $[\text{M}^++\text{H}]$ 510.2596, $[\text{M}^++\text{Na}]$ 532.2411.

2A.6.3 Materials and methods

2A.6.3.1 Materials

Synthesis of basic region of HIV-1 Tat peptide (*Ac*-FGRKKRRQRRR-*NH*₂) and other modifications of Tat peptides (shown in Table 2A.1) were synthesised by using standard Fmoc chemistry protocols. ctDNA was obtained from Sigma-Aldrich. The concentration of ctDNA was determined spectrophotometrically at 260 nm using the molar extinction coefficient $6600 \text{ M}^{-1}\text{cm}^{-1}$. Milli-Q water was used to prepare all stock solutions. Other reagents of analytical grade quality were used without any further purification. All experiments were performed using 10 mM phosphate buffer at pH 7.0.

2A.6.3.2 CD Spectroscopy

CD spectra of peptide-ctDNA complexes were recorded on a Jasco spectropolarimeter (model J815, Japan) equipped with a thermoelectrically controlled cell holder. The path length of the cuvette used to measure structural changes was 1 cm. CD spectra were recorded from 320 nm to 195 nm, with averaging of 3 accumulations at 25 °C. Each spectrum was collected at a rate of 100 nm/min, and 1 nm data pitch. The buffer solution contained 10 mM potassium phosphate buffer at pH 7.0. For all the CD experiment ctDNA concentration was fixed at 100 μM and peptide concentration was increased from 50-300 μM .

The CD were measured for peptides alone using a J-815 spectropolarimeter (Jasco, Japan). The spectra were recorded at a scan speed of 100 nm/min from 300 nm to 190 nm in water. An average of three scans was collected for each peptide. The final concentration of the peptides was 500 μM . The acquired CD signal spectra were converted to the molar ellipticity using the equation: $[\theta] = (\theta \times 1000)/(c \times l)$, where, $[\theta]$ is the molar ellipticity ($\text{deg.cm}^2.\text{dmol}^{-1}$), θ is the observed ellipticity corrected for the buffer at a given wavelength (mdeg), c is the peptide concentration (M), l is the path length (cm).

2A.6.3.3 Temperature-dependent UV Spectroscopy (UV melting)

Temperature dependent UV melting experiments were carried out using a Cary 100 (Varian) Spectrophotometer with thermoelectrically controlled cell holder. A quartz cell of 1 cm path length was used for all absorbance studies. Temperature dependent absorption spectra were obtained at 260 nm with 0.5 °C/min rate of increase in temperature, from 40 to 100 °C. In these experiments the concentration of ctDNA was kept 50 µM and peptide concentration was increased from 0-3 molar ratio. The buffer solution contained 10 mM potassium phosphate buffer at pH 7.0.

2A.6.3.4 Agarose gel Electrophoresis

Electrophoretic mobility of peptide-plasmid DNA complexes at different charge ratios was studied by agarose gel electrophoresis on 0.8 % agarose gels containing 30 µg/mL of ethidium bromide in TAE buffer. Experiments were run at 80V for 90 min. Gels were visualised by UV transillumination.

2A.6.3.5 Cellular uptake and cytotoxicity studies

2A.6.3.5.1 Flow Cytometry :

HeLa cells were seeded in 24-well plates at a density of 50,000 cells/well and incubated for 24 h. The fluorescently tagged peptides were added to the cells at concentrations of 5 µM in 300 µL of serum-free medium. After 4h incubation at 37 °C, cells were washed with PBS containing heparin (1 mg/mL) to remove membrane bound peptides.³² Thus, the fluorescence-positive cells (Figure2A.7) that were obtained are indicative of internalized peptides alone and exclude those superficially and externally associated with the cell membrane. Cells were then collected by trypsinization and resuspended in PBS and placed on ice. Flow cytometry measurements were carried out on a BD Accuri™ C6 Flow Cytometer System using BD Accuri C6 Software. 10,000 live cells were used for each analysis at room temperature. Flow cytometry measurements at 37 °C, subsequent to treating the cells with peptides at the same temperature were carried out using the same protocols as mentioned above. The uptake experiments were repeated in triplicates.

2A.6.3.5.2 Confocal microscopy

Cells were seeded at a density of 10,000 cells/well in a 12-well plate (NEST biotech, China) and incubated for 24 h. Labeled peptides (5 µM) were added to the cells in serum-free media and incubated at 37 °C for 4 h. After 4 h of incubation at 37 °C, cells were washed twice with ice

cold 1× phosphate buffered saline (PBS) and fixed with 4 % paraformaldehyde. The cells then treated with 500 nM of DAPI solution for 5 min at 37 °C. The excess of DAPI was again washed off using 1X PBS twice and cells were again incubated with 100 nM LysoTracker solution for 3 min at 37 °C. Finally cells were washed with 1X PBS twice before imaging to remove residual traces of LysoTracker. Imaging was done at room temperature on an inverted LSM510 META laser scanning microscope (Carl Zeiss, Germany) using the 488 nm line of an argon laser for fluorescein.

2A.6.3.5.3 Cytotoxicity studies :

The cytotoxicity of peptides to HeLa cells was determined by the MTT cell viability assay. All cells were plated overnight in 96-well plates at a density of 10,000 cells per well in 0.2 ml of appropriate growth medium with 10 % FBS at 37 °C. Different concentrations of peptides up to a maximum of 50 µM were incubated with the cells for 12 h, following which, the peptides were removed by replacing the media by fresh media. The cell culture medium alone and with cells, both without peptides, were included in each experiment as controls. After 12 h incubation, 10 µL of a 5 mg/ml solution of 3-(4,5-dimethylthiazol-2-yl)-2,5-diphenyl-tetrazolium bromide (MTT) was added and further incubated for 4 h. Conversion of MTT into purple formazan product by metabolically active cells is used as an indication of cell viability. The crystals of formazan were dissolved with DMSO and the optical density was measured at 570 nm using a microplate reader VarioskanFlash (4.00.53), for quantification of cell viability. All assays were run in triplicates.

2A.6.3.5.4 Hemolysis assay :

Human red blood cells (hRBCs) with additive K₂ EDTA (spray-dried) were washed using PBS buffer many times and centrifuged at 1000 g for 10 min until a clear supernatant was observed. The hRBCs were re-suspended in PBS to get a 0.5 % v/v suspension. Peptides dissolved in PBS were added to a sterile 96-well plate to a volume of 75 µL in each well. Then 75 µL of 0.5% v/v hRBC solution was added to make up a total volume of 150 µL in each well. TritonX-100 and PBS were used as positive and negative controls respectively. The plate was then incubated at 37 °C for 1 h, followed by centrifugation at 3500 rpm for 10 min. The supernatant (120 µL) was transferred to fresh wells and absorbance was measured at 414 nm on a VarioskanFlash (4.00.53) Microplate Reader. Results were with respect to the positive (Triton X-100) and

negative (PBS) controls. % hemolysis was determined by the equation: % hemolysis = $(\text{Abs.}_{\text{sample}} - \text{Abs.}_{\text{PBS}}) / (\text{Abs.}_{\text{Triton-X 100}} - \text{Abs.}_{\text{PBS}}) \times 100$.

2A.6.3.6 Trypsin Digestion Assay:

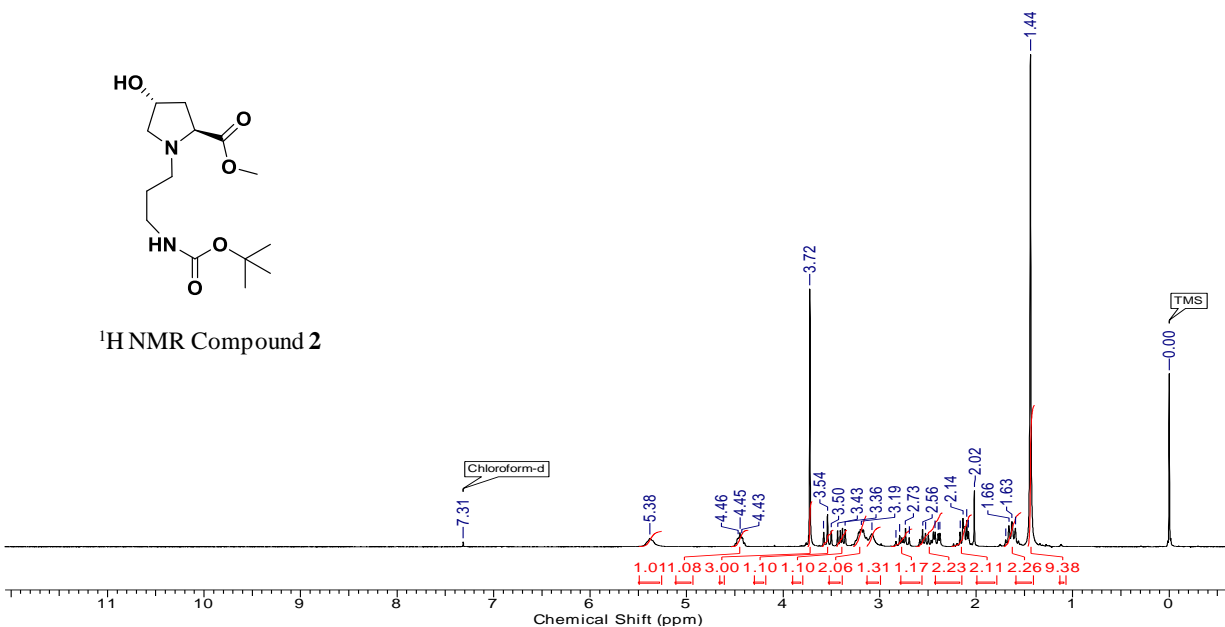
A reverse phase high-performance liquid chromatography (RP-HPLC) assay was used to assess proteolytic susceptibility. Peptide concentration was calculated by measuring the absorbance at 260 nm and using the extinction coefficient $\epsilon_{260\text{nm}} = 200 \text{ M}^{-1}\text{cm}^{-1}$ for phenylalanine. Peptide stock solutions were prepared in Tris-EDTA buffer. Cell culture grade trypsin from bovine pancreas was purchased from Thermo Fisher Scientific. Each trypsinolysis experiment was carried out at a peptide concentration of 10 mM, and run in triplicate. Following addition of trypsin (1 μL of 1X Tryple Express enzyme in 100 μL peptide solution), aliquots of the reaction were removed at different time intervals and quenched by combining a 10 μL aliquot of the trypsinolysis mixture with 10 μL of 2 % trifluoroacetic acid in acetonitrile. A portion (20 μL) of the quenched reaction mixture was subjected to RP-HPLC and the peaks obtained were analyzed. The extent of peptide trypsinolysis was determined by integrating the area of the peak corresponding to the intact peptide. The peaks observed in the HPLCs were collected and analyzed by matrix-assisted laser desorption/ionization–time of flight (MALDI-TOF) to identify the peptide fragments.

2A.7 Appendix A

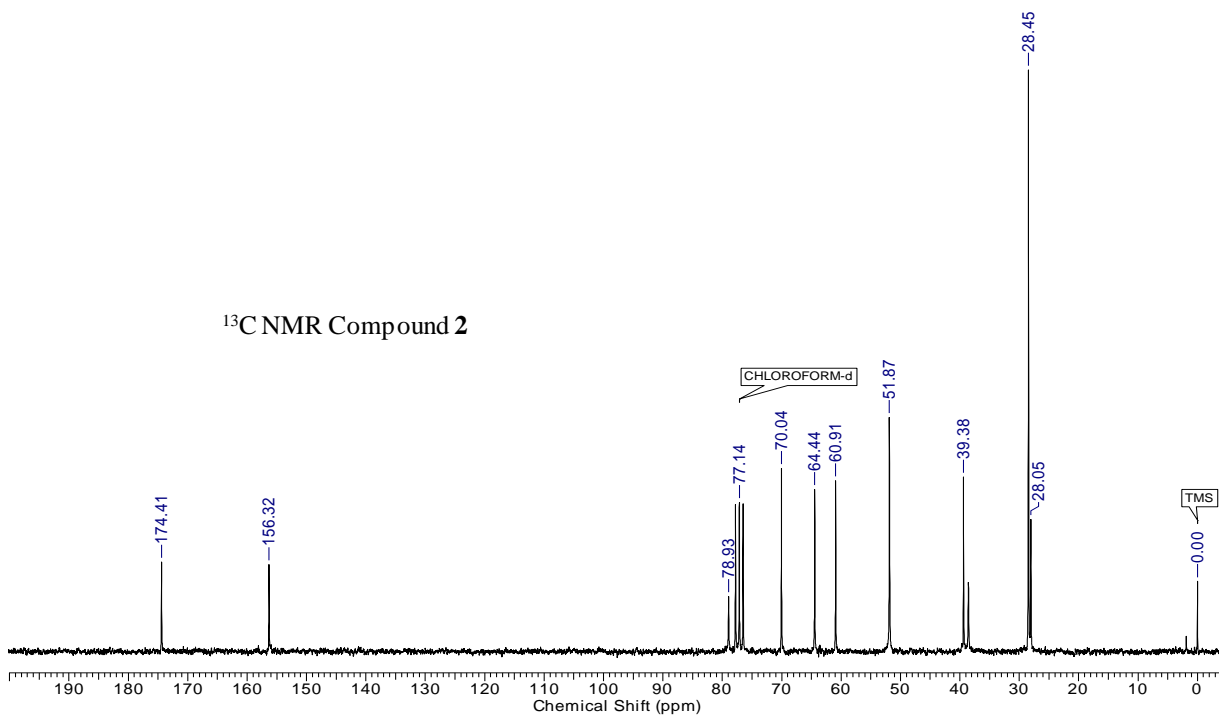
Compound and characterization	Page No.
Compound 2 : ^1H , ^{13}C & DEPT NMR, HRMS	65 - 66
Compound 3 : ^1H , ^{13}C & DEPT NMR, HRMS	67 - 68
Compound X : ^1H , ^{13}C & DEPT NMR, HRMS	69 - 70
RP-HPLC Chromatograms of the Tat peptides	71 - 72
MALDI-TOF spectra of peptides	73 - 76

(2*S*, 4*R*)-methyl-1-(3-(*tert*-butyloxycarbonyl-amino)propyl)-4-hydroxypyrrolidine-2-carboxylate (2)

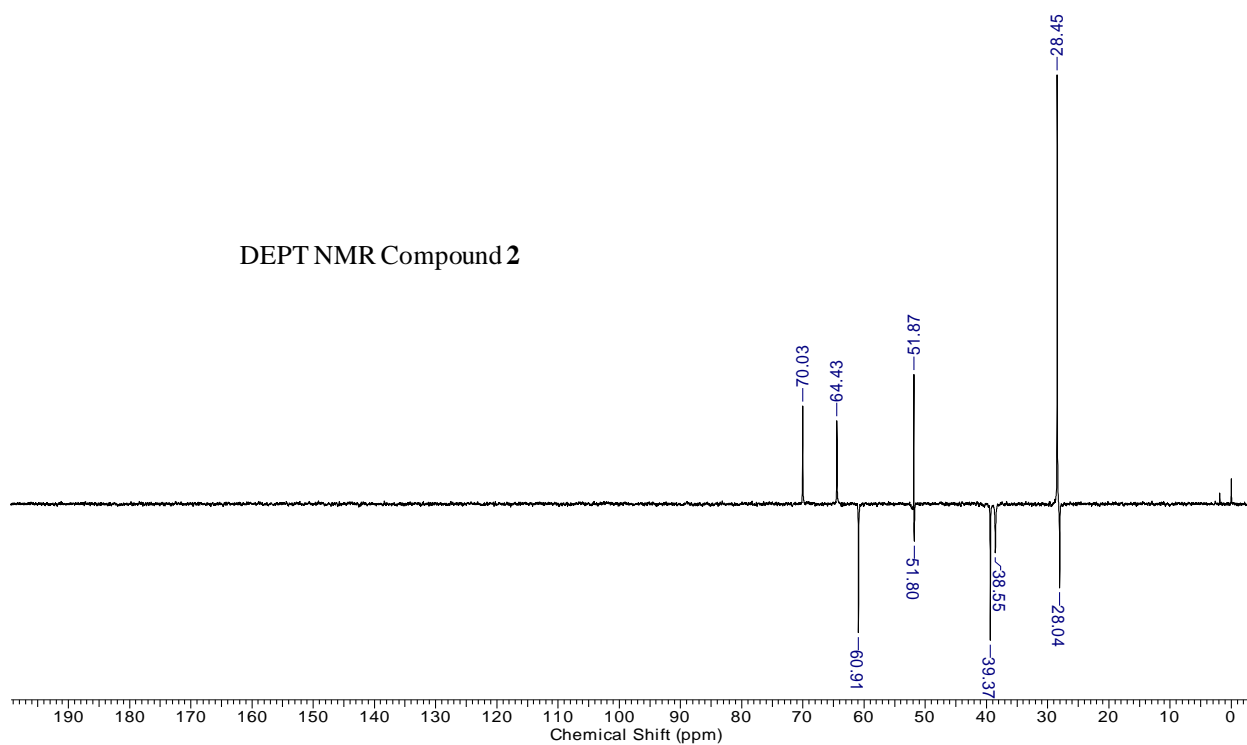
¹H NMR (200 MHz; CDCl₃) spectra of compound 2:



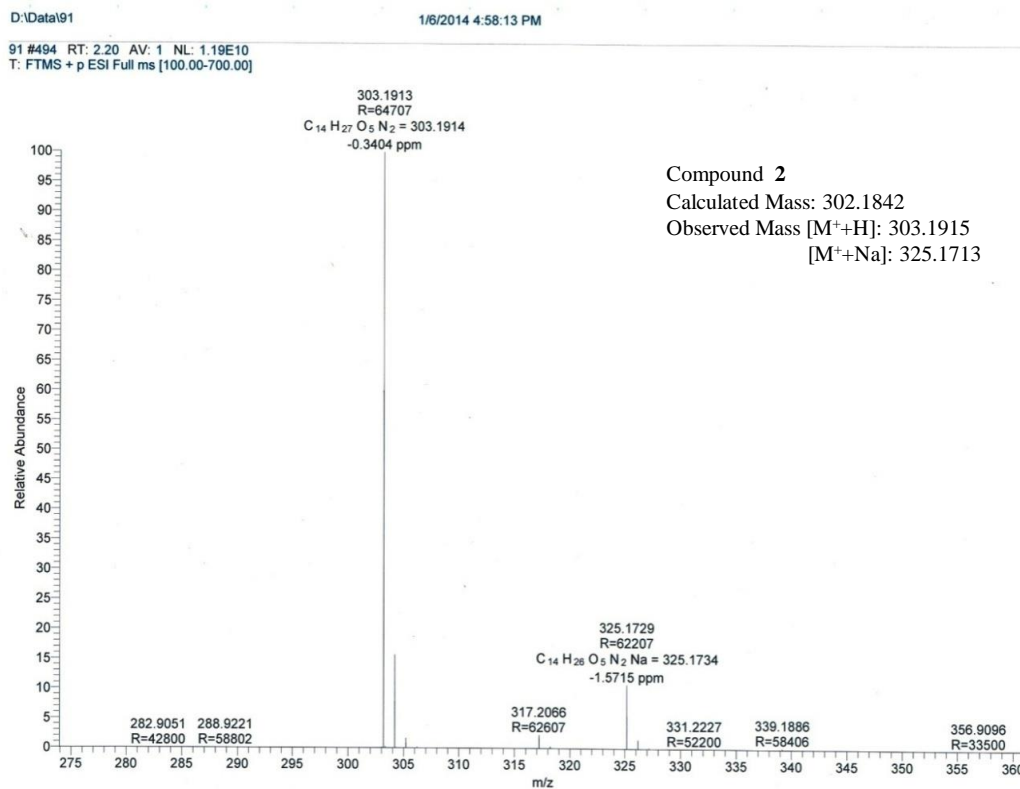
¹³C NMR (50 MHz; CDCl₃) spectra of compound 2:



DEPT NMR (50 MHz; CDCl₃) spectra of compound 2:

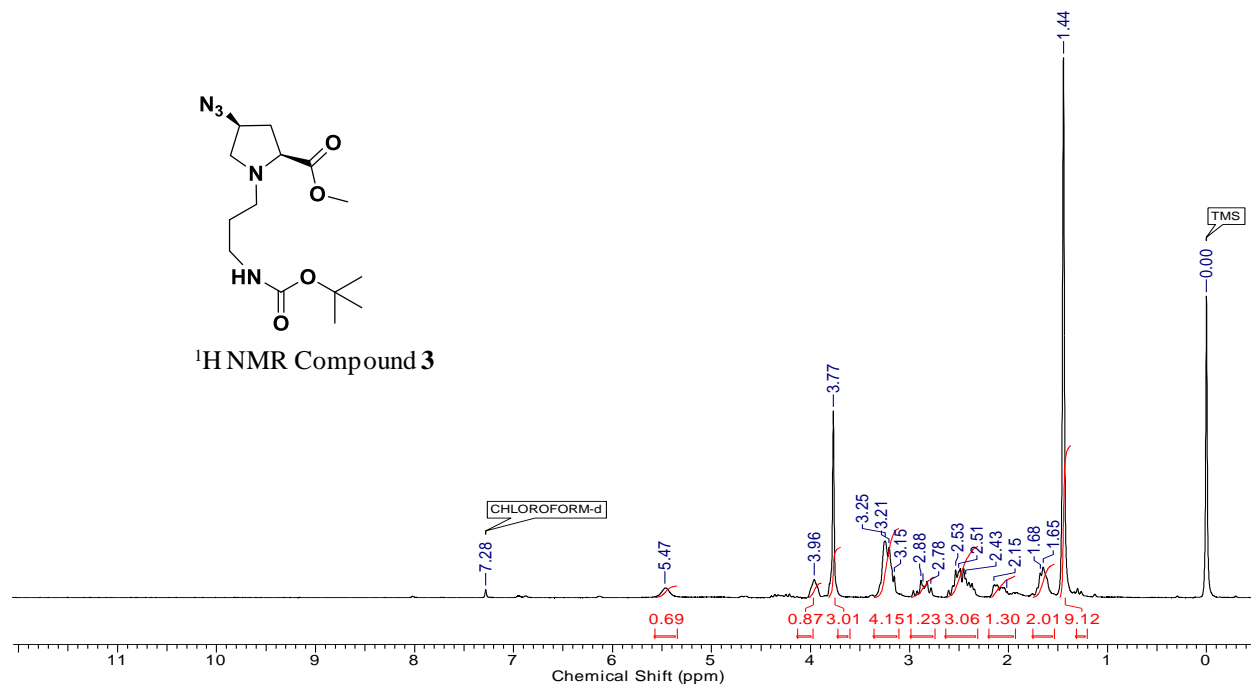


HRMA spectra of compound 2:

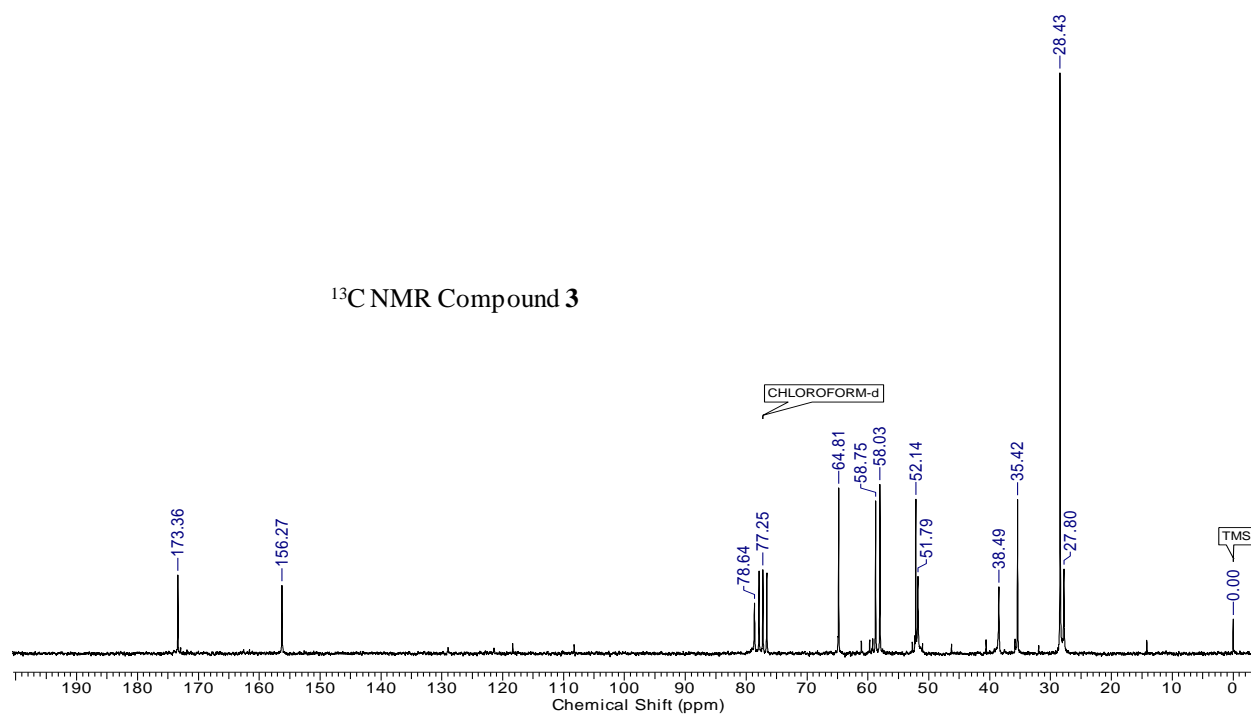


(2S,4S)-methyl-4-azido-1-(3-(*tert*-butyloxycarbonyl-amino)ethyl)pyrrolidine-2-carboxylate (3)

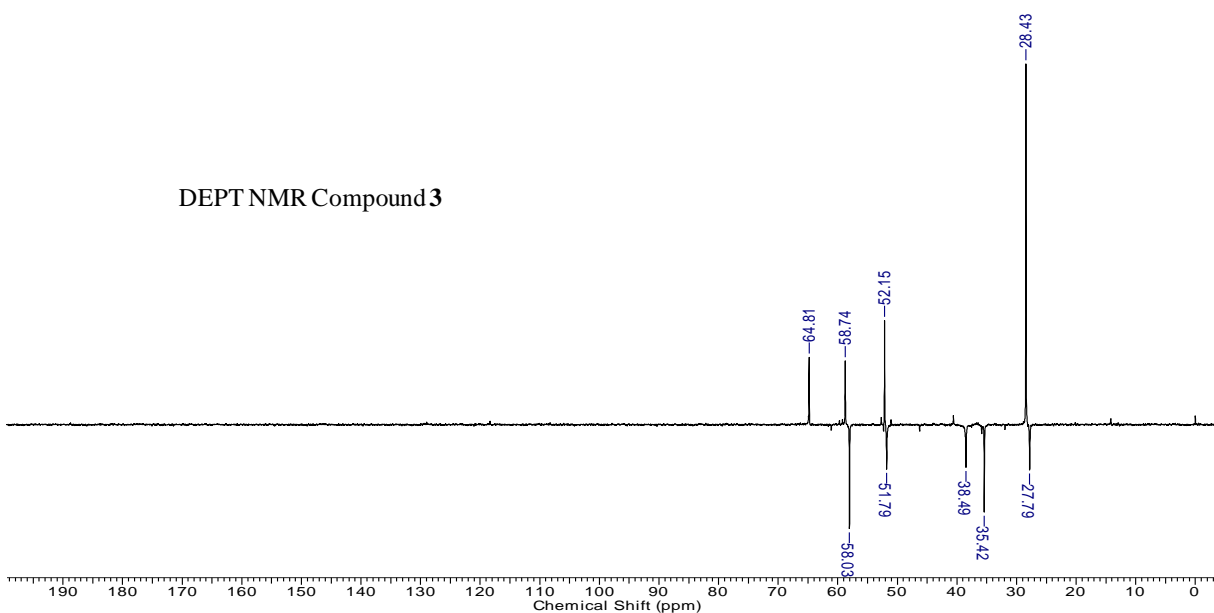
¹H NMR (200 MHz; CDCl₃) spectra of compound 3:



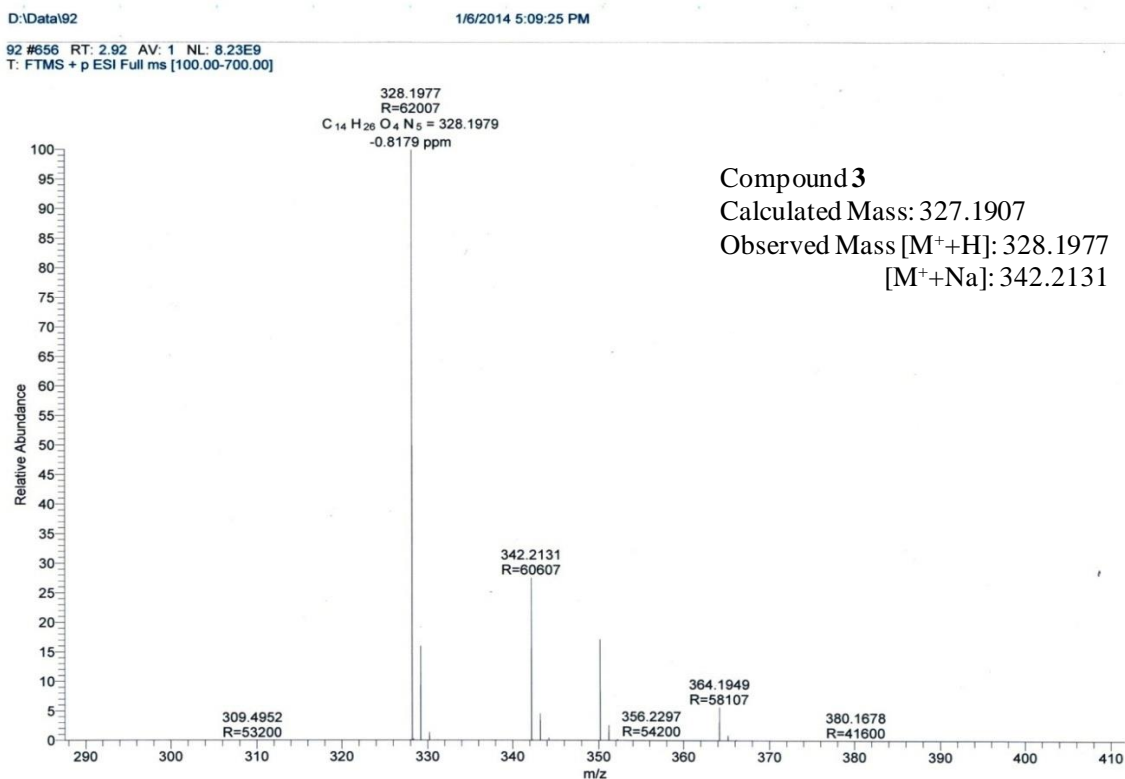
¹³C NMR (50 MHz; CDCl₃) spectra of compound 3:



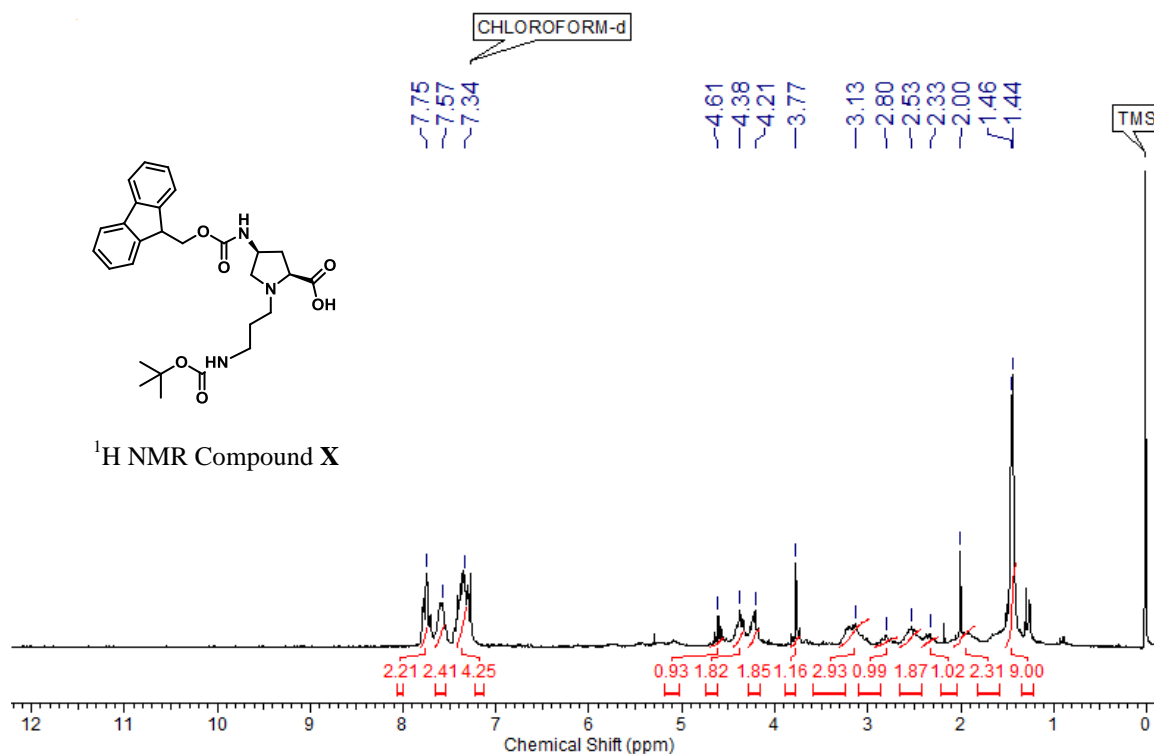
DEPT NMR (50 MHz; CDCl₃) spectra of compound **3**:



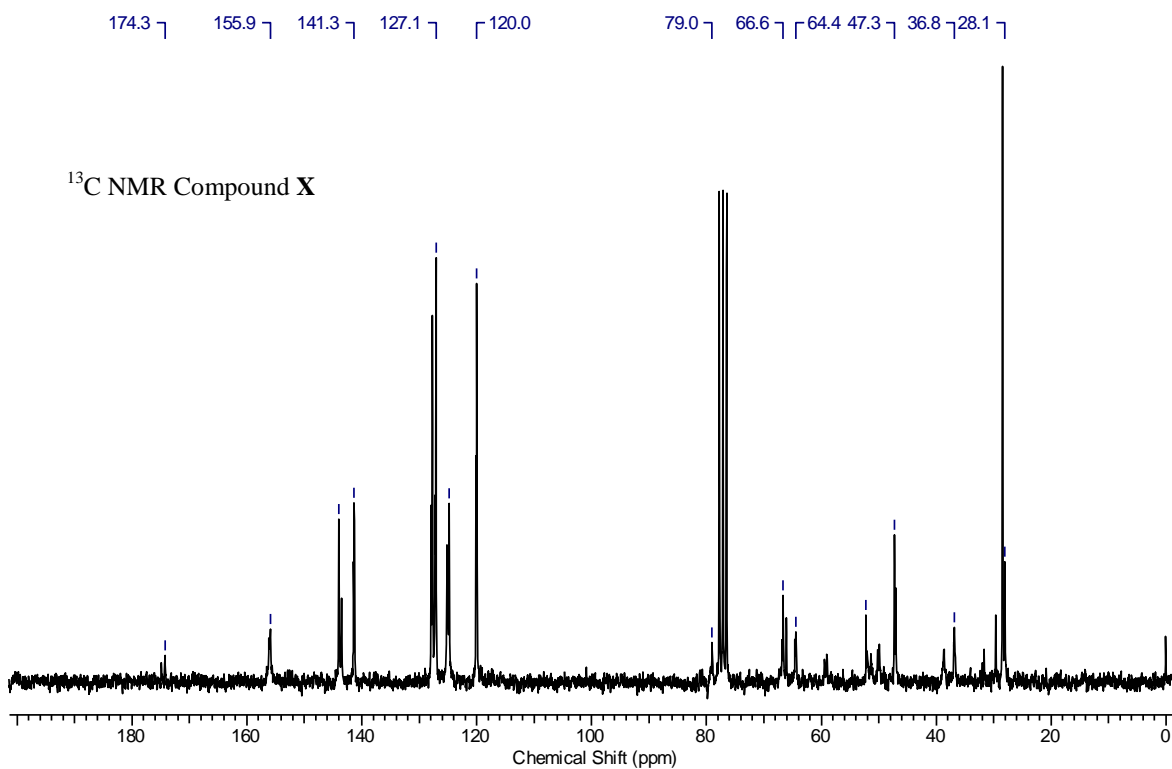
HRMA spectra of compound **3**:

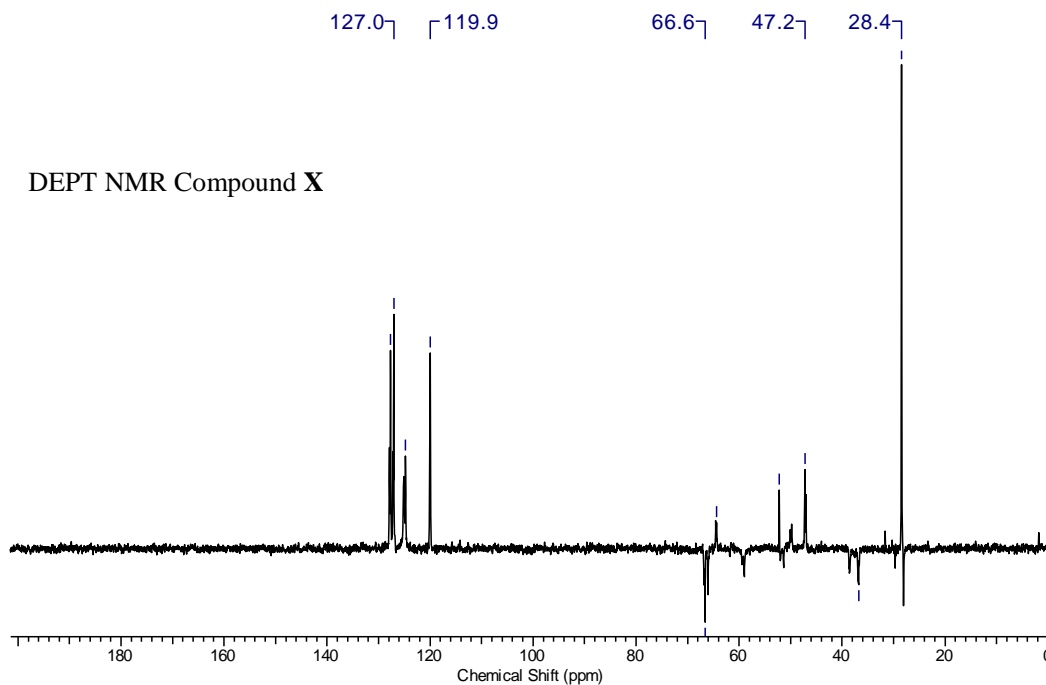


^1H NMR (200 MHz; CDCl_3) spectra of compound **X**:

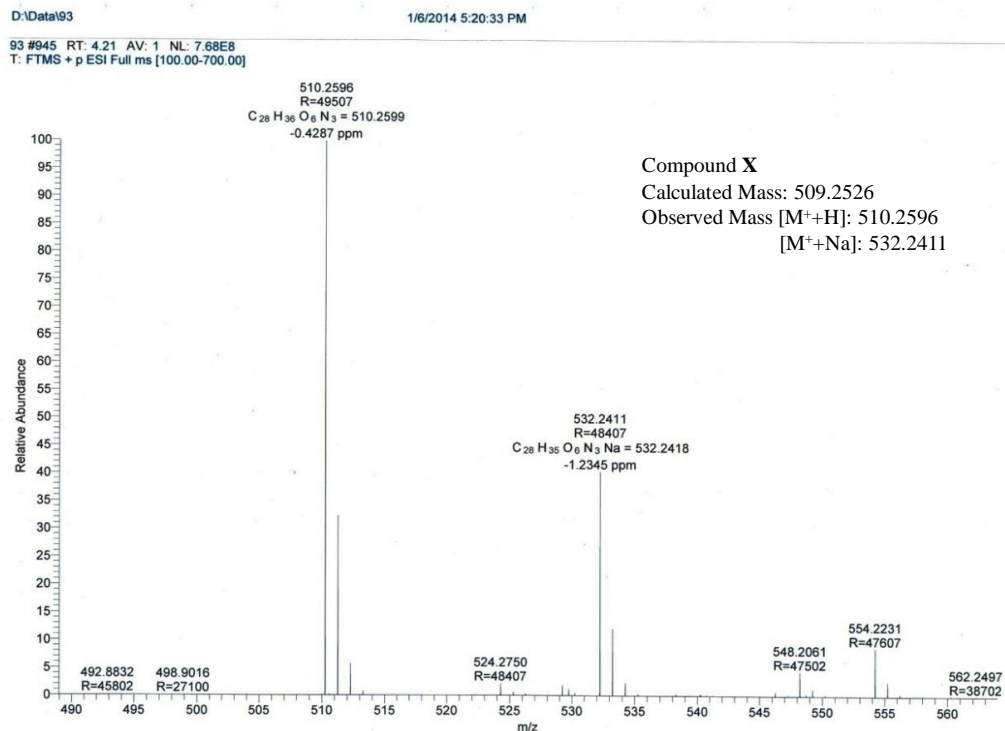


^{13}C NMR (50 MHz; CDCl_3) spectra of compound **X**:

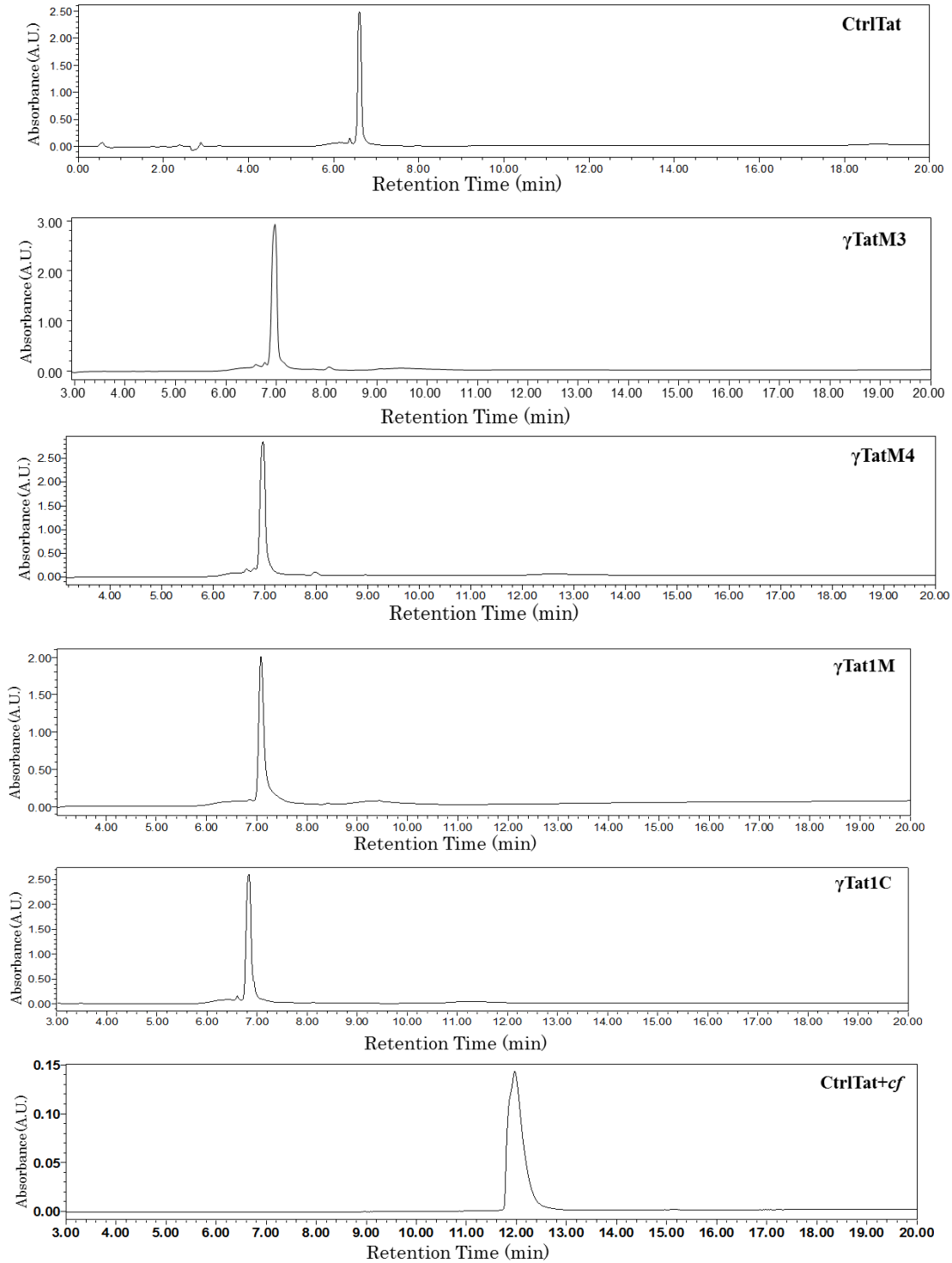


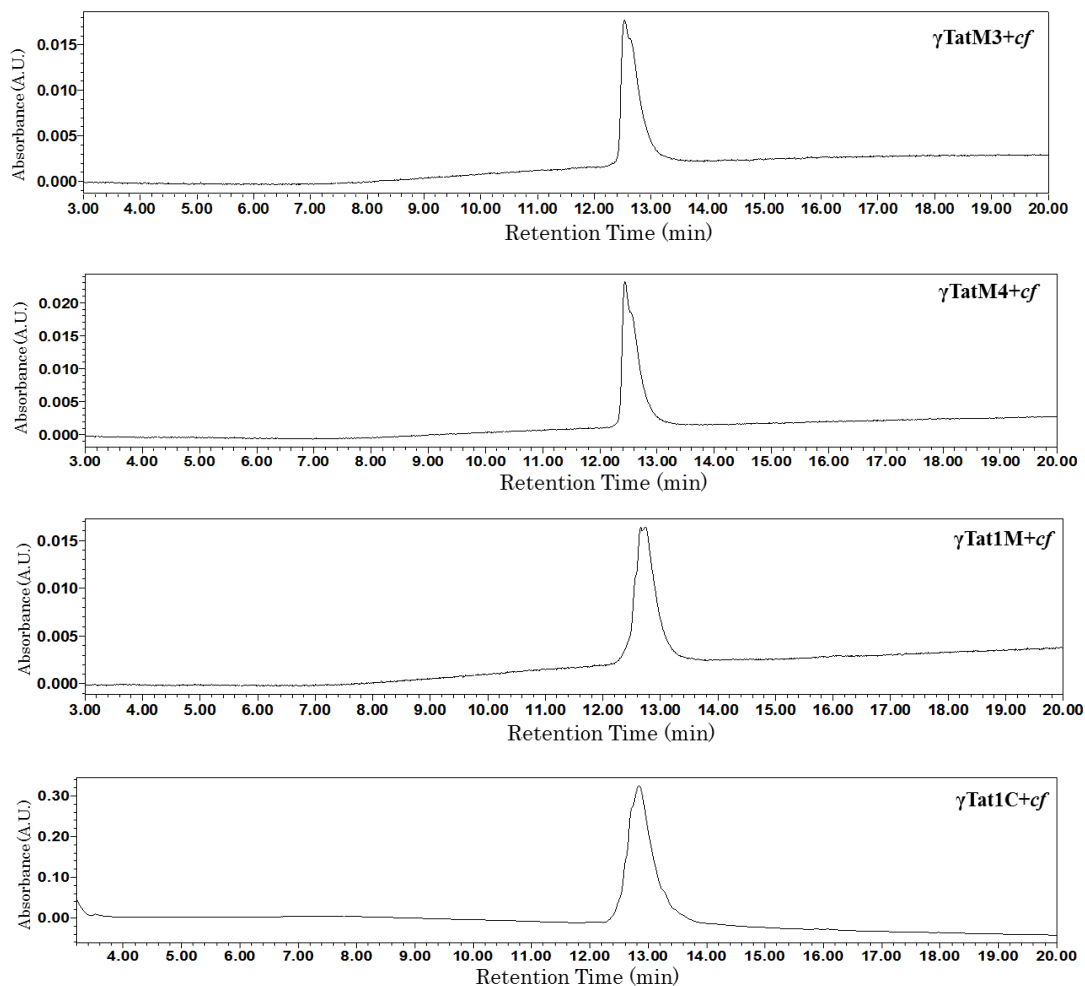
DEPT NMR (50 MHz; CDCl₃) spectra of compound X:

HRMA spectra of compound X:



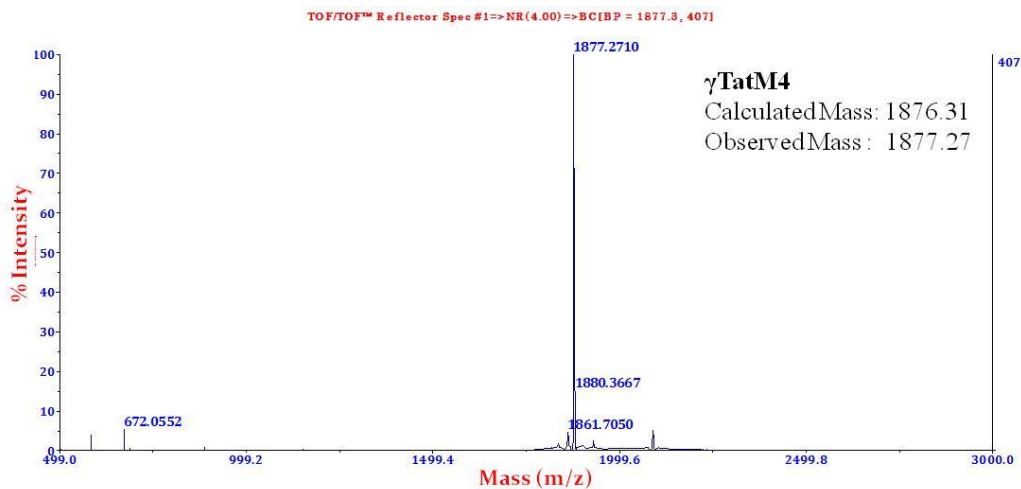
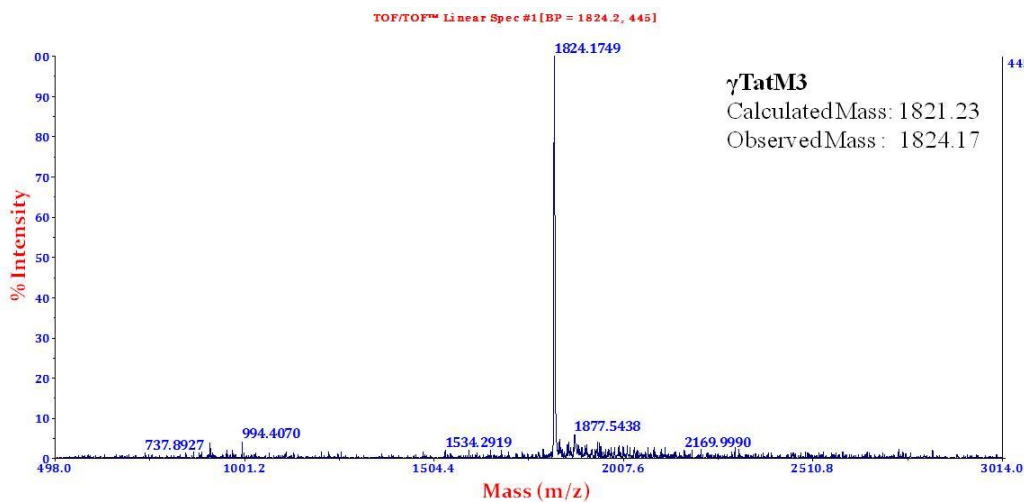
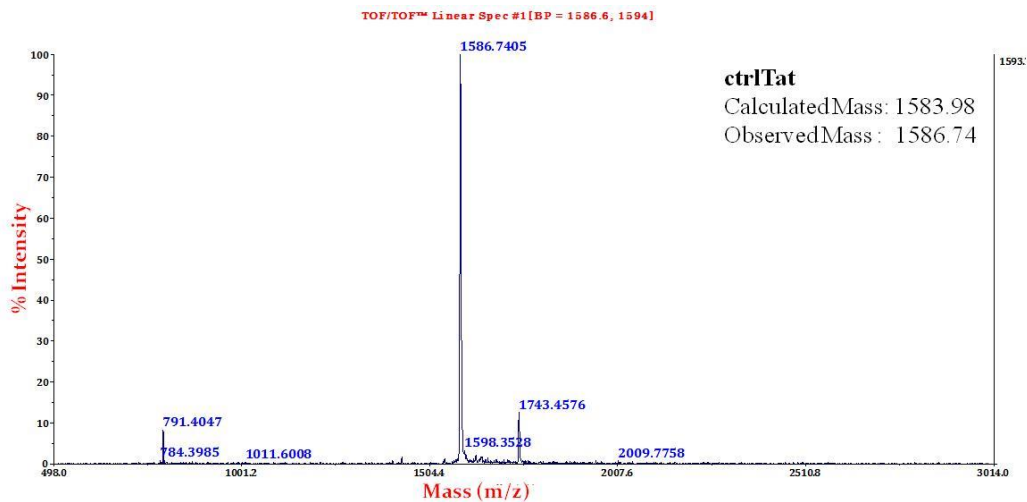
RP-HPLC chromatogram

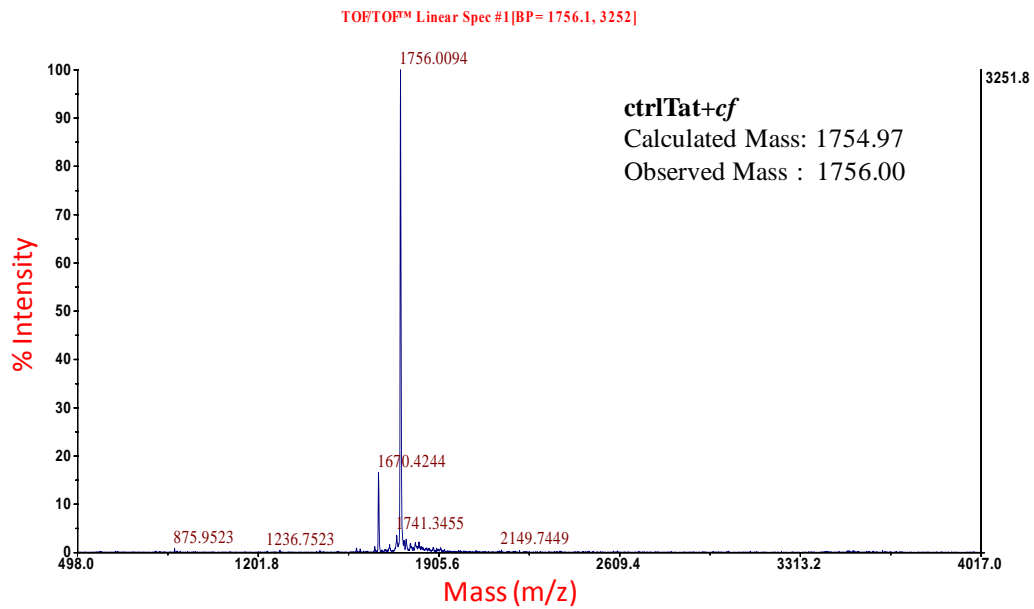
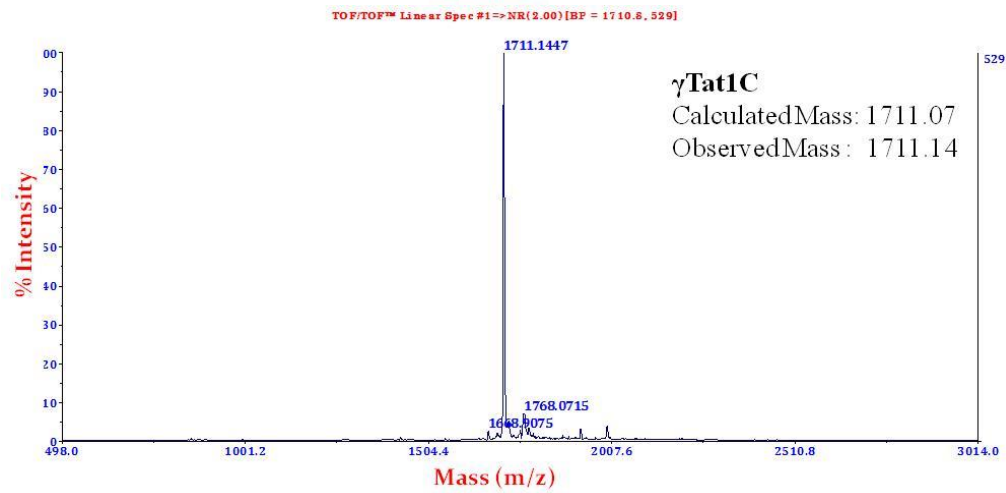
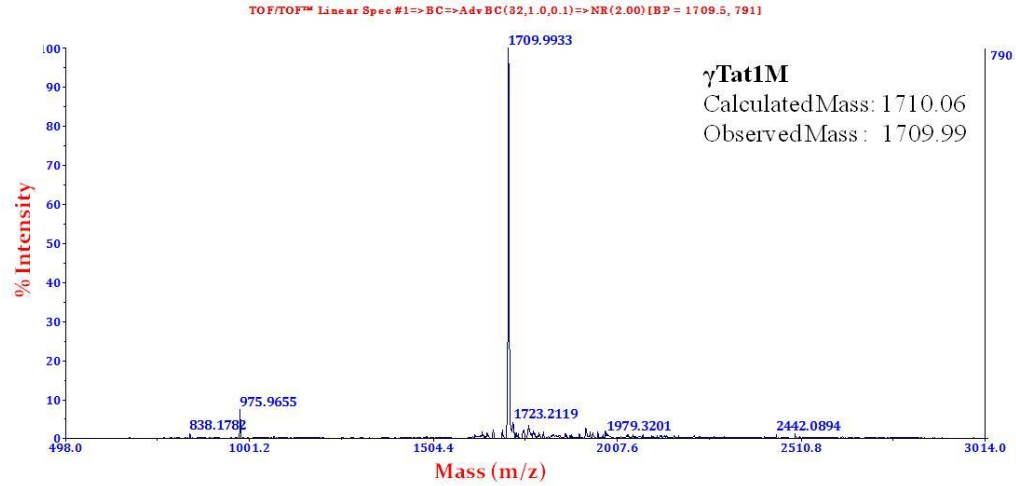


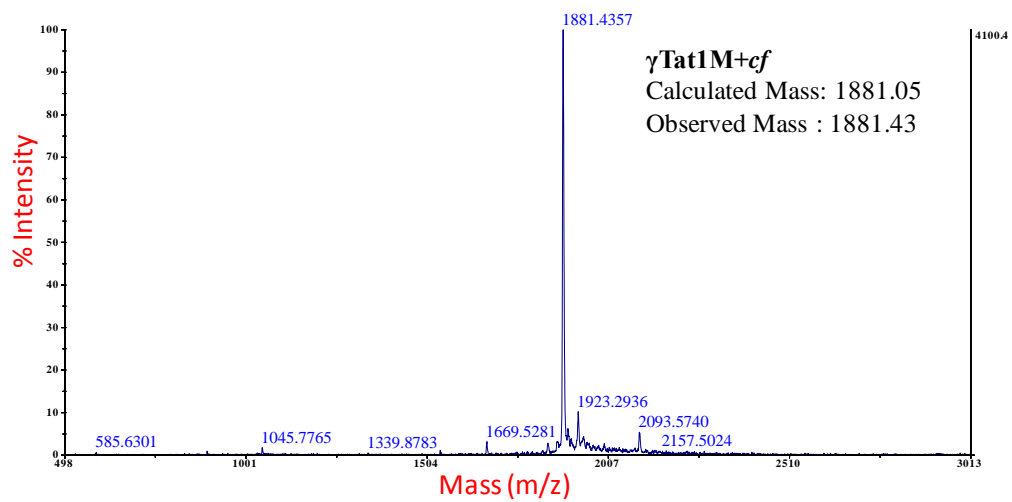
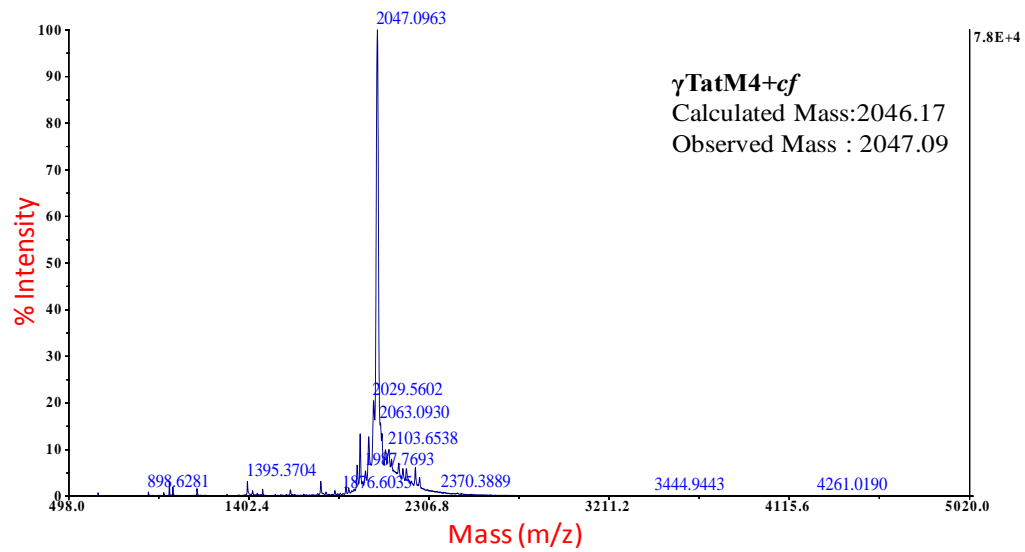
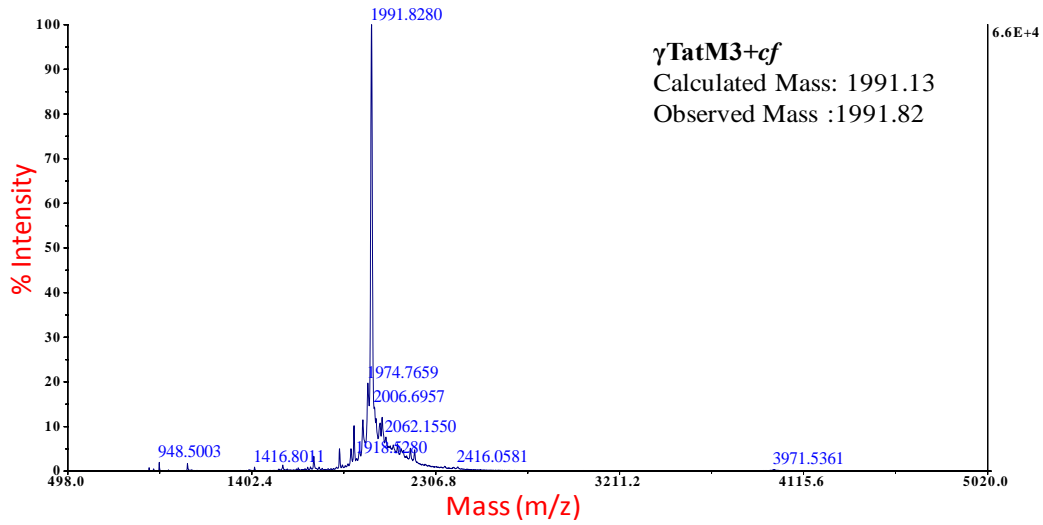


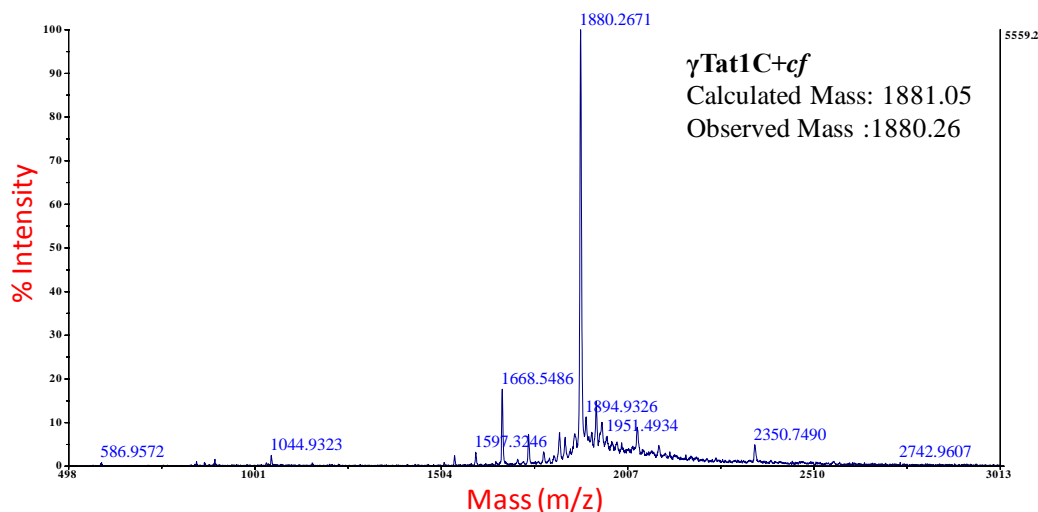
HPLC conditions: For unlabelled peptides, an increasing gradient of 5 to 50 % CH₃CN in water containing 0.1 % TFA in 10 min, followed by 50% CH₃CN/H₂O. For *cf*-labelled peptides, an increasing gradient of 5 to 50 % CH₃CN in water containing 0.1 % TFA in 20 min. The absorbance was monitored at 220 nm and 254 nm; the HPLC profiles at 220 nm are shown above.

MALDI-TOF spectra of peptides









2A.7 References

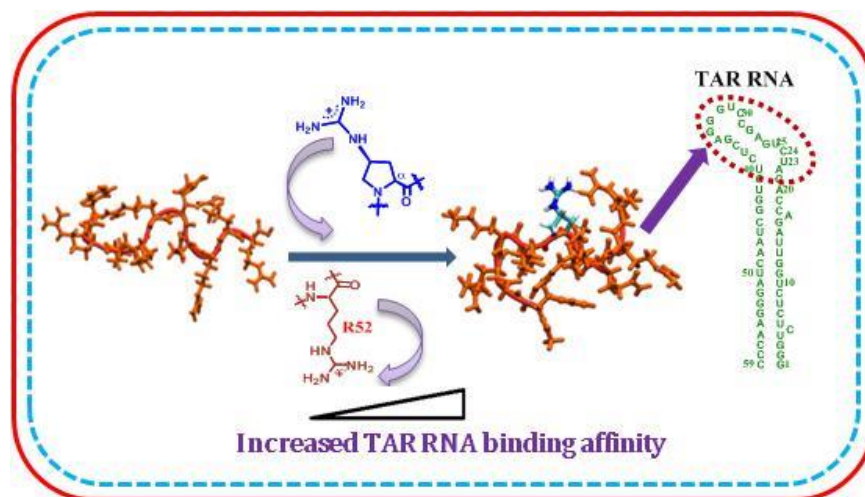
1. Takakura, Y.; Nishikawa, M.; Yamashita, F.; Hashida, M.; *Eur J Pharm Sci.*, **2001**, *13*,71–76.
2. Plank, C.; Tang, M. X.; Wolfe, A.R.; Szoka Jr, F.C.; *Hum Gene Ther*, **1999**, *10*, 319–32.
3. Kim, H.H.; Lee, W.S.; Yang, J.M.; Shin, S.; *BiochimBiophysActa*, **2003**, *1640*,129–36.
4. Bloomfield, V.A.; *CurrOpinStructBiol*, **1996**, *6*, 334–41.
5. Wolfert, M.A.; Seymour, L.W.; *Gene Ther.*, **1998**, *5*, 409–14.
6. Lewis, J.G.; Lin, K. Y.; Kothavale, A.; Flanagan, W. M.; Matteucci, M. D.; DePrince, R. B.; Mook, Jr, R. A.; Hendren, R. W.; Wagner. R. W.; *Proc.Natl.Acad.Sci. USA*, **1996**, *93*, 3176–3181.
7. Gottschalk, S.; Sparrow, J.T.; Hauer, J.; Mims, M.P.; Leland, F.E.; Woo, S.L.; Smith, L.C.; *Gene Therapy*, **1996**, *3*, 448–457.
8. Fant, K.; Rner, E.E.; Jenkins, A.; *Mol. Pharm.* **2010**, *7*, 1734–1746.
9. Ferrer-Miralles, N.; Vazquez, E.; Villaverde, A.; *Trends Biotechnol*, **2008**, *26*, 267–75.
10. Ignatovich, I.A.; Dizhe, E.B.; Pavlotskaya, A.V.; Akifiev, B.N.; Burov, S.V.; Orlov, S.V.; Perevozchikov, A.P.; *J. Biol.Chem.*, **2003**, *278*, 42625–36.
11. Manickam, D.; Bisht, H.; Wan, L.; Mao, G.; Oupicky, D.; *Journal of Controlled Release*, **2005**, *102*, 293–306.
12. Chauhan, A.; Tikoo, A.; Kapur, A.K.; Singh, M.; *Journal of Controlled Release*, **2007**, *117*, 148–162
13. Bhosle, G. S.; Nawale, L.; Yeware, A.; Sarkar, D.; Fernandes, M. *Unpublished data, Submitted.*

14. Gangamani, B. P.; Kumar, V. A.; Ganesh, K. N. *Tetrahedron*, **1996**, *57*, 15017–15030.
15. a) Patil, K. M.; Naik, R. J.; Rajpal; Fernandes, M.; Ganguli, M.; Kumar, V. A.; *Journal of the American Chemical Society*, **2012**, *134*, 7196–7199. b) Patil, K. M.; Naik, R. J.; Vij, M.; Yadav, A. K.; Kumar, V. A.; Ganguli, M.; Fernandes, M.; *Bioorg. Med. Chem. Lett.*, **2014**, *24*, 4198–4202.
16. (a) Chilukuri, H.; Kolekar, Y. M.; Bhosle, G. S.; Godbole, R. K.; Kazi, R. S.; Kulkarni, M. J.; Fernandes, M.; *RSC Adv.* **2015**, *5*, 77332–77340.
17. Pyle, A.M.; Rehmann, J.P.; Meshoyrer, R.; Kumar, C.V.; Turro, N.J.; Barton, J.K.; *J. Am. Chem. Soc.*; **1989**, *111*, 3051–3058.
18. Shahabadi, N.; Kashanian, S.; Khosravi, M.; Mahdavi, M.; *Trans. Metal Chem.* **2010**, *35*, 699–705.
19. Tabassum, S.; Al-Asbahy, W.M.; Afzal, M.; Arjmand, F.; Bagchi, V.; *Dalton Trans.* **2012**, *41*, 4955–5964.
20. Loret, E. P.; Georgel, P.; Johnson Jr., W. C.; Ho, P. S.; *Proc. Natl. Acad. Sci. USA*, **1992**, *89*, 9734–9738.
21. Demizu, Y.; Oba, M.; Okitsu, K.; Yamashita, H.; Misawa, T.; Tanaka, M.; Kurihara, M.; Gellman, S. H.; *Org. Biomol. Chem.*, **2015**, *13*, 5617–5620.
22. Lundberg, M.; Wikstrom, S.; Johansson, M.; *Mol. Ther.*; **2003**, *8*, 143.
23. Farrera-Sinfreu, J.; Giralt, E.; Castel, S.; Albericio, F.; Royo, M.; *J. Am. Chem. Soc.* **2005**, *127*, 9459–9468
24. Olsen, J. V.; Ong, S.-E.; Mann, M.; *Mol. Cell. Proteomics*, **2004**, *3*, 608–614.

CHAPTER 2

SECTION B

Superior HIV-1 TAR-Binders with Conformationally Constrained R52 Arginine Mimics in Tat (48-57) Peptide.



RNA–protein interactions, along with protein–protein interactions, control many functions in a living cell such as transcription, splicing, replication, transport, and catalysis. Realising the importance of RNA-mediated biological processes, molecules that can selectively bind and regulate the function of RNA have enormous potential application in biotechnology and therapeutics. In this chapter we reported the incorporation of two novel synthetic conformationally constrained arginine mimics, (2S,4S)-4-guanidinoproline and (2S,4S)-4-amino-N-(3-guanidinopropyl)-proline, instead of R52, which is known to be essential for specific binding to TAR RNA, in the Tat(48-57) peptide. The results indicated that the α Tat1M peptide containing (2S,4S)-4-guanidinoproline is far superior to γ Tat1M containing (2S,4S)-4-amino-N-(3-guanidinopropyl)-proline, or even the control Tat peptide, in binding to TAR RNA. The Tat mimetics were further found have better cell uptake properties in comparison to the control Tat peptide and were relatively non-toxic to mammalian cells, thus increasing their application potential as specific TAR-binding molecules to counter viral transactivation and thus, HIV-1.

2B.1 Introduction

Ribonucleic acid (RNA) is one of the important biomolecule which has many important functions *in vivo*. Many of these functions have been unexplored in the past decade. Although there are large numbers of literature reports, for the number of potential RNA targets. Although there are large number of reports for small molecules targeting DNA and proteins but comparatively few compounds are reported that target RNA with high affinity and specificity.^{1,2} Even though there are many naturally occurring modified nucleotides in RNA,^{3,4} it is originated from only four nucleobases. Chemical similarity of RNA with DNA and its less complexity than protein makes it unique target in many diseases. There are many classes of small molecules that bind DNA but not with RNA. This is due to the deep and narrow minor groove of RNA makes binding difficult to natural products. The binding to DNA occurs through base stacking and by interacting with the minor groove which is shallow and broad.^{5,6} The 3-dimensional structures of DNA and RNA are very different *in vivo*. The DNA has double stranded structure and gives helical shape but RNA has single stranded structure which folds into different secondary structures to minimize its energy similar to proteins. RNA forms unique binding pockets for small molecules, and this structural variation can be explored to design small molecules that specifically target RNA. Binding of antibiotics to the ribosome is the most well studied model.⁷ Structural diversity of RNA offers potential for selective recognition by small molecules. Hence targeting RNA could be a strategy for treating diseases. There is a scarcity of knowledge about the chemical scaffolds that are specific to bind RNA. The biased nature of high-throughput screening process for small molecules libraries to bind proteins makes them less successful. The most well-explored classes of compounds that modulate RNA function include antibiotics such as macrolides, aminoglycosides, oxazolidinones, and tetracyclines. In general, these compounds and derivatives have moderate affinities and selectivities for RNA. There are literature reports where use of these scaffolds were made to target RNA secondary structures, such as bulges^{8,9} and helices.¹⁰

As the interaction with RNA involves large surface area for recognition and tight binding is needed to achieve ideal RNA binding. The structural dynamics of RNA which results in to structural heterogeneity makes RNA targeting difficult task.¹¹

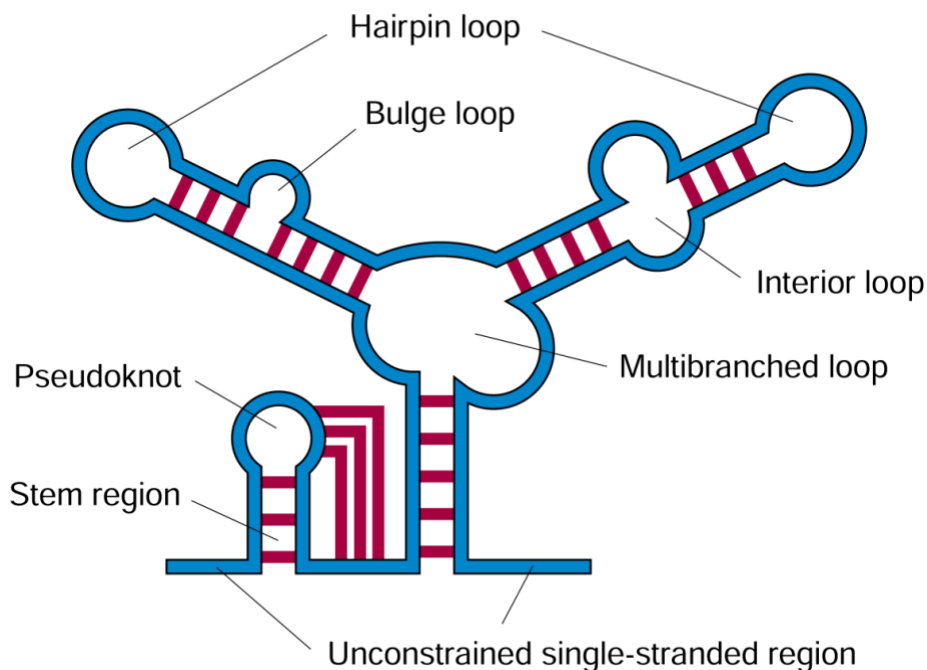


Figure 2B.1 Possible secondary structures in RNA.¹²

As RNA forms variety of secondary structures (Figure 2B.1) like hairpins, bulges, stems, loops, pseudo knots, and turns. The tertiary structures formed by the folding of these local structures such as bulges, loops, hairpins, stem etc. helps in recognition of RNA.¹² The ability of RNA to offer three-dimensional structure make it possible to target at a level that is not offered by DNA. However, the discovery of RNA-binding small molecules is not an easy task, since poor selectivity is a major hurdle, and RNA-targeting remains unachieved target.¹³ The most favorite approach of rational, structure-based RNA-targeted drug discovery is still in its initial stage, making the design of RNA ligands difficult.¹⁴ Designing of ligands for targeting RNA based on the knowledge of target RNA sequence is difficult. RNA-targeted gene silencing can be achieved using antisense or RNA interference technologies.¹⁵ There are several siRNAs are in clinical trials even though there are severe issues with drug characteristics such as cellular delivery, stability, and off-target effects.^{15,16}

Due to key role of human immunodeficiency virus-1 (HIV-1) transactivation response element (TAR) in viral replication, it is one of the most studied RNA target.¹⁷ HIV-1 TAR (Figure 2B.2) is made up of 59-nucleotide stem-bulge-loop secondary structure, which is found at the 5'-end of all nascent HIV-1 transcripts.¹⁸ The region from +19 to +42 bases of HIV-1 TAR consist of

hexanucleotide loop at the end of a helical stem containing a single, trinucleotide pyrimidine bulge. HIV-1 TAR RNA is the target of the 101-amino-acid Tat protein, which is the virally encoded trans-activator of HIV-1 transcription.¹⁹ Basal viral transcription is very low when the Tat protein is not associated with HIV-1 TAR, and short RNA transcripts are generated.²⁰ When the Tat–TAR RNA complex is formed, cofactors such as cyclin T1 and its cognate kinase CDK9 stimulate efficient transcription from the long terminal repeat (LTR).¹⁹ To control the proliferation of the virus and provides a potential anti-HIV therapy, blocking this Tat–TAR interaction is a potent strategy for HIV-1 AIDS.

2B.2 Rationale, design and objectives of the present work

Drugs that exhibit novel modes of action are most important because resistance to current HIV therapies has been observed.²¹ Till date no drug has been reached to the clinic even though significant efforts from scientific community has been made. Different strategies have been employed to inhibit the Tat–TAR interaction.^{13,22-27} TAR RNA decoys^{28,29} has been investigated but their large size causing serious issues in delivery. Compounds of intermediate size like oligomeric amines³⁰ and β -hairpin peptidomimetics^{31,32} can be an ideal choice as therapeutics to target Tat-TAR interactions. The compounds with intermediate size offers better overlap with the large surface area of RNA. Recently cyclic peptide L50 has shown inhibition of Tat-dependent transcription process and the reverse transcription which results in to increased antiviral activity.³³ The interaction of Tat protein with TAR RNA leads to the formation of more copies of viral transcript leading to the progression of AIDS.³⁵ The Tat-TAR interactions are localized mainly to a trinucleotide pyrimidine bulge (residues U23-U25) and adjacent duplex region in TAR RNA³⁶ and the 11-amino acid basic region of Tat³⁷ (residues 47-57, YGRKKRRQRRR) (Figure 2B.2). The disruption of this interaction, is thus, an area of much research towards the control of HIV-1. In this direction, a variety of ligands²⁵ including peptides³⁸ besides Tat, peptidomimetics,³⁹ peptoids,⁴⁰ peptide nucleic acids⁴¹ and small molecules like aminoglycoside, macrolide, oxazolidinone, and tetracycline antibiotics⁴²⁻⁴⁷ were reported.

Backbone-modified Tat analogues including a D-peptide⁴⁸, an oligocarbamate,⁴⁹ an oligoureia⁵⁰ and various peptoid-based structures⁴⁶ have been reported and preserve the side chains of the Tat (47-57) peptide, but vary (in spacing and/or chirality) the relative positions of the functional

groups. The success of these analogues in disrupting the Tat-TAR interaction further endorses the importance of the cationic nature of the peptide and also the relative presentation of cationic groups in determining the binding affinity. In spite of these reports, there still exists a pressing need for newer effective agents that can selectively and strongly bind TAR RNA and thus act against HIV by inhibiting viral transactivation. Further, although proteolytically stable peptide derivatives have been used previously to target TAR,^{48,51} linear peptide analogues were found highly flexible and therefore bound various RNAs, preventing sufficient activity in cells. Therefore, we focused our attention on conformationally constrained mimics of HIV-1 Tat. Arginine 52 (R52) has been shown to be essential for TAR-binding,⁵² through possible bidentate hydrogen-bonding specifically with the two phosphates between residues A22-U23-C24, and possibly also with the ribose 2'-OH groups, of the trinucleotide bulge region of TAR RNA. The presentation of the forked arginine guanidine group in the context of flanking cationic residues is particularly important for the binding of Tat(47-57) to TAR RNA. We therefore chose to replace R52 with conformationally constrained mimics, and envisioned the modulation of Tat-TAR binding through the use of proteolytically stable analogues. Our designed synthetic arginine mimics- two non-natural pyrrolidine-based amino acids- (2*S*,4*S*)-4-guanidinoproline and (2*S*,4*S*)-4-amino-*N*-(3-guanidinopropyl)-proline, were incorporated at position 52 of the Tat(48-57) peptide, in lieu of arginine (Figure 2B.2). We report herein the interesting effect of the inclusion of these arginine mimics on the binding ability of the resulting Tat peptides to TAR RNA, and find that these are distinctly different.

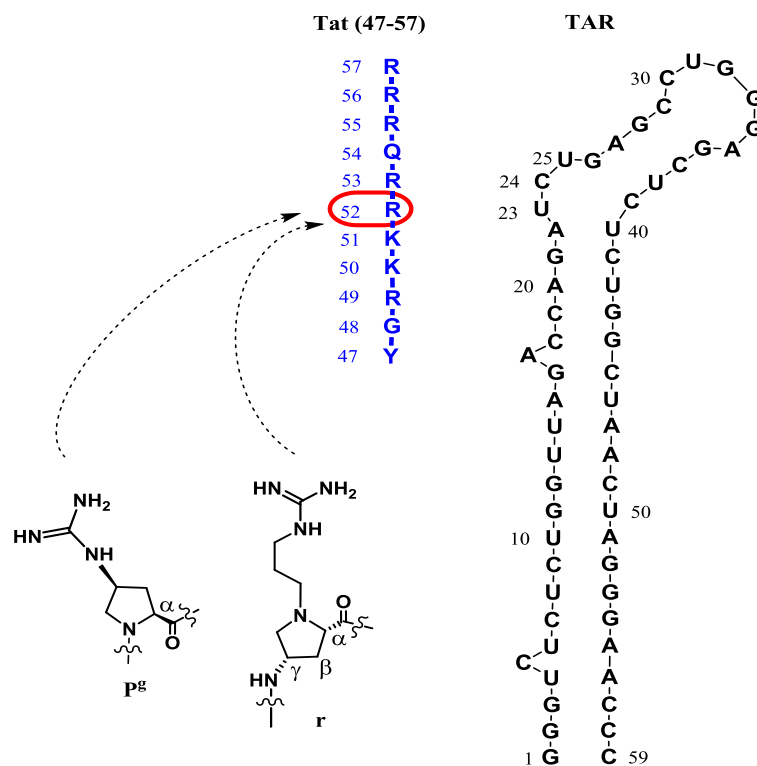


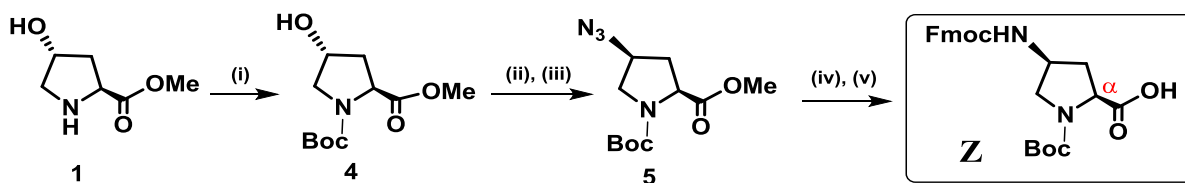
Figure 2B.2. TAR RNA, the Tat (47-57) peptide and proposed arginine mimics.

2B.3 Results and Discussion

2B.3.1 Synthesis of arginine surrogates

The synthesis of the non-natural arginine surrogates (Figure 2B.2) was accomplished as described earlier.^{53,54} In brief, the orthogonally protected precursor for (2*S*,4*S*)-4-guanidinoproline, i.e., (2*S*,4*S*)-*N*1-Boc-4-(Fmoc-amino)proline **Z** (Scheme 2B.1),⁵³ was synthesized starting from naturally occurring (2*S*,4*R*)-4-hydroxyproline, following sequential steps of *N*-Boc protection, esterification, S_N2 inversion of the 4(*R*)-hydroxy group to the corresponding 4(*S*)-azide through a mesyl intermediate, reduction of the azide by hydrogenation, Fmoc-protection of the resulting amine and finally ester hydrolysis to yield the *N*1-Boc-4(*S*)-(Fmoc-amino)-proline derivative (**Z**) suitable for use in solid phase synthesis. The 4-amino group in **Z** was converted to the corresponding guanidino derivative, **P^g** (Figure 2B.2), subsequent to peptide synthesis, just prior to cleavage from the solid support. The precursor to (2*S*,4*S*)-4-Amino-*N*1-(3-guanidinopropyl)-proline, i.e., (2*S*,4*S*)-4-(Fmoc-amino)-*N*1-((3-Boc-

amino)propyl)-proline, **X** (Scheme 2A.1), was also synthesized from the naturally occurring (2*S*,4*R*)-4-hydroxyproline as described earlier,⁵⁴ following sequential steps of



Scheme 2B.1. Synthesis of the monomer **Z**, precursor to arginine mimic **P^g**.

Reagents and conditions: (i) (Boc)₂O, NaOH, H₂O-dioxane, 84 % (ii) MsCl, Et₃N, CH₂Cl₂, 71 % (iii) NaN₃, DMF, 65°C, 67 % (iv) (a) H₂, Pd/C, MeOH, (b) LiOH, then HCl, 62 % over (a) and (b) (v) (a) Fmoc-Cl, NaHCO₃, H₂O-dioxane, (b) Dowex H⁺ resin. 58 % over (a) and (b).

esterification, *N*-alkylation, S_N2 inversion of the 4(*R*)-hydroxy function to the corresponding 4(*S*)-azide through a mesyl intermediate, reduction of the azide to the corresponding amine followed by ester hydrolysis and finally amine protection as an Fmoc-derivative to yield the orthogonally protected monomer **X**, suitable for use in solid phase synthesis. The pendant amino group of the *N*3-aminopropyl segment was converted to its guanidino derivative, **r** (Figure 2B.2), subsequent to peptide synthesis, just prior to cleavage from the solid support.

2B.3.2 Synthesis of Tat peptide oligomers

The orthogonally protected monomers **Z** and **X** (For **X** described in section A) described above were utilized in the solid phase synthesis of the αTat1M and γTat1M peptides respectively, listed in (Table 2B.1). The chemical structures of the peptides are illustrated in Figure 2B.3.

The peptides were assembled on MBHA resin by either Fmoc- or Boc-chemistry protocols, as required. β-Alanine was coupled as the first spacer amino acid, followed by the coupling of other amino acids. All the coupling steps were done in dry DMF in presence of DIPEA, with HOBT and TBTU as coupling agents. Removal of the Boc-protecting group was achieved using 50% TFA in CH₂Cl₂, while the Fmoc group was removed using 20% piperidine in DMF. A phenylalanine residue was added at the *N*-termini of the peptides in order to facilitate concentration calculation from the absorbance.

Guanidinylation of monomers **Z** and **X** to arginine surrogates **P^g** and **r** respectively were performed on the solid support after *N*-acetylation of the phenylalanine residue at *N*-terminus,

and deprotection of the appropriate amino group, using 1*H*-pyrazole-1-carboxamide hydrochloride and DIPEA in dry DMF. The peptides α Tat1M and γ Tat1M thus contain one P^g and r unit respectively, towards the middle of the oligomer.

Table 2B.1 Oligomers of the study.

Code	Peptide
CtrlTat	Ac-FGRKKRRQRRR-NH ₂
α Tat1M	Ac-FGRKKP ^g RQRRR- β Ala-NH ₂
γ Tat1M	Ac-FGRKKrRQRRR- β Ala-NH ₂
CtrlTat- <i>cf</i>	<i>cf</i> -GRKKRRQRRR-NH ₂
α Tat1M- <i>cf</i>	<i>cf</i> -GRKKP ^g RQRRR- β Ala-NH ₂
γ Tat1M- <i>cf</i>	<i>cf</i> -GRKKrRQRRR- β Ala-NH ₂
TAR RNA:	
5'-r(GCAGAUUCUGAGCCUGGGAGCUCUCUGC)	

A control Tat peptide (CtrlTat) was also synthesized for comparison. For cell uptake studies, the peptides were tagged with fluorescein at their N-termini by treating them with 5/6-carboxyfluorescein in the presence of HOBt and diisopropyl carbodiimide (DIPCDI) as coupling agents. This yielded fluorescein-tagged peptides Ctrl-*cf*, α Tat1M-*cf* and γ Tat1M-*cf*. The synthesized peptides were cleaved from the resin by the TFA-TFMSA cleavage protocol and purified by RP-HPLC on a C18 column. Their purity was re-checked by analytical HPLC and all the peptides were characterized by MALDI-TOF analysis.

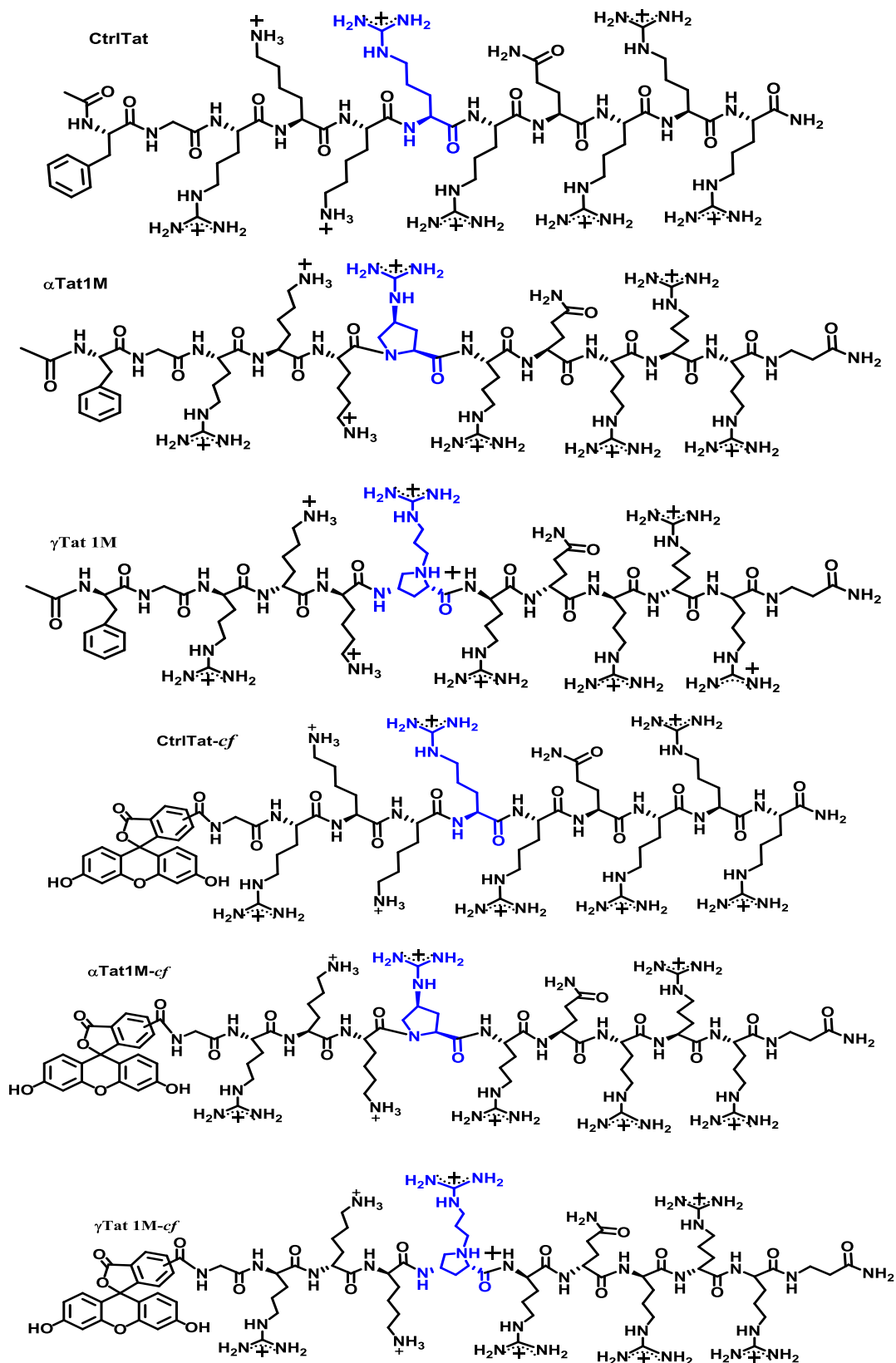


Figure 2B.3. Chemical structures of peptide of the study.

2B.3.3 UV-Melting Studies

UV-melting experiments were performed to test the thermal stability of the TAR RNA hairpin in the absence and presence of varying amounts of Tat peptide. The UV melting curves for the TAR RNA hairpin duplex in the absence and presence of the peptide, at a peptide to RNA ratio of 0:1, 1:1, 2:1, and 3:1 are shown in Figure 2B.4. The data are listed in Table 2B.2. The TAR RNA itself exhibited a T_m of 67.0 °C, as reported earlier.⁵⁵ Increase in the thermal stability of the RNA has been observed in the presence of peptide as increase in T_m was clearly observed. The addition of peptide at a [peptide]/[RNA] ratio of 1:1 led to peptide-induced T_m enhancement ($\Delta T_m = 0.9$ to 1.7 °C). Higher [peptide]/[RNA] ratios resulted in a further increase in the T_m of the RNA hairpin ($\Delta T_m = 1.7$ to 3.7 °C for a ratio of 1:3). This increase in the T_m at higher ratios is probably a result of secondary binding events.

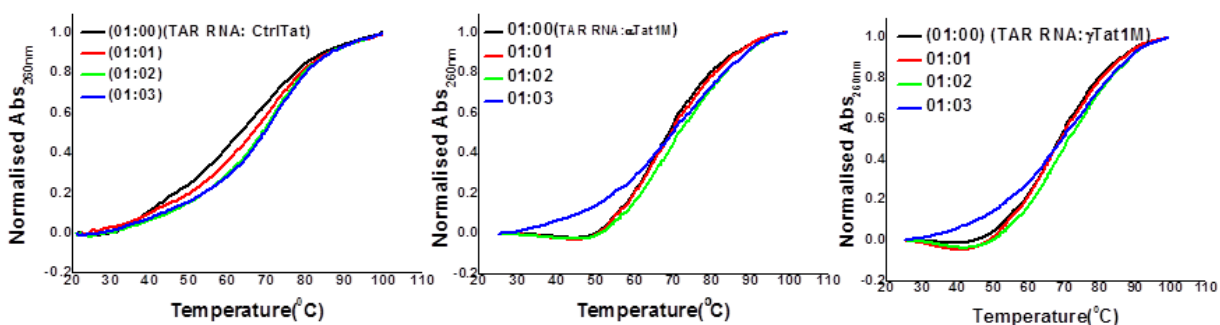


Figure 2B.4. UV-thermal melting profiles of HIV-1 TAR RNA alone and in the presence of the Tat peptides of the study.

Table 2B.2. UV-thermal melting data of HIV-1 TAR RNA alone and in the presence of the Tat peptides .

Peptide	UV- T_m in °C (ΔT_m , °C)*		
	TAR RNA: peptide ratio		
	1:1	1:2	1:3
CtrlTat	68.0 (1.0)	69.2 (2.2)	70.1 (3.1)
α Tat1M	68.7 (1.7)	69.3 (2.3)	70.7 (3.7)
γ Tat1M	67.9 (0.9)	67.8 (0.8)	68.7 (1.7)

*The values of ΔT_m in parentheses indicate the difference in T_m between the TAR RNA:peptide complex and TAR RNA alone. T_m of TAR RNA alone = 67.0 °C. Experiments were carried out in triplicates (± 1).

2B.3.4 Isothermal Titration Calorimetric evaluation of the Tat-TAR binding

Measuring thermodynamic parameters of peptide binding to RNA offers valuable information of the molecular forces involved in complex formation that cannot be obtained by structural studies alone. Thermodynamic analysis plays important role in designing and development of peptides as future drugs. Isothermal titration calorimetry (ITC) was therefore carried out to thermodynamically evaluate the binding of the Tat peptides to TAR RNA. Figure 2B.5 shows representative ITC profiles resulting from the injection of the Tat peptides into a solution of the TAR RNA stem-loop. The upper panels of Figure 2B.5, shows that each of the heat burst curves corresponds to a single peptide injection. The injection heats were determined by integrating the areas under these heat burst curves. The correction of injection heats were done by subtraction of the corresponding dilution heats derived from the injection peptides into buffer alone.⁵⁵

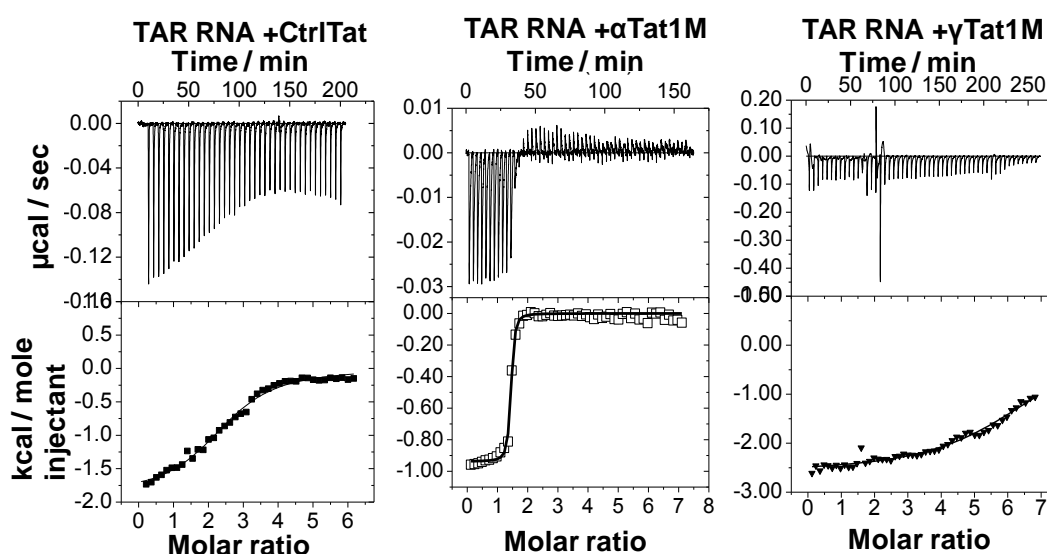


Figure 2B.5. ITC profiles for the interaction of Tat peptides of the study with TAR RNA. Upper panels: each of the heat burst curves corresponds to a single peptide injection. Lower panels: corrected injection heats as a function of the [peptide]/[RNA] ratio.

In Figure 2B.5, the bottom panels show the resulting corrected injection heats plotted as a function of the [peptide]/[RNA] ratio. The injection heat data corresponding to the titration of the RNA with peptide were fitted with a model for one set of binding sites. The derived parameters from these fits are summarized in Table 2B.3. ITC studies showed that α Tat1M peptide binds to one site on TAR RNA with strong affinity, $K_a = 2.40 \times 10^6 \text{ M}^{-1}$ compared to γ Tat1M and CtrlTat peptides with K_a values $3.03 \times 10^4 \text{ M}^{-1}$ and $2.94 \times 10^4 \text{ M}^{-1}$ respectively. As observed from Table

2B.3, the binding is associated with a binding stoichiometry (n) of approximately 1.4 peptide molecule/RNA in case of α Tat1M. However the binding of CtrlTat and γ Tat1M is accompanied by a stoichiometry (n) of 2.5 and 6.7 respectively. The lower stoichiometry for the α Tat1M binding is probably indicative of specific and strong binding, in contrast to non-specific binding due to electrostatics alone. The entropy change (ΔS) associated with the binding of α Tat1M to TAR RNA (0.030 Kcal/mol) is also higher compared to CtrlTat and γ Tat1M (0.0189 and 0.0164 Kcal/mol respectively).

Table 2B.3. ITC-Derived Parameters at 25 °C for the complexation of Tat peptides with TAR RNA.

Peptide	K_a (M^{-1})	Stoichiometry (n)	ΔH Kcal/mol	T ΔS Kcal/mol	ΔG Kcal/mol
CtrlTat	$2.94 \times 10^4 \pm 2.84 \times 10^{-3}$	2.5 \pm 0.1	-1.89 \pm 0.04	5.66	-7.55
α Tat1M	$2.40 \times 10^6 \pm 1.07 \times 10^{-5}$	1.4 \pm 0.1	-0.937 \pm 0.08	9.23	-10.17
γ Tat1M	$3.03 \times 10^4 \pm 2.35 \times 10^{-3}$	6.7 \pm 0.1	-2.59 \pm 0.03	4.91	-7.50

Moreover, inspection of Table 2B.3 indicates that the binding of α Tat1M is associated with largely favourable enthalpy (ΔH) and entropy (ΔS) changes, whereas these changes with respect to γ Tat1M binding to TAR RNA are much lower in magnitude. These favourable changes for the binding of α Tat1M could be a consequence of increased specific hydrogen bonding contacts with TAR RNA, accompanied by release of large number of ordered water molecules upon complex formation, in comparison to CtrlTat or γ Tat1M. The importance of such a network of hydrogen bonds has been previously demonstrated in NMR studies of RNA and arginine-rich peptides.⁵⁶

2B.3.5 Electrophoretic Gel Mobility Shift Assay

The electrophoretic mobility shift assay (EMSA) is routinely used to evaluate ligand-RNA interactions and it is possible to distinctly and efficiently resolve free from bound RNA. The method exploits the charged nature of nucleic acids as the main factor to ensure differential migration through the polyacrylamide gel under the influence of an applied electric field. Tat peptides at increasing molar ratios (peptide:TAR RNA) of 5, 10, 15 and 20 were added to TAR RNA, and the resulting complexes analyzed by PAGE (Figure 2B.6). As seen in the figure, the band of free TAR RNA is seen to decrease with increasing concentration of the Tat peptides.

This is apparent for the α Tat1M peptide, where the TAR RNA band is not visible even at the ratio of 10, further supporting its strong binding to TAR RNA. Several increasingly retarded bands are also visible on the gel, probably indicative of higher order associations of the Tat peptides with TAR RNA. These are probably due to electrostatic association, rather than specific interactions such as hydrogen bonding, with the TAR RNA.

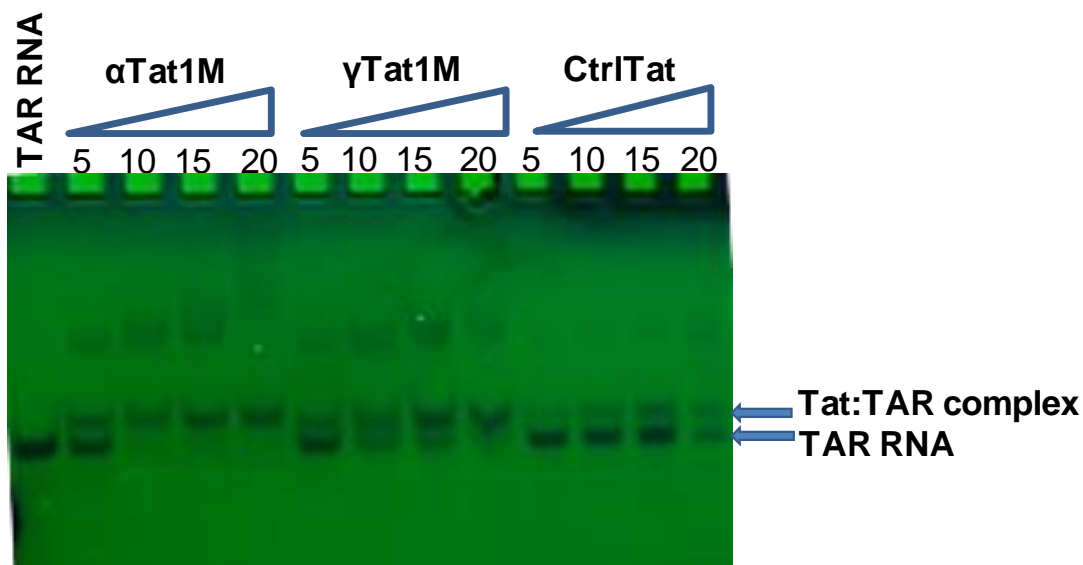


Figure 2B.6. EMSA of the Tat peptides of the study. Tat peptides were added at increasing molar ratios (peptide:TAR RNA) of 5, 10, 15 and 20. The bands were visualized by UV-shadowing. TAR RNA was taken at a concentration of 200 μ M.

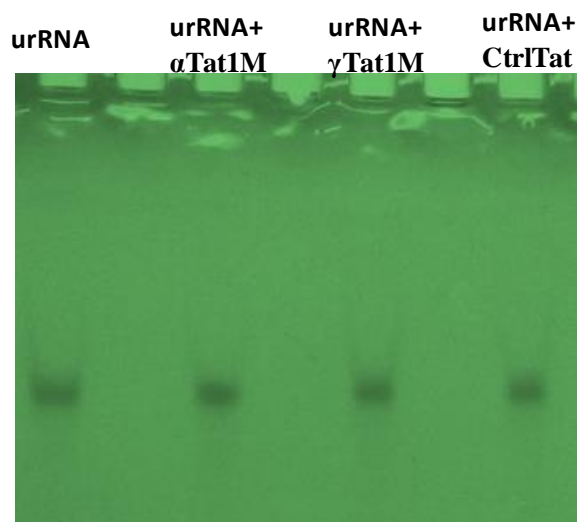


Figure 2B.7. EMSA of the Tat peptides of the study with urRNA. Tat peptides were taken at 1: 15 (urRNA: peptide) molar ratios.

A similar EMSA study with an unrelated RNA (urRNA, 5'-r(GGA GAA UGG AGU CAA UGU)) revealed no binding (Figure 2B.7) of the Tat peptides, thus revealing that the observed binding of the peptides to TAR RNA is specific and not merely driven by electrostatic interactions.

2B.3.6 Circular Dichroism Spectroscopic Studies

The arginine mimics described in this study being conformationally constrained, were expected to influence the structure of the derived Tat1M peptides. This kind of conformational pre-organization often offers an entropic advantage in binding to specific targets. In order to evaluate this, the CD spectra of the Tat peptides of the study were recorded in water as well as in presence of the secondary structure-inducing solvent, trifluoroethanol (TFE). The spectra are shown in Figure 2B.8. The Tat(47-58) peptide is reported to display a CD signature equivalent to an unstructured⁵⁷ random coil structure, even in the presence of TFE.^{57,58} The CtrlTat peptide in our study displayed a random coil structure in water, as reported earlier,⁵⁹ but contrary to the earlier report, showed a significant change towards the α -helical structure in the presence of TFE (Figure 2B.8 B).

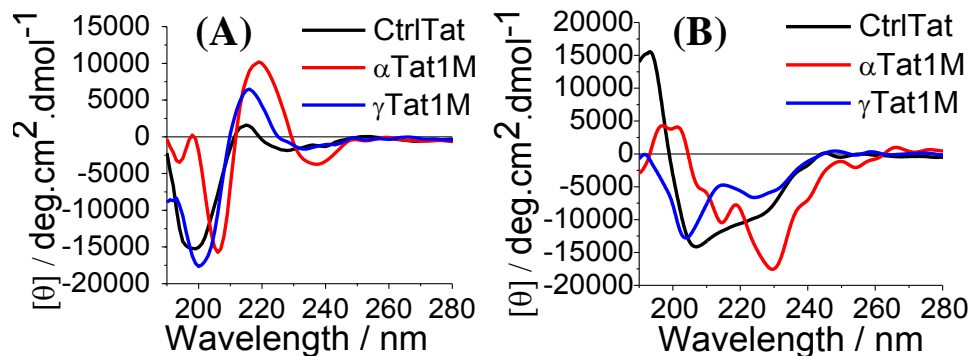


Figure 2B.8. CD spectra of the Tat peptides of the study in (A) water and (B) TFE.

A similar trend was observed for the γ Tat1M peptide, which displayed a CD signature similar to CtrlTat in water. In TFE, two distinct negative bands at 225 and 205 nm were observed, similar to an α -helical structure observed with α -peptides. The α Tat1M peptide, on the other hand, displayed distinctly different CD signatures in both, water and TFE, indicating a possible structure pre-organization induced by the presence of the conformationally constrained arginine mimic P^g. In water, a maxima at 230 nm and minima at \approx 237 and \approx 206 nm were observed,

whereas in TFE, a strong minimum at 230 nm, and another at ≈ 215 nm were observed, indicating a markedly different CD signature for this peptide in comparison to CtrlTat and γ Tat1M. Thus, the structural pre-organization of α Tat1M could be an instrumental factor in its superior binding to TAR RNA.

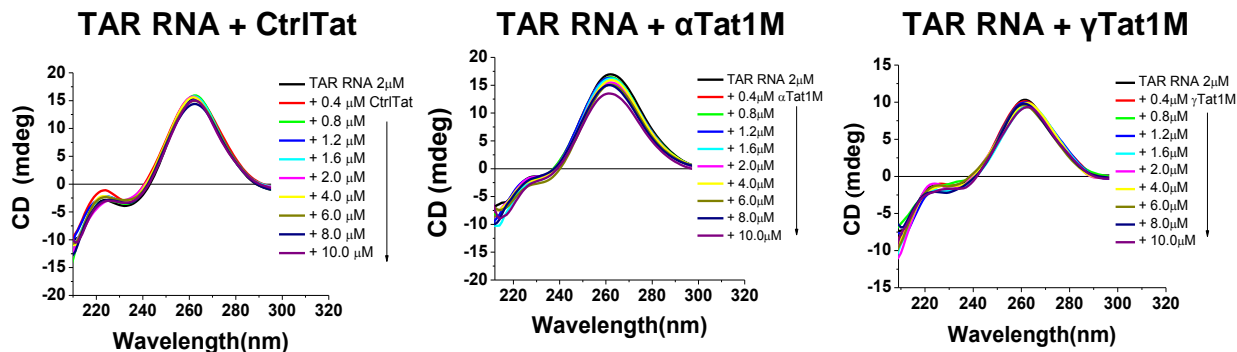


Figure 2B.9. CD spectra of TAR RNA (2 μ M) with increasing concentration of Tat peptides (0 to 10 μ M) recorded in 10 mM sodium cacodylate buffer, pH 7.5.

We further investigated the effect of the binding of the Tat peptides on the structure of TAR RNA. CD spectra allow detection of even slight conformational changes in the nucleic acid structures due to possible binding reactions. Figure 2B.9 represents the CD spectra of TAR RNA, taken at 2 μ M, in the presence of increasing concentration of Tat peptides, ranging from 0 to 10 μ M. As observed, the overall structure of TAR RNA remains unchanged, with a maximum observed at ~ 261 nm and a small minimum at ~ 233 nm. Upon addition of the Tat peptides, a decrease in the amplitude at 261 nm, which is sensitive to base-stacking interactions, was apparent in the case of α Tat1M, while this remained almost unchanged with CtrlTat and very low with γ Tat1M (Figure 2B.9). This change in the CD spectrum is also probably indicative of the stronger interactions between α Tat1M and TAR RNA, in comparison to CtrlTat or γ Tat1M.

2B.3.7 Computational analysis of Tat peptides binding to TAR RNA

This structural pre-organization of α Tat1M could be an instrumental factor in its superior binding to TAR RNA. Molecular dynamics simulations further supported the structural pre-organization of the α Tat1M peptide in comparison to CtrlTat.

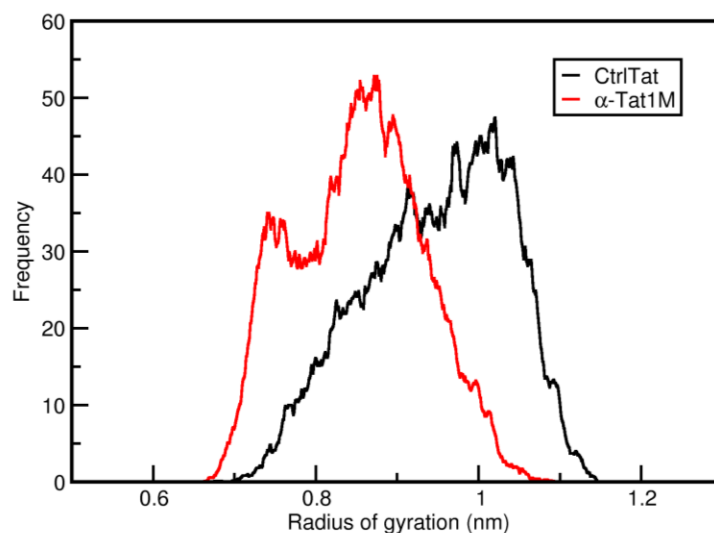


Figure 2B.10. Plot of radius of gyration of CtrlTat (black) and α Tat1M (red) peptides simulations in bulk water.

These peptides were modeled as extended conformations and simulated in water for 1 μ s each. On an average, peptides were unstructured, although the α Tat1M analogue appeared to be more compact, as evident from its lower radius of gyration in comparison to CtrlTat (Figure 2B.10). All the structures from simulations were clustered and representative structures from the top three clusters were chosen for structural studies. Interestingly, CtrlTat exhibited a large number of clusters with lower population in the top three clusters, indicating a higher dynamics compared to α Tat1M probably owing to the conformational constraint and pre-organization induced by $P^{\#}$ at position 52 in the latter (Figure 2B.11).

To unravel the basis of improved binding of α Tat1M peptide to TAR RNA, molecular dynamics simulations of α Tat1M and CtrlTat with TAR RNA were performed, and interaction energies of the complexes were calculated. The peptides were docked to TAR RNA using NPDock server. The docked complexes are shown in Figure 2B.12. The complexes were scored using CHARMM36 force-field. The interaction energies of most favourable complexes are -1520.5622 kJ/mol for CtrlTat as compared to -1821.2571 kJ/mol for α Tat1M indicating an improved binding of α Tat1M. The α Tat1M-TAR RNA complex exhibits larger number of hydrogen bonds, salt bridges and overall contacts compared to CtrlTat (Table 2B.4). These increased contacts are due to the compact and pre-organized nature of α Tat1M.

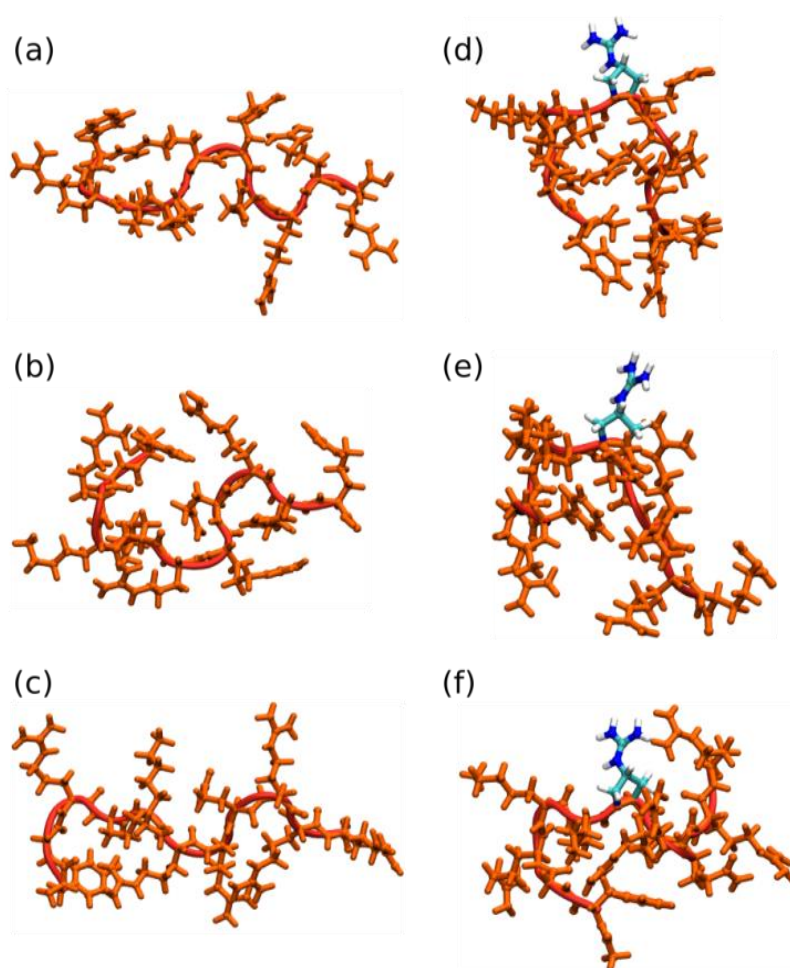


Figure 2B.11. Snapshots of most populated clusters from CtrlTat (a-c) and α Tat1M (d-f) peptides simulations. The P⁵² residue at position 52 (TMP52) is coloured in the latter according to atom names. The Tat peptides are rendered in Licorice representation and shown in orange.

The simulation studies reveal increased interactions between α Tat1M and TAR RNA in comparison to CtrlTat (Table 2B.4), which could account for its observed stronger binding. In particular, the increased intermolecular hydrogen bonding contacts (Table 2B.4) that are observed for this peptide (totally 15 Vs 8 in CtrlTat) contribute in a major way, with increased contacts with sugar atoms (6 in α Tat1M Vs 1 in CtrlTat) and those involving the peptide backbone (9 in α Tat1M Vs 7 in CtrlTat).

Additionally, the CtrlTat peptide was observed mainly to contribute in the form of hydrogen bond donors, while the α Tat1M peptide exhibited significant number of donor as well as acceptor contributions in binding to TAR RNA (Figure 2B.12 and Table 2B.5). From an analysis

of the TAR residues involved in hydrogen bonding with the Tat peptides, it appears that α Tat1M not only binds through increased contacts in the trinucleotide bulge region, as is known for

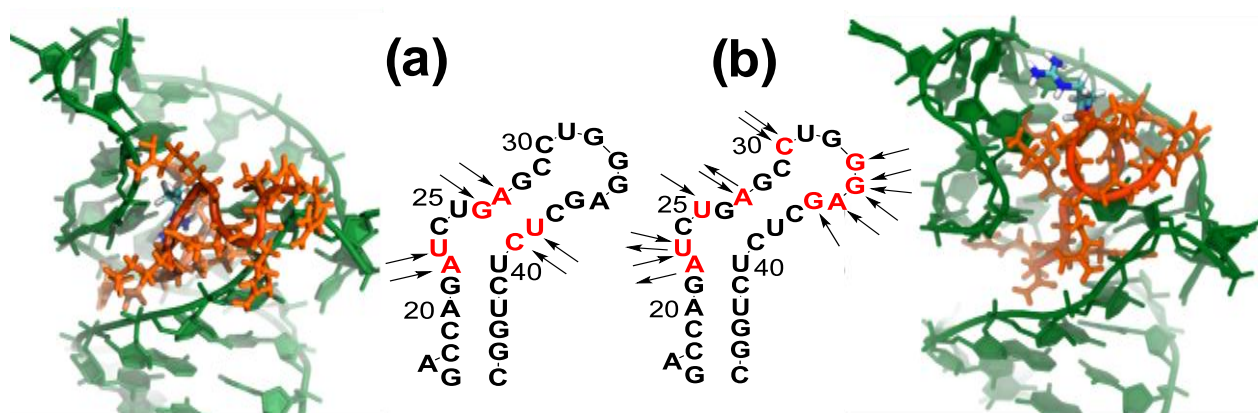


Figure 2B.12. Docked complexes of (a) CtrlTat and (b) α Tat1M peptides with TAR RNA. The Tat peptides are rendered in Licorice representation and shown in orange. Modified residue P^S and R52 are shown as CPK representation. TAR RNA is shown in green. Insets: H-bonding contacts as observed in the simulation studies with CtrlTat and α Tat1M. The hydrogen bond donors/acceptors are indicated by means of arrows pointing away or towards the residue respectively. Nucleotides in red indicate TAR residues involved in these interactions.

Table 2B.4. Interactions between Tat peptides and TAR RNA.

	CtrlTat	α Tat1M
Total interaction energy* (kJ/mol)	-1520.562	-1821.257
Number of intermolecular hydrogen bonds	8	15
Number of intermolecular salt bridge interactions	6	7
Number of contacts between Tat and TAR RNA within 2 Å cutoff	16	20

*Total interaction energies calculated after energy minimization in GROMACS.

CtrlTat, but additionally, has significant number of hydrogen bonding interactions with residues in the loop region (Residues C30 through G36, Figure 2B.12). These loop interactions were not observed in the case of CtrlTat, which bound mainly the bulge region and part of the adjoining stem (Figure 2B.12). The number of interactions within a 2Å limit (Table 2B.4) were also more for α Tat1M (20) in comparison to CtrlTat (16). It is clear that the specificity of the α Tat1M binding to TAR RNA is derived mainly from specific hydrogen bonding contacts between the

two, and is not merely electrostatic. In fact, the γ Tat1M peptide possesses an extra charge (totally 9 positive charges, experimental section) in comparison to α Tat1M (totally 8 positive charges), but still fails to bind as strongly to TAR RNA, emphasizing the specificity of this interaction, and the importance of the relative presentation of positive charges, and in particular, specific guanidine moieties (as we have shown, for R52) along the backbone.

Table 2B.5. Comparison of Hydrogen bonding pairs in the CtrlTat:TAR RNA and α Tat1M:TAR RNA complexes.

CtrlTat:TAR RNA					α Tat1M:TAR RNA				
Donor		Acceptor		Donor-Acceptor distance	Donor		Acceptor		Donor-Acceptor distance
Residue/ Base	Atom	Residue/ Base	Atom		Residue/ Base	Atom	Residue/ Base	Atom	
ARG55	NE2	A22	O5'	2.91	A22	N6	ARG57	O	2.73
ARG52	NE1	U23	O4	2.78	ARG56	NE2	U23	O5'	2.84
TYR47	N	G26	O6	2.86	U23	N3	ARG53	O	3.09
LYS50	NZ	G26	N7	2.95	PHE47	N	U23	O2'	2.91
TYR47	N	A27	N1	2.83	ARG56	NE2	U25	O2'	2.90
TYR47	N	U38	O4	3.14	ARG53	NE2	A27	O5'	2.92
GLY48	N	U38	O4	2.77	A27	N6	ARG55	O	2.80
TYR47	N	C39	N3	2.97	ARG55	NE1	C30	O2	2.76
					LYS50	NZ	G33	O2'	2.80
					LYS50	NZ	G34	O4'	2.97
					ARG56	N	A35	N7	3.28
					ARG55	NE1	G36	O6	2.63
					TMP52	ND	C30	O2	3.50
					TMP52	ND	G34	O6	3.00
					TMP52	NZ2	G34	O6	2.76

2B 3.8 Cell uptake studies and Cytotoxicity

An attractive advantage of developing Tat peptide analogues as RNA ligands is their ability to penetrate cells. We therefore, sought to evaluate the effect that the inclusion of P^8 and r as arginine mimics would have on the cell-penetrating properties of the derived Tat peptides. Thus, the peptides were labeled with a fluorescent tag (Table 2B.1) and their uptake in HeLa cells was

studied by flow cytometry (Figure 2B.13). The effect of a similar pre-organized β -amino acid was recently reported to have a positive effect on the cell-permeation properties of the Tat peptide,⁵⁹ although in this report, three β -amino acid residues were simultaneously included in the derived Tat peptide. HeLa cells were treated with the *cf*-labeled Tat peptides at 5 μ M concentration and incubated for 4 h at 37 °C. In order to remove the cell surface-bound peptides, the cells were washed with heparin (1 mg/ml) before flow cytometric analysis.⁶⁰

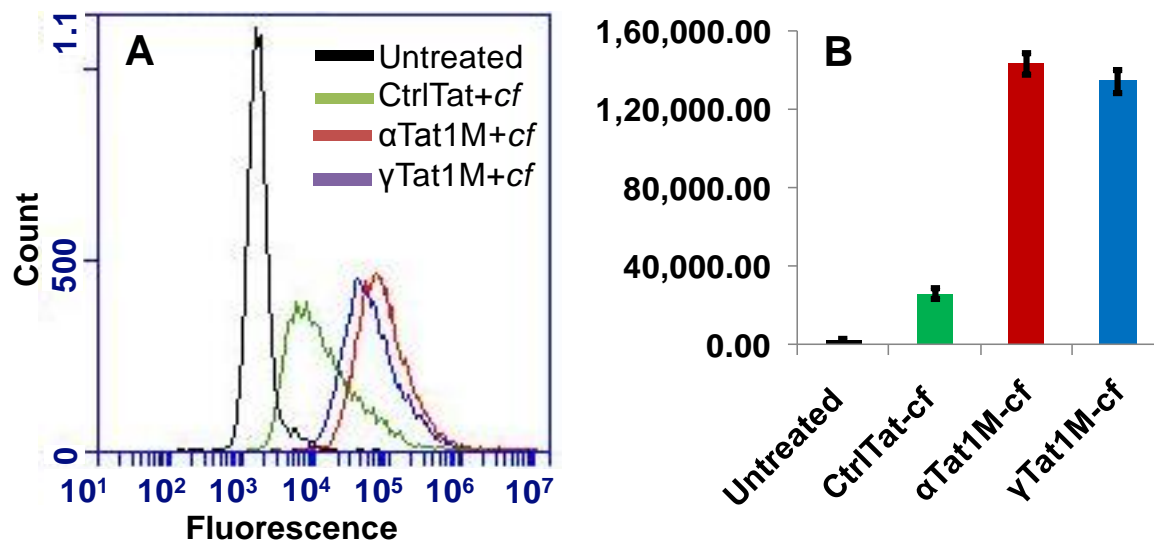


Figure 2B.13. Flow cytometry data for the uptake of Tat peptides in HeLa cells. (A) Number of positive cells and (B) Mean fluorescence.

Thus, the fluorescence-positive cells (Figure 2B.13 A) that were obtained are indicative of internalized peptides alone and exclude those superficially and externally associated with the cell membrane. Both, α Tat1M and γ Tat1M were internalized by >95% of the counted cells, although the mean fluorescence of cells treated with γ Tat1M was slightly lower than those treated with α Tat1M. Significantly, both α Tat1M and γ Tat1M possess far superior cell-penetrating ability than the CtrlTat peptide.

Confocal microscopy revealed that the peptides are distributed throughout the cytoplasm and are also visible in the nuclei and nucleoli (Figure 2B.14), indicating their ability to traverse cell and nuclear membranes. Considering fluorescein as a model cargo molecule, it may be foreseen that a similar conjugation strategy be applied for covalently conjugating other cell-impermeable

drugs to the Tat peptides to deliver them into cells for more effective therapeutic applications. This improves the prospects of these Tat peptide molecules described herein as promising candidates for development of anti-HIV agents, either by themselves, or in combination with other known drug molecules for this virus.

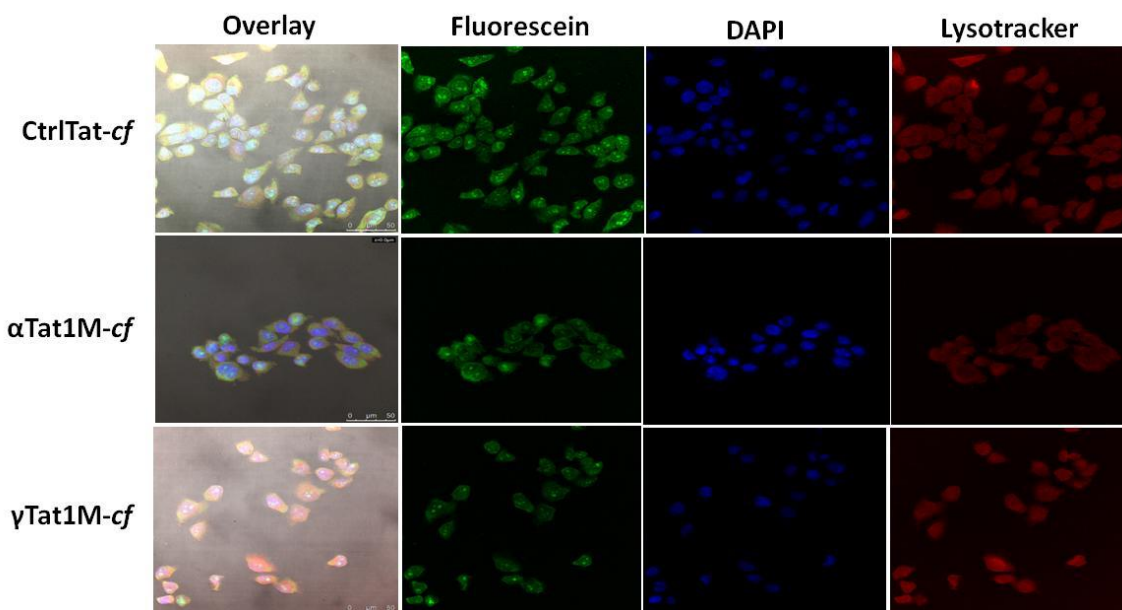


Figure 2B.14. Confocal microscopy images of HeLa cells treated with the peptides of the study at 5 μM concentration, for 4 h at 37 $^{\circ}\text{C}$ and visualized after staining with fluorescein, DAPI or Lysotracker. Scale bar = 50 μm .

We further evaluated the effect of the Tat peptides on cell viability. This was assessed by the standard MTT cell viability and hemolysis assays. Figure 2B.15 (A) shows the cell viability profile in the MTT assay. HeLa cells were treated with increasing concentrations of the Tat peptides and the cell viability assayed after 12 h. Upto 10 μM concentration, the αTat1M peptide caused no decrease in cell viability, while in the presence of CtrlTat or γTat1M , a $\approx 10\%$ drop in cell viability was seen. At a higher concentration of 50 μM , a slight drop in cell viability was observed, with $\sim 85\%$ cell viability for the Tat peptides. The cytotoxicity of the Tat peptides was further evaluated by the hemolysis assay, when human RBCs were treated with the peptides for 1 h. As evident from Figure 2B.14 (B), the Tat peptides had a very low hemolytic effect ($\leq 10\%$). Thus, the Tat peptides of the study were demonstrated to be relatively non-toxic to mammalian cells, while demonstrating good cell penetration properties.

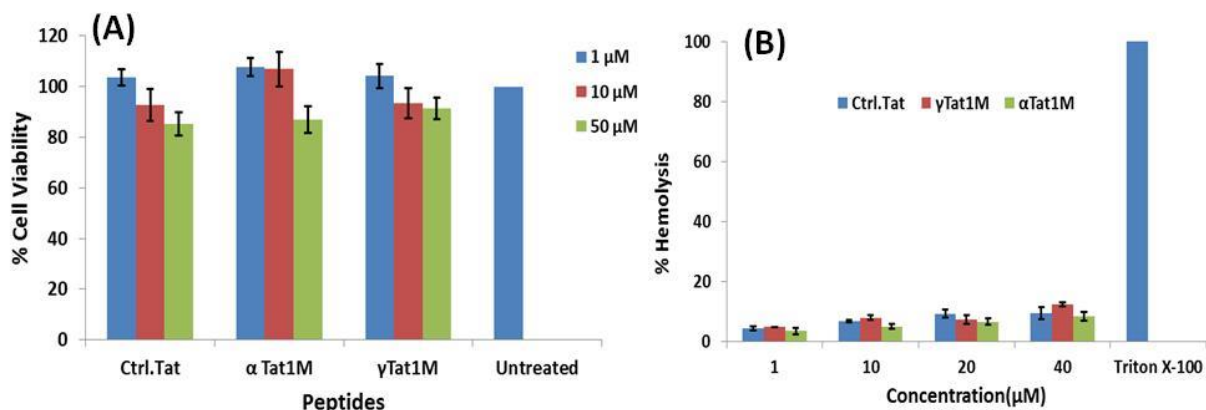


Figure 2B.15. (A) Cell viability assessed by the MTT assay. (B) Hemolysis assay.

2B.4 Summary and Conclusions

In summary, conformationally constrained non-natural arginine mimics were designed and incorporated into Tat(48-57) at position 52 in lieu of arginine. The differences in the arginine mimics in terms of presentation of the guanidine moiety and peptide backbone translated into significantly different TAR-binding abilities. α Tat1M was shown to bind TAR RNA with a higher affinity than CtrlTat, possibly due to its compact nature and increased interactions, including specific hydrogen bonding contacts with the TAR residues in the bulge and loop regions, salt bridges and also electrostatic and other interactions. The superior binding of α Tat1M to TAR RNA in comparison to γ Tat1M or even CtrlTat, and its ability to compete with and prevent the binding of CtrlTat, coupled with its good cell penetration and low cytotoxicity make it a promising candidate for further evaluation in the search for selective TAR-binding ligands with a potential to target Tat-TAR interaction and prevent viral transactivation. In addition to being able to prevent Tat binding to TAR, the Tat analogues presented herein possess enhanced cell penetration properties and could also be utilized to act as molecular transporters to transport anti-HIV drugs into cells, thus acting as a double-headed hammer against the virus. It is indeed noteworthy that the modification of a single residue in Tat can lead to such extreme differences in binding to TAR RNA, and potentially prevent the viral process of transactivation of transcription.

2B.5 Experimental Section

2B.5.1 General Information

All the reagents used were obtained commercially and were of $\geq 95\%$ purity and used without further purification. DMF, CH_2Cl_2 , pyridine were dried over P_2O_5 , CaH_2 , KOH respectively. DMF, CH_2Cl_2 were stored by adding 4 Å molecular sieves and pyridine by adding KOH. Column chromatography was performed for purification of compounds on silica gel (100- 200 mesh or 60-120 mesh, Merck). TLCs were performed on pre-coated with silica gel 60 F254 (Merck) aluminium sheets. TLCs were performed using petroleum ether-ethyl acetate and ethyl acetate-methanol solvent systems. TLCs were visualised after spraying with ninhydrin reagent and heating. ^1H and ^{13}C NMR spectra were recorded on a Bruker AV 200 or AV 400 or AV 500 spectrometer fitted with an Aspect 3000 computer and all the chemical shifts (ppm) are referred to internal TMS, chloroform-d for ^1H and/or ^{13}C NMR. ^1H NMR data are reported in the order of chemical shift, multiplicity (s, singlet; d, doublet; t, triplet; q, quartet; br, broad; br s, broad singlet; m, multiplet and/ or multiple resonance), number of protons. HRMS mass spectra were recorded on a Thermo Scientific Q-Exactive, Accela 1250 pump MALDI-TOF spectra were obtained from a Voyager-De-STR (Applied Biosystems) and CHCA (α -Cyano-4-hydroxycinnamic acid) matrix was used to analyze MALDI-TOF samples. All final compounds and oligomers were $\geq 95\%$ pure, as determined by ^1H NMR, ^{13}C NMR, HRMS, HPLC and/or MALDI-TOF analysis, as applicable. UV absorbance was performed on a Varian Cary 300 UV-VIS spectrophotometer.

2B.5.2 Experimental procedures and spectral data

2S,4R)-methyl-1-(*tert*-butyloxycarbonyl)-4-hydroxypyrrolidine-2-carboxylate (4)

To a solution of *trans*-4-hydroxy-L-proline methyl ester **1** (10 g, 68.9 mmol) dissolved in dioxane:water (1:1, 25 ml), sodium hydroxide (8.26 g, 206.7 mmol) was added. The reaction mixture was stirred for 30 min at room temperature, followed by drop-wise addition of di-*tert*-butyl dicarbonate (19.54 g, 89.5 mmol) dissolved in dioxane:water (1:1). The reaction was further stirred at RT for 4 h and monitored by TLC. Upon completion of reaction, the dioxane was removed under vacuum and ethyl acetate was added. The layers were separated, and the aqueous phase was extracted with ethyl acetate. The combined organic extracts were washed with brine and dried over Na_2SO_4 . The solvent was evaporated and the crude residue was

purified by silica gel column chromatography to give the title compound **4** as a white crystalline solid (14.2 g, 84%). $[\alpha]_D^{20} = -134.30$ (*c* 0.080, CHCl₃).

Molecular Formula: C₁₁H₁₉NO₅ ; **Molecular weight:** 245.1263

¹H NMR (200 MHz, CDCl₃) δ : 4.43 (m,1H), 4.36 (m,1H), 3.70 (s,3H), 3.56 (d, *J* = 3.4 Hz,1H), 3.52 (d, *J* = 11.6 Hz,1H), 2.25 (m, 1H), 2.01 (m,1H), 1.42 (s, major) & 1.37 (s, minor), 9H.

¹³C NMR (50 MHz, CDCl₃) δ : 173.7, 154.0, 80.4, 69.1, 57.9, 54.6, 52.0, 39.0, 28.2.

¹³C DEPT (50 MHz, CDCl₃) δ : 69.1, 57.9, 54.6, 52.0, 39.0, 28.2.

HRMS (ESI) : *m/z* calculated for C₁₁H₁₉NO₅: 245.1263; Observed: [M⁺+Na] 268.1151.

(2*S*,4*S*)-methyl-1-(*tert*-butyloxycarbonyl)-4-azidopyrrolidine-2-carboxylate (5)

Dry triethylamine (6 mL) was added to a solution of compound **4** (3.0 g, 12.2 mmol) in dry CH₂Cl₂. The reaction mixture was stirred for 30 min and mesyl chloride (1.42 mL, 18.4 mmol) was added drop-wise and stirring continued for another 30 min at 0-5 °C. The reaction was monitored by TLC. Upon completion of reaction, excess CH₂Cl₂ and water (100 mL) were added. The layers were separated, and the aqueous phase was extracted with CH₂Cl₂ (3 x 100 mL). The combined organic extracts were washed with brine (100 mL), dried over Na₂SO₄. The solvents were evaporated *in vacuo* and the mesylate obtained was used in the further reaction. To a flask containing the mesyl compound dissolved in dry DMF, was added sodium azide (2 g, 6.19 mmol) portion-wise at room temperature with constant stirring. The reaction was heated at 65 °C for 10 h, and monitored by TLC. Upon completion of reaction, the solvent was evaporated *in vacuo* and ethyl acetate and water were added to the residue. The layers were separated, and the aqueous phase was further extracted with ethyl acetate. The combined organic extracts were washed with brine and dried over Na₂SO₄. The solvent was evaporated under vacuum and the crude product was purified by silica gel column chromatography to give the title compound **5** as a thick gummy liquid (1.12 g, 67%). $[\alpha]_D^{20} = -71.13$ (*c* 0.065, CHCl₃).

Molecular Formula: C₁₁H₁₈N₄O₄ ; **Molecular weight:** 270.1328

¹H NMR (200 MHz, CDCl₃) δ : 4.41 (min) & 4.31 (maj) (m, 1H), 4.15 (m, 1H), 3.73 (s, 3H), 3.66 (d, J = 4.0 Hz, 1H), 3.46 (d, J = 4.0 Hz, 1H), 2.44 (m, 1H), 2.16 (dd, J = 1.0 & 4.0 Hz, 1H), 1.45 (min) & 1.39 (maj) (s, 9H).

¹³C NMR (50 MHz, CDCl₃) δ : 172.2, 153.0, 80.5, 59.2, 52.2, 51.2, 35.0, 28.1.

¹³C DEPT (50 MHz, CDCl₃) δ : 59.2, 57.6, 52.2, 51.2, 35.9, 28.1.

HRMS (ESI) : m/z calculated for C₁₁H₁₈N₄O₄: 270.1328; Observed: [M⁺+Na] 293.1214.

(2*S*,4*S*)-4-(((9H-fluoren-9 yl)methoxy)carbonyl)amino)-1-(*tert* butoxycarbonyl)pyrrolidine-2-carboxylic acid (Z**)**

To a solution of azido compound **5** (1.5 g, 5.5 mmol) dissolved in dry MeOH (25 mL), 10% palladium on charcoal (300 mg, 20% w/w) was added, the resulting reaction mixture stirred under hydrogen gas at 50 psi for 3 h and the reaction was monitored by TLC. After completion of reaction, it was filtered through celite and water and methanol (1:1, 10 mL) were added. 2 N LiOH (15 mL) was further added to the reaction mixture and stirred for 30 min. Methanol was evaporated under reduced pressure and the resulting mixture was neutralised with dil. HCl. Solvents were evaporated and the residue was suspended in methanol and filtered. The supernatant collected was evaporated *in vacuo* to obtain the corresponding amino acid. The amino acid obtained was dissolved in 1, 4-dioxane:water (1:1), and NaHCO₃ (3.6 g, 43.4 mmol) was added to ensure an alkaline pH. The resulting reaction mixture was stirred at room temperature for 30 min and Fmoc-Cl (1.33 g, 5.1 mmol) was added in portions. The reaction mixture was stirred overnight at room temperature and monitored by TLC. Upon completion of reaction, the reaction mixture was slightly acidified by addition of Dowex H⁺ resin and the resin was subsequently filtered off. The dioxane was evaporated under vacuum and ethyl acetate was added. The product was extracted in ethyl acetate. The organic extracts were washed with brine and dried over sodium sulfate. The solvents were evaporated *in vacuo* and the product was washed repeatedly by petroleum ether and diethyl ether to give title compound **Z** (1.13 g, 58%) as a solid yellowish foam. $[\alpha]_D^{20}$ -69.60 (c 0.050, CHCl₃).

Molecular Formula: C₂₅H₂₈N₂O₆ ; **Molecular weight:** 452.1947

¹H NMR (200 MHz, CDCl₃) δ : 7.74 (m, 2H), 7.57 (m, 2H), 7.40 (m, 4H), 5.80 (m, 1H), 4.49 (m, 2H), 4.34 (m, 3H), 4.20 (m, 1H), 3.53 (m, 2H), 2.38 (m, 1H), 1.50 & 1.44 (s, 9H).

¹³C NMR (50 MHz, CDCl₃) δ : 174.5, 156.7, 156.0, 143.8, 142.6, 141.3, 127.8, 120.0, 82.4, 67.1, 58.4, 47.1, 28.3.

¹³C DEPT (50 MHz, CDCl₃) δ : 125.8, 125.2, 122.3, 118.1, 65.2, 56.5, 51.8, 45.2, 31.7, 26.4.

HRMS (ESI): *m/z* calculated for C₂₅H₂₈N₂O₆: 452.1947; Observed: [M⁺+Na] 475.1832.

2B.5.3 Materials

The CtrlTat peptide and analogues were synthesised using standard Fmoc- and/or Boc- chemistry protocols. Further, these peptides were purified by RP-HPLC and characterized by MALDI-TOF analysis. The 27-nucleotide long bulged stem loop of HIV-1 TAR RNA 5'-r(GCAGAUCUGAGCCUGGGAGCUCUCUGC) was purchased from Sigma-Aldrich and the concentration was determined spectrophotometrically by measuring the absorbance at 260 nm at 25 °C and using the molar extinction co-efficient 251,800 M⁻¹ cm⁻¹. Other reagents were of analytical grade and were used without any further purification.

2B.5.4 Temperature-dependent UV-melting studies

Temperature-dependent UV-melting experiments were carried out using a Cary 100 (Varian) spectrophotometer equipped with a Peltier-controlled cell holder. A quartz cell of 1 cm path length was used. Temperature-dependent absorbance changes were recorded at 260 nm with a heating rate of 0.5 °C/min, from 25 to 100 °C. Before the start of the experiments, each sample was held for at least 2 min at the initial temperature to attain the required temperature. In all the melting experiments, concentration of TAR RNA was 1 μ M and peptide concentration was varied from 0 to 3 μ M. The samples were prepared in 10 mM sodium cacodylate buffer containing 0.1 mM EDTA and 70 mM NaCl at pH 7.5. For each melting experiment, the melting temperature (*T_m*) was determined using previously described methods.²¹

2B.5.5 Isothermal titration calorimetry (ITC) studies

Isothermal titration calorimetry experiments were conducted at 25 °C on a Microcal VP-ITC (Microcal, Inc.; Northampton MA). Titration of HIV-1 TAR with Tat and different modified peptides was done by injecting 6 μ L aliquots of 350 μ M peptide from a 280 μ L capacity rotating

syringe (350 rpm) into an isothermal sample chamber containing 1.5 mL HIV-1 TAR RNA solution at 10 μM concentration. Each experiment of this type was accompanied by the corresponding control experiment in which 350 μM peptide was injected into a solution of buffer alone. The duration of each injection was 12 s and the delay between the injections was 180 s or 300 s, the initial delay prior to the first injection was 300 s. Each injection generated a heat burst curve (microcalories/second vs. seconds) and the area under each curve was determined by integration [using the Origin version 7.0 software (Microcal, Inc.; Northampton, MA)] to obtain the measure of the heat associated with that injection. The buffer corrected ITC profiles for the binding of Tat and different modified peptides was fit with a model for one site of binding.²² The net enthalpy change for HIV-1 TAR RNA stem loop interaction with Tat and different modified peptides were determined by subtraction of the heat of dilution from each binding isotherm.

2B.5.6 Electrophoretic gel mobility shift assay for Tat-TAR binding

The TAR RNA binding ability of the Tat peptide and its analogues was assessed by non-denaturing polyacrylamide gel electrophoresis using 20% gels. For the gel, TAR RNA (200 μM) was mixed with peptides at varying concentrations, as indicated, in TAE buffer and incubated at room temperature for 30 min prior to loading on the gel. The gel was run in TAE buffer at a voltage of 150 V at 4 °C till the bromophenol blue dye had migrated to 3/4th of the gel length. The bands were visualized by UV-shadowing.

2B.5.7 Computational analysis of Tat peptides binding to TAR RNA

2B.5.7.1 Structure : The 3D structure of wild type Tat peptide (CtrlTat), corresponding to residues 47-57 [YGRKKRRQRRR], was taken from the crystal structure of the HIV-1 Tat protein (PDB ID: 1JFW). This structure was further used to build the modified αTat1M peptide by replacement of R52 by the modified residue (TMP) and Y47 by F47 (in line with the synthetic Tat peptides of the study) using Discovery Studio Visualizer.²³

2B.5.7.2 Molecular dynamics simulations : Molecular dynamics simulations were performed for the conformational sampling of the Tat peptides using the GROMACS v5.0.5 software package.²⁴ The CHARMM36 force field²⁵ was used to represent the peptides and water. The parameters for the modified residue were obtained from CGenFF program.²⁶ The wild type and αTat1M peptides were independently solvated using TIP3P water molecules and the structures were energy minimized using the steepest descent algorithm. The systems were equilibrated

under NVT conditions for 100 ps, together with position restraints on peptides, followed by simulations in an NPT ensemble for 1 ns. The system temperatures were maintained at 300 K using the v-rescale algorithm.²⁷ A constant pressure of 1 bar was maintained isotropically using ParrinelloRahman algorithm.²⁸ Production runs of 1 μ s were performed for each system.

2B.5.7.3 Docking : The structures sampled in the simulations were clustered using g_cluster program implemented in GROMACS, with a RMSD cutoff of 0.25 nm. The representative conformations of three most populated clusters were used for docking studies. These peptides were docked on HIV-1 TAR RNA (PDB ID: 1ARJ) using NPDock server.²⁹ The docked complexes with the best scores were selected and scored on the basis of interaction energies.

2B.5.7.4 Analysis of docked complexes : In order to understand the binding affinity associated with the peptide-RNA complexes, the minimized structures of Tat-TAR complexes were analyzed. The docked poses obtained were further relaxed by performing energy minimization. The interaction energies were calculated as the sum of the Lennard Jones and Coulombic electrostatics terms using the CHARMM36 force-field in GROMACS v5.0.5. The number of intermolecular hydrogen bonds was calculated by HBPLUS program,³⁰ where hydrogen bond was defined by these criteria - maximum donor-acceptor distance of 3.9 nm and donor-H-acceptor angle greater than 90°. The intermolecular salt bridge interactions were determined as the distance between charged moieties of amino acid residues and nucleotides must be less than 0.4 nm. The packing interactions between Tat peptide and TAR RNA were examined using VMD-1.9.2³¹ by considering intermolecular contacts with a distance cut-off of 0.2 nm. All figures were rendered using VMD-1.9.2.

2B.5.8 Circular dichroism (CD) spectroscopic studies.

Circular dichroism experiments were performed on a Jasco J-815 spectropolarimeter equipped with a Peltier-controlled cell holder in a quartz cuvette of 1 cm path length. The spectra of the peptides alone were recorded at a concentration of 500 μ M from 300 to 190 nm as accumulations of 3 scans at a scann speed of 100 nm/min in water and 90% TFE (Sigma). The ellipticity in the acquired CD spectra was converted to the molar ellipticity using the equation: $[\theta] = \theta / (10 \times c \times l)$, where, $[\theta]$ is the Molar ellipticity ($\text{deg.cm}^2.\text{dmol}^{-1}$), θ is the observed ellipticity corrected for the buffer at a given wavelength (mdeg), c is the molar concentration and l is the path length

(cm). For the complexes of peptides with TAR RNA, CD spectra were recorded from 320 nm to 200 nm as accumulations of 3 spectra at 25 °C. Each spectrum was collected at a speed of 100 nm/min and 1 nm data pitch. The buffer solution contained 10 mM sodium cacodylate buffer, 0.1 mM EDTA and 70 mM NaCl at pH 7.5. For the titration experiments, TAR RNA was taken at a concentration of 2 μ M and the peptides were added in increasing concentrations from 0 to 10 μ M. The baseline was corrected for every spectrum under identical conditions.

2B.5.9 Cell uptake and cytotoxicity studies

2B.5.9.1 Flow Cytometry :

As described previously in section A (2A.6.3.5.1).

2B.5.9.2 Confocal microscopy :

As described previously in section A (2A.6.3.5.2).

2B.5.9.3 Cytotoxicity studies :

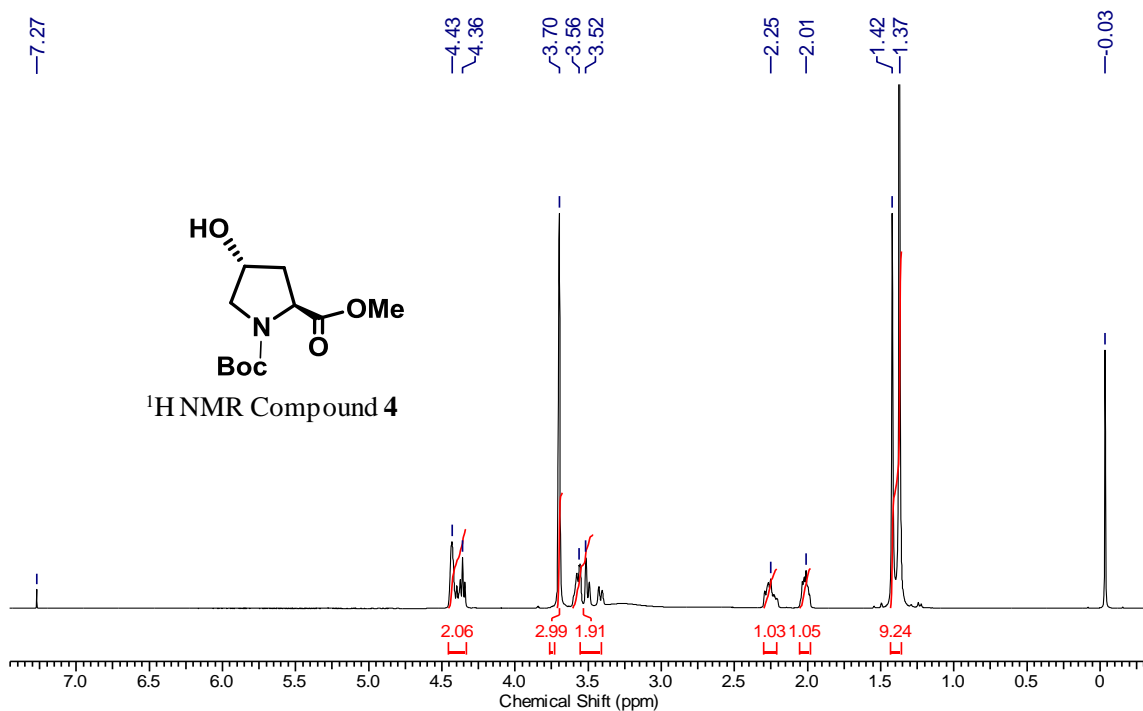
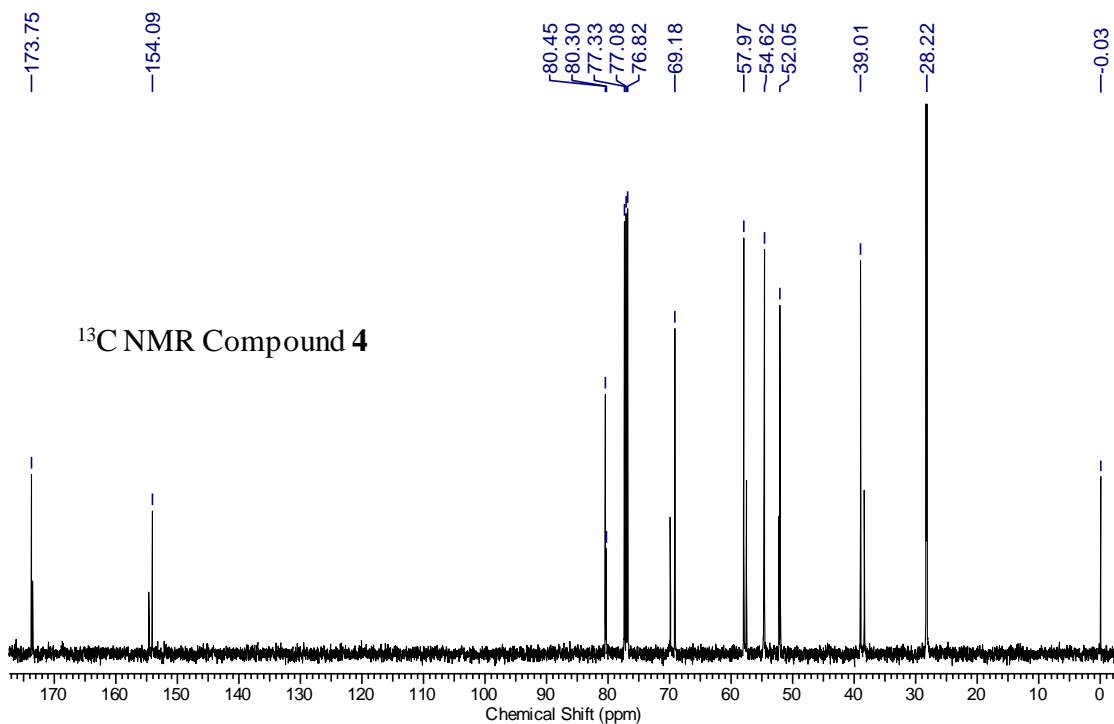
As described previously in section A (2A.6.3.5.3).

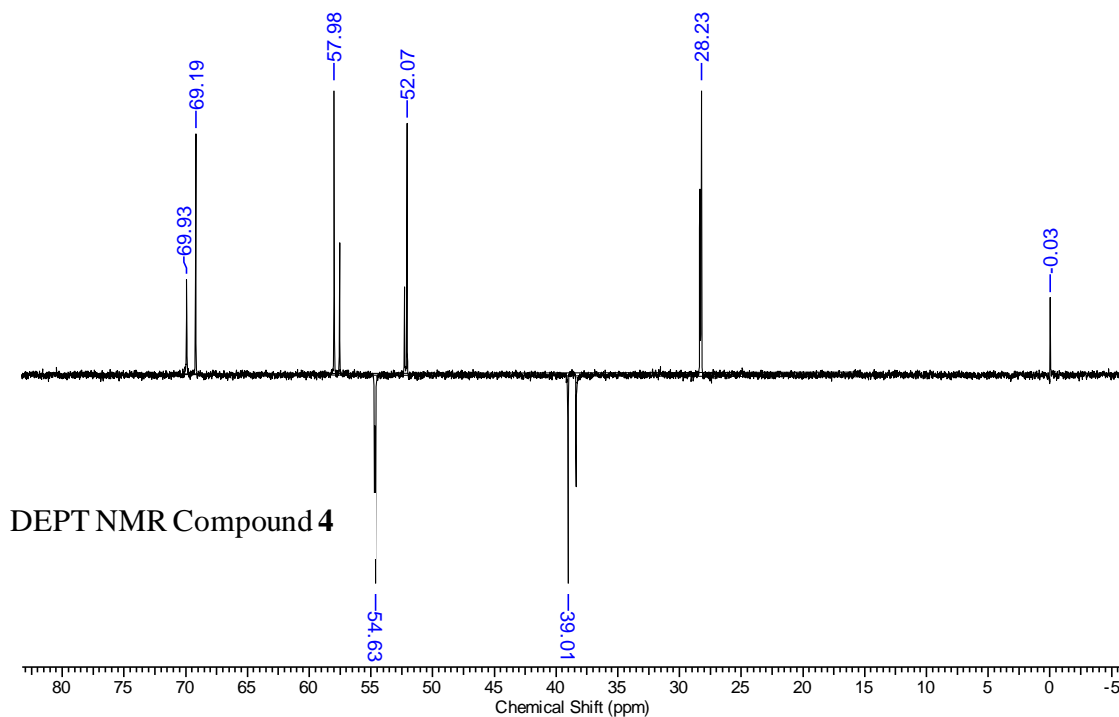
2B.5.9.4 Hemolysis assay :

As described previously in section A (2A.6.3.5.4).

2B.6 Appendix B

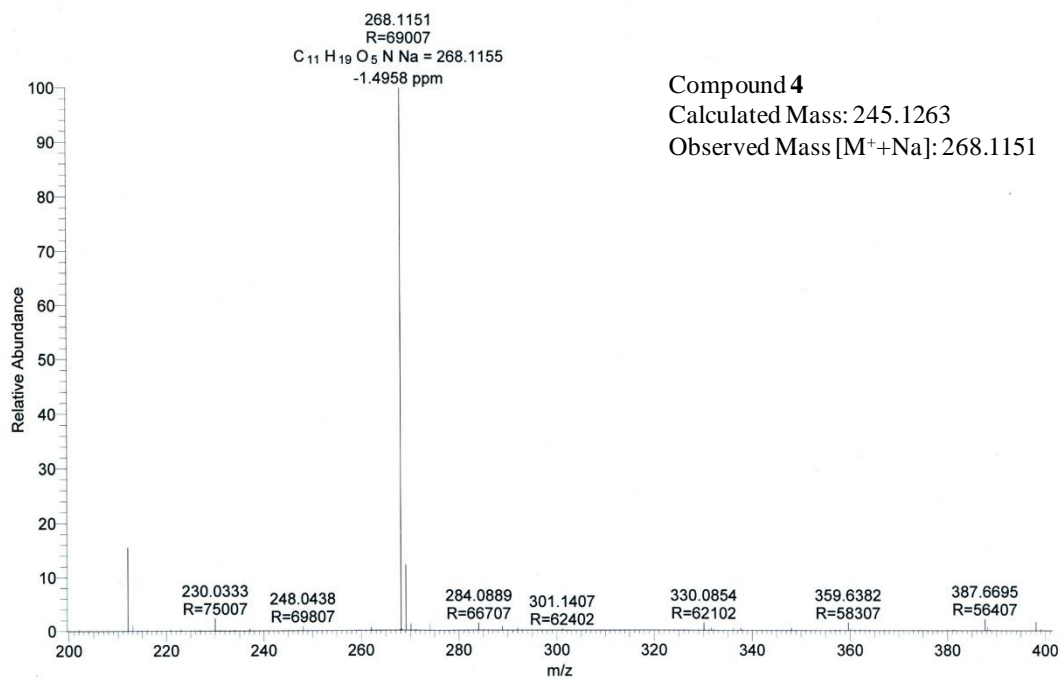
Compound and characterization	Page No.
Compound 4: ¹ H, ¹³ C NMR, ¹³ C DEPT, HRMS	107 - 108
Compound 5: ¹ H, ¹³ C NMR, ¹³ C DEPT, HRMS	109 - 110
Compound X: ¹ H, ¹³ C NMR, ¹³ C DEPT, HRMS	111 - 112
RP-HPLC Chromatograms of the Tat peptides	113
MALDI-TOF spectra of peptides	114 - 115

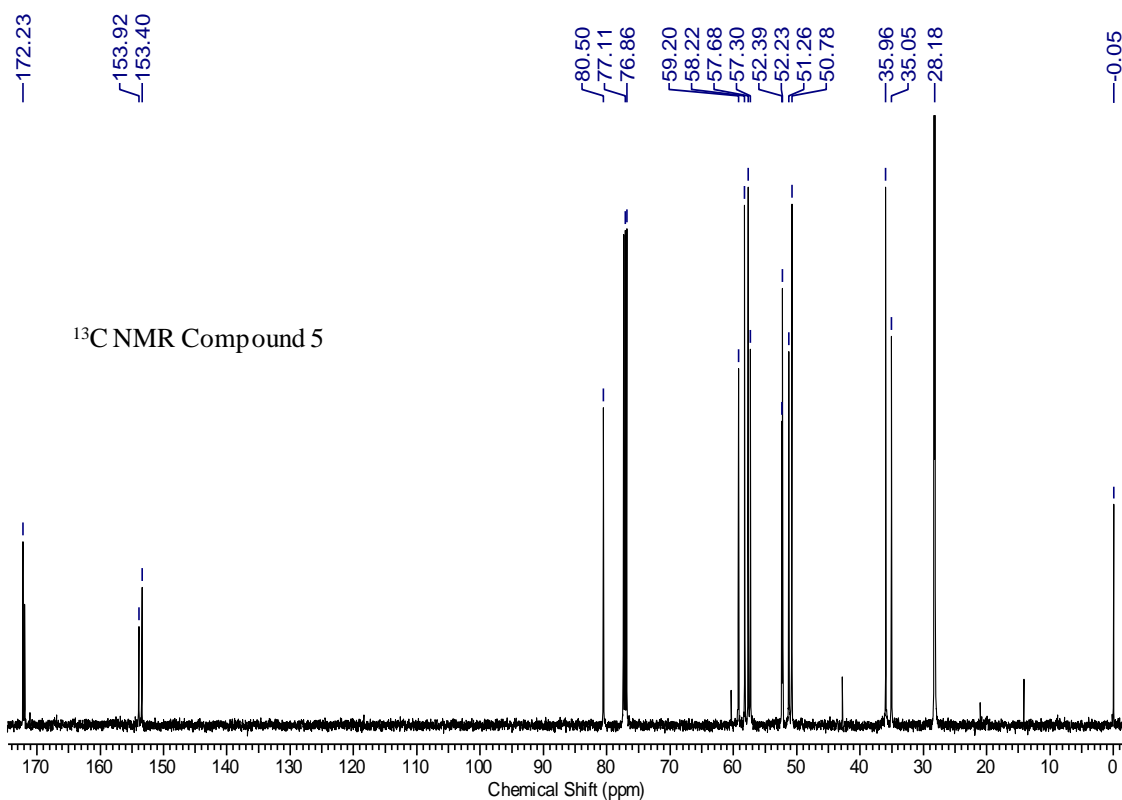
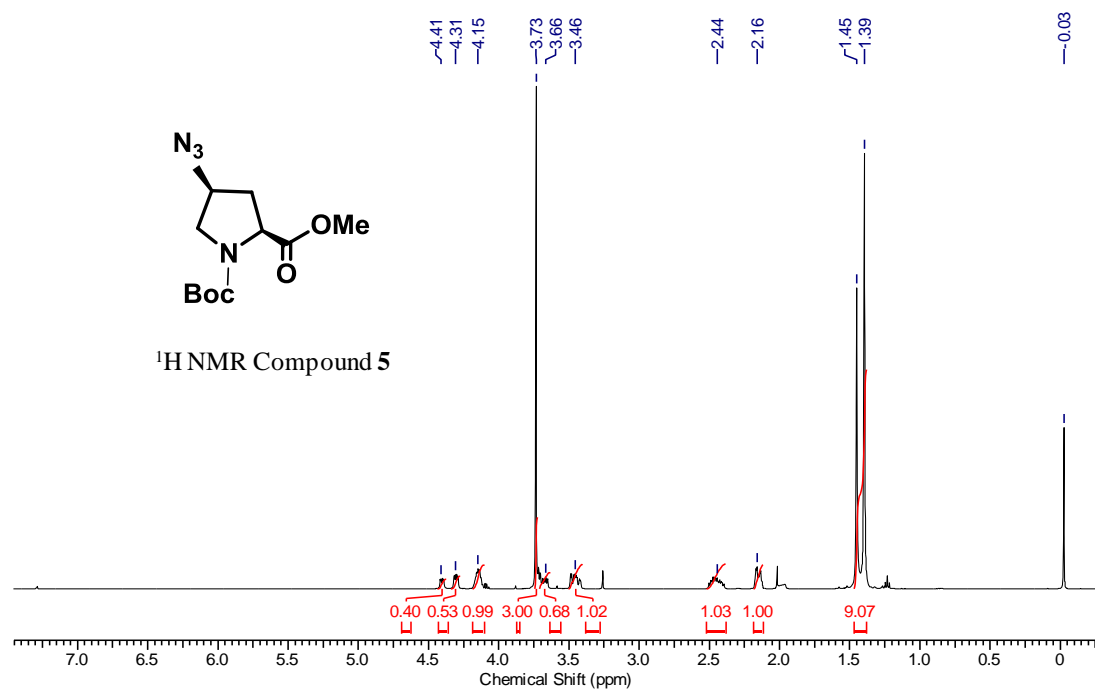
(2*S*,4*R*)-methyl-1-(*tert*-butyloxycarbonyl)-4-hydroxypyrrolidine-2-carboxylate (4)¹H NMR (200 MHz; CDCl₃) spectra of compound 4:¹³C NMR (50 MHz; CDCl₃) spectra of compound 4:

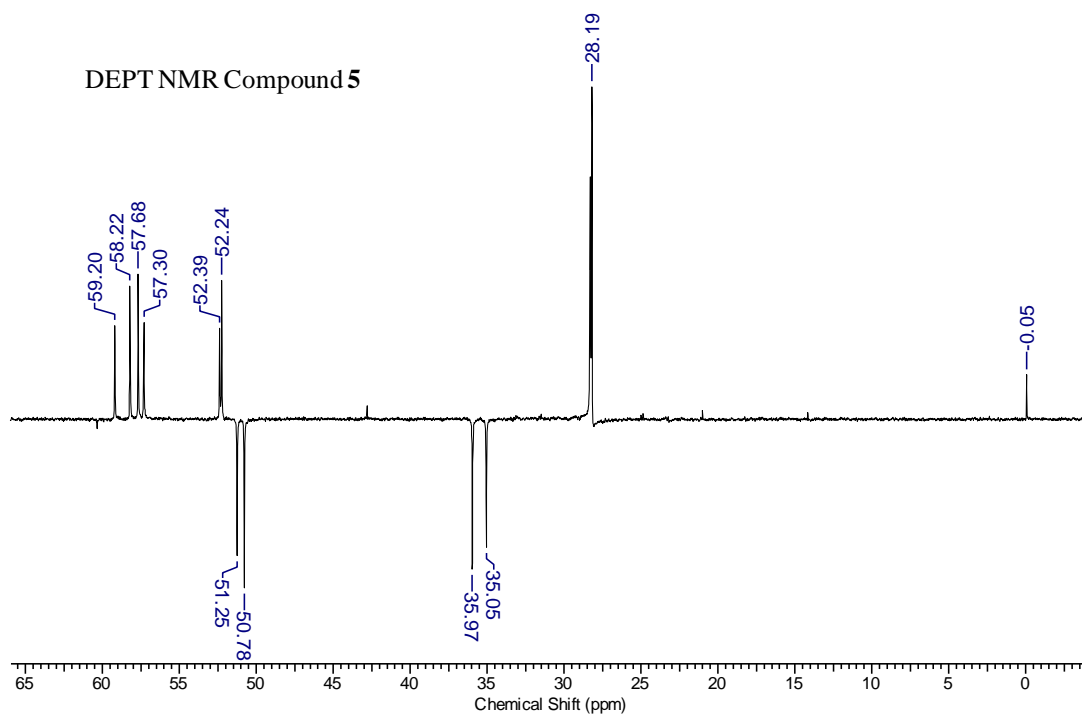


D:\Data\GB-1

6/11/2015 6:16:22 PM

GB-1 #97 RT: 0.43 AV: 1 NL: 6.51E8
T: FTMS + p ESI Full ms [100.00-1500.00]

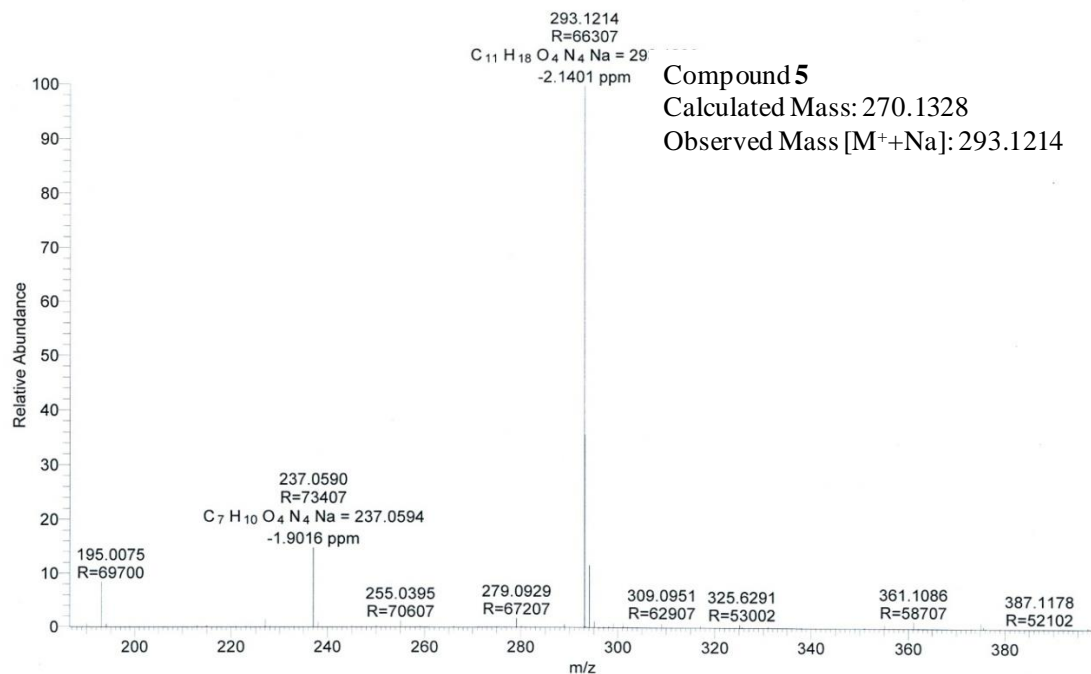
(2S,4S)-methyl-1-(*tert*-butyloxycarbonyl)-4-azidopyrrolidine-2-carboxylate (5)

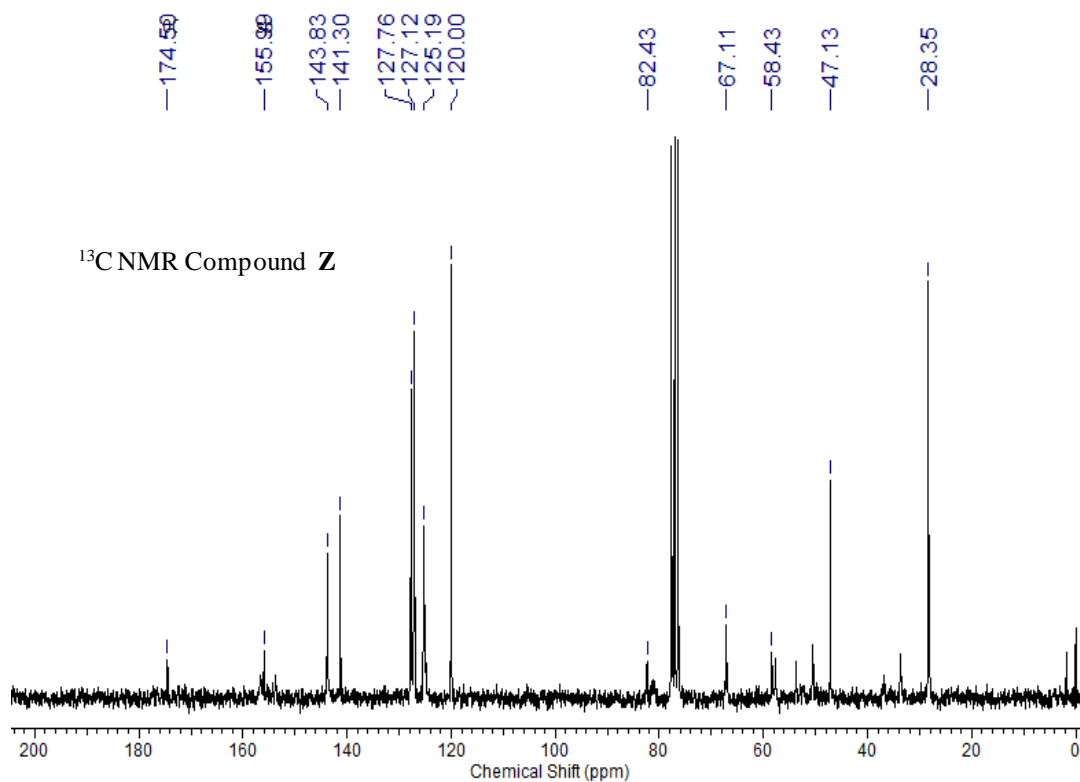
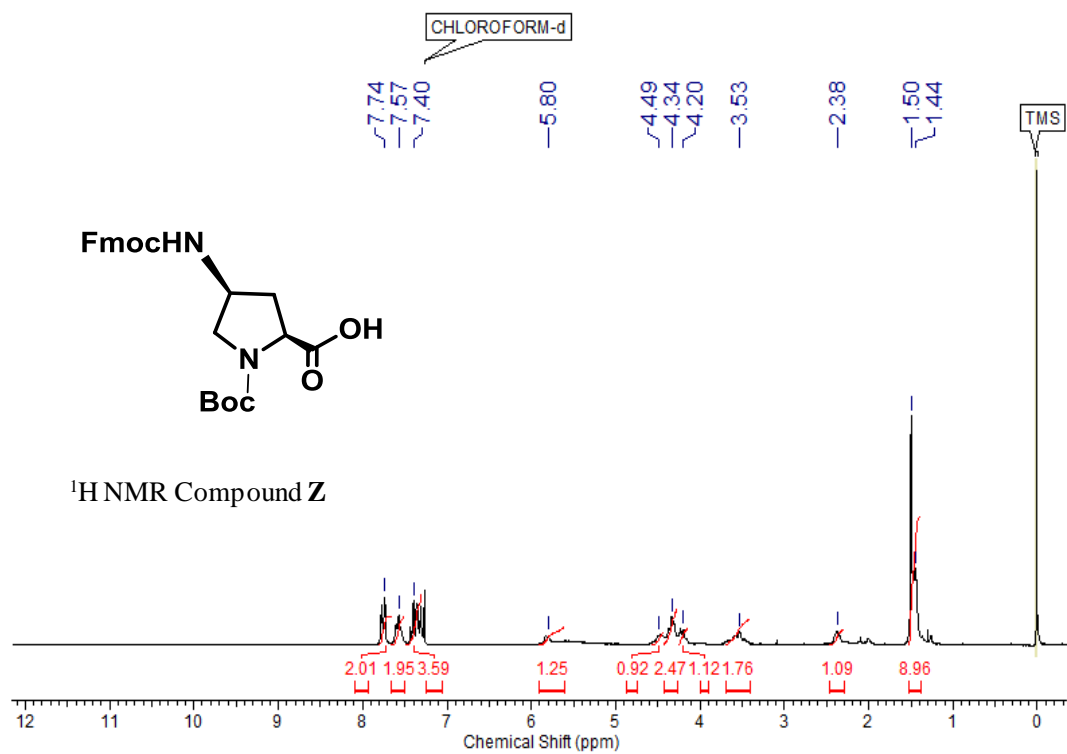


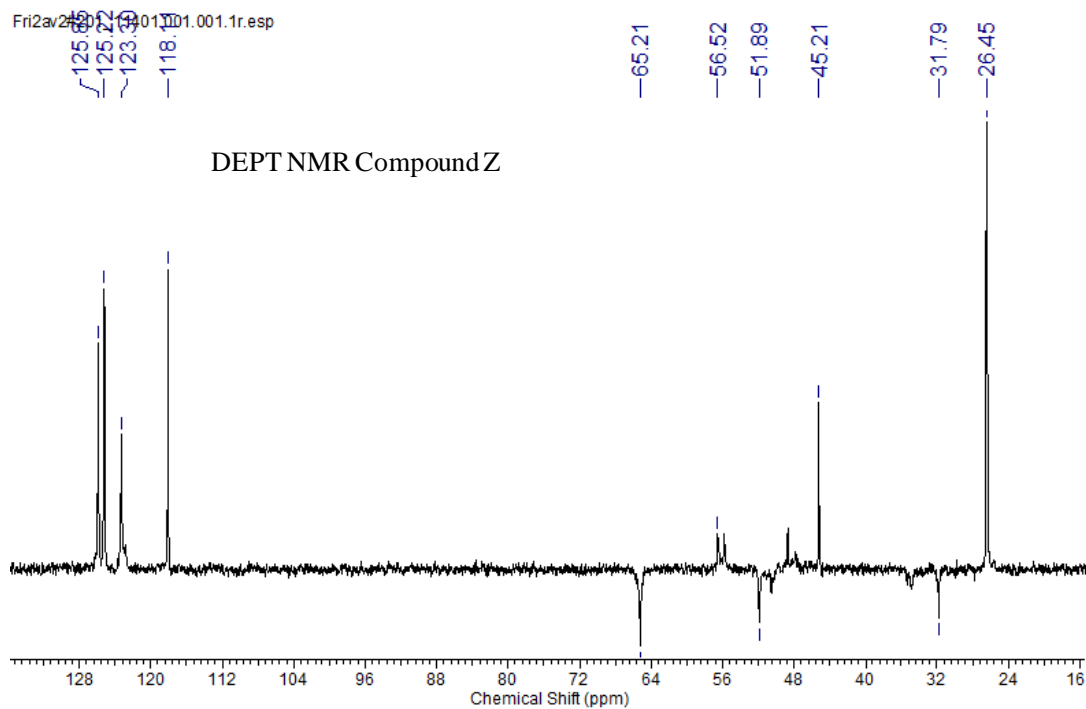
D:\Data\GB-2

6/11/2015 6:20:31 PM

GB-2 #102 RT: 0.45 AV: 1 NL: 9.29E8
 T: FTMS + p ESI Full ms [100.00-1500.00]

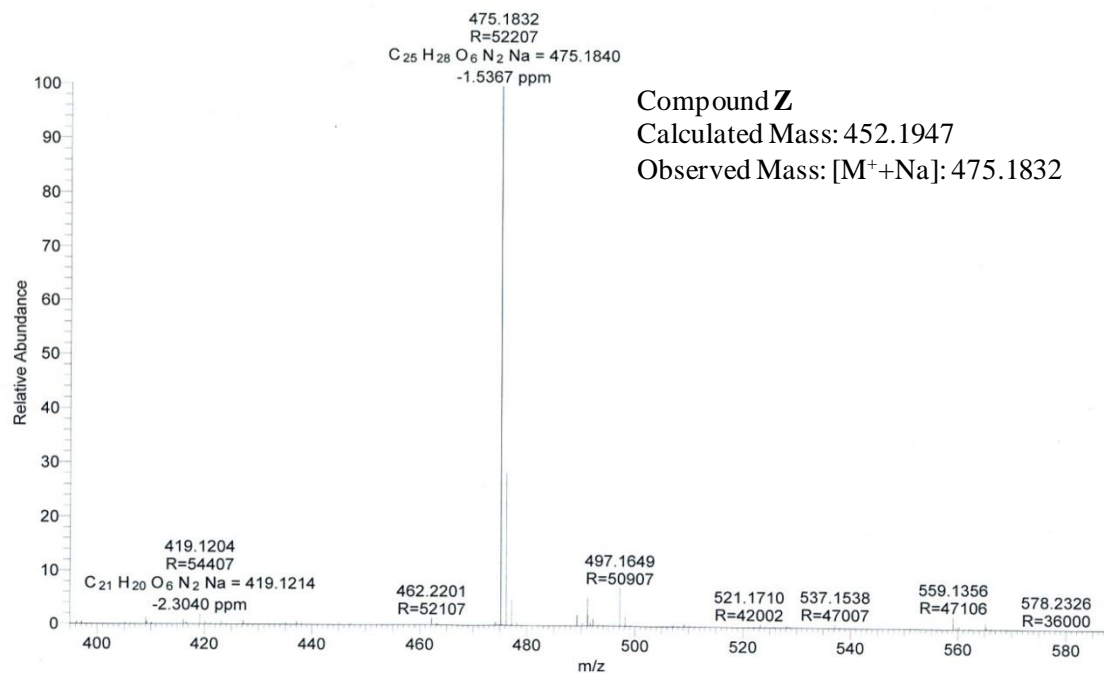


(2S,4S)-4-(((9H-fluoren-9-yl)methoxy)carbonyl)amino)-1-(tert butyloxycarbonyl)-pyrrolidine-2-carboxylic acid (Z)

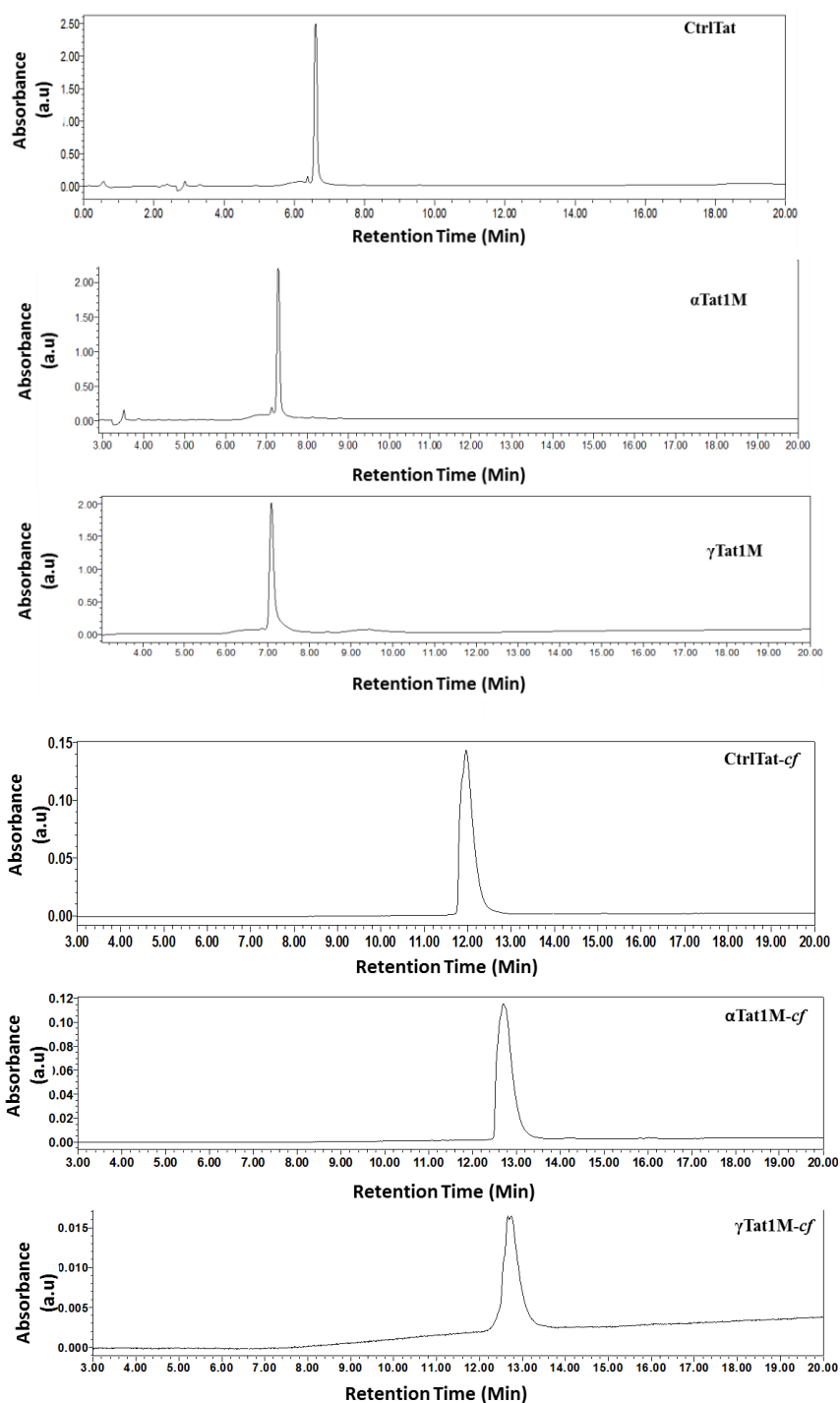


D:\Data\GB-3

6/11/2015 6:24:39 PM

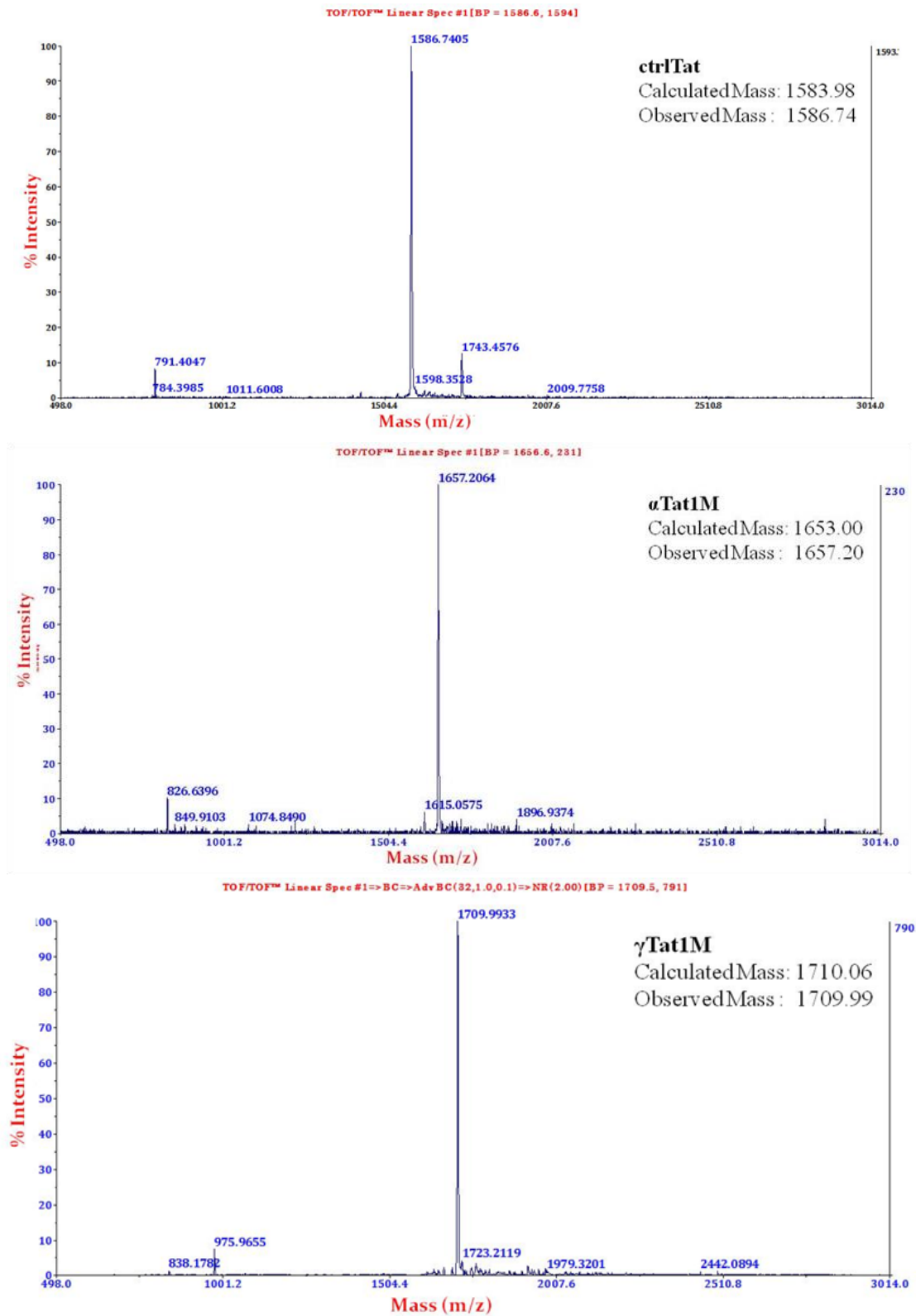
GB-3 #119 RT: 0.53 AV: 1 NL: 2.23E8
T: FTMS + p ESI Full ms [100.00-1500.00]

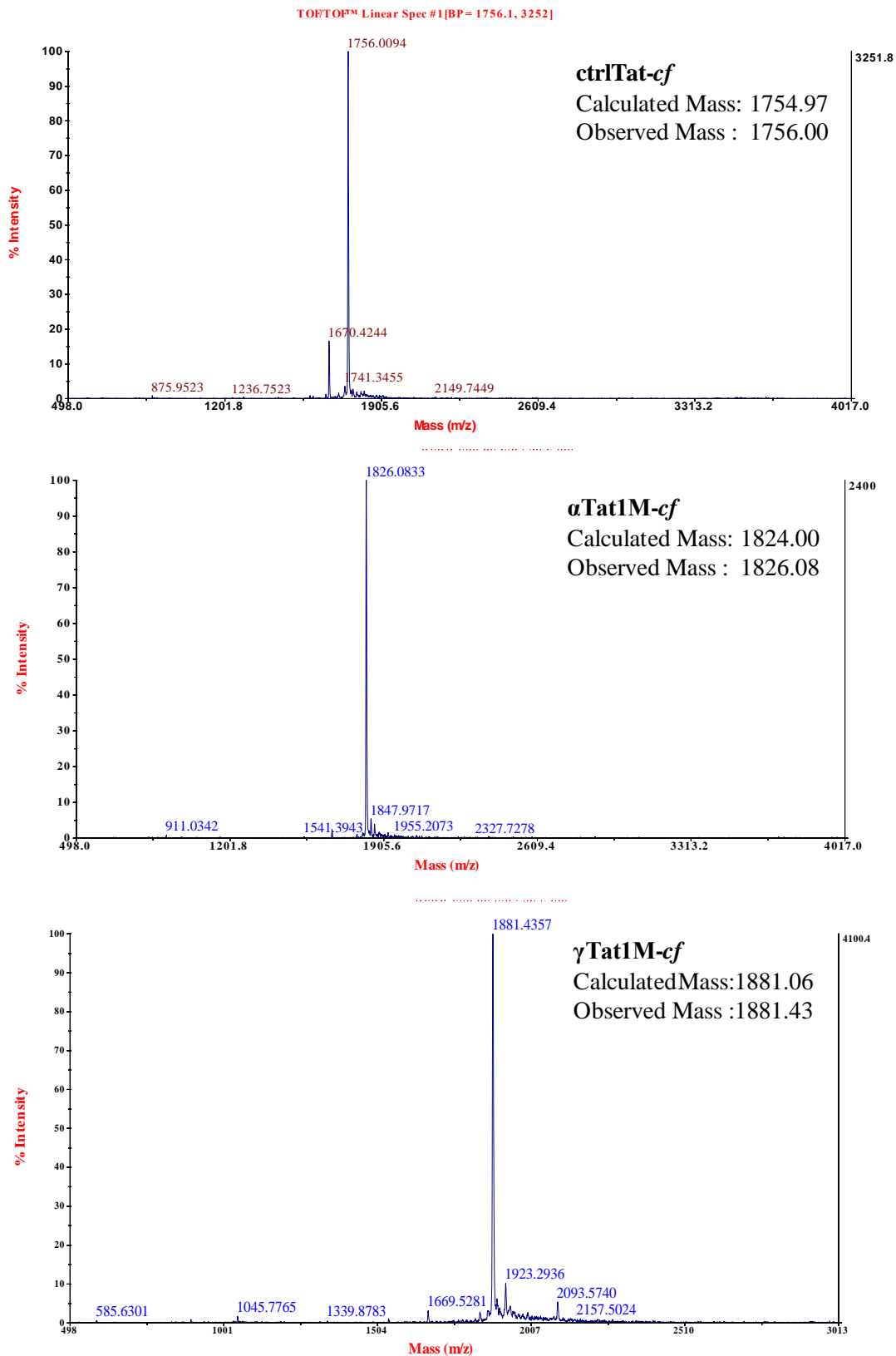
RP-HPLC Chromatograms of the Tat peptides



HPLC conditions: For unlabelled peptides, an increasing gradient of 5 to 50 % CH₃CN in water containing 0.1 % TFA in 10 min, followed by 50% CH₃CN/H₂O. For *cf*-labelled peptides, an increasing gradient of 5 to 50 % CH₃CN in water containing 0.1 % TFA in 20 min. The absorbance was monitored at 220 nm and 254 nm; the HPLC profiles at 220 nm are shown above.

MALDI-TOF Spectra





2B.7 References

1. Palchaudhuri, R.; Hergenrother, P. J.; *Curr. Opin. Biotechnol.*, **2007**, *18*, 497–503.
2. Rask-Andersen, M.; Almen, M. S.; and Schioth, H. B.; *Nat. Rev. Drug Discovery*, **2011**, *10*, 579–590.
3. Limbach, P. A.; Crain, P. F.; McCloskey, J. A.; *Nucleic Acids Res.*, **1994**, *22*, 2183–2196.
4. Czerwoniec, A.; Dunin-Horkawicz, S.; Purta, E.; Kaminska, K. H.; Kasprzak, J. M.; Bujnicki, J. M.; Grosjean, H.; and Rother, K., *Nucleic Acids Res.*, **2009**, *37*, 14.
5. Bischoff, G.; Hoffmann, S.; *Curr. Med. Chem.*, **2002**, *9*, 312–348.
6. Doss, R. M.; Marques, M. A.; Foister, S.; Chenoweth, D. M.; Dervan, P. B.; *J. Am. Chem. Soc.*, **2006**, *128*, 9074–9079.
7. Edward, C. S.; (Ralph, A. W., Ed.), **2010**, 139–166.
8. Meyer, S. T.; Hergenrother, P. J.; *Org. Lett.*, **2009**, *11*, 4052–4055.
9. Liu, Y.; Peacey, E.; Dickson, J.; Donahue, C. P.; Zheng, S.; Varani, G.; Wolfe, M. S., *J. Med. Chem.*, **2009**, *52*, 6523–6526.
10. Zengeya, T.; Li, M.; Rozners, E.; *Bioorg. Med. Chem. Lett.*, **2011**, *21*, 2121–2124.
11. Lu, J.; Kadakkuzha, B. M.; Zhao, L.; Fan, M.; Qi, X.; Xia, T.; *Biochemistry*, **2011**, *50*, 5042–5057.
12. Zaman, G. J. R.; Michiels, P. J. A.; van Boeckel, C. A. A.; *Drug Discovery Today*, **2003**, *8*, 297–306.
13. Thomas, J. R.; Hergenrother, P. J.; *Chem. Rev.* **2008**, *108*, 1171–1224.
14. Lee, M. M.; Pushechnikov, A.; Disney, M. D.; *ACS Chem. Biol.*, **2009**, *4*, 345–355.
15. Davidson, B. L.; McCray, P. B.; *Nat. Rev. Genet.*, **2011**, *12*, 329–340.
16. Watts, J. K.; Corey, D. R.; *Bioorg. Med. Chem. Lett.*, **2010**, *20*, 3203–3207.
17. Stevens, M.; De Clercq, E.; Balzarini, J.; *Med. Res. Rev.*, **2006**, *26*, 595–625.
18. Rana, T. M.; Jeang, K.-T.; *Arch. Biochem. Biophys.*, **1999**, *365*, 175–185.
19. Bannwarth, S.; Gatignol, A.; *Curr. HIV Res.* **2005**, *3*, 61–71.
20. Keen, N. J.; Gait, M. J.; Karn, J.; *Proc. Natl. Acad. Sci. U.S.A.*, **1996**, *93*, 2505–2510.
21. Hirsch, M. S.; Brun-Vézinet, F.; Clotet, B.; Conway, B.; Kuritzkes, D. R.; D’Aquila, R. T.; Demeter, L. M.; Hammer, S. M.; Johnson, V. A.; Loveday, C.; Mellors, J. W.; Jacobsen, D. M.; Richman, D. D.; *Clin. Infect. Dis.*, **2003**, *37*, 113–128.
22. Tao, J.; Frankel, A. D.; *Proc. Natl. Acad. Sci. U.S.A.*, **1992**, *89*, 2723–2726.

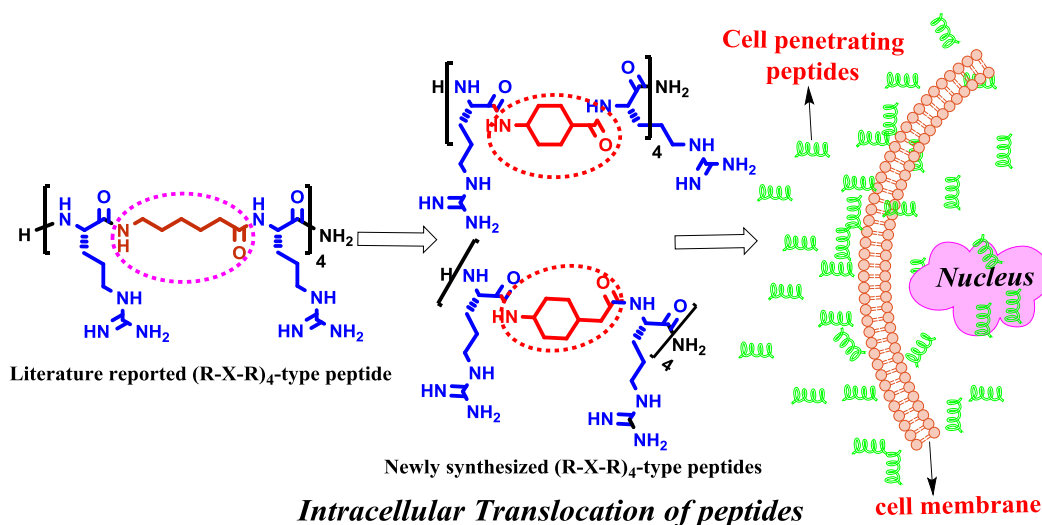
23. Pang, R.; Zhang, C.; Yuan, D.; Yang, M.; *Biorg. Med. Chem.*, **2008**, *16*, 8178–8186.
24. Hwang, S.; Tamilarasu, N.; Ryan, K.; Huq, I.; Richter, S.; Still, W. C.; Rana, T. M.; *Proc. Natl. Acad. Sci. U. S. A.*, **1999**, *96*, 12997–13002.
25. Mei, H. Y.; Mack, D. P.; Galan, A. A.; Halim, N. S.; Heldsinger, A.; Loo, J. A.; Moreland, D. W.; Sannes-Lowery, K. A.; Sharmeen, L.; Truong, H. N.; Czarnik, A. W.; *Bioorg. Med. Chem.*, **1997**, *5*, 1173–1184.
26. Davis, B.; Afshar, M.; Varani, G.; Murchie, A. I.; Karn, J.; Lentzen, G.; Drysdale, M.; Bower, J.; Potter, A. J.; Starkey, I. D.; Swarbrick, T.; Aboul-ela, F.; *J. Mol. Biol.*, **2004**, *336*, 343–356.
27. Murchie, A. I.; Davis, B.; Isel, C.; Afshar, M.; Drysdale, M. J.; Bower, J.; Potter, A. J.; Starkey, I. D.; Swarbrick, T. M.; Mirza, S.; Prescott, C. D.; Vaglio, P.; Aboul-ela, F.; Karn, J.; *J. Mol. Biol.*, **2004**, *336*, 625–638.
28. Michienzi, A.; Li, S.; Zaia, J. A.; Rossi, J. J.; *Proc. Natl. Acad. Sci. U.S.A.*; **2002**, *99*, 14047–14052.
29. Bohjanen, P. R.; Colvin, R. A.; Puttaraju, M.; Been, M. D.; GarciaBlanco, M. A.; *Nucleic Acids Res.*, **1996**, *24*, 3733–3738.
30. Wang, D.; Iera, J.; Baker, H.; Hogan, P.; Ptak, R.; Yang, L.; Hartman, T.; Buckheit, R. W. Jr.; Desjardins, A.; Yang, A.; Legault, P.; Yedavalli, V.; Jeang, K. T.; Appella, D. H.; *Bioorg. Med. Chem. Lett.*, **2009**, *19*, 6893–6897.
31. Davidson, A.; Leeper, T. C.; Athanassiou, Z.; Patora-Komisarska, K.; Karn, J.; Robinson, J. A.; Varani, G.; *Proc. Natl. Acad. Sci. U.S.A.*, **2009**, *106*, 11931–11936.
32. Athanassiou, Z.; Patora, K.; Dias, R. L.; Moehle, K.; Robinson, J. A.; Varani, G.; *Biochemistry*, **2007**, *46*, 741–751.
33. Lalonde, M. S.; Lobritz, M. A.; Ratcliff, A.; Chamanian, M.; Athanassiou, Z.; Tyagi, M.; Wong, J.; Robinson, J. A.; Karn, J.; Varani, G.; Arts, E. J.; *PLoS Pathog.*, **2011**, *7*, e1002038.
34. a) Tor, Y.; *ChemBioChem*, **2003**, *4*, 998–1007. b) Hermann, T.; *Curr. Opin. Struct. Biol.*, **2005**, *15*, 355–366.
35. Kao, S.-Y.; Calman, A. F.; Luciw, P. A.; Peterlin, B. M. *Nature (London)* 1987, **330**, 489–493.

36. a) Dingwall, C.; Ernberg, I.; Gait, M. J.; Green, S. M.; Heaphy, S.; Karn, J.; Lowe, A. D.; Singh, M.; Skinner, M. A.. *EMBO J.* **1990**, *9*, 4145- 4153. b) Cordingley, M. G.; LaFemina, R. L.; Callahan, P. L.; Condra, J. H.; Sardana, V. V.; Graham, D. J.; Nguyen, T. M.; LeGrow, K.; Gotlib, L.; Schlabach, A. J. COLONNO, R.J.; *Proc. Natl. Acad. Sci. U.S.A.*, **1990**, *87*, 8985-8989.
37. Weeks, K. M.; Ampe, C.; Schultz, S. C.; Steitz, T. A.; Crothers, D. M.; *Science*, **1990**, *249*, 1281-1285.
38. (a) Athanassiou, Z.; Dias, R. L.A.; Moehle, J.; Dobson, N.; Varani, G.; Robinson, J. A.; *J. Am. Chem. Soc.*, **2004**, *126*, 6906-6913. (b) Bryson, D. I.; Zhang, W.; McLendon, P. M.; Reineke, T. M.; Santos, W. L.; *ACS Chem. Biol.*, **2012**, *7*, 210–217. (c) Bryson, D. I.; Zhang, W.; Ray, W. K.; Santos, W. L.; *Mol. BioSyst.*, **2009**, *5*, 1070–1073. (d) Hwang, S.; Tamilarasu, N.; Ryan, K.; Huq, I.; Richter, S.; Still, W. C.; Rana, T. M., *Proc. Natl. Acad. Sci. U. S. A.*, **1999**, *96*, 12997–13002. (e) Lalonde, M. S.; Lobritz, M. A.; Ratcliff, A.; Chamanian, M.; Athanassiou, Z.; Tyagi, M.; Wong, J.; Robinson, J. A.; Karn, J.; Varani, G.; Arts, E. J., *PLoS Pathogens*, **2011**, *7*, 1-17. (e) Zhang, W.; Bryson, D. I.; Crumpton, J. B.; Wynn, J.; Santos, W. L., *Chem. Commun.*, **2013**, *49*, 2436-2438.
39. (a) Athanassiou, Z.; Patora, K.; Dias, R. L.; Moehle, K.; Robinson, J. A.; Varani, G.; *Biochemistry*, **2007**, *46*, 741–751. (b) Tamilarasu, N.; Huq, I.; Rana, T. M.; *Bioorg. Med. Chem. Lett.*, **2001**, *11*, 505-507.
40. (a) Simon, R. J.; Kania, R. S.; Zuckermann, R. N.; Huebner, V. D.; Jewell, D. A.; Banville, S.; Ng, S.; Wang, L.; Rosenberg, S.; Marlowe, C.K.; *Proc. Natl. Acad. Sci. U.S.A.* **1992**, *89*, 9367-9371. (b) Kesavan, V.; Tamilarasu, N.; Cao, H.; Rana, T. M. *Bioconjugate Chem.* **2002**, *13*, 1171-1175.
41. Das, I.; Désiré, J.; Manvar, D.; Baussanne, I.; Pandey, V. N.; Décout, J.-L. *J. Med. Chem.* **2012**, *55*, 6021–6032.
42. Carter, A. P.; Clemons, W. M.; Brodersen, D. E.; Morgan-Warren, R. J.; Wimberly, B. T.; Ramakrishnan, V.; *Nature*, **2000**, *407*, 340–348.
43. Tor, Y.; *Biochimie*, **2006**, *88*, 1045–1051.
44. Brodersen, D. E.; Clemons, W. M.; Jr, Carter, A. P.; Morgan- Warren, R. J.; Wimberly, B. T.; Ramakrishnan, V.; *Cell*, **2000**, *103*, 1143–1154.
45. Wilson, D. N.; Harms, J. M.; Nierhaus, K. H.; Schlünzen, F.; Fucini, P.; *Biol. Chem.* **2005**,

- 386, 1239–1252.
46. Hermann, T.; *Curr. Opin. Struct. Biol.*, **2005**, *15*, 355–366.
47. Leach, K. L.; Swaney, S. M.; Colca, J. R.; McDonald, W. G.; Blinn, J. R.; Thomasco, Lisa M.; Gadwood, R. C.; Shinabarger, D.; Xiong, L.; Mankin, A. S.; *Mol. Cell*, **2007**, *26*, 393–402.
48. Huq, I.; Ping, Y.-H.; Tamilarasu, N.; Rana, T. M. *Biochemistry*, **1999**, *38*, 5172-5177.
49. Wang, X.; Huq, I.; Rana, T. M.; *J. Am. Chem. Soc.* **1997**, *119*, 6444- 6445.
50. Tamilarasu, N.; Huq, I.; Rana, T. M.; *J. Am. Chem. Soc.* **1999**, *121*, 1597-1598.
51. Hamy, F.; Felder, E. R.; Heizmann, G.; Lazdins, J.; Aboul-ela, F.; Varani, G.; Karn, J.; Klimkait, T. *Proc. Natl. Acad. Sci. U.S.A.* **1997**, *94*, 3548–3553.
52. Calnan, B. J.; Tidor, B.; Biancalana, S.; Hudson, D.; Frankel, A. D. *Science*, **1991**, *252*, 5009, 1167-1171.
53. (a) Zanardi, F.; Burreddu, P.; Rasso, G.; Auzzas, L.; Battistini, L.; Curti, C.; Sartori, A.; Nicastro, G.; Menchi, G.; Cini, N.; Borronocetti, A.; Raspanti, S.; Casiraghi, G.; *J. Med. Chem.*, **2008**, *51*, 1771-1782. (b) Gangamani, B. P.; Kumar, V. A.; Ganesh, K. N. *Tetrahedron*, **1996**, *57*, 15017–15030. (c) Bhosle, G. S.; Nawale, L.; Sarkar, D.; Fernandes, M. *Unpublished data, Communicated*.
54. (a) Chilukuri, H.; Kolekar, Y. M.; Bhosle, G. S.; Godbole, R. K.; Kazi, R. S.; Kulkarni, M. J.; Fernandes, M.; *RSC Adv.*, **2015**, *5*, 77332-77340. (b) Bhosle, G. S.; Nawale, L.; Sarkar, D.; Fernandes, M.; *Unpublished data, Communicated*.
55. (a) Suryawanshi, H.; Sabharwal, H.; Maiti, S.; *J. Phys. Chem. B*, **2010**, *114*, 11155-11163. (b) Kumar, S.; Maiti, S. *PLOS ONE*, **2013**, *8*, 10, 1-9.
56. Melckebeke, H. V.; Devany, M.; Di Primo, C.; Beaurain, F.; Toulmé, J.-J.; Bryce, D. L.; Boisbouvier, J.; *Proc. Natl. Acad. Sci. USA*, **2008**, *105*, 27, 9210–9215.
57. Campbell, G. R.; Loret, E. P.; *Retrovirology*, **2009**, *6*, 50.
58. Loret, E. P.; Georgel, P.; Johnson Jr., W. C.; Ho, P. S.; *Proc. Natl. Acad. Sci. USA*, **1992**, *89*, 9734-9738.
59. Demizu, Y.; Oba, M.; Okitsu, K.; Yamashita, H.; Misawa, T.; Tanaka, M.; Kurihara, M.; Gellman, S. H.; *Org. Biomol. Chem.*, **2015**, *13*, 5617-5620.
60. Lundberg, M.; Wikstrom, S.; Johansson, M.; *Mol. Ther.*, **2003**, *8*, 143.

CHAPTER 3

(R-X-R)₄-motif peptides containing conformationally constrained cyclohexane-derived spacers: Effect on cellular uptake.



Cell-Penetrating Oligomers (CPOs) are useful tools to deliver variety of cell impervious bioactive cargoes across the cell membrane. Chemical modifications in naturally occurring CPOs could enhance the efficiency of these peptides. Numerous type of CPOs have been reported such as Cell-Penetrating Peptides (CPPs), oligocarbamates, oligocarbonates, etc. Cell uptake mechanism of these oligomers is not understood completely, but it is known that it may vary and depend on their structural backbone, amphipathicity, associated cargo, etc. Many of these CPOs were found to have enhanced uptake properties with good biocompatibility. In this chapter, we have designed, synthesized and shown the applicability of Cyclohexanoic and Cyclohexyl acetic acid-derived, (R-X-R)₄-motif Peptides as CPPs. Their cellular uptake property was studied by flow cytometry and confocal microscopy analysis. Incorporation of these constrained, non-proteinogenic amino acid spacers in the CPPs has led to enhanced proteolytic stability.

3.1 Introduction

Despite numerous successes in identification and capacity to tackle therapeutic targets inside cells, therapeutic drug molecules fail to be effective because of their insufficient and/or non-specific cellular uptake. The hydrophobic plasma membrane of the cells is an crucial barrier which allows trafficking of essential molecules while preventing access to extracellular unnatural drugs or macromolecules. This highly selective barrier of the cell membranes does not easily allow the entry of essential therapeutic drug molecules inside cells. Thus in the treatment of diseases, crossing the membrane barrier is sometimes necessary but a difficult task in the absence of active transport.¹

Many promising drug candidates failed in clinical trials because they are unable to meet the necessary requirements of physical properties such as water solubility, lipophilicity and amphipathicity, which allow them to cross the cell membrane. They are either too non-polar (water insoluble) for administration and distribution or too polar for passive cellular entry. These drug molecules can be natural or synthetic, such as peptides, oligonucleotides, small molecules, nanoparticles, etc. To overcome these drawbacks, a smart drug delivery agent² is required, which will have good pharmacokinetic properties and effectiveness to transport associate cargoes to intracellular targeted sites.³ Currently, drug delivery is not only important in the treatment of diseases but also becoming important in prevention and diagnosis of diseases. In recent years, efficient drug delivery to the specific site is preferred because it influences the vital sites and hence are useful to avoid any undesirable side effects or repetitive high doses of the drug. Optimisation of cell penetrating peptides (CPPs) is necessary to improve physicochemical (such as size and amphipathicity with surface functional groups) and biological (such as enzymatic stability) properties of CPPs. The optimized CPPs are then taken up by cells more easily and can be used as successful drug delivery agents. Surface PEGylation to decorate some of these nano-drug carriers has also been studied widely to improve the blood circulation time,⁴ which could also enhance accumulation of drug near to targeted tumor site and hence passively transport drug to the targeted tumor cells.^{5,6}

CPPs are short peptides which facilitate the transport of hydrophobic/ hydrophilic small- or macro-molecules across the cell membranes of living cells. The CPPs such as proline-rich

peptides,⁷ β -peptides⁸ and cationic amphiphilic polyproline helices^{9,10} have been shown to have good cell-penetrating abilities, possibly because of favorable backbone structure while interacting with the cell membrane. A significant number of most effective CPPs are cationic in nature and contain at least six amino acids such as lysine or arginine which are positively charged at physiological pH. It was demonstrated that the guanidine head-group of arginine in polyarginine peptides was the critical component for their membrane penetration efficiency.^{11,12} An optimum balance of hydrophilic-hydrophobic components together with the favorable spatial presentation of guanidine moieties to interact with functional groups on the cell membrane was found to be important to achieve efficient cell penetration. Synthetic polyarginines in which the arginine residues were spaced by alkyl chains (RX)_n of differing lengths showed enhanced cellular uptake relative to the polyarginines themselves.¹³

3.2 Rationale, design and objectives of the present work

One of the most successful type of arginine- rich cell-penetrating peptide, is the (R-X-R)_n-motif peptides,¹⁴ where X is a non-natural amino acid, either 6-aminohexanoic acid (Ahx) or 3-aminopropanoic acid (β -alanine). Conjugates of such (R-X-R)₄-CPP with peptide nucleic acid (PNA) and phosphorodiamidate morpholino (PMO) oligomers are reported for splice correction¹⁵ and exon-skipping activity.¹⁶ Recently, it was reported that intracellular biological activity of PMO conjugated to (R-X-R)₄-peptide can be influenced by the spacing between the charges, hydrophobicity of the linker between the R residues and stereochemistry of the R units.¹⁷ To improve the cell-penetrating ability of (R-X-R)₄-type peptides, our group previously reported replacing the backbone amide linkages by carbamates, which resulted in improved cellular uptake and cargo delivery properties with decreased cytotoxicity.¹⁸ Our group also reported earlier that incorporation of five-membered pyrrolidine spacers (X') derived from proline in the (R-X'-R)₄-motif improved cell-penetrating ability of (α - ω - α)-peptides as molecular transporters.¹⁹ Five-membered rings are known to be conformationally more flexible relative to the six-membered rings. We therefore, chose to study the inclusion of a six-membered ring as a part of the spacer (X), where 6-aminohexanoic acid is replaced by its analogues containing a conformationally constrained cyclohexane ring. Specifically, we studied the inclusion of *cis*- and

trans-4-aminocyclohexanecarboxylic acid (X_{CHA} and X_{THA} respectively) and *cis*- and *trans*-4-aminocyclohexaneacetic acid (X_{CHAA} and X_{THAA} respectively) as spacers (X) in place of aminohexanoic acid (X_{HA}) (Figure 3.1). The rigidity and stereochemistry of the 6-membered ring structure in 4-aminocyclohexanecarboxylic acid and 4-aminocyclohexaneacetic acid units would allow variation of the conformational constraint and backbone chirality in the peptide. Thus, the designed 4-aminocyclohexaneacetic acid and 4-aminocyclohexanecarboxylic acid spacers (X) differ in stereochemistry at the C4 position, being derived from either the *cis* or *trans* configurations of the spacers. Further, the *cis*- and *trans*-4-aminocyclohexaneacetic acid spacers (X_{CHAA} and X_{THAA} respectively) may allow controlled flexibility by virtue of the acetic acid substituent (Figure 3.1). This study is aimed at fine-tuning the length and flexibility in the spacer “X”, in order to optimize cellular uptake.

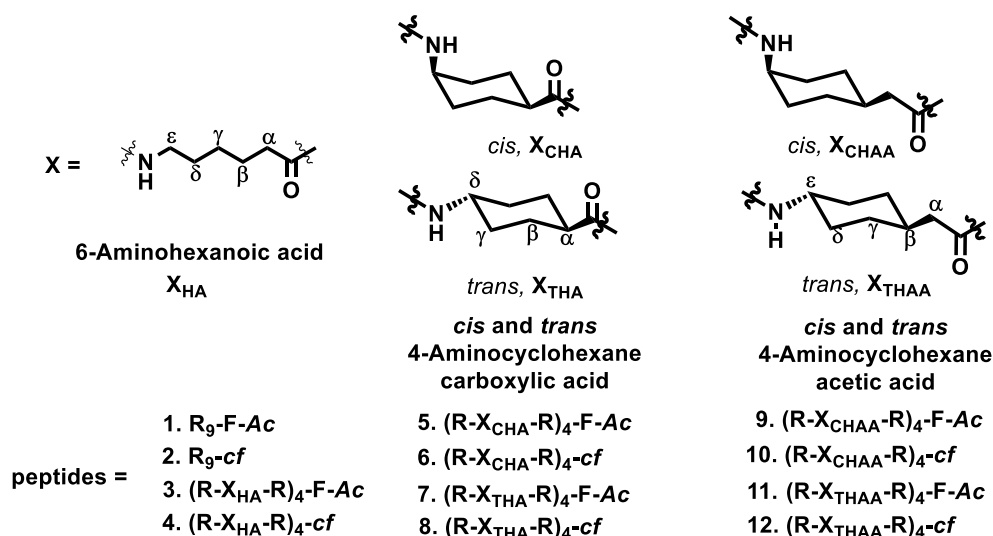


Figure 3.1. The ($-X-$) units in designed $(R-X-R)_4$ -peptides.

3.3 Results and discussion

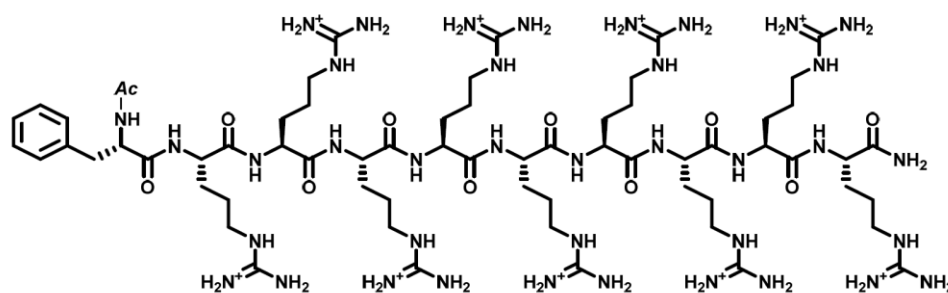
3.3.1 Solid phase peptide synthesis of (R-X-R)-motif CPPs

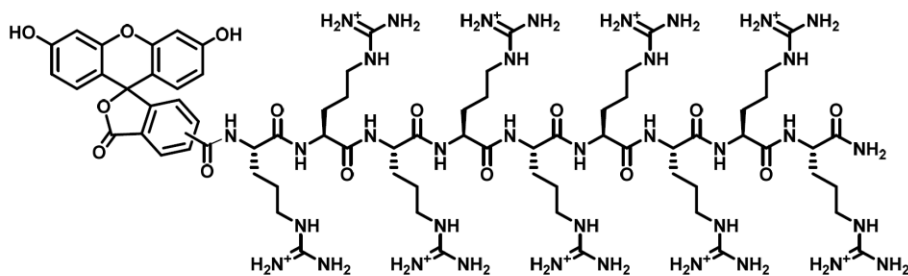
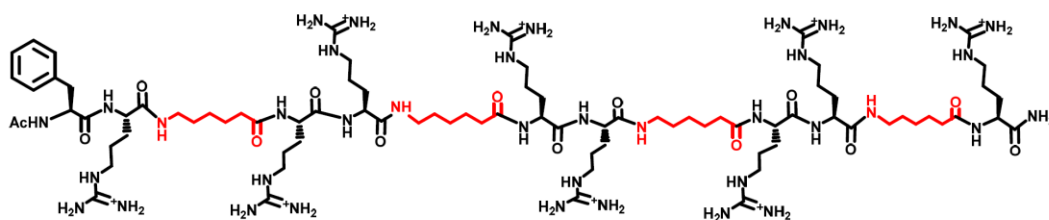
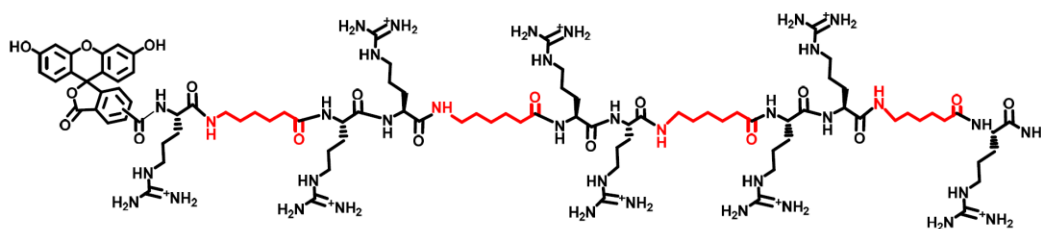
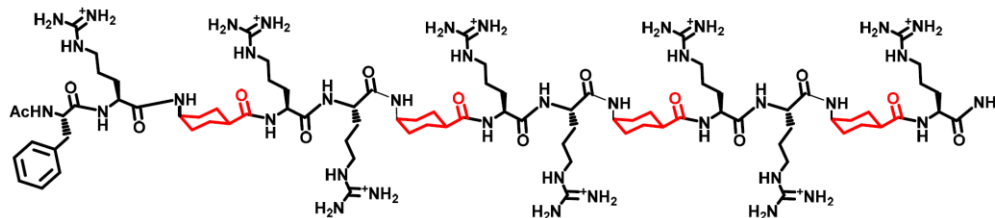
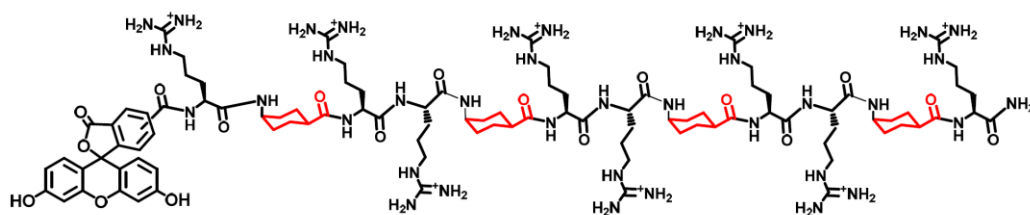
All the peptide sequences (Table 3.1) were synthesized using standard Fmoc-chemistry protocol and MBHA (4-methyl-benzylhydramine) resin as the solid support. Synthesis was carried out on 50 μ mol scale manually. Deprotection of the Fmoc protecting group was carried out in the presence of 20% piperidine in DMF. Further, coupling reactions were performed by using three equivalents each of monomer amino acid, TBTU, HOBt and DIPEA in DMF for 4h. Successive

deprotection, coupling and washing steps were carried out as iterative cycles (Chapter 2, Section A, Scheme 2A.2) until the desired length of peptide was synthesized. Deprotection and coupling reactions were monitored by the Kaiser test.

The four Fmoc-protected cyclohexane-derived monomer units amenable for solid phase peptide synthesis were commercially obtained and used as such without further purification. The protected non-natural amino acid monomers (X), were incorporated at predetermined positions in the desired arginine-rich (R-X-R)-motif peptides on solid support (MBHA resin) using Fmoc-chemistry protocol by following repetitive cycles of deprotection and coupling. For cell uptake studies, a portion of the synthesized CPPs was labeled at its N-terminal by coupling 5(6)-carboxyfluorescein(*cf*) in the presence of *N,N'*-diisopropylcarbodiimide(DIPCDI) and HOBt in DMF. In the absence of *cf*, a phenylalanine (F) residue was coupled at the N-terminal to facilitate concentration determination by UV-absorbance. The synthesized peptides were cleaved from the solid support using the standard TFA-TFMSA cleavage protocol, purified by RP-HPLC and characterized by MALDI-TOF mass spectroscopic analysis, after re-checking their purity by analytical RP-HPLC on a C18 column. The synthesized CPPs are listed in Table 3.1 and structures are depicted in Figure 3.2. The control R-X-R peptides (entries 3, 4) where X = aminohexanoic acid (X_{HA}) and peptides without spacer X (entries 1, 2) were also synthesized using similar protocols. The peptides (R- X_{CHA} -R) $_4$ -F-Ac and (R- X_{THA} -R) $_4$ -F-Ac contain *cis*-4-amino cyclohexanoic acid and *trans*-4-amino cyclohexanoic acid as the spacer unit (-X-) respectively, whereas peptides (R- X_{CHAA} -R) $_4$ -F-Ac and (R- X_{THAA} -R) $_4$ -F-Ac contain *cis*-4-amino cyclohexane acetic acid and *trans*-4-amino cyclohexane acetic acid as spacers respectively (Figure 3.2).

R₉-F-Ac



R₉-cf**(R-X_{HA}-R)₄-F-Ac****(R-X_{HA}-R)₄-cf****(R-X_{CHA}-R)₄-F-Ac****(R-X_{CHA}-R)₄-cf**

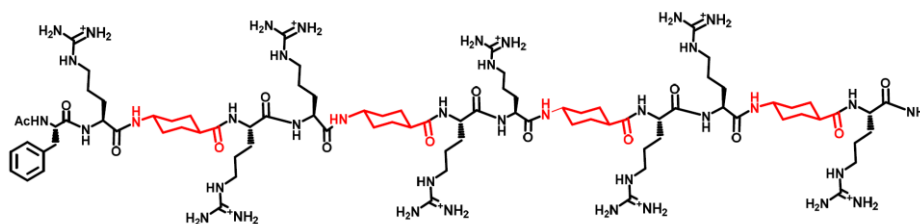
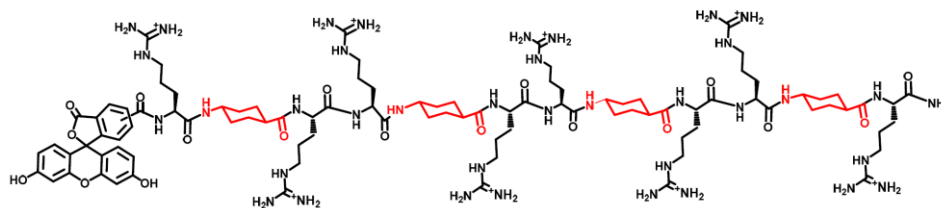
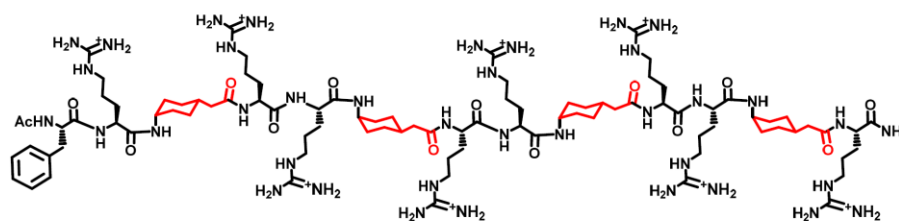
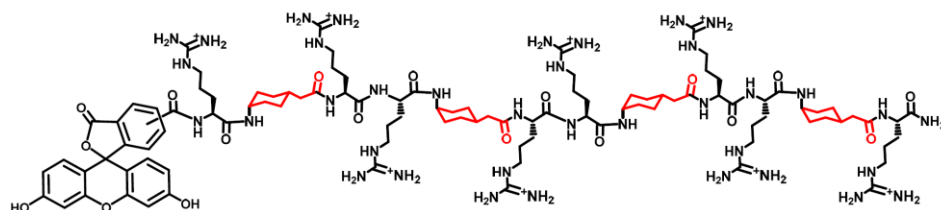
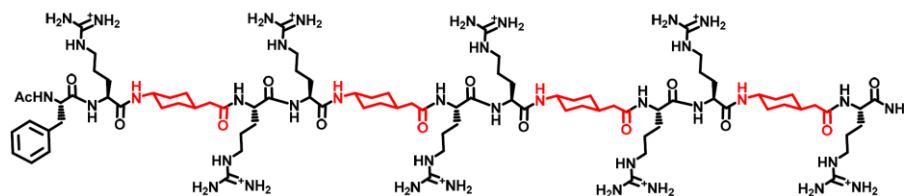
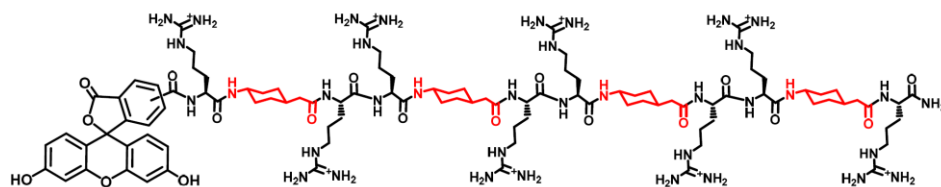
(R-X_{THA}-R)₄-F-Ac**(R-X_{THA}-R)₄-cf****(R-X_{CHAA}-R)₄-F-Ac****(R-X_{CHAA}-R)₄-cf****(R-X_{THAA}-R)₄-F-Ac****(R-X_{THAA}-R)₄-cf****Figure 3.2.**Chemical structures of the designed peptides.

Table 3.1. Synthesized peptides of the study.

Entry	Peptide Name	Mass (MALDI-TOF)	
		Calculated	Observed
1	R ₉ -F-Ac	1611.01	1609.80
2	R ₉ -cf	1781.99	1784.60
3	(R-X _{HA} -R) ₄ -F-Ac	1921.30	1917.75
4	(R-X _{HA} -R) ₄ -cf	2078.23	2079.67
5	(R-X _{CHA} -R) ₄ -F-Ac	1955.25	1954.28
6	(R-X _{CHA} -R) ₄ -cf	2126.23	2123.59
7	(R-X _{THA} -R) ₄ -F-Ac	1955.25	1953.91
8	(R-X _{THA} -R) ₄ -cf	2126.23	2127.33
9	(R-X _{CHAA} -R) ₄ -F-Ac	2011.31	2010.38
10	(R-X _{CHAA} -R) ₄ -cf	2182.29	2179.51
11	(R-X _{THAA} -R) ₄ -F-Ac	2011.31	2009.81
12	(R-X _{THAA} -R) ₄ -cf	2182.29	2179.58

cf = 5(6)-carboxyfluorescein; HA = 6-aminohexanoic acid; R = L-Arginine; F = L-Phenyl alanine; Ac-Acetate; X_{CHA} = Cis-4- Amino cyclohexanoic acid; X_{THA} = Trans-4- Amino cyclohexanoic acid; X_{CHAA} = Cis-4- Amino cyclohexane acetic acid; X_{THAA} = Trans-4- Amino cyclohexane acetic acid;

3.3.2 Circular Dichroism analysis of synthesized peptides

The structural features of the CPPs were analyzed using circular dichroism (CD) spectroscopy, to examine the effect induced by the chiral cyclohexane-based spacers in the (R-X-R)₄-motif CPPs in comparison to the control (R-X_{HA}-R)₄-F-Ac peptide, comprising the achiral spacer, 6-aminohexanoic acid as X. CD spectra were recorded in water, when all the synthesized CPPs showed similar CD spectra (Figure 3.3), with maxima at 215 nm and minima at 205 nm. The cyclohexane-derived spacers were found to exert no major structural effect in the (R-X-R)₄-motif peptides.

Thus, the chirality of the spacer and conformational restrictions due to cyclohexane ring structures seem to have minimal effect on the CPP secondary structure.

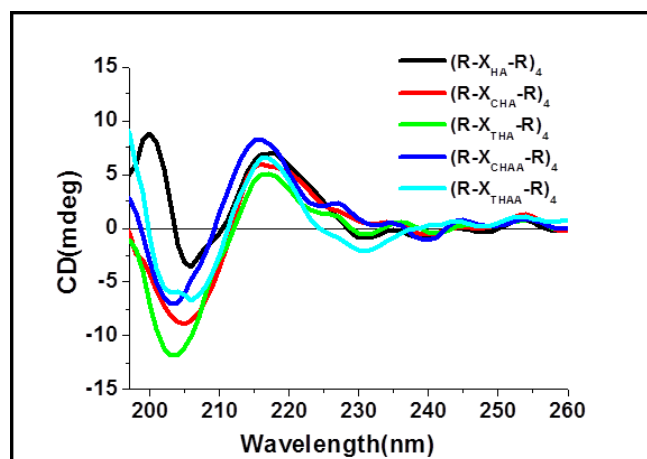


Figure 3.3. CD spectra of peptides in water at 10 μ M peptide concentration.

3.3.3 Flow Cytometry analysis

3.3.3.1 General principle of Flow Cytometry analysis

Flow cytometry is a method which is used to examine and determine the expression of intracellular molecules and the cell surface and to define and characterize distinct cell types. It is also used in determining the cell volume and cell size and to evaluate the purity of sub-populations which are isolated. This allows the multi-parameter evaluation of single cells at about the same time. Flow cytometry is used in measuring the intensity of fluorescence which is produced due to fluorescently labeled antibodies which help to identify proteins or ligands that bind to associated cells. (Figure 3.4).

Generally, flow cytometry includes three sub-systems mainly. They are the fluidics, the electronics, and the optics. In flow cytometry, five main components are available which are used in cell sorting. They are, a flow cell (a stream of liquid that is used to transport them and align the cells for optical sensing process), a system of measurement (can be of different systems including, mercury and xenon lamps, high power water-cooled or low power air-cooled lasers or diode lasers), an ADC; Analog to Digital Converter system, amplification system and a computer for analysis. The acquisition is the process by which the data is collected from the samples using flow cytometer. This process is mediated by a computer which is connected with the flow cytometer. The software present in the computer analyzes the information fed to the computer

from the flow cytometer. The software also has the ability in adjusting parameters of the experiment controlling the flow cytometer.

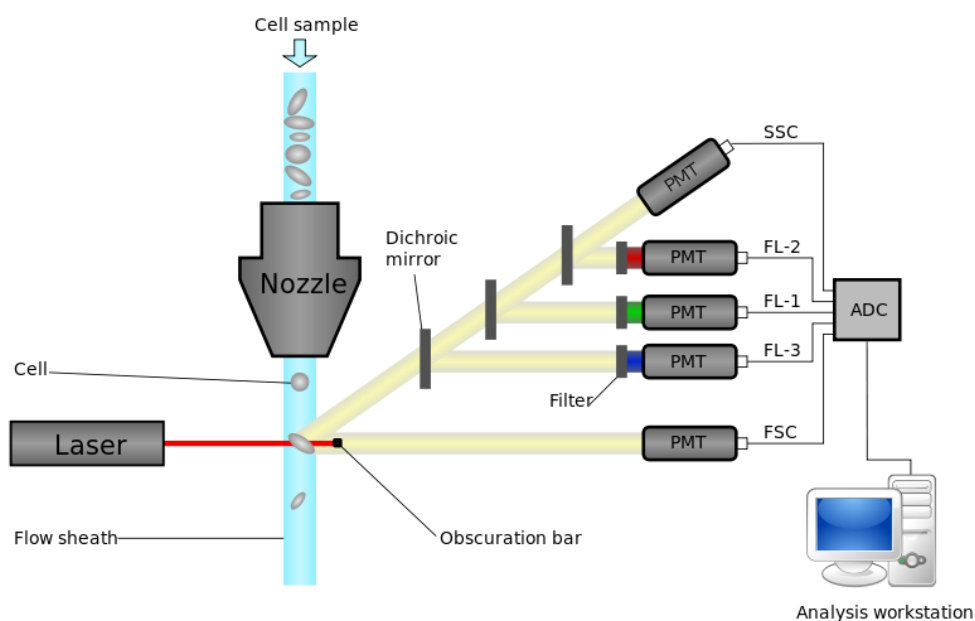


Figure 3.4. Principle of Flow cytometry (Source : Wikipedia).

Once light signals have been converted to electronic pulses and then converted to channel numbers by the Analog-to-Digital Converter (ADC), data is stored according to a standard format, the flow cytometry standard (FCS) format. According to the FCS standard, a data storage file includes a description of the sample acquired, the instrument on which the data was collected, the data set, and the results of data analysis. Multiple (approximately 10,000 events) are collected for a single sample. Once a data file has been saved, cell populations can be displayed in several different formats. A single parameter such as FSC or FITC (FL1) can be displayed as a single parameter histogram, where the horizontal axis represents the parameter's signal value in channel numbers and the vertical axis represents the number of events per channel number. Each event is placed in the channel that corresponds to its signal value. Signals with identical intensities accumulate in the same channel. Brighter signals are displayed in channels to the right of the dimmer signals.

Two parameters can be displayed simultaneously in a plot. One parameter is displayed on the x-axis and the other parameter is displayed on the y-axis. Three-dimensional data can also be viewed where the x- and y-axis represent parameters and the z-axis displays the number of events per channel.

3.3.3.2 Flow cytometry analysis of *cf*-labeled (R-X-R)-motif peptides

The cell penetration properties of the synthesized *cf*-labeled (R-X-R)-motif peptides were evaluated by flow cytometry (Figure 3.5). As seen in Figure 3.5 (A), all the modified peptides showed improved cellular uptake compared to the control peptide, (R-X_{HA}-R)₄-*cf*. Figure 3.5 (B) shows the mean fluorescence, where the peptide (R-X_{THA}-R)₄-*cf* with X = *trans*-4-aminocyclohexanecarboxylic acid was far superior to the others. On the whole, peptides containing 4-aminocyclohexanecarboxylic acid spacers displayed a higher mean fluorescence in comparison to those containing 4-aminocyclohexane acetic acid, which were similar to the controls, R₉-*cf* and (R-X_{HA}-R)₄-*cf*.

In order to understand the energy-dependence of the (R-X-R)₄-motif peptides' cell-uptake, cells were incubated with the peptides in medium containing sodium azide, a known inhibitor of energy-dependent uptake *via* an ATP depletion pathway, followed by flow cytometry analysis. The uptake of all the peptides was found to be significantly impeded, as seen in (Figure 3.6) The uptake was also found to be significantly inhibited at a lower temperature of 4 °C in comparison to 37 °C (Figure 3.6), confirming the energy-dependence of the uptake process. These results are in agreement with earlier reports^{19,20} and suggest endocytosis as the predominant mechanism of uptake.

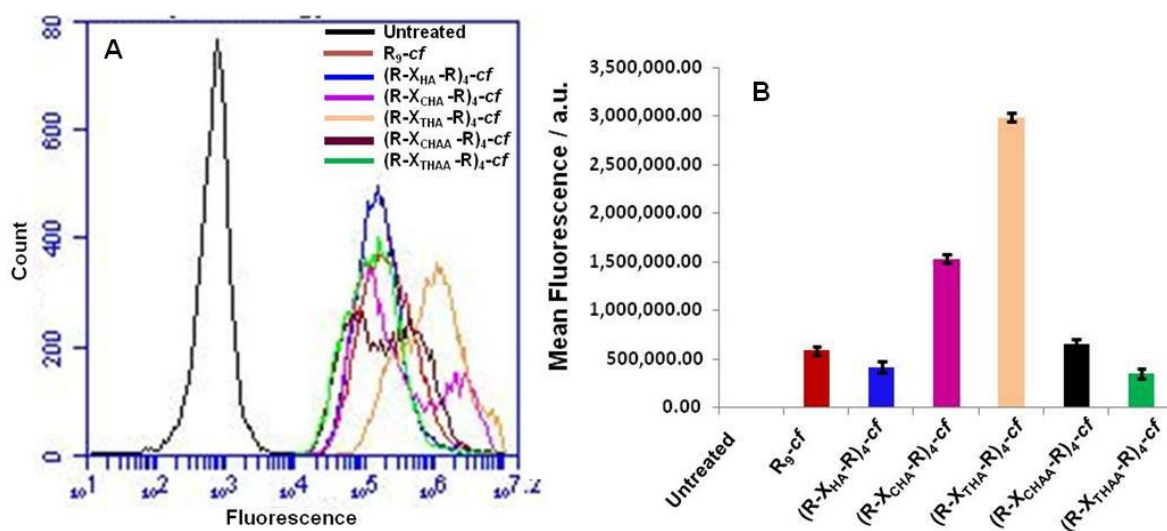


Figure 3.5 Flow cytometry analysis of HeLa cells treated with the peptides (5 μ M) for 4 h at 37 $^{\circ}$ C. (A) Number of positive cells. (B) Mean fluorescence. SD was calculated from three independent experiments.

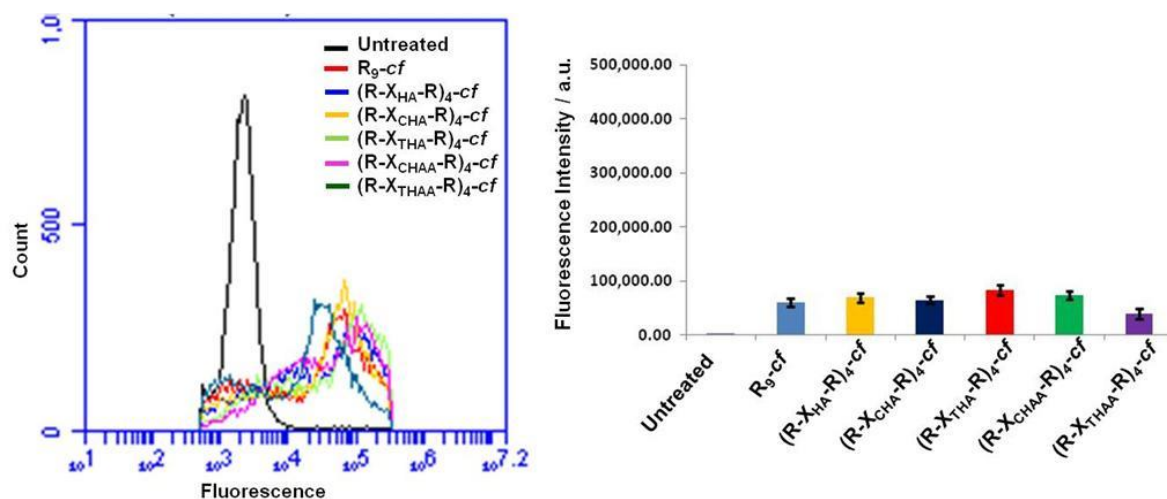


Figure 3.6. Flow cytometry analysis of peptides (5 μ M) in presence of 25 mM NaN₃ at 37 $^{\circ}$ C. SD was calculated from three independent experiments.

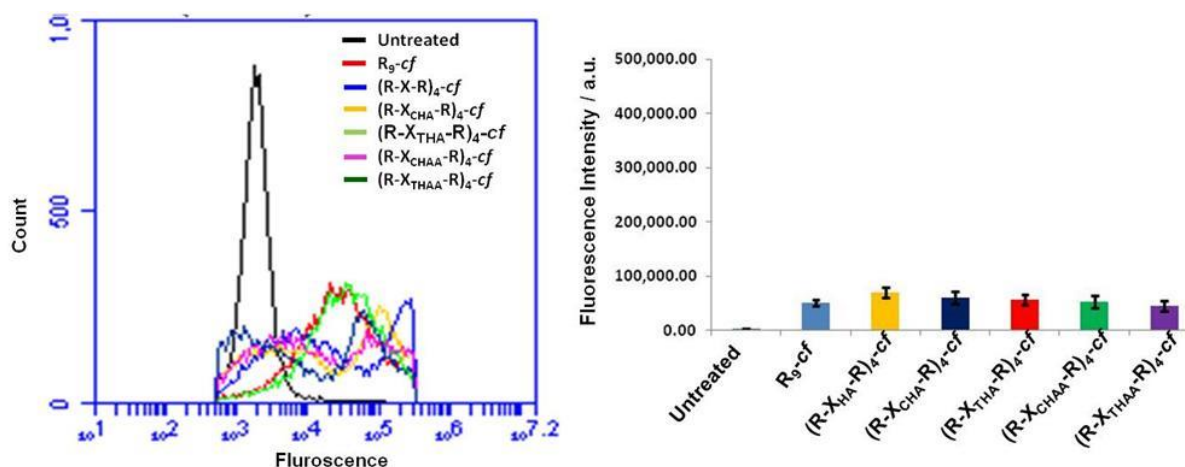


Figure 3.7. Flow cytometry analysis of peptides (5 μ M) in HeLa cells at 4 °C. SD was calculated from three independent experiments.

3.3.4 Confocal microscopy analysis

3.3.4.1 Principle of confocal microscopy

The confocal microscope is so-named because of the arrangement of the light path. There is sharing of focal plane achieved by 2 pinholes that are equidistant to the specimen in the detection and illumination of light path. Krypton/Argon and Helium/Neon mixed gas lasers gives a range of different distinct wavelengths, hence they are used in confocal microscope. The resultant light is then sent through a pinhole and reflected by a beamsplitter to the objective and specimen.

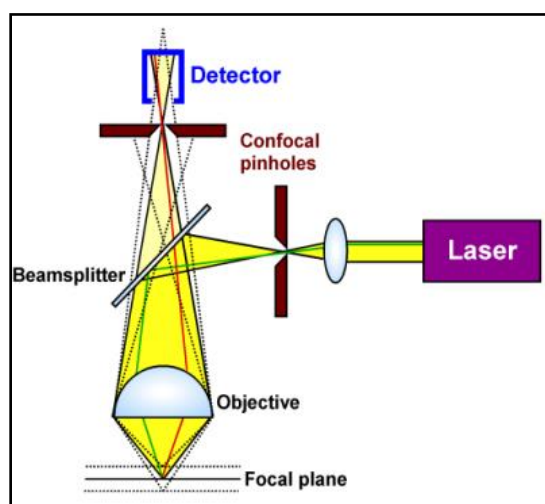


Figure 3.8 principle of confocal microscopy.²¹

Therefore, the emitted light from the specimen (which has a wavelength spectrum above the excitation wavelength) can go through the beamsplitter to the detection pinhole and the detector (actually the beamsplitter now has been replaced by an acousto-optical device). As a consequence of the pinhole arrangement, light arriving at the detector comes predominantly from a narrow focal plane, which improves the z-resolution significantly compared to conventional microscopy. At the high end, it is possible to achieve axial resolution in the submicron range.²¹

3.3.4.2 Confocal microscopic analysis of synthesized peptides

To know the intracellular localization of the CPPs, confocal microscopic analysis was carried out after incubating the cells with fluorescein-labelled CPPs. All the (R-X-R)-motif CPPs showed significant presence in the cytoplasm and also inside the nuclei and nucleoli (Figure 3.9). Their distribution was punctate, rather than diffuse, suggesting the endocytosis mode of uptake,²² as observed from the energy-dependence uptake experiments.

Considering carboxyfluorescein as a model cargo molecule, one may expect that other similarly conjugated cargo molecules such as drugs, especially those with poor cell-penetration properties, may be transported into cells by the peptides of this study. Further, as has been shown for other (R-X-R)-motif peptides^{17,18,23} and cationic CPPs, it is highly probable that these peptides will also be able to condense larger cargo molecules such as oligonucleotides or pDNA through charge interactions, enabling their transport into cells as well.

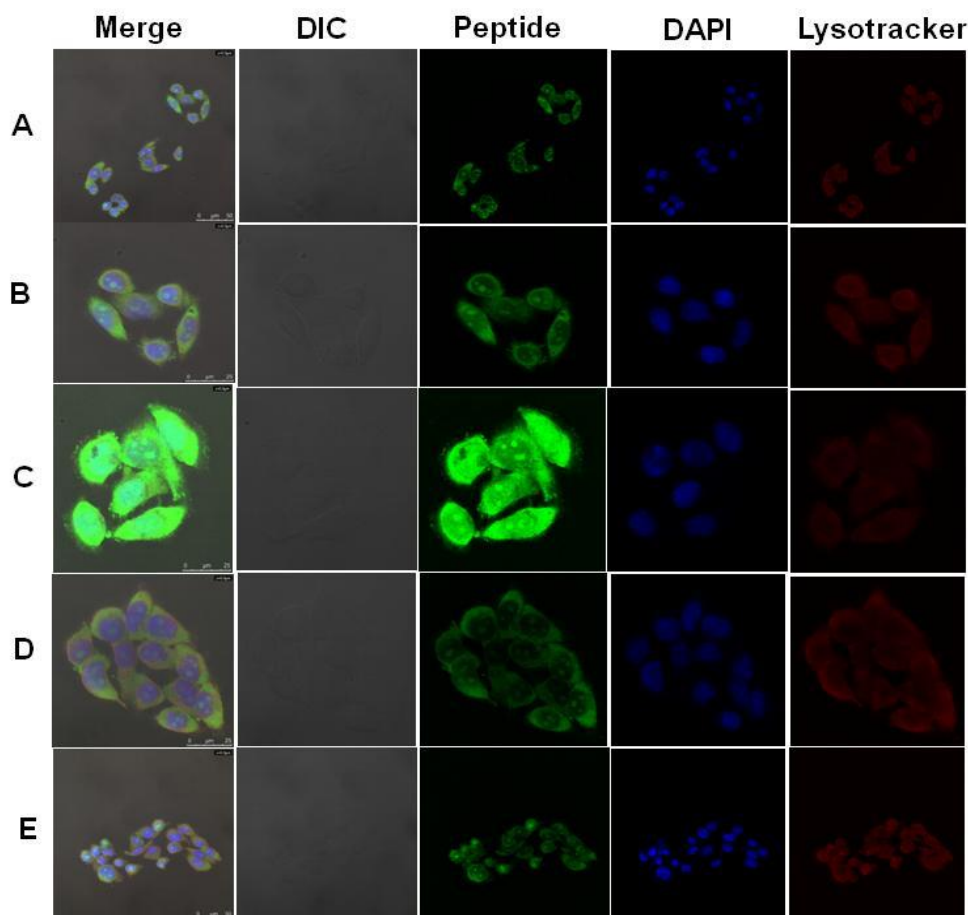


Figure 3.9. Confocal microscopy images of HeLa cells after 4 h incubation at 37 °C with the appropriate peptide (5 μM). A = $(\text{R-X}_{\text{HA}}\text{-R})_4\text{-cf}$, B = $(\text{R-X}_{\text{CHA}}\text{-R})_4\text{-cf}$, C = $(\text{R-X}_{\text{THA}}\text{-R})_4\text{-cf}$, D = $(\text{R-X}_{\text{CHAA}}\text{-R})_4\text{-cf}$, E = $(\text{R-X}_{\text{THAA}}\text{-R})_4\text{-cf}$. Scale bar: A, E = 50 μ . B, C, D = 25 μ . Merge = merged image of peptide, DAPI and Lysotracker. DIC = Differential interference contrast image. Peptide = Carboxyfluorescein labeled peptides. DAPI = Nucleus stain, Lysotracker = Lysosome stain

3.3.5 Cytotoxicity studies by the MTT and Hemolysis assays

The cytotoxicity of the synthesized CPPs was estimated in HeLa cells by the standard MTT cell viability assay. This is a colorimetric assay based on the formation of a purple formazan derivative upon reduction of 3-(4,5-dimethylthiazol-2-yl)-2,5-diphenyl tetrazolium bromide by enzymes present in viable cells. A high colour intensity is therefore, indicative of low cell toxicity and high viability. Accordingly, the synthesized CPPs were incubated with HeLa cells separately at a range of concentrations from 1 to 50 μM for 4 h, followed by evaluation of their cytotoxicity by measuring the cell viability. All the synthesized CPPs $(\text{R-X}_{\text{HA}}\text{-R})_4\text{-cf}$, $(\text{R-X}_{\text{CHA}}\text{-R})_4\text{-cf}$,

(R-X_{THA}-R)₄-cf, (R-X_{CHAA}-R)₄-cf and (R-X_{THAA}-R)₄-cf were found to be almost non-toxic, with cell viability \geq 80 % even at the highest concentration studied (Figure 3.10).

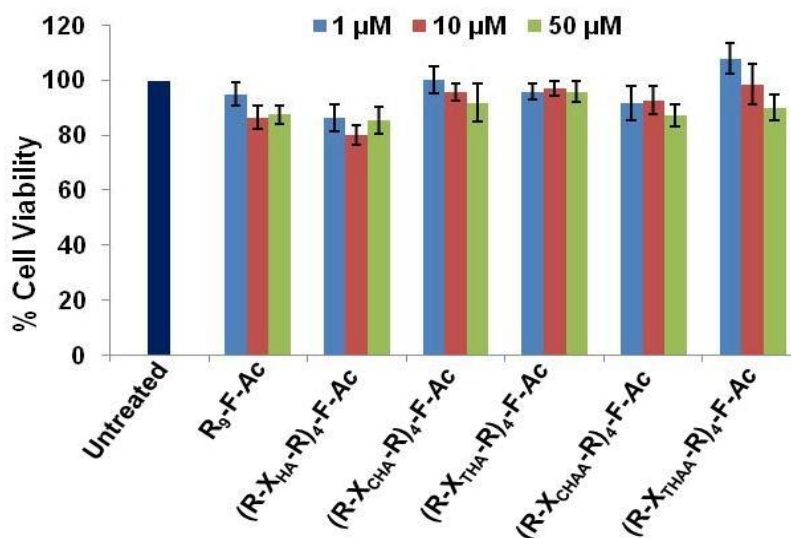


Figure 3.10. Cytotoxicity analysis of synthesized peptides by the MTT cell viability assay. SD was calculated from three independent experiments.

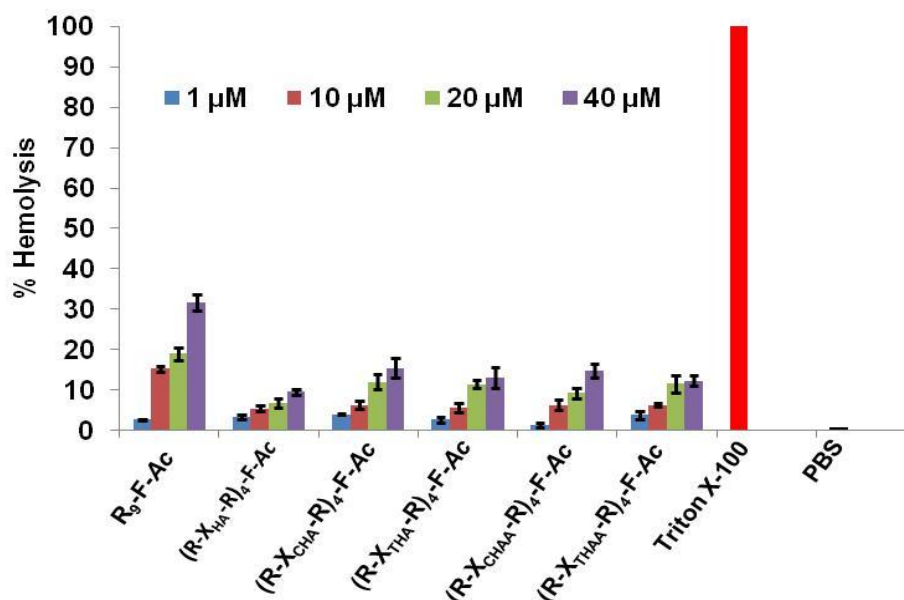


Figure 3.11. Hemolytic activity of synthesized peptides. SD was calculated from three independent experiments.

The effect of the (R-X-R)-motif peptides on mammalian cells was further investigated by the hemolysis assay,²⁴ where, disruption of the red blood cell (RBC) membrane is an indication of

toxicity, resulting in release of hemoglobin, that can be measured spectrophotometrically. An increase in absorbance is therefore, indicative of increased hemolysis and toxicity. All the (R-X-R)-motif peptides were found to have lower hemolytic activity compared to the R₉-F-Ac control peptide that contained the cationic residues concentrated together, without any spacers (Figure 3.11). Treatment with Triton X-100 and phosphate buffered saline served as positive and negative controls respectively. The results are in agreement with the cytotoxicity data obtained by the MTT assay (Figure 3.10).

3.3.6 Protease stability of Peptides

A major limitation in the applications of CPPs is their degradation by proteases. We examined the susceptibility of the various peptides to trypsin, a commercially available protease. Trypsin specifically catalyzes the hydrolysis of C-terminal amide bonds of lysine and arginine, making it an ideal enzyme for our study, as the (R-X-R)-motif peptides described herein contain multiple cleavage sites in the form of residues with cationic side chains (arginine). The introduction of non-natural amino acids in peptides is known to result in resistance to protease degradation.²⁵ We evaluated the effect of 4-amino cyclohexane-carboxylic acid and 4-amino cyclohexane acetic acid units on the protease stability of the derived (R-X-R)₄-motif peptides. The HPLC traces of the trypsin resistance study for peptide are shown in experimental section.

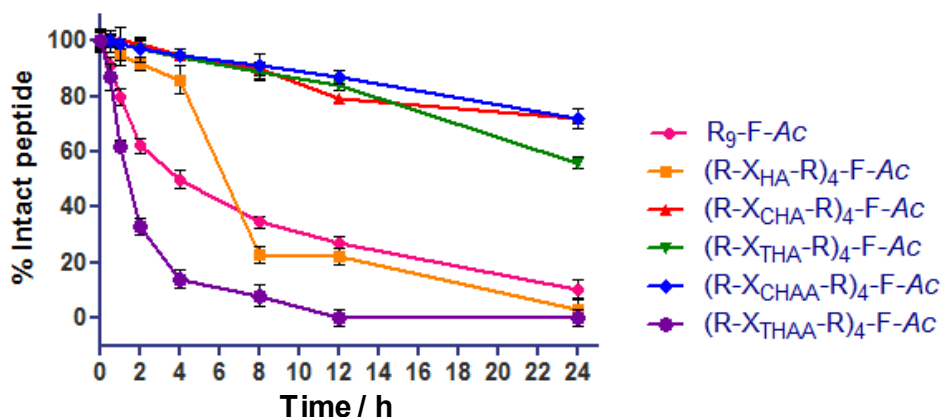


Figure 3.12. Stability of the peptides to hydrolysis by trypsin, as a function of time. SD was calculated from three independent experiments.

All the peptides containing cyclohexane spacers with the exception of (R-X_{THAA}-R)₄-F-Ac were found to be significantly resistant to trypsin digestion. The peptides bearing *cis*-4-amino-cyclohexane carboxylic acid- and *cis*-4-amino-cyclohexane acetic acid- spacers were 24-fold more resistant to hydrolysis, while those bearing *trans*-4-amino-cyclohexane carboxylic acid-spacers were 18-fold more resistant to hydrolysis, when compared to (R-X_{HA}-R)₄-F-Ac after 24 h (Figure 3.12 and Table 3.2). Thus, in general, the *cis* stereochemistry of both- the 4-amino-cyclohexane carboxylic acid and 4-amino-cyclohexane acetic acid spacers- was found to be advantageous in enhancing the stability of the derived peptides towards enzymatic hydrolysis.

Table 3.2. Percentage of peptides remaining intact after treatment with trypsin.

Time (h)	Intact peptide (%)					
	R ₉ -F-Ac	(R-X _{HA} -R) ₄ -F-Ac	(R-X _{CHA} -R) ₄ -F-Ac	(R-X _{THA} -R) ₄ -F-Ac	(R-X _{CHAA} -R) ₄ -F-Ac	(R-X _{THAA} -R) ₄ -F-Ac
0	100	100	100	100	100	100
0.5	91.4	100	100	100	100	87
1	79.8	95	100	99	99	62
2	62.3	92	99	97	97	33
4	50.1	86	95	94	95	14
8	34.5	23	90	89	91	8
12	26.7	22	79	84	87	0
24	10	3	72	56	72	0

Surprisingly, the peptides bearing *trans*-4-amino-cyclohexane carboxylic acid- and 4-amino-cyclohexane acetic acid- spacers displayed dramatically different stabilities towards trypsin hydrolysis; the *trans*-4-amino-cyclohexane acetic acid-derived (R-X_{THAA}-R)₄-F-Ac peptide was found to be completely degraded in 12 h, even faster than the control R₉-F-Ac and (R-X_{HA}-R)₄-F-Ac peptides, while the (R-X_{THA}-R)₄-F-Ac peptide displayed a stability comparable to the peptides containing the other cyclohexane-derived spacers (Figure 3.12). The reason for this unexpectedly high susceptibility of the (R-X_{THAA}-R)₄-F-Ac peptide is not known at

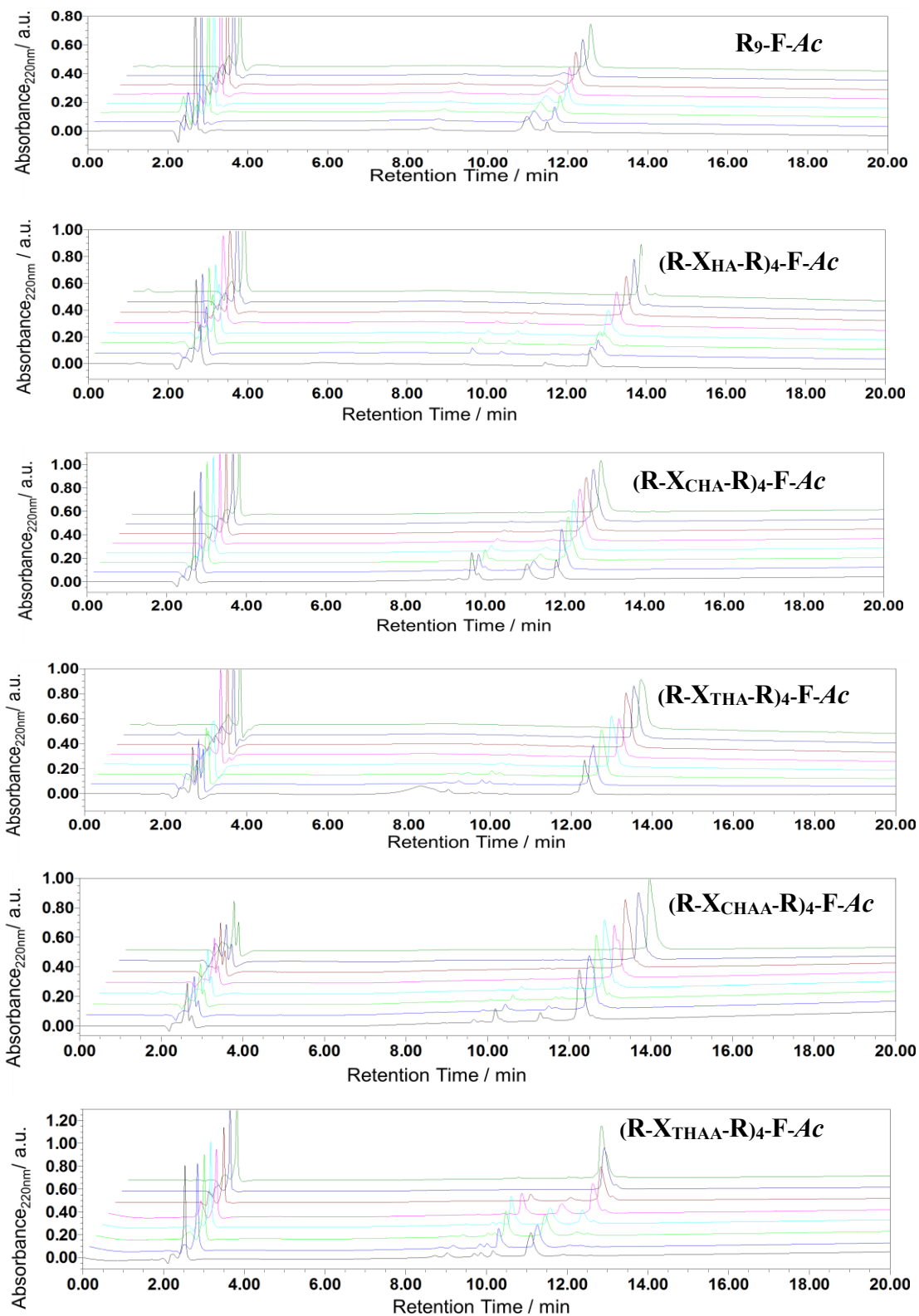


Figure 3.13. RP-HPLC profiles of the peptides to hydrolysis by trypsin.

present, but this low stability of (R- $X_{\text{THAA}}\text{-R}$)₄-F-Ac towards protease hydrolysis could account for its low cell uptake in comparison to the other peptides. The peptides (R- $X_{\text{CHA}}\text{-R}$)₄-F-Ac and (R- $X_{\text{CHAA}}\text{-R}$)₄-F-Ac were found to be the most stable, with 72 % peptide still intact after 24 h, followed by (R- $X_{\text{THA}}\text{-R}$)₄-F-Ac, (56 %). The control peptides, R₉-F-Ac and (R- $X_{\text{HA}}\text{-R}$)₄-F-Ac were almost completely degraded in 24 h, with only 10 % and 3 % intact peptide remaining at this time point (Figure 3.13). Thus, in most cases, the presence of 4-amino cyclohexane carboxylic acid and 4-amino cyclohexane acetic acid spacers confers a remarkable advantage in protecting the derived peptide from proteolysis.

3.4 Summary and conclusions

The use of chiral cyclohexanecarboxylic acid- and cyclohexane acetic acid-derived spacers in designed polycationic (R-X-R)-motif CPPs is demonstrated in a study of their cellular uptake properties. The cellular uptake followed an endocytosis pathway and the peptides were relatively non-cytotoxic in nature. The relative stereochemistry of the 1,4-substituents in the spacer, as well as its contribution to the hydrophobicity and controlled flexibility of the derived CPPs were found to significantly influence their cell-penetrating properties. The peptide containing *trans*-4-aminocyclohexanecarboxylic acid (X_{THA}) was found to possess the best cell-penetration and enzymatic stability properties in the present study.

3.5 Experimental procedure and spectral data

3.5.1 CD analysis

Circular Dichroism (CD) analysis was performed on a JASCO J-815 spectrophotometer using a 10mm cell. CD spectra were recorded as accumulations of 3 scans using a scan speed of 100nm/min, resolution of 1.0 nm, band-width 1.0 nm and a response of 1 sec. The spectra were smoothed and plotted using OriginPro 6.1. Peptides were taken at a concentration of 500 μM .

3.5.2 Cellular Uptake Assay by Fluorescence Flow Cytometry

As described previously in section A of chapter 2. (2A.6.3.5.1)

3.5.3 Experiments to evaluate the energy-dependence of cell uptake using azide

HeLa cells were seeded in 24-well culture plates (50,000 cells/well) and incubated overnight in 400 μ L of DMEM containing 10% fetal bovine serum (FBS). The medium was then replaced with fresh medium containing 10% FBS. Cells were pre-incubated at 37 °C for 30 min in the presence of 25 mM NaN_3 . A peptide solution (5 μ M) was added to each well. The medium was removed after 4h incubation, and cells were washed with ice-cold PBS with heparin (20 units/mL) and trypsinized. After the addition of medium containing 10% FBS, cells were centrifuged at 1,600 rpm for 3 min at 4 °C. The cell pellets obtained were suspended in ice-cold PBS with heparin and centrifuged at 1,600 rpm for 3 min at 4 °C. Flow cytometry measurements were carried out on BD Accuri™ C6 Flow Cytometer System using BD Accuri C6 Software. 10,000 live cells were used for each analysis at room temperature.

3.5.4 Confocal microscopy

As described previously in section A of chapter 2. (2A.6.3.5.2)

3.5.5 Cytotoxicity

As described previously in section A of chapter 2. (2A.6.3.5.3)

3.5.6 Hemolysis assay

As described previously in section A of chapter 2. (2A.6.3.5.1)

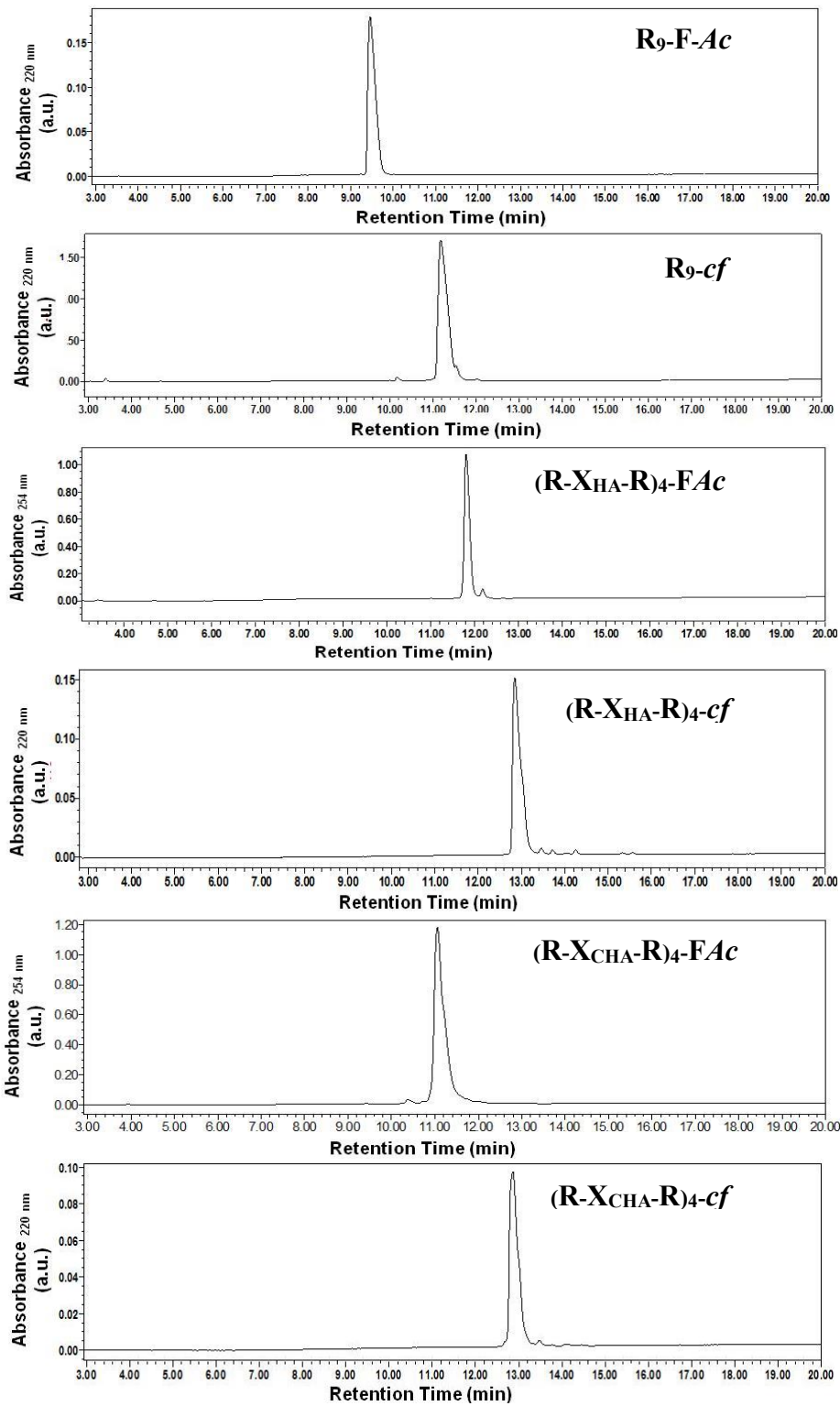
3.5.7 Trypsin Digestion Assay

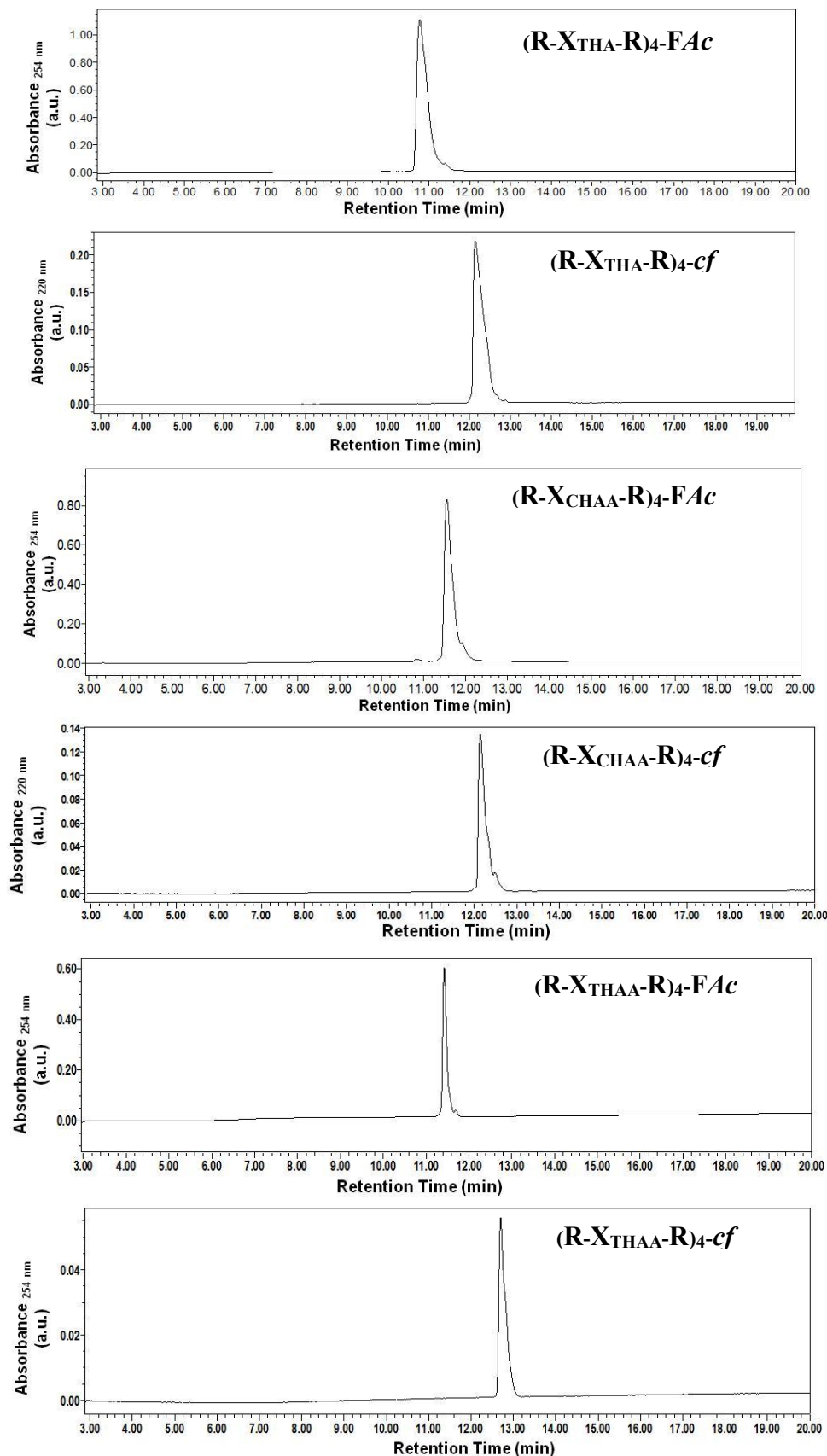
As described previously in section A of chapter 2. (2A.6.3.6)

3.6 Appendix C

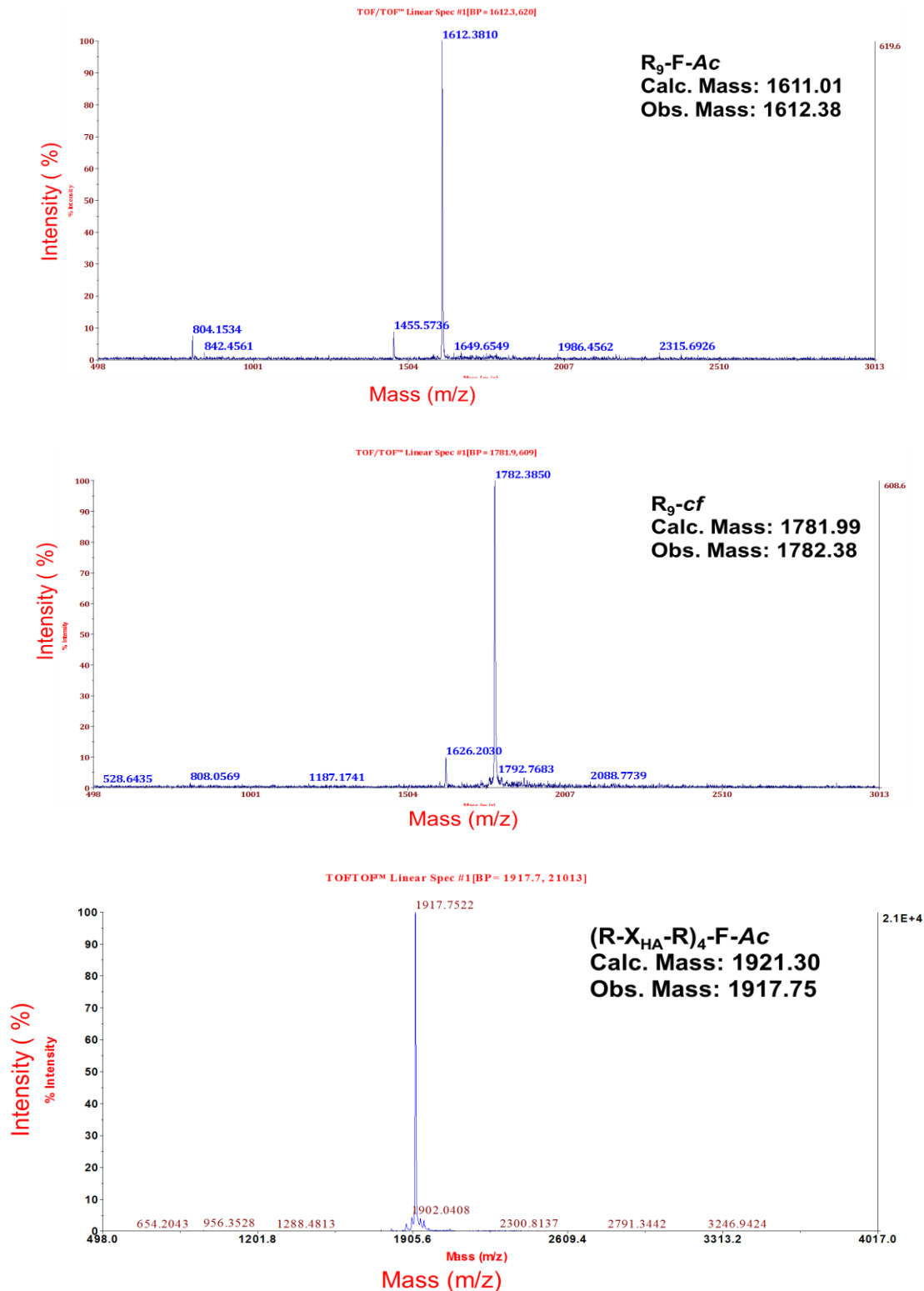
Compound and characterization	Page No.
RP-HPLC Chromatograms of Peptides	140- 141
MALDI-TOF Spectra of Peptides	142 - 145

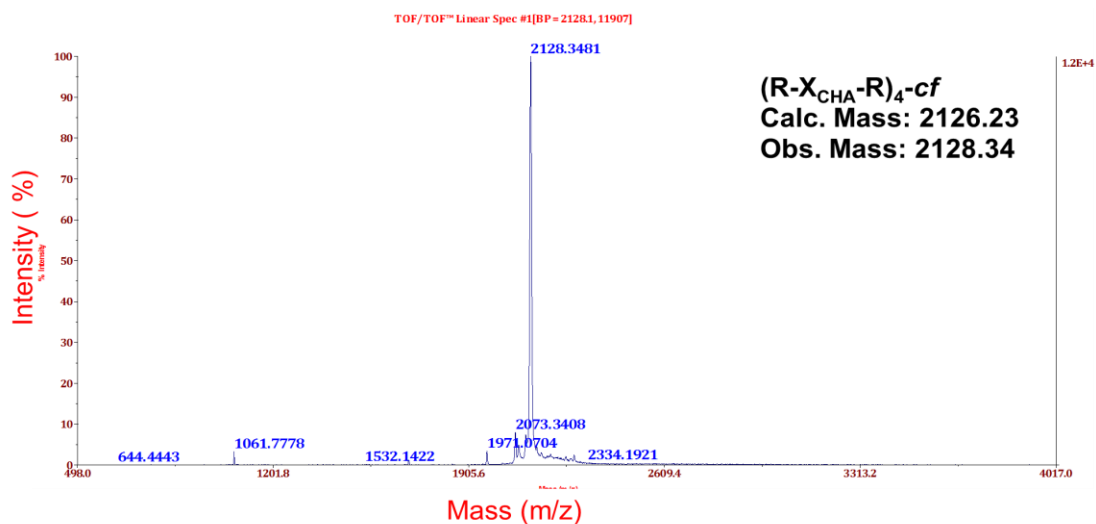
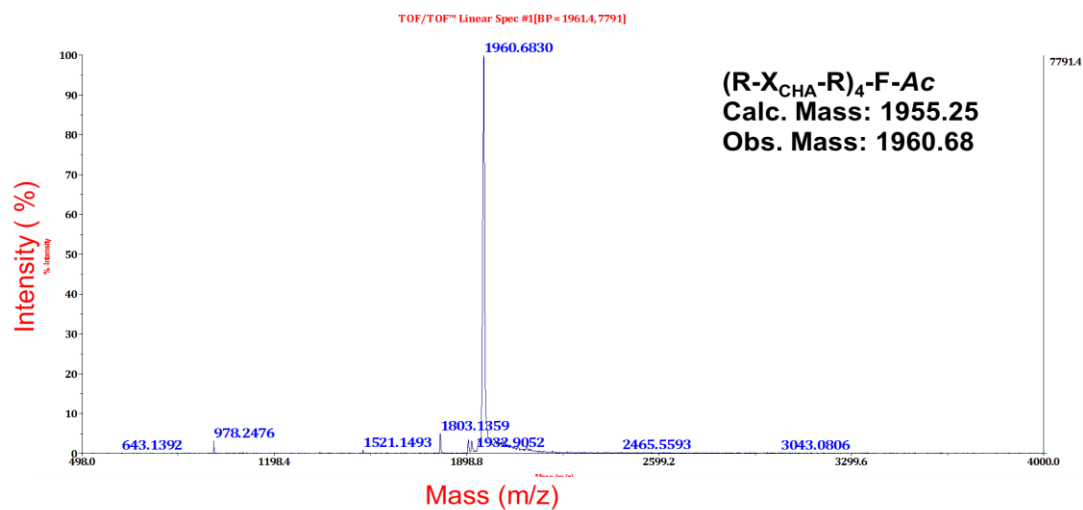
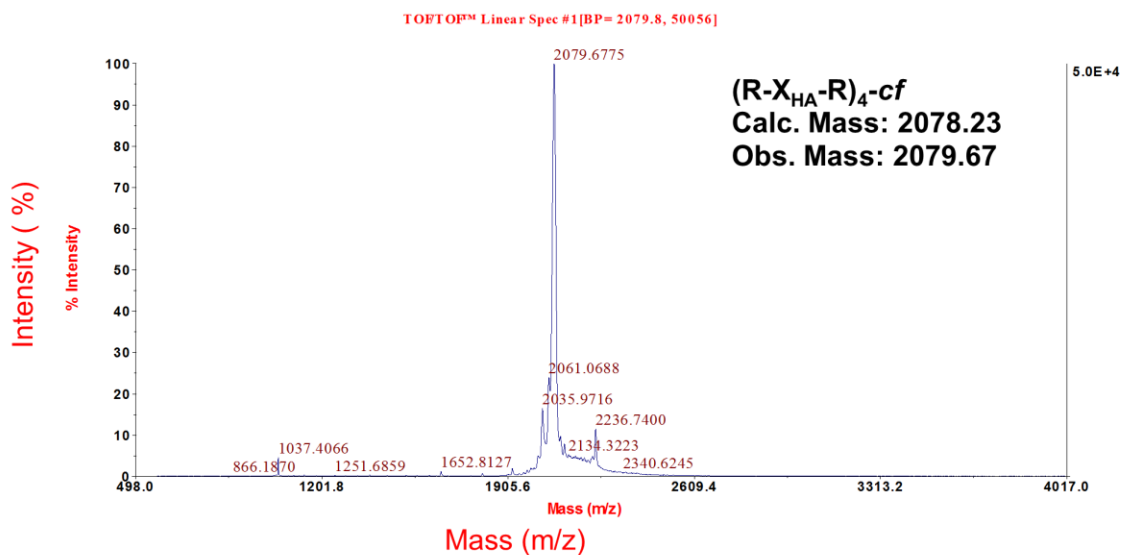
RP-HPLC Chromatograms of Peptides

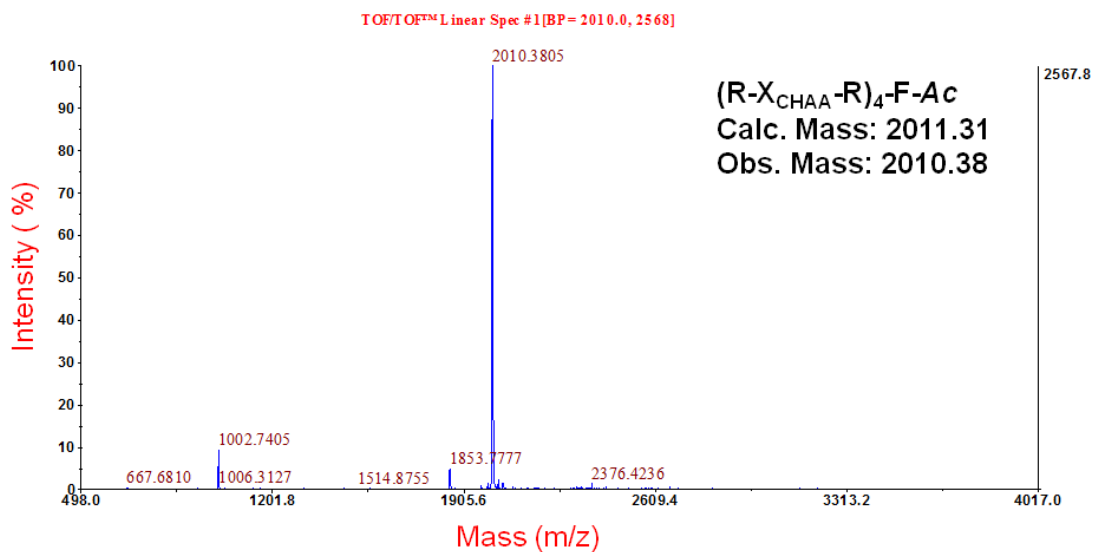
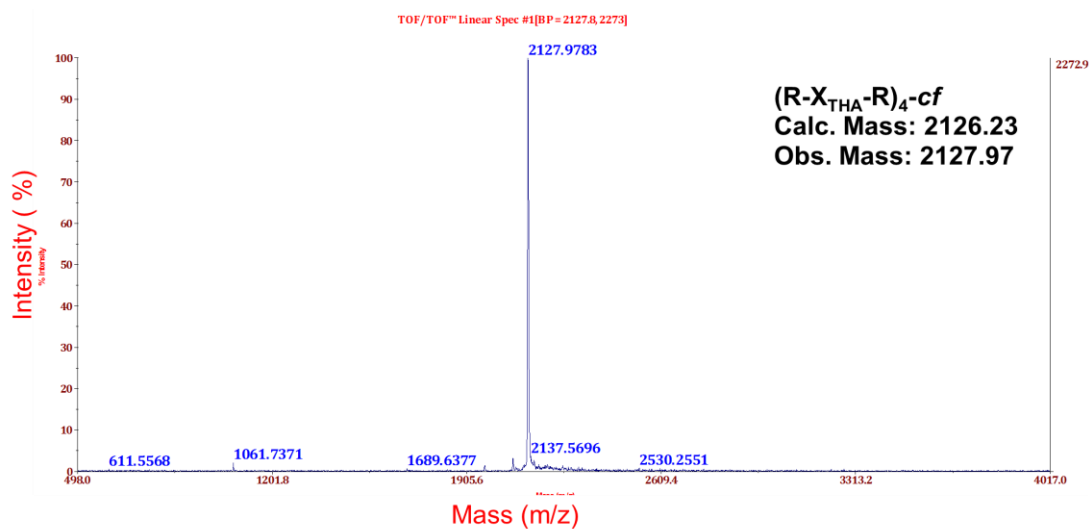
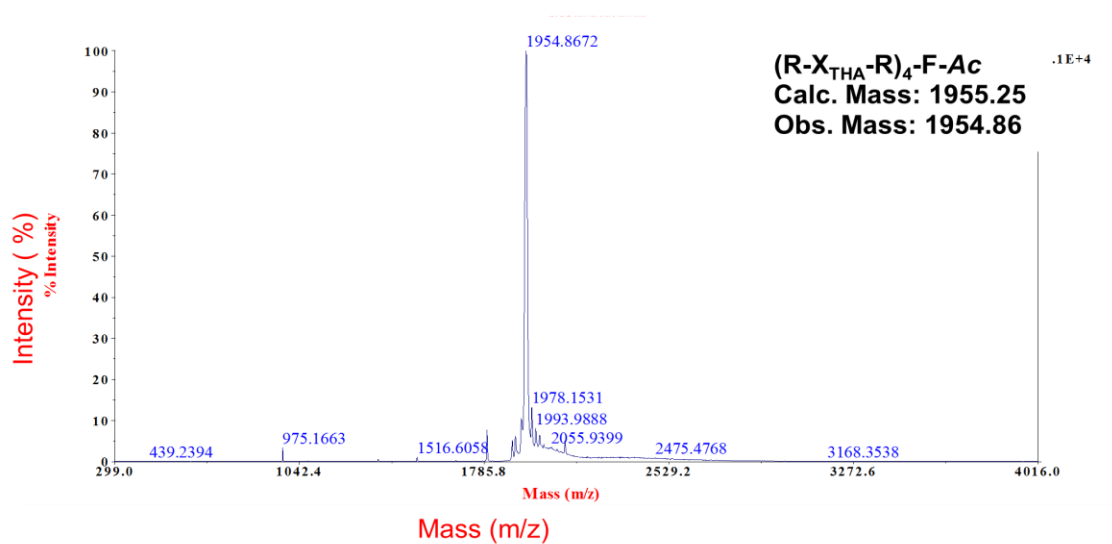


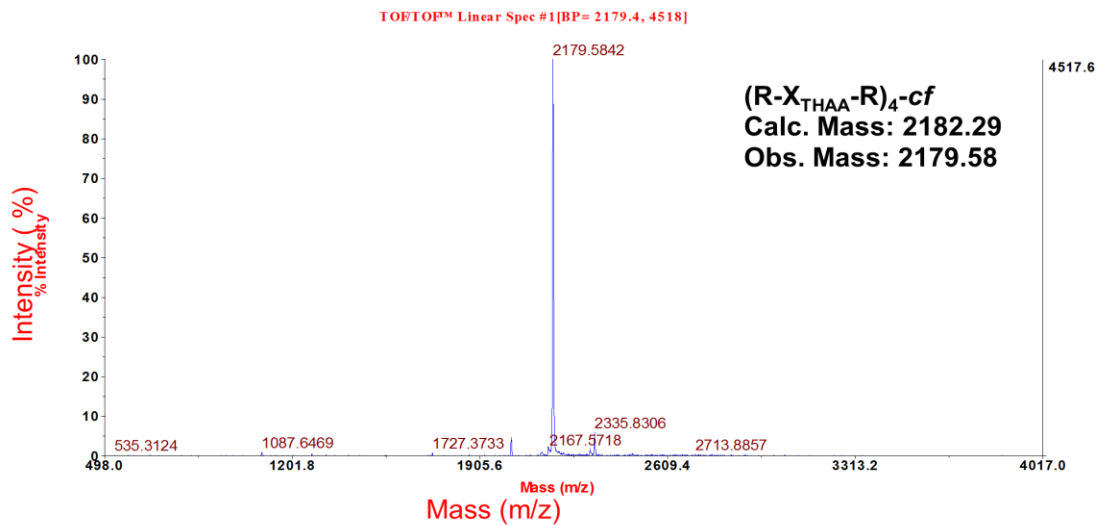
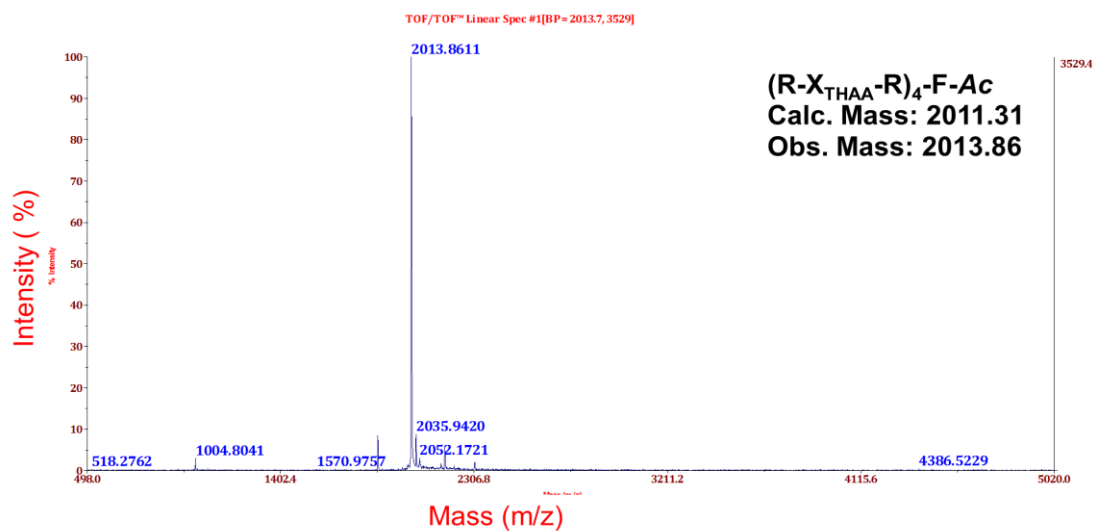
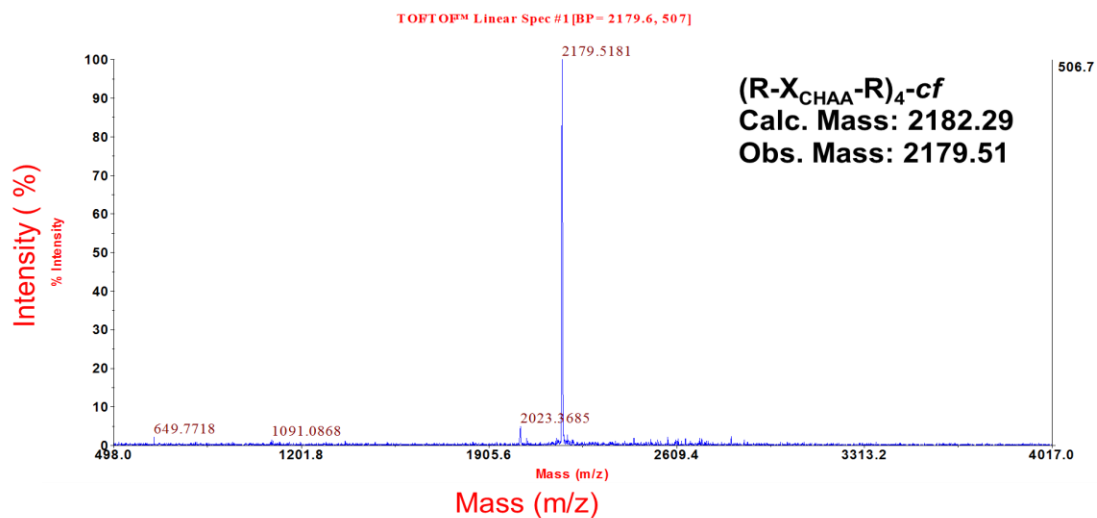


MALDI-TOF Analysis of Peptides









3.7 References

1. Bae, Y.; Park, K.; *Journal of Controlled Release*, **2011**, *153*, 198-205.
2. (a) Xia, H.; Gu, G.; Hu, Q.; Liu, Z.; Jiang, M.; Kang, T.; Miao, D.; Song, Q.; Yao, L.; Tu, Y.; Chen, H.; Gao, X.; Chen, J.; *Bioconjugate Chemistry*, **2013**, *24*, 419-430. (b) Jin, E.; Zhang, B.; Sun, X.; Zhou, Z.; Ma, X.; Sun, Q.; Tang, J.; Shen, Y.; Van Kirk, E.; Murdoch, W. J.; Radosz, M.; *Journal of the American Chemical Society*, **2012**, *135*, 933-940.
3. Kelley, S.; Stewart, K.; Mourrada, R.; *Pharmaceutical Research*, **2011**, *28*, 2808-2819.
4. De Jong, W.; Borm, P.; *International Journal of Nanomedicine*, **2008**, *3*, 133-149.
5. Wilczewska, A.; Niemirowicz, K.; Markiewicz, K.; Car, H.; *Pharmacological Reports*, **2012**, *64*, 1020-1037.
6. Suri, S.; Fenniri, H.; Singh, B.; *Journal of Occupational Medicine and Toxicology, (London, England)* **2007**, *2*, 16.
7. a) Sinfreu, J.F.; Giralt, E.; Castel, S.; Albericio, F.; Royo, M.; *Journal of the American Chemical Society*, **2005**, *127*, 9459-9468; b) Pujals, S.; Giralt, E.; *Adv. Drug Delivery Rev.* **2008**, *60*, 473-484; c) Martn, I.; Teixidj, M.; Giralt, E. *ChemBio-Chem*, **2011**, *12*, 896-903; d) Daniels, D. S.; Schepartz, A.; *Journal of the American Chemical Society*, **2007**, *129*, 14578-14579.
8. a) Potocky, T. B.; Menon, A. K.; Gellman, S.; *Journal of the American Chemical Society*, **2005**, *127*, 3686-3687; b) Seebach, D.; Beck, A. K.; Bierbaum, D. J.; *Chem. Biodiversity*, **2004**, *1*, 1111-1140.
9. Geisler, I.; Chmielewski, J.; *Bioorg. Med. Chem. Lett.*, **2007**, *17*, 2765-2768.
10. Kalafut, D.; Anderson, T. N.; Chmielewski, J.; *Bioorg. Med. Chem. Lett.*, **2012**, *22*, 561-563.
11. Mitchell, D. J.; Kim, D. T.; Steinman, L.; Fathman, C. G.; Rothbard, J. B.; *J. Pept. Res.* **2000**, *56*, 318-325.
12. Naik, R. J.; Chandra, P.; Mann, A. Ganguli, M.; *J. Biol. Chem.*, **2011**, *286*, 18982-18993.
13. Rothbard, J. B.; Kreider, E.; VanDeusen, C. L.; Wright, L.; Wylie, B. L.; Wender, P. A.; *J. Med. Chem.*, **2002**, *45*, 3612-3618.
14. Hassane, F. S.; Saleh, A. F.; Abes, R.; Gait, M. J.; Lebleu, B.; *Cell. Mol. Life Sci.*, **2010**, *67*,

715–726.

15. Moulton, H. M.; Nelson, H. M.; Hatlevig, A. S.; Reddy, T. M.; Iversen, L. P.; *Bioconjugate Chem.*, **2004**, *15*, 290–299.

16. McClorey, G.; Moulton, M. H.; Iversen, L. P.; Fletcher, S.; Wilton, D. S.; *Gene Ther.*, **2006**, *13*, 1373–1381.

17. Abes, R.; Moulton, H. M.; Clair, P.; Yang, S. T.; Abes, S.; Melikov, K.; Prevot, P.; Youngblood, D. S.; Iversen, P. L.; Chernomordik, L. V.; Lebleu, B.; *Nucleic Acids Res.*, **2008**, *36*, 20, 6343–6354.

18. Patil, K. M.; Naik, R. J.; Rajpal; Fernandes, M.; Ganguli, M.; Kumar, V. A.; *Journal of the American Chemical Society*, **2012**, *134*, 7196–7199.

19. Patil, K. M.; Naik, R. J.; Vij, M.; Yadav, A. K.; Kumar, V. A.; Ganguli, M.; Fernandes, M.; *Bioorg. Med. Chem. Lett.*, **2014**, *24*, 4198–4202.

20. Trabulo, S.; Cardoso, A. L.; Mano, M.; Pedroso de Lima, M. C.; *Pharmaceuticals*, **2010**, *3*, 961–993.

21. JB, P. *Handbook of Biological Confocal Microscopy second Edition. New York, London: Plenum Press 1995.*

22. (a) Farrera-Sinfreu, J.; Giralt, E.; Castel, S.; Albericio, F.; Royo, M.; *Journal of the American Chemical Society*, **2005**, *127*, 9459–9468;

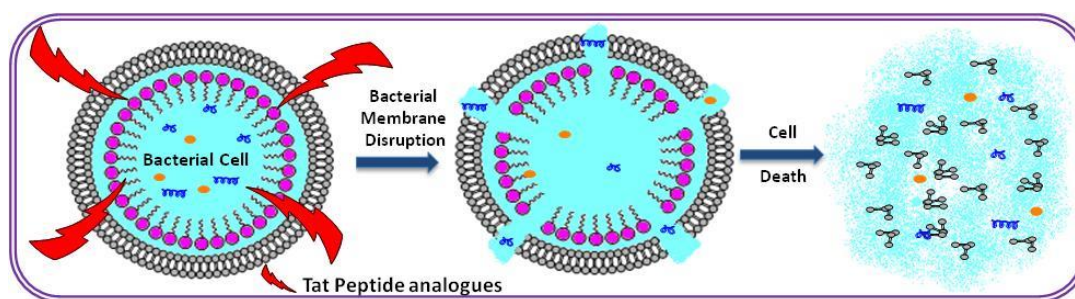
23. (a) Vij, M.; Natarajan, P.; Yadav, A. K.; Patil, K. M.; Pandey, T.; Gupta, N.; Santhiya, D.; Kumar, V. A.; Fernandes, M.; Ganguli, M.; *Mol. Pharmaceutics*, **2016**, *13*, 1779–1790. (b) Youngblood, D. S.; Hatlevig, S. A.; Hassinger, J. N.; Iversen, P. L.; Moulton, H. M.; *Bioconjugate Chem.*, **2007**, *18*, 50–60.

24. Porter, E. A.; Wang, X. F.; Lee, H. S.; Weisblum, B.; Gellman, S. H.; *Nature*, **2000**, *404*, 565.

25. Meng, H.; Kumar, K.; *Journal of the American Chemical Society*, **2007**, *129*, 15615–15622.

CHAPTER 4

Antibacterial and anti-TB Tat-peptidomimetics with improved efficacy and half life.



Non-natural antimicrobial peptides are ideal candidates for next generation antibiotics because of their ability to circumvent the problems of drug resistance and *in vivo* instability. We report herein, novel all- α - and α,γ -mixed non-natural Tat peptide analogues as potential antibacterial and anti-TB agents. These all- α - and α,γ -peptides showed broad spectrum antibacterial activities against Gram-positive and Gram-negative bacteria and also against active and dormant forms of *Mycobacterium tuberculosis*, including strains that are resistant to antibiotics. The introduction of the non-natural amino acids of the study in the Tat peptide analogues resulted in increased resistance to degradation by proteolysis, significantly increasing their half-life. The peptides appear to act by a membrane disruption mechanism. Fluorescence and transmission electron microscopy studies support this finding. The Tat peptide analogues are shown to have only a low cytotoxic effect on mammalian cells by the MTT and hemolysis assays, thereby increasing the scope for their further development as effective antibacterial and anti-TB agents.

4.1 Introduction

Antimicrobial peptides (AMPs) are small, cationic, amphipathic peptides between 15 and 30 amino acids that often form alpha helices and intercalate within the bacterial cell membrane to form pores; eventually leading to cell lysis. In order for bacteria to evade the action of AMPs, they are required to significantly alter their cell membrane composition, which drastically decreases their viability. For this reason, resistance to AMPs is uncommon which constitutes one of their greatest advantages over the traditional small-molecule antibiotics used in clinics today.¹ AMPs are part of the innate immune systems of many living organisms and serve as a first line of protection against invading bacterial, viral or fungal infections.^{2,3,4,5,6} They represent an exciting potential new class of antibacterial therapies as their novel mode of action prevents bacteria from easily evolving resistance to AMPs.

In general, AMPs can have both a direct antimicrobial effect and have the ability to activate the adaptive immune system.⁷ When only considering the direct antimicrobial effect, many different mechanisms of action have been proposed for AMPs, but, in general, AMPs are either membrane-interacting or membrane-penetrating. The membrane-interacting AMPs are believed to either cause lysis of the cells through pore formation/dissolution of the membrane or to bind to the membrane or a membrane component (both specific lipids and proteins) in a way that prevents normal function of the cell.^{8,9} (Figure 4.1) The membrane-penetrating AMPs are believed to interact with an intracellular target, which in most cases has been proposed to be DNA.^{10,11}

To improve the stability to enzymatic hydrolysis and to increase bioavailability, several synthetic, non-natural AMPs¹² and mimetics have been reported.¹³ Many AMPs have a helical component that has been shown to be necessary for their antimicrobial activity. Among these, recently, Nepal *et al.*¹⁴ described cationic and amphiphilic proline-rich polyproline type II (PPII) helices for effective cell penetration of macrophages that also exerted potent antibacterial activity. PPII¹⁵ and other helical peptides such as 12-helical β -peptides have been reported by several groups to have varying degrees of antimicrobial activities,^{16,17,18} including against some species that are resistant to common antibiotics such as vancomycin or penicillin. Several other groups have reported peptoids,¹⁹ α -aminoxy-peptides,²⁰ α/β -peptides,^{21,22} or azapeptides,^{23,24} as synthetic mimics of AMPs.

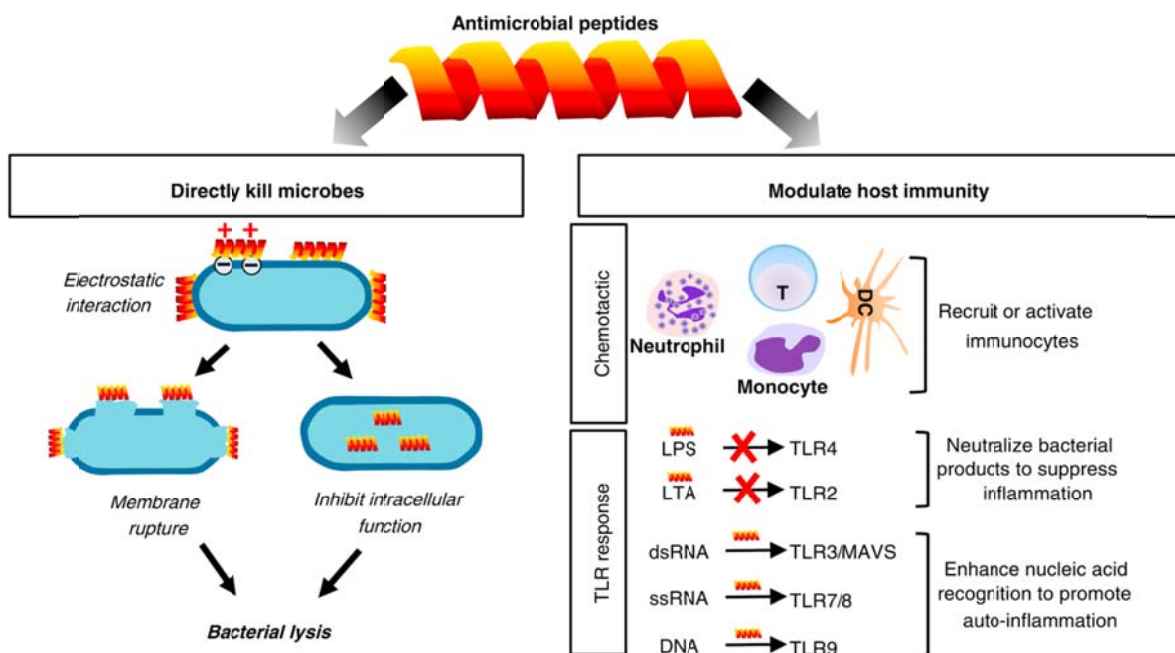


Figure. 4.1 Examples of the different mechanisms used by antimicrobial peptides to induce killing of bacteria.²⁵ AMPs bind to bacterial membranes through electrostatic interactions either to disrupt the membrane or to enter the bacterium to inhibit intracellular function. Some AMPs also modulate host immunity by recruiting/activating immunocytes or by influencing Toll-like receptor (TLR) recognition of microbial products and nucleic acids released upon tissue damage. (DC - dendritic cell; LPS - lipopolysaccharide; LTA - lipoteichoic acid; MAVS - mitochondrial antiviral signaling protein.)

4.2 Rationale, design and objectives of the present work

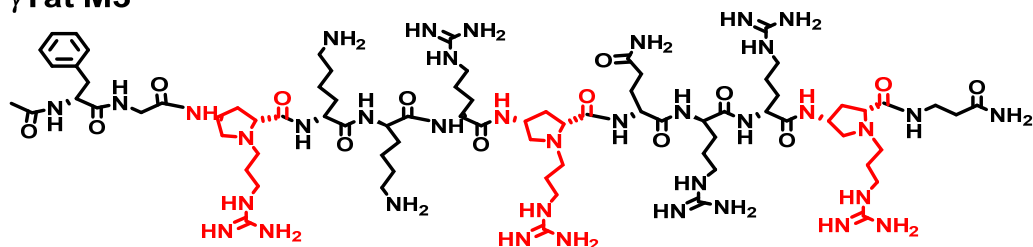
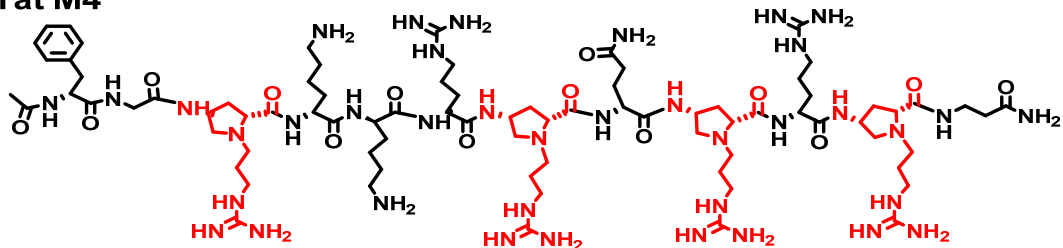
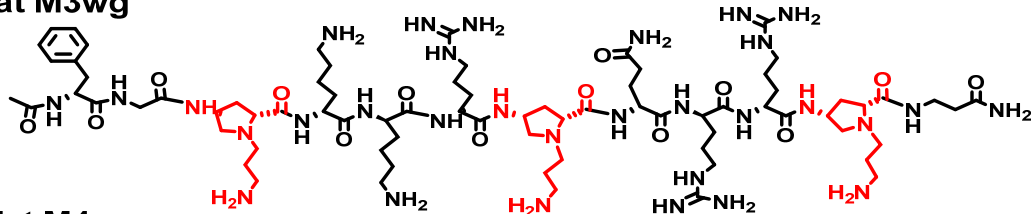
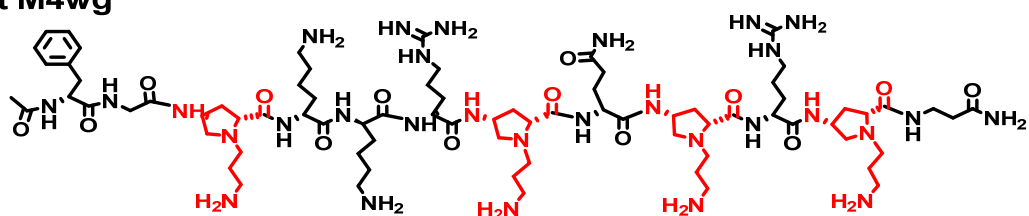
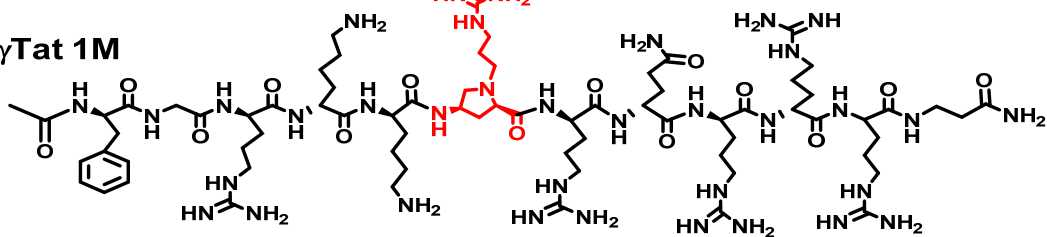
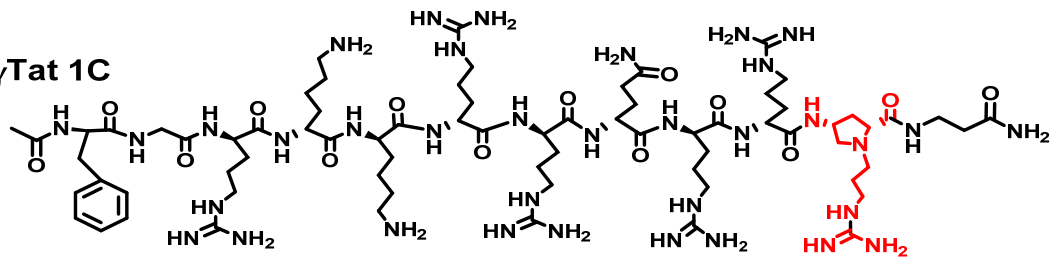
The basic translocating region (48-60) of the trans-activating transcriptional activator (Tat) peptide,²⁶ derived from the human immunodeficiency virus 1 (HIV-1) tat protein is a positively charged peptide, rich in arginine, and is highly studied for cell penetration and delivery of a variety of cargo molecules.^{27,28,29,30} The membrane translocation does not usually occur by endocytosis,³¹ but could vary, depending on the cargo.³² The contribution of the positive charges and the guanidine head groups are known to be important in this process.³³ The presence of several arginine residues, in addition to lysine residues, makes it particularly susceptible to the degradative action of enzymes, precluding its possible application in biological systems. Several reports of modifications in the Tat peptide have appeared in literature, where non-natural amino acids³⁴ as well as backbone linkages^{35,36} have been explored in relation to cell penetration. They have, however, not been studied for antimicrobial activity. Cell-penetrating peptides (CPPs) and AMPs share many features such as the presence of cationic residues and

amphipathic/amphiphilic nature. It is therefore, not unreasonable to surmise that cationic and amphipathic CPPs could function additionally as AMPs. There have appeared few reports^{37,38,39,40,41,42} of the antibacterial properties involving the cell-penetrating Tat peptide that involved the use of Tat peptide dimers,³⁷ Tat peptide-porphyrin conjugates,³⁹ D-Tat⁴⁰ (with D-amino acids instead of L-amino acids) and cholesterol-conjugated Tat peptides,⁴¹ besides the Tat peptide itself,⁴⁰ that were shown to form nanoparticles and one report of its antifungal activity against human pathogenic fungi.⁴² Studies with model membranes^{37,38} suggested that membrane disruption was the mode of antibacterial action of the cell-penetrating Tat peptide. The activity of the Tat peptide against mycobacteria, specifically *Mycobacterium tuberculosis* (Mtb), has not been reported. We thus, studied the antibacterial and anti-TB effects of novel synthetic analogues of the Tat(48-57) peptide (GRKKRRQRRR). Their microcidal effect was envisioned considering the amphipathicity, overall charge and possible interaction with bacterial cell membranes. The effect of the chiral monomers on structural pre-organization of the derived peptides is also investigated to determine if this, in turn, influences their antimicrobial activity. The novel Tat peptide analogues may also be envisioned to overcome the limitation of bacterial resistance development that is frequently encountered in the use of antibiotics, since AMPs⁴² are less likely to lead to development of resistance,⁴³ being known to act by targeting the microbial membranes,⁴⁰ rather than metabolic processes, as in the case of small molecule drugs.^{44,45}

4.3 Results

4.3.1 Synthesis of Tat peptide analogues

The protected non-natural amino acids **X** and **Z** were used as surrogates of lysine and arginine, in the solid phase synthesis of Tat peptide derivatives. The synthesis of amino acids **X** and **Z** has been described in section A and B of Chapter 2 (Schemes 2A.1 and 2B.1 respectively). Peptides were assembled on MBHA resin by either Fmoc- or Boc-chemistry protocols. β -Alanine was coupled as the first amino acid as a spacer, followed by the coupling of other amino acids. All the coupling steps were done in dry DMF in presence of DIPEA, with HOBt and TBTU as coupling agents. Removal of the Boc-protecting group was achieved using 50% TFA in CH_2Cl_2 , while the Fmoc group was removed using 20% piperidine in DMF. A phenylalanine residue was added at the N-termini of the peptides in order to facilitate concentration calculation from the UV absorbance.

γ Tat M3 γ Tat M4 γ Tat M3wg γ Tat M4wg γ Tat 1M γ Tat 1C

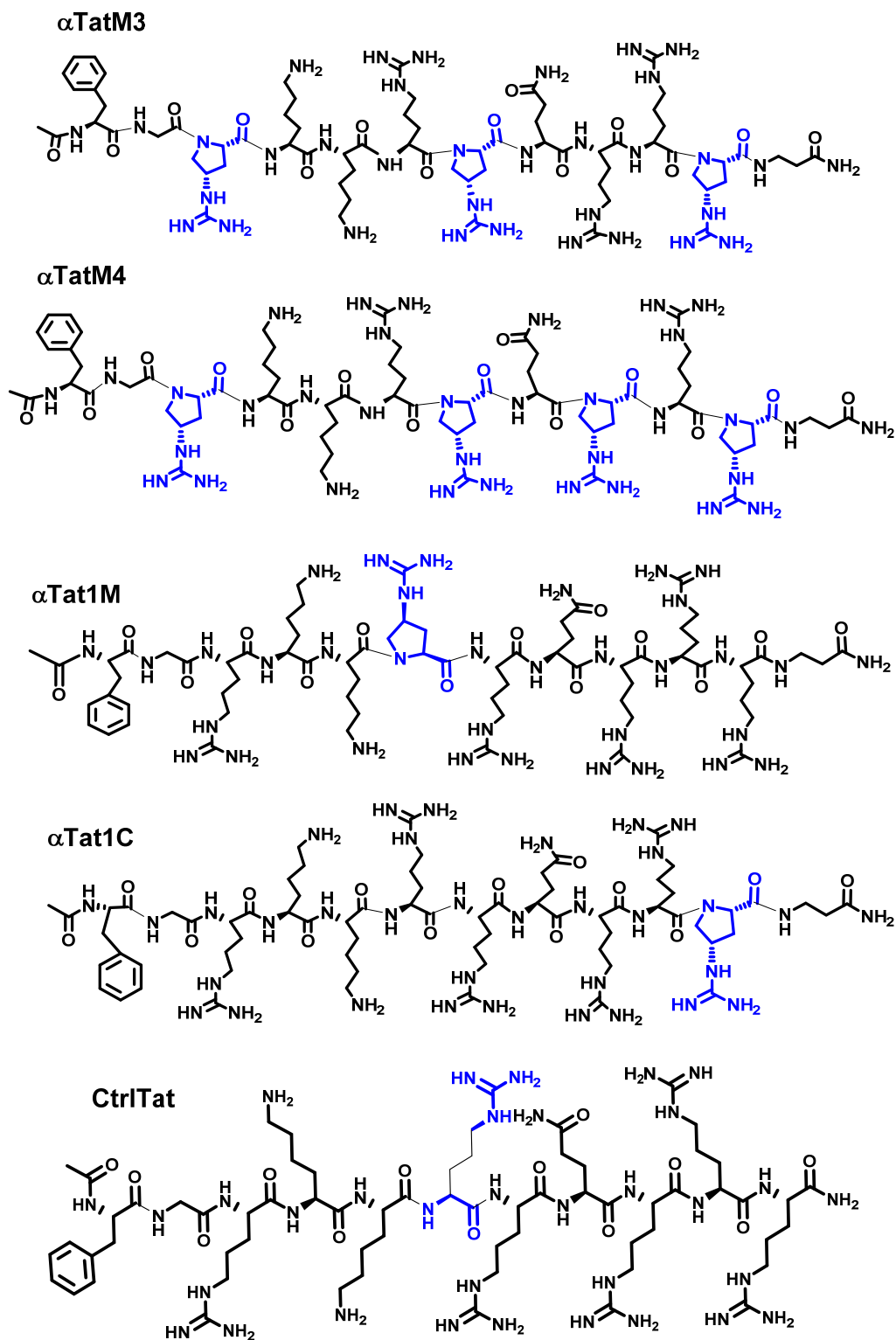


Figure 4.2. Chemical structures of the Tat peptides of the study.

Guanidinylation of monomer **Z** to arginine surrogate **P^g** was performed on the solid support after *N*-acetylation of the phenylalanine residue at *N*-terminus, and removal of the Fmoc protecting group, using 1*H*-pyrazole-1-carboxamide hydrochloride and DIPEA in dry DMF (Scheme 2B.2). The synthesized peptides were cleaved from the resin by the TFA-TFMSA cleavage protocol and purified by RP-HPLC on a C18 column. Their purity was re-checked by analytical HPLC and all the peptides were characterized by MALDI-TOF analysis. Table 4.1 lists the peptides synthesized, while the chemical structures are in Figure 4.2. The peptides γ Tat1M and γ Tat1C (Table 4.1, entries 1 and 2 respectively) contain one **r** unit, either in the middle of the oligomer, or at the 'C'-terminal. Likewise, the α Tat1M and α Tat1C peptides (Table 1, entries 7 & 8 respectively) contain one **P^g** unit in the middle and 'C'-terminal positions respectively. γ TatM3, γ TatM3wg and α TatM3 peptides contain three units each of **r**, **k** or **P^g** respectively, distributed across the oligomer (Table 4.1, entries 3, 4 & 9 respectively), while γ TatM4, γ TatM4wg and α TatM4 peptides contain four units each of **r**, **k** or **P^g** respectively, distributed across the oligomer (Table 4.1, entries 5, 6 & 10 respectively). A control Tat peptide (ctrlTat) was also synthesized (Table 4.1, entry 11) for comparison.

Table 4.1. Peptides of the study

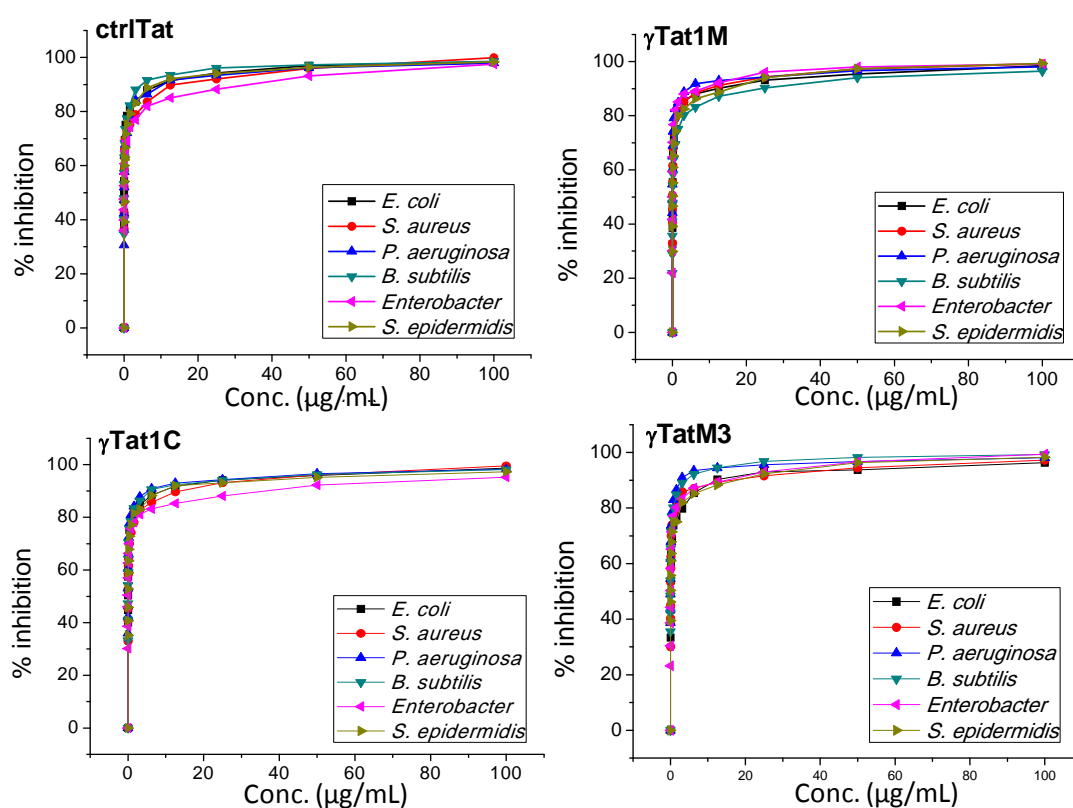
Entry	Code	Sequence	Mass (MALDI-TOF)	
			Calcd.	Obsd.
1	γ Tat1M	<i>Ac</i> -FGRKK r RQRRR- β Ala-NH ₂	1710.06	1709.99
2	γ Tat1C	<i>Ac</i> -FGRKKRRQRR r - β Ala-NH ₂	1711.07	1711.14
3	γ TatM3	<i>Ac</i> -F Gr KKR r QRRR- β Ala-NH ₂	1821.23	1824.17
4	γ TatM3wg	<i>Ac</i> -F Gk KKR k QRR k - β Ala-NH ₂	1695.11	1696.79
5	γ TatM4	<i>Ac</i> -F Gr KKR r Q r R r - β Ala-NH ₂	1876.31	1877.27
6	γ TatM4wg	<i>Ac</i> -F Gk KKR k Q k R k - β Ala-NH ₂	1708.15	1707.79
7	α Tat1M	<i>Ac</i> -FGRKK P^g RQRRR- β Ala-NH ₂	1653.00	1657.20
8	α Tat1C	<i>Ac</i> -FGRKKRRQRR P^g - β Ala-NH ₂	1653.00	1659.46
9	α TatM3	<i>Ac</i> -F P^g KKR P^g QRR P^g - β Ala-NH ₂	1649.94	1650.40
10	α TatM4	<i>Ac</i> -F P^g KKR P^g Q P^g R P^g - β Ala-NH ₂	1647.93	1647.10
11	ctrlTat	<i>Ac</i> -FGRKKRRQRRR-NH ₂	1583.98	1586.74

r = (2*S*,4*S*)-4-amino-*N*-(3-guanidinopropyl)-proline, **k** = (2*S*,4*S*)-4-amino-*N*-(3-aminopropyl)-proline, **P^g** = (2*S*,4*S*)-4-guanidinoproline.

4.3.2 Antibacterial activity of the Tat peptide analogues of the study

The novel Tat peptides of the study were tested for antimicrobial activity against Gram-positive (*Staphylococcus aureus*, *Bacillus subtilis*, *Staphylococcus epidermidis*) and Gram-negative (*Escherichia coli*, *Pseudomonas aeruginosa*, *Enterobacter spp.*) bacteria. The data obtained are summarized as IC₉₀ or MIC values in Table 4.2. The dose response curves are shown in Figure 4.3. These plots illustrate the percent inhibition of bacterial growth as a function of peptide concentration.

Among all the peptides, the γ TatM4 peptide displayed the best activity, with the lowest MIC values against Gram-positive as well as Gram-negative bacteria. Specifically, the MIC values for γ TatM4 against *E. coli*, *P. aeruginosa*, *Enterobacter spp.*, *S. aureus*, *B. subtilis* and *S. epidermidis* were 1.12, 0.61, 1.35, 1.26, 0.71 and 1.12 μ M respectively (Table 4.2).



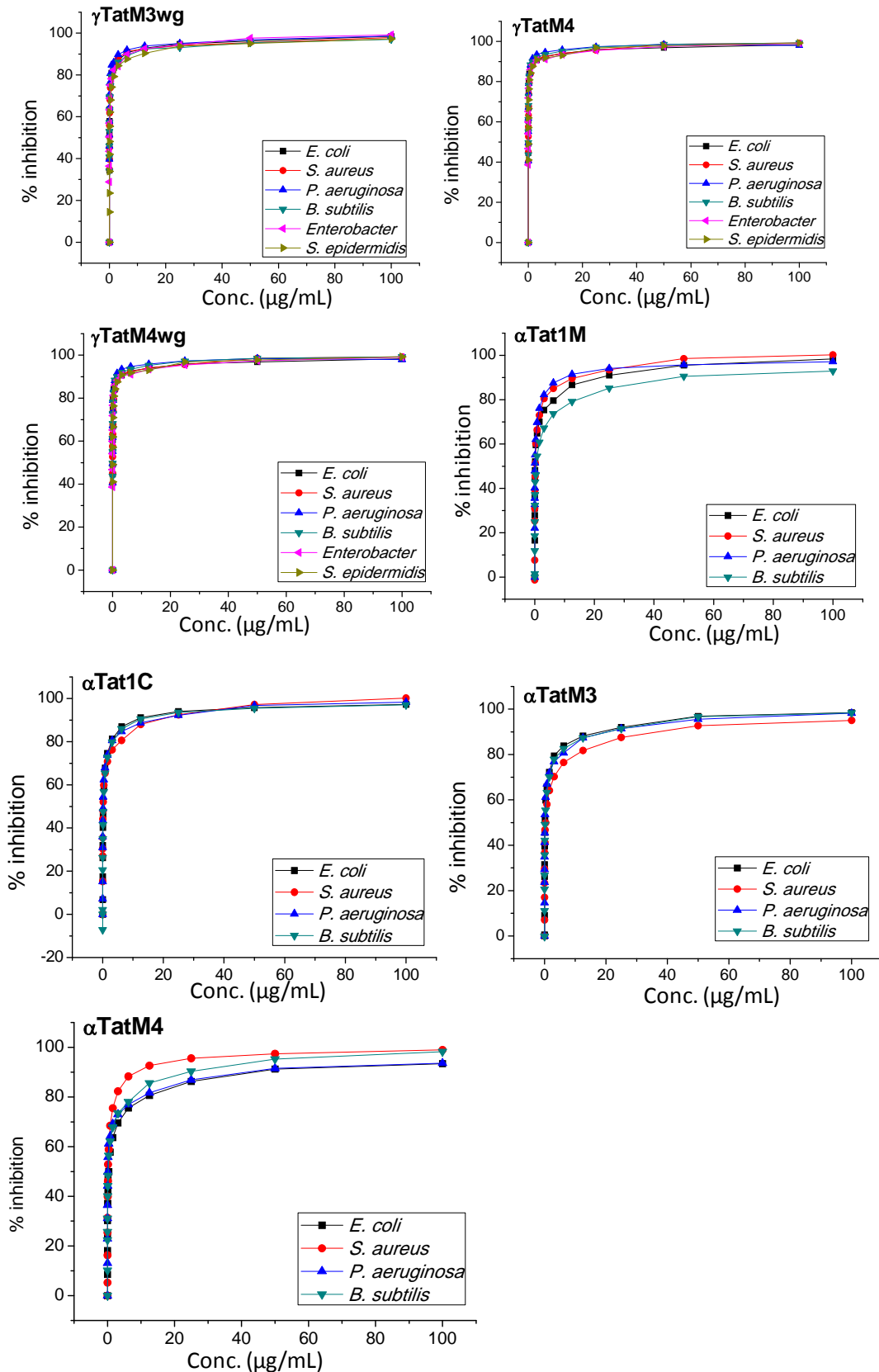


Figure 4.3 Dose response curves of the peptides against Gram-positive and Gram-negative bacteria.

Table 4.2. MIC data for peptides of the study against Gram-positive and Gram-negative bacteria.

Entry	MIC ^a (μM) of peptides with SD (±)					
	Gram-negative			Gram-positive		
	<i>E. coli</i>	<i>P. aeruginosa</i>	<i>Enterobacter spp.</i>	<i>S. aureus</i>	<i>B. subtilis</i>	<i>S. epidermidis</i>
γTat1M	7.25± 0.06	2.67± 0.04	4.70 ± 0.49	5.25 ± 0.11	14.1 ± 0.47	8.95 ± 1.2
γTat1C	5.71 ± 0.04	3.35 ± 0.03	18.85±1.28	8.47 ± 0.17	3.56 ± 0.04	4.92 ± 0.5
γTatM3	7.58 ± 0.03	1.82 ± 0.005	8.01 ± 0.58	9.05 ± 0.33	2.81 ± 0.02	9.44 ± 0.82
γTatM3wg	3.52 ± 0.08	2.32 ± 0.047	4.65 ± 0.23	3.02 ± 0.05	4.16 ± 0.06	7.25 ± 0.64
γTatM4	1.12 ± 0.01	0.61 ± 0.03	1.35 ± 0.21	1.26 ± 0.02	0.71± 0.005	1.12 ± 0.23
γTatM4wg	2.34 ± 0.05	2.2 ± 0.02	4.51 ± 0.44	3.02 ± 0.03	3.79 ± 0.08	3.94 ± 0.54
αTat1M	13.49±0.02	6.53 ± 0.42	nd	8.65 ± 0.18	29.8 ± 1.15	nd
αTat1C	6.73 ± 0.03	10.26 ± 0.03	nd	10.95 ± 0.66	7.96 ± 0.12	nd
αTatM3	11.8±0.018	12.62 ± 0.06	nd	20.54 ± 0.85	13.2 ± 0.54	nd
αTatM4	27.73±0.04	25.98 ± 0.79	nd	5.59 ± 0.42	15.13± 0.73	nd
ctrlTat	6.27 ± 0.05	7.46 ± 0.69	21.60±1.95	9.91 ± 0.25	3.34 ± 0.04	5.78 ± 0.51
Ampicillin ^b	4.17±0.036	12.5 ± 0.09	nd	2.8 ± 0.01	29.5 ± 0.3	nd
Kanamycin ^b	3.3 ± 0.024	1.01 ± 0.06	nd	>61.9 ± 0.6	2.8 ± 0.027	nd

^a The values are expressed as the mean of triplicates. Antibacterial activity of each peptide was determined by serial dose dependent dilutions. ^b Standard antibacterial drug and positive control. SD (±) = standard deviation. nd = not determined.

4.3.3 Activity against *Mycobacterium tuberculosis*

The activity of the peptides of the study against Mtb and MDR-Mtb are depicted as their MIC values in Figure 4.4 and listed in Table 4.3. The respective dose response curves are shown in Figure 4.5. Against Mtb, γTat1M was the most active against the dormant and active forms (MIC 13.8 and 20.1 μM respectively).

Against MDR-Mtb, the γTatM4wg and αTatM3 peptides showed the best activity, with MIC values of 6.6 μM and 6.0 μM respectively against the dormant form and 12.8 μM and 15.0 μM respectively, against the active form. The γTat1M peptide also showed moderate activity against MDR-Mtb, with MIC values of 10.6 μM and 13.0 μM against the dormant and active forms respectively.

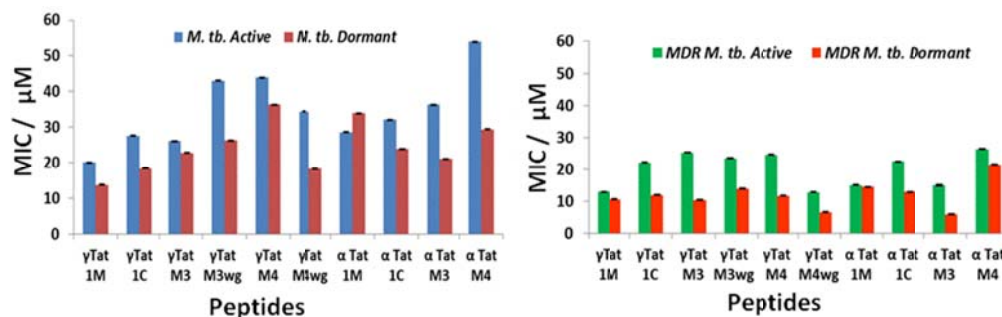
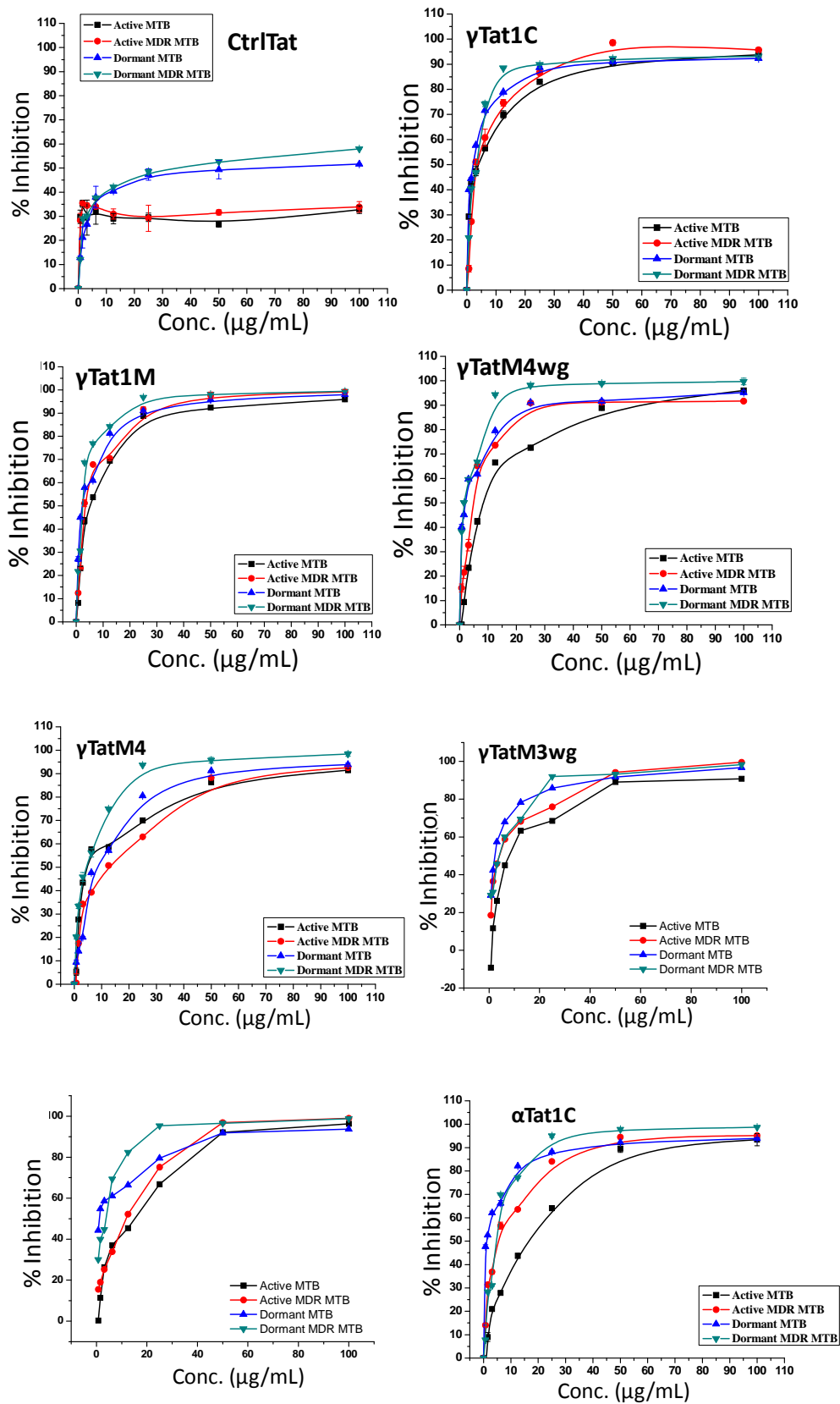


Figure 4.4. Activity of the peptides of the study against *Mycobacterium tuberculosis*.

Table 4.3 MIC data (μM) for peptides of the study against *Mycobacterium tuberculosis* *in vitro*.

Peptide	MIC (μM) values of peptides with SD (\pm)			
	Mtb H37Ra (ATCC 25177)		MDR-Mtb	
	Dormant	Active	Dormant	Active
$\gamma\text{Tat}1\text{M}$	13.8 ± 0.001	20.1 ± 0.00076	10.6 ± 0.0015	13 ± 0.0035
$\gamma\text{Tat}1\text{C}$	18.4 ± 0.001	27.6 ± 0.00064	12.0 ± 0.001	22.1 ± 0.003
$\gamma\text{Tat}M3$	22.8 ± 0.003	26.1 ± 0.003	10.4 ± 0.0014	25.3 ± 0.0014
$\gamma\text{Tat}M3\text{wg}$	26.3 ± 0.003	43.0 ± 0.0029	14.0 ± 0.001	23.5 ± 0.001
$\gamma\text{Tat}M4$	36.3 ± 0.003	43.9 ± 0.0026	11.7 ± 0.001	24.6 ± 0.0023
$\gamma\text{Tat}M4\text{wg}$	18.3 ± 0.003	34.4 ± 0.003	6.6 ± 0.001	12.0 ± 0.002
$\alpha\text{Tat}1\text{M}$	33.9 ± 0.0042	28.6 ± 0.0042	14.5 ± 0.0026	15.1 ± 0.0026
$\alpha\text{Tat}1\text{C}$	23.9 ± 0.003	32.10 ± 0.003	12.9 ± 0.002	22.5 ± 0.0025
$\alpha\text{Tat}M3$	21.1 ± 0.0045	36.3 ± 0.0047	6.0 ± 0.0034	15.0 ± 0.0034
$\alpha\text{Tat}M4$	29.4 ± 0.004	53.9 ± 0.0036	21.5 ± 0.003	26.4 ± 0.0026
Rifampicin ^a	0.91 ± 0.005	0.97 ± 0.005	$>12.1 \pm 0.0037$	$>12.1 \pm 0.0043$
Pyrazinamide ^a	> 100	> 100	> 100	> 100

Anti-TB activity of each peptide was determined by serial dose dependent dilutions. Data are expressed as the mean values of triplicates. ^aStandard anti-TB drug and positive control.



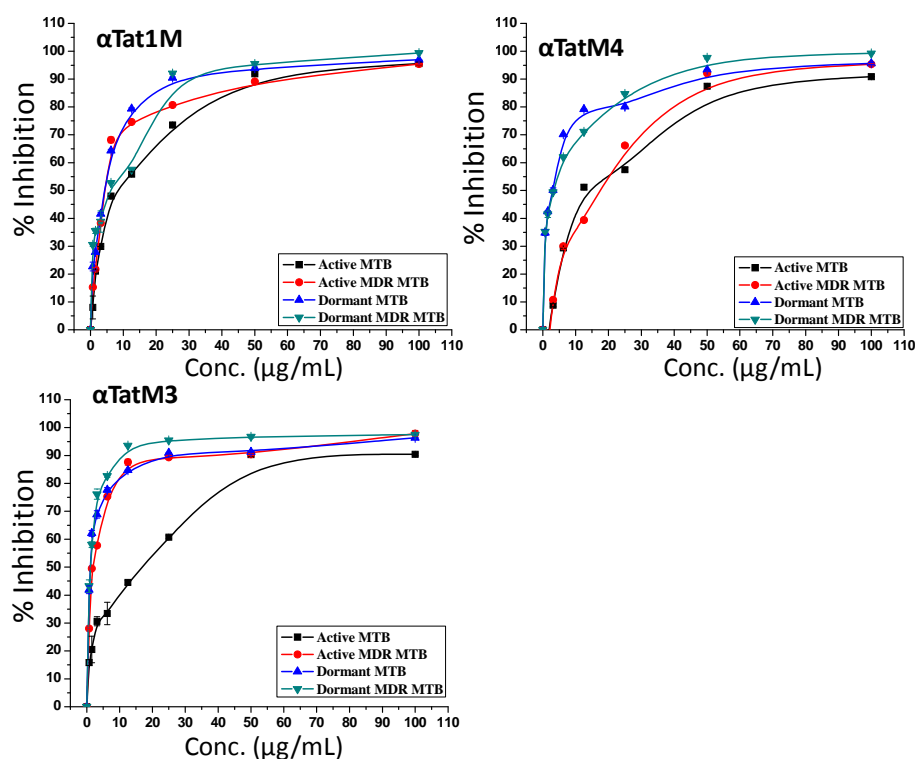


Figure 4.5 Dose response curves of the peptides against active and dormant strains of *Mycobacterium tuberculosis* and multidrug resistant *Mycobacterium tuberculosis*.

4.3.4 Circular Dichroism studies

The CD spectra of the Tat peptides of the study were recorded in water as well as in presence of the secondary structure-inducing solvent, trifluoroethanol (TFE). The spectra are shown in Figure 4.6. The ctrlTat peptide displayed a random coil structure in water, as reported earlier,⁴⁶ but showed a significant change towards the α -helical structure in the presence of TFE (Figures 4.6 (a) and 4.6 (b) respectively).

A similar trend was observed for the all- α -peptides of this study. The α,γ -peptides, on the other hand, displayed differing CD signatures. The γ TatM4, γ TatM4wg and γ TatM3wg peptides were found to display markedly different CD signatures from the other α,γ -peptides. This trend was also found in these peptides in the presence of TFE. The γ Tat1C peptide was found to display a CD signature very similar to that of the ctrlTat peptide in TFE, and tending towards the signature observed for α -helices⁴⁷ in the case of α -peptides. Coincidentally, this peptide also had very similar antibacterial activity to the ctrlTat peptide against the bacteria tested, as evident from Table 4.2.

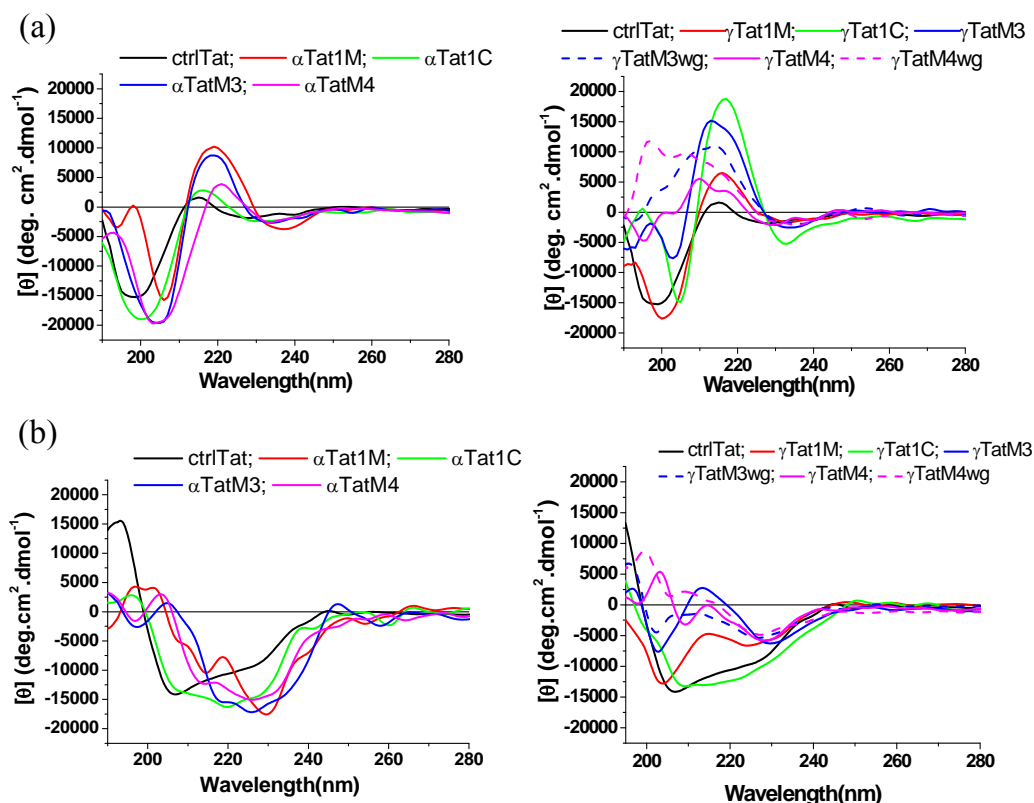


Figure 4.6. CD spectra of the all- α -Tat peptides and α,γ -Tat peptides of the study in water (a) and in 90% TFE-water (b).

4.3.5 Fluorescence- and transmission electron microscopy analysis

Fluorescence microscopy images were recorded using a dual staining method [LIVE/DEAD™ BacLight™ Bacterial Viability Kit, (Invitrogen)] employing SYTO 9 and propidium iodide (PI) dyes. As seen in Figure 4.7, significantly increased staining with PI is observed in cells treated with a representative peptide of the study in comparison to untreated cells.

Representative Tat-peptides that displayed relatively higher antibacterial activity were studied by TEM to examine their effect on the bacterial cell walls. Specifically, the effect of the peptides γ TatM4 and γ Tat1C were studied on cells of *S. aureus* and *E. coli* as Gram-positive and Gram-negative bacteria respectively and are depicted in Figures 4.8 and 4.9 and on Mtb (Figure 4.10). Extensive damage to the bacterial membranes was observed.

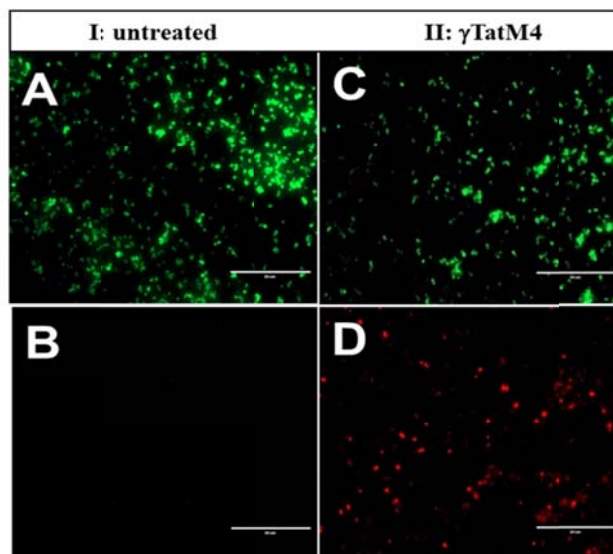


Figure 4.7. Fluorescence micrographs of *S. aureus*. A and C are green channel (SYTO 9)-; B and D are red channel (PI)- images captured for untreated cells (I) and cells treated with γ TatM4 (II) under 60X magnification respectively. Scale bar = 50 μ .

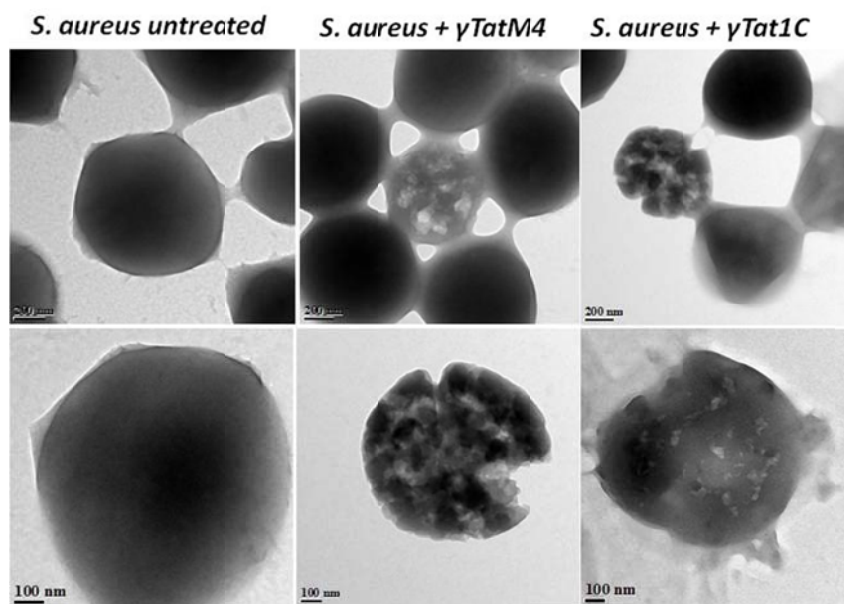


Figure 4.8. TEM images of *S. aureus* untreated and after treatment with representative peptides of the study. Scale bar: upper panel = 200 nm; lower panel = 100 nm.

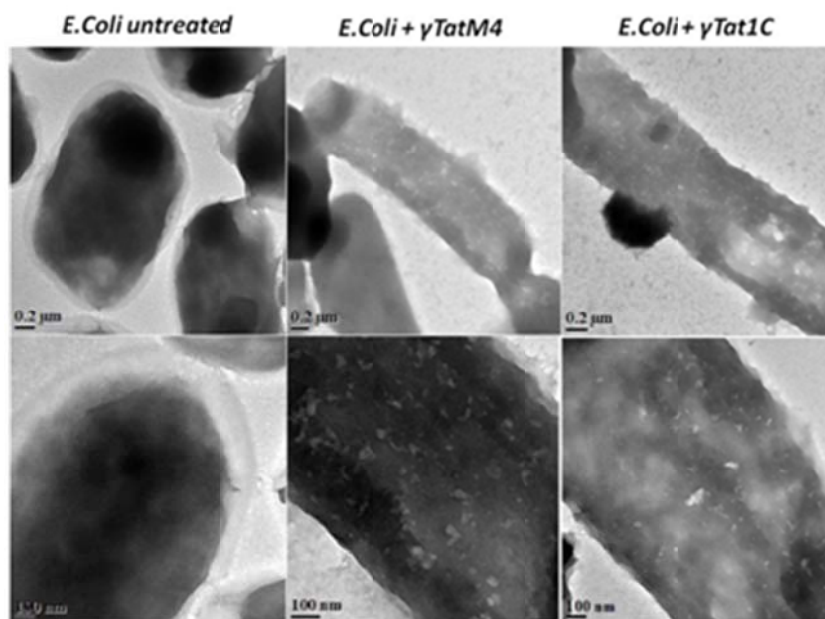


Figure 4.9. TEM images of *E. coli* untreated and after treatment with representative peptides of the study. Scale bar: upper panel = 200 nm; lower panel = 100 nm.

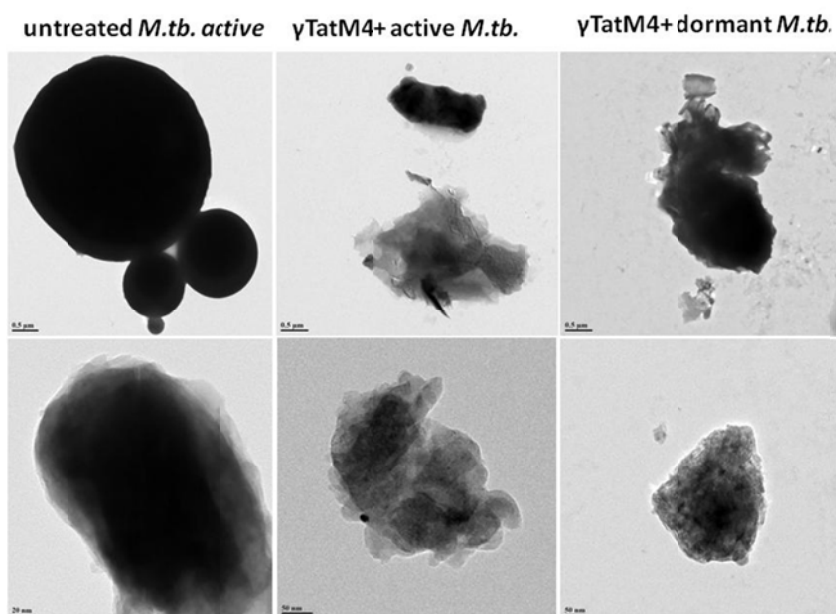


Figure 4.10. TEM images of *M. tuberculosis* untreated and after treatment with γ TatM4, a representative peptide of the study. Scale bar: upper panel = 0.5 μ ; lower panel = 50 nm.

4.3.6 Cytotoxicity studies

The cytotoxicity of the Tat peptides of the study on mammalian cells was estimated by the standard MTT cell viability assay. HeLa cells were treated with the peptides of the study at varying concentrations for 24 h and the cell viability was estimated. The results are depicted in Figure 4.11. As seen in the plot, the peptides of the study show very low cytotoxicity to mammalian cells. The cell viability is $\geq 80\%$ for almost all the peptides even at the higher concentrations studied. The cytotoxicity of the peptides was also evaluated in HCT116 and HUVEC cells.

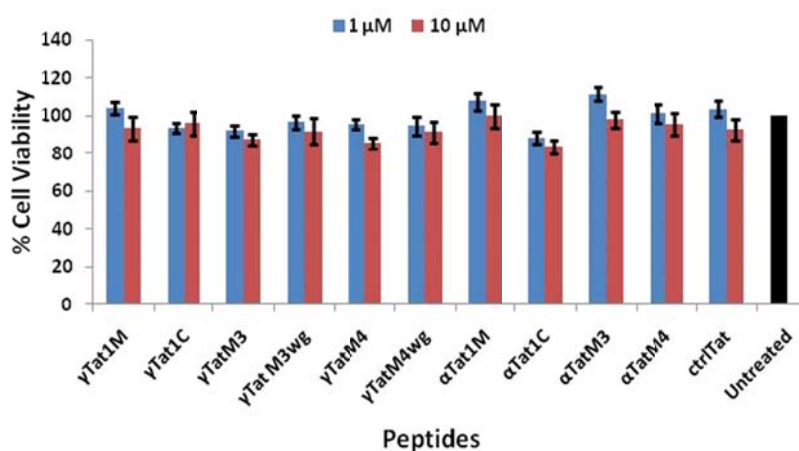


Figure 4.11. MTT cell viability assay upon treatment with Tat peptides of the study with HeLa cells. SD were calculated from three independent experiments.

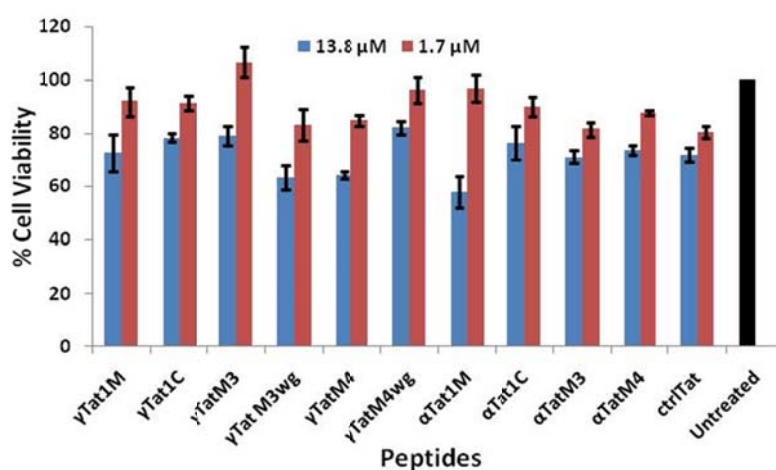


Figure 4.12. MTT cell viability assay upon treatment with Tat peptides of the study with Human Umbilical Vein Endothelial Cells (HUVEC) cells. SD were calculated from three independent experiments.

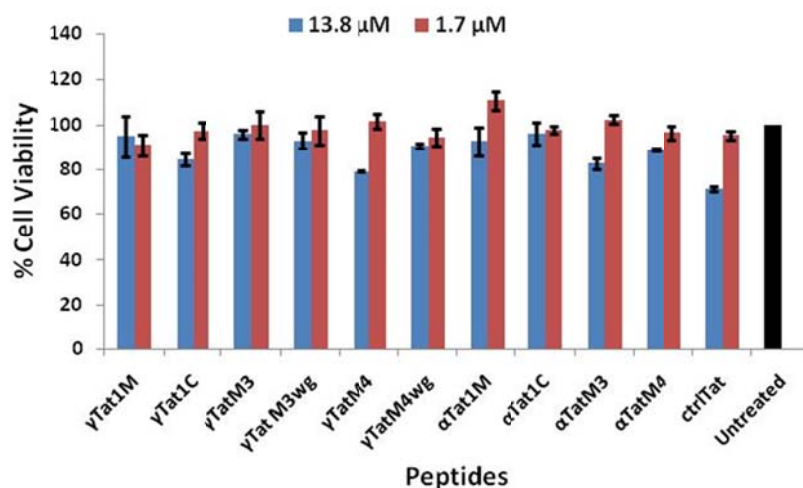


Figure 4.13. MTT cell viability assay upon treatment with Tat peptides of the study with Human colon carcinoma (HCT116) cells. SD were calculated from three independent experiments.

The hemolytic activity of a representative Tat peptide analogue, γ TatM4, in comparison to the ctrlTat peptide, was measured as an indication of its effect on the mammalian cell membrane. This *in vitro* assay is an indicator of red blood cell lysis and evaluates the hemoglobin released in the plasma spectrophotometrically at 540 nm, after exposure to the test peptides. An increase in absorbance at this wavelength, is therefore, indicative of increased hemolysis and toxicity. The γ TatM4 peptide showed lower hemolytic activity compared to ctrlTat peptide (Figure 4.14). Treatment with Triton X-100 and phosphate buffered saline were used as positive and negative controls respectively. The results are in agreement with the cytotoxicity data obtained by the MTT assay (Figure 4.11).

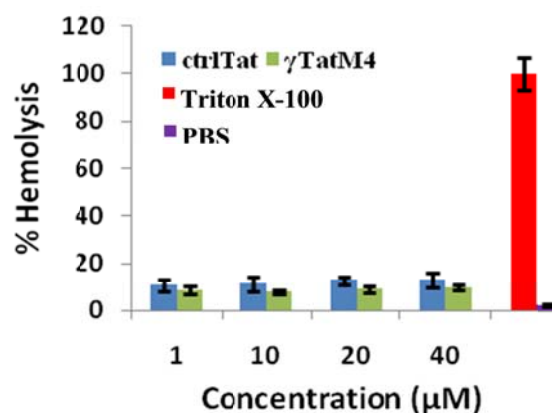


Figure 4.14. Hemolytic activity of representative peptides. SD were calculated from three independent experiments.

4.3.6 Protease resistance studies

The stability of the Tat peptides of the study to hydrolytic digestion by enzymes was studied by treating the peptides with trypsin, a commercially available protease, and estimating the percent intact peptide remaining over time by HPLC analysis. The results of the study with γ TatM4 as a representative example, in comparison to the control Tat peptide (ctrlTat) was studied, as described in Chapter 2A, Section 2A.4.7. It is evident that the introduction of the arginine surrogate *r* within the Tat peptide sequence conferred the derived peptide with significant resistance to digestion by trypsin. In particular, the $t_{1/2}$ of γ TatM4 was found to be 16 h in comparison to 4 h for the ctrlTat peptide. After 24 h, 30 % of the γ TatM4 peptide still remained intact, while only 4 % of the ctrlTat peptide was found to be intact at the same time point. The fragments obtained after digestion with trypsin were analysed by MALDI-TOF, in order to elucidate the cleavage sites. The details of the experiment are elaborated in Chapter 2A.

4.4 Discussion

Gram-positive and Gram-negative bacteria differ in the structure and composition of their cell walls, which could lead to differential interactions on their surface. However, both types of bacterial cell surfaces are negatively charged. The negative charge in Gram-positive bacteria is mainly due to the teichoic acid polymeric chains which bear anionic phosphates in the glycerolphosphate units, while in Gram-negative bacteria, this comes mainly from the phosphates and carboxylates of sugar acids. The overall negative charge makes them amenable to interaction with positively charged ligands, such as the Tat-peptides of the present study. The antibacterial effect of the α,γ -peptides of the study is far superior to that of the all- α -peptides. Among all the peptides, the γ TatM4 peptide displayed the best activity. The MIC values of the γ TatM4 peptide (0.61 to 1.35 μ M) are in the range or even better than those of some of the most effective antibiotics, e.g., ampicillin and kanamycin, currently used against the tested bacteria. This activity is also significantly more than reported for some natural antimicrobial peptides such as indolicidin, defensin, mellitin and magainin, against some of the tested bacteria.⁴⁸ The α,γ -peptides were also more active than the all- α -peptides against Mtb. It is indeed noteworthy that while the control Tat peptide showed insignificant activity against active and dormant forms of Mtb and MDR-Mtb (MIC > 150 μ M), all the peptides of the study were active to different

extents. Although the MIC values for the Tat peptides of the study were not as low as for rifampicin against Mtb, it is noteworthy that many of the peptides are active against both, active and dormant forms of MDR-Mtb. We have also compared MIC of Tat Peptide analogues with pyrazinamide for comparison of anti-TB activity. Pyrazinamide is the only anti-TB drug that is known to act by disrupting the bacterial membrane energetic and affecting membrane transport. However, this drug is inactive in assays in vitro (MIC > 100 μ M). It may be pointed out that most of the currently used drugs against Mtb, including rifampicin, act less effectively against the dormant forms. Importantly, the peptides reported herein act to a greater extent against MDR-Mtb than against Mtb itself. This is a particularly significant finding, since the treatment of MDR-Mtb is known to be increasingly challenging.

The observed antimicrobial properties of the Tat peptide analogues of this study could be a consequence of their increased amphipathic character, caused by the inclusion of the non-natural amino acid surrogates. The increased hydrophobicity in comparison to ctrlTat could partly contribute to the cell membrane disruption and hence antimicrobial properties⁴² of the Tat peptide analogues described herein. The presence of the guanidine group rather than the amino group was also shown to be favourable for increased activity. The ability of the guanidine group to partake in bidentate hydrogen-bonding makes oligomers bearing this function more potent than those bearing simple amines. Thus, the peptide γ TatM4 was more active than the peptide γ TatM4wg. The highest activity was observed for the γ TatM4 peptide that bears four units of the γ -amino acid, **r**, while the peptides with fewer **r** units or bearing the α -amino acid, **P^s**, displayed lower antimicrobial activity. In general, the non-natural amino acid **r**, presenting the guanidino group on a relatively flexible alkyl spacer had a more positive effect on the antimicrobial properties of the resulting peptide, rather than the amino acid **P^s**, where the guanidino group is attached directly to the pyrrolidine ring in a more rigid disposition. The flexibility associated with the alkyl spacer could be the reason for more favourable interactions of the guanidines with the cell membrane in the derived α,γ -peptides, thus leading to their enhanced activity. The potent antimicrobial activity of Tat-derived AMPs indicated that they have potential to be used alone for the treatment of infections caused by both Gram-positive and Gram-negative bacteria. Although the use of a single agent to treat infections is the most commonly used practice, combination treatment can potentially eliminate drug resistant strains, delay the evolution of drug resistance and reduce the size of the dose, which can circumvent the side-effects.

The Tat₄₇₋₅₈ peptide is reported to display a CD signature commensurate with a random coil structure, even in the presence of TFE,^{34,46} while the longer Tat₄₇₋₇₂ peptide was reported to display a significant increase in the alpha-helical content in 80% TFE.^{46,39} The ctrlTat peptide in our study displayed a random coil structure in water, as reported earlier,^{46,39} but showed a significant change towards the α -helical structure in the presence of TFE. The CD studies suggest a possible correlation between the secondary structure of the peptides and their antimicrobial activity. Further, our studies indicate that the peptides that lack a defined secondary structure as seen for α -peptides, even in presence of the secondary structure-inducing solvent, trifluoroethanol (TFE), are more effective antibacterial agents in comparison to those that show a signature similar to that of an α -helix in the case of α -peptides, in presence of TFE. Thus, our findings suggest that though the structure of the Tat peptide analogues does seem to play a role in deciding their antibacterial activity, the helical component in the structure may not be as important as previously suggested in several literature reports.^{14,16,17,18} A helical predisposition may prove beneficial in terms of antimicrobial activity in the case of some peptides, but is not an absolute requirement, and potent activity may still be achieved with peptides that are not helically predisposed.

Of the two dyes used in the fluorescence microscopy studies, SYTO 9 can penetrate the cell membrane and bind strongly to DNA; it can be used to stain both live and dead cells. When bound to double-stranded DNA, its green fluorescence emission at 503 nm is enhanced (excitation maximum = 483 nm). PI, on the other hand, is membrane impermeant and is generally excluded from viable cells. It is therefore, commonly used to identify dead cells (where the cells are ruptured, with a release of the intracellular constituents into the extracellular space) in a mixed population of dead and viable cells. When intercalated in nucleic acids, its emission maximum is at 617 nm (excitation at 535 nm). The relatively higher level of PI-staining in relation to SYTO9-staining in the case of the γ TatM4 peptide analogue (Figure 4.7) is therefore, indicative of their higher ability to disrupt bacterial membranes in comparison to untreated. The TEM images (Figures 4.8 and 4.9) clearly illustrate the extensive damage that is caused to the bacterial cell walls, as previously suggested by studies with model membranes,^{31,38} upon treatment with the Tat-peptides of the study. Further, the disruptive effects of the peptides are seen to affect both, Gram-positive as well as Gram-negative bacteria, with similar efficacy. The permeation of the cell wall can be seen in several cases in the form of pores or holes, causing the

leakage of intracellular contents and leading to the formation of empty or dead cells. A similar devastating effect was observed with Mtb, when both active and dormant forms were significantly found to be affected (Figure 4.10), leading to permeation of the cell membranes and cell death.

The cytotoxicity of the Tat peptides of the study on mammalian cells (HeLa) was estimated by the MTT cell viability assay. It is a colorimetric assay that is based on the reduction of the tetrazolium dye, 3-(4,5-dimethylthiazol-2-yl)-2,5-diphenyltetrazolium bromide to a purple formazan derivative, that is achieved by enzymes present in viable cells. A decreased colour intensity is therefore indicative of low cell viability as a result of increased cytotoxicity. The peptides of the study showed low cytotoxic effects, with viability ≥ 70 -80 % at elevated concentrations (Figure 4.11, 4.12, 4.13). The low cytotoxic effect was also estimated and confirmed by the hemolysis assay, when the γ TatM4 peptide showed lower hemolytic activity than the ctrlTat peptide (Figure 4.14). The difference in deleterious effects observed with bacteria/ Mtb *vis-a-vis* mammalian cells could be attributed to the difference in composition of the bacterial and mammalian cell membranes, which may be expected to influence the interaction properties of the peptides with the respective membranes.

One major limitation of antimicrobial peptides in their commercial use as therapeutics is their inactivation by proteases. Poor protease stability severely limits the clinical use of potentially therapeutic peptides. The Tat-peptide contains multiple arginine and lysine residues, which constitute the major sites of proteolytic cleavage. The non-natural amino acids used in the present work confer the derived peptide with improved protease resistance properties, increasing their application potential in biological systems, by increasing their half-life significantly.

4.5 Summary and Conclusions

The Tat peptide analogues reported herein are shown to possess good activity against Gram-positive and Gram-negative bacteria and also Mtb. Further, in contrast to the antifungal effect, where no disruption of fungal membranes was observed, the antibacterial and anti-TB effects were found to be due to the interaction with and disruption of microbial membranes, leading to cell lysis and death, as earlier reported. Both electrostatic as well as hydrophobic interactions are possibly involved in bringing about this effect. From our TEM results, the anti-TB effect appears to be by membrane disruption, as with Gram-positive and Gram-negative bacteria. Tat peptide

analogues are active particularly against the dormant forms of Mtb, in addition to the active form, makes them promising for further study and development. Their low potential for resistance development, higher bio-stability, owing to the presence of non-natural amino acids, further adds to their potential towards therapy. The applicability of the peptides reported herein could be enhanced, perhaps synergistically, by combination with known antimicrobial agents such as antibiotics.

4.6 Experimental Section

4.6.1 Anti-bacterial activity

All bacterial cultures were first grown in LB media at 37 °C at 180 rpm. Once the culture reached an absorbance of 1 OD, as measured at 620 nm, it was used for anti-bacterial assays. Bacterial strains *E. coli* (NCIM 2688), *P. aeruginosa* (NCIM 2036), Enterobacter spp (NCIM 5392) as Gram-negative and *B. subtilis* (NCIM 2079), *S. aureus* (NCIM 2010), *S.epidermis* (5270) as Gram-positive were obtained from NCIM (CSIR-NCL, Pune) and were grown in Luria Bertani medium (Himedia, India). 0.1 % of 1 OD culture at 600 nm was used for screening. 0.1 % inoculated culture was added into each well of the 96-well plate containing the compounds to be tested. Optical density for each plate was measured at 620 nm after 8 h for Gram-negative bacteria and after 12 h for Gram-positive bacteria.

4.6.2 Anti-TB assay

All the synthetic peptides were screened for their *in vitro* activity against *M. tuberculosis* H37Ra (Mtb) (ATCC 25177) and multidrug resistant *M. tuberculosis* H37Ra (MDR-Mtb). MICs were determined in both these strains by using the standard XTT Reduction Menadione Assay (XRMA) protocol previously described by Singh *et al.*⁴⁵ Briefly, 2.5 µl aliquots of 2-fold serially diluted peptides were mixed in 247.5 µl of *Mtb*/MDR *Mtb* inoculated cultures (~ 5 x 10⁵ cells/ml) in 96-well plates and sealed with plate sealer (Nunc Inc.). After incubation at 37 °C, the XTT menadione assay was performed after 8 days for detection of active stage inhibitors and 12 days for detection of dormant stage inhibitors respectively, by removing the plate sealer. Absorbance was measured at 470 nm and percentage inhibition was calculated using the formula:

% inhibition = $[(\text{Control} - \text{Test}) / (\text{Control} - \text{Blank})] \times 100$, where 'Control' is the absorbance in the absence of added compounds, 'Test' is the absorbance in the presence of compounds and 'Blank' is the absorbance of the culture medium without mycobacteria.

4.6.3 CD analysis

The secondary structures of the peptides in different environments were measured using a J-815 spectropolarimeter (Jasco, Japan). The spectra were recorded at a scan speed of 100 nm/min at wavelengths ranging from 190 to 300 nm in water and 90 % TFE (Sigma). An average of three scans was collected for each peptide. The final concentration of the peptides was 500 μM . The acquired CD signal spectra were converted to the molar ellipticity using the equation: $[\theta] = (\theta \times 1000) / (c \times l)$, where, $[\theta]$ is the molar ellipticity ($\text{deg} \cdot \text{cm}^2 \cdot \text{dmol}^{-1}$), θ is the observed ellipticity corrected for the buffer at a given wavelength (mdeg), c is the peptide concentration (M), l is the path length (cm).

4.6.4 Fluorescence microscopy images

S. aureus was allowed to grow to the mid-log phase and then incubated with the peptides (10 $\mu\text{g}/\text{mL}$) at 37 °C for 4 h. The solution was centrifuged at 1000 g for 10 min. The supernatant was removed and the bacterial pellets were washed with PBS three to four times. PI (5 $\mu\text{g}/\text{mL}$) was added and incubated for 15 min in the dark. Excess dye was removed by PBS washes ($\times 3$). Next, the cells were incubated with SYTO 9 (10 $\mu\text{g}/\text{mL}$ in water) for 15 min in the dark and excess dye was removed, followed by PBS washes ($\times 3$). The bacteria were then examined under oil-immersion objective (60 X) by using the Invitrogen™ EVOS™ FL Cell Imaging Microscope.

4.6.5 Transmission Electron Microscopy images

E. coli and *S. aureus* were cultured to mid-log phase. The cells were harvested by centrifugation at $1,000 \times g$ for 10 min, washed thrice with 10 mM PBS and re-suspended to an $\text{OD}_{600\text{nm}}$ of 0.2. The cell suspension was incubated at 37 °C for 60 min with different peptides at their MIC. Following the incubation, the cells were centrifuged and washed with PBS 3 times at 5,000 g for 5 min. Microbial cell pellets were then fixed overnight with 2.5 % (v/v) glutaraldehyde in PBS at 4 °C and washed twice with PBS. After pre-fixation with 2.5 % glutaraldehyde overnight, the cell pellets were washed 3 times with PBS and post-fixed with 2 % osmium tetroxide in PBS for 70 min. The samples were washed twice with PBS, followed by dehydration for 9 min in a

graded ethanol series (50%, 70%, 90% and 100%), and incubated for 10 min each in 100% ethanol, a mixture (1:1) of 100% ethanol and acetone, and absolute acetone. These samples were then transferred to a constant-temperature (37 °C) incubator overnight. Finally, the specimens were observed using a transmission electron microscope.

4.6.6 Cytotoxicity studies: MTT cell viability and hemolysis assays

As previously described in section A of chapter 2 (2A. 6.3.5.3 and 2A. 6.3.5.4).

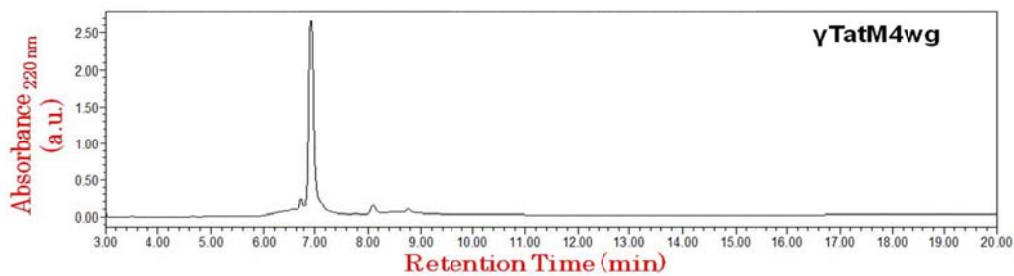
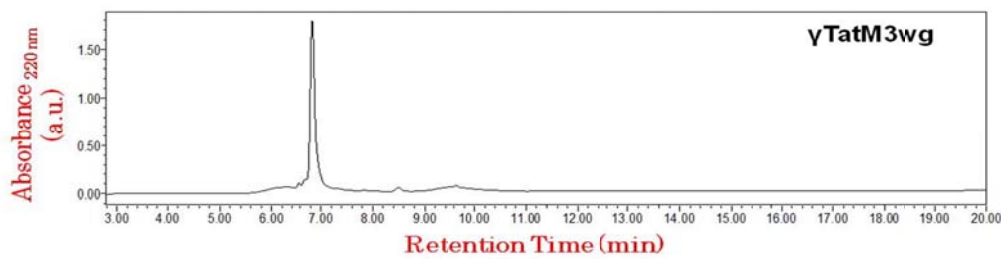
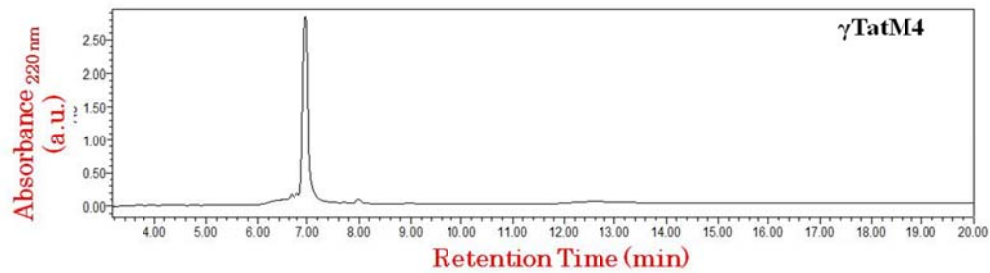
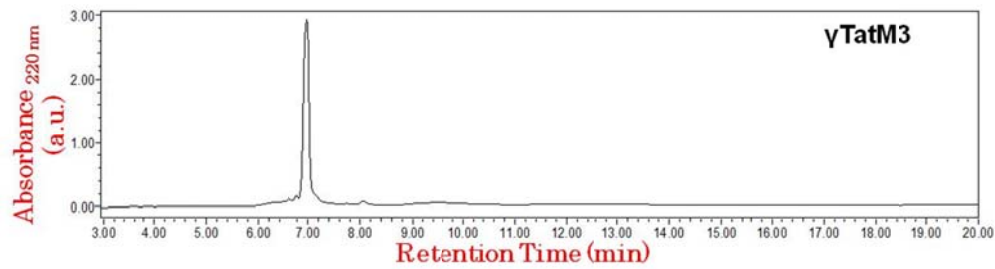
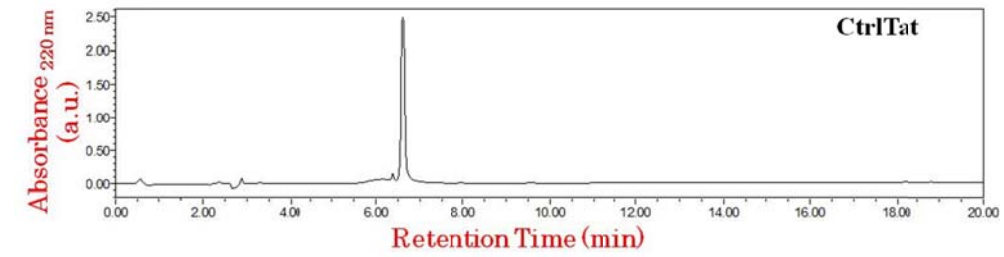
4.6.7 Protease resistance studies

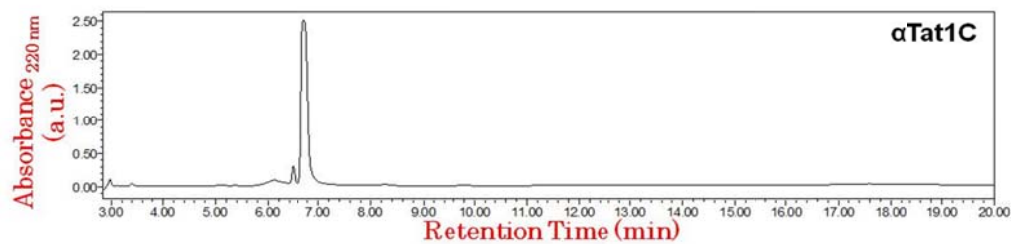
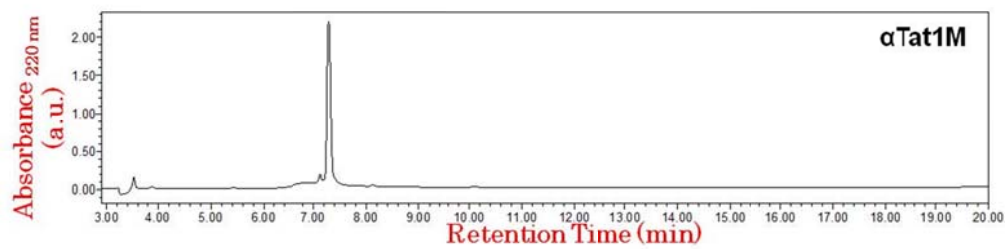
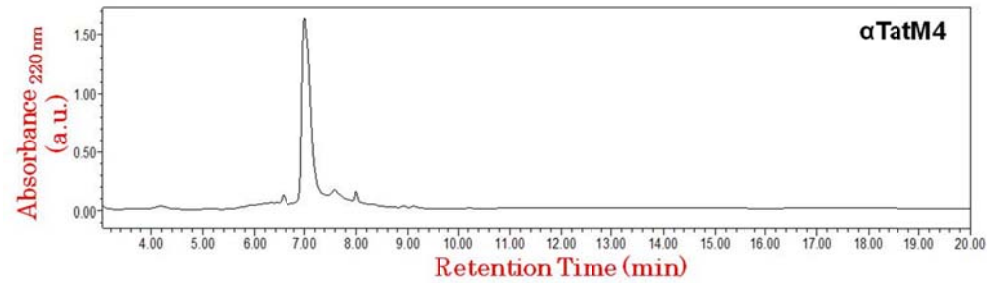
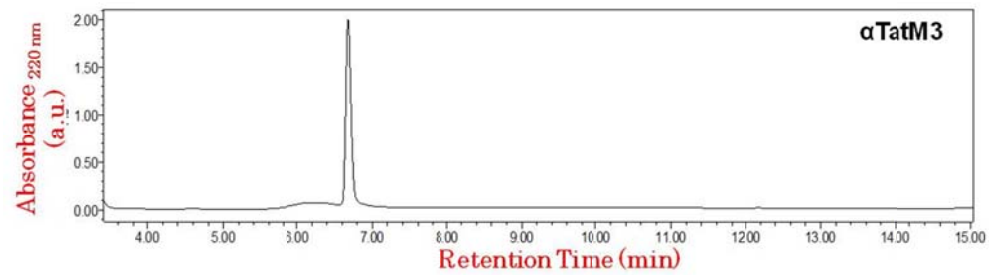
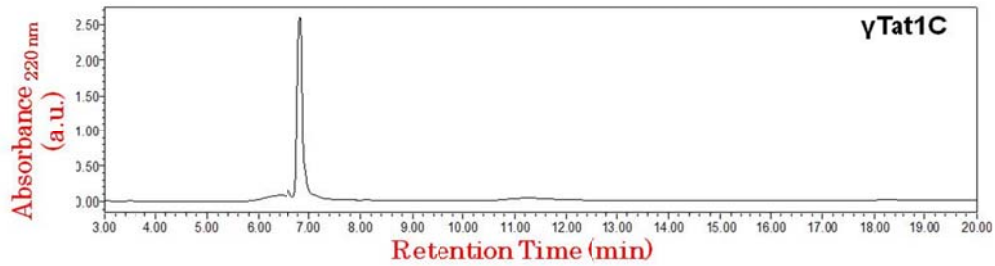
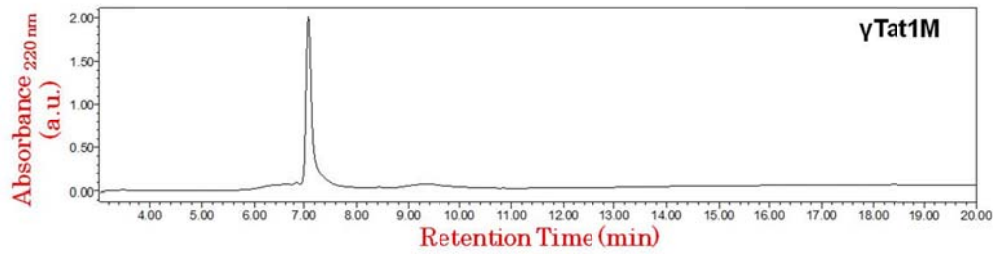
As previously described in section A of chapter 2 (2A. 6.3.6).

4.7 Appendix D

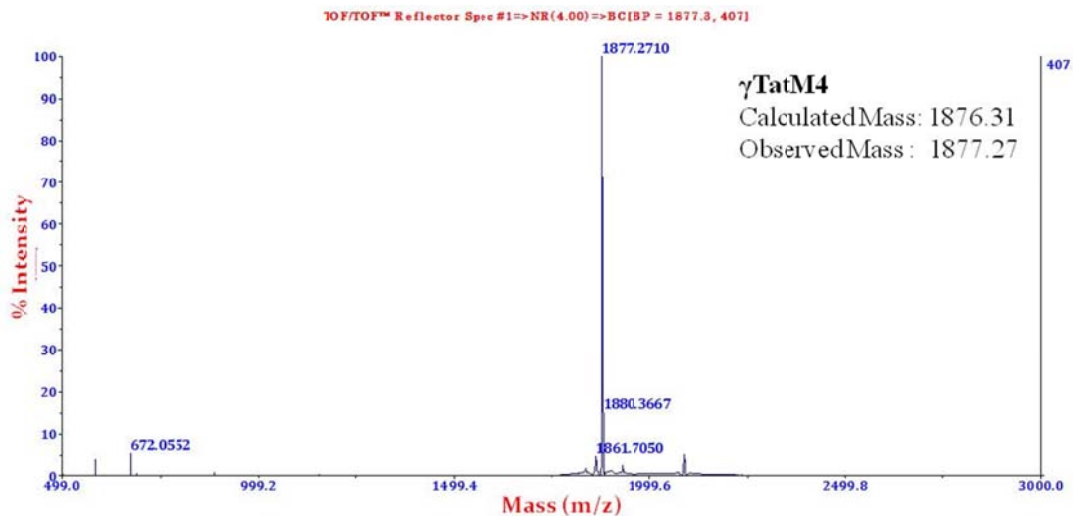
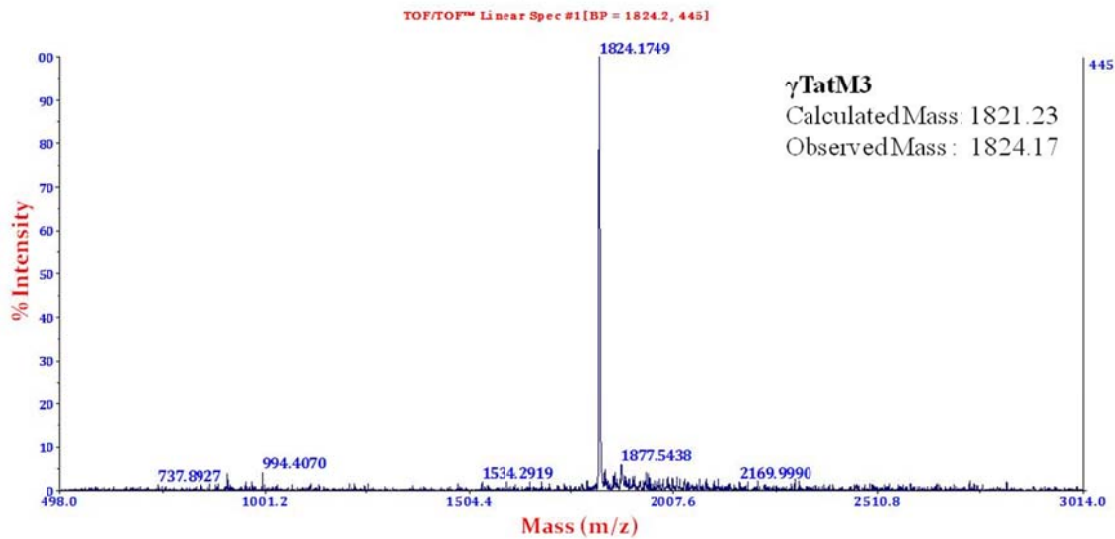
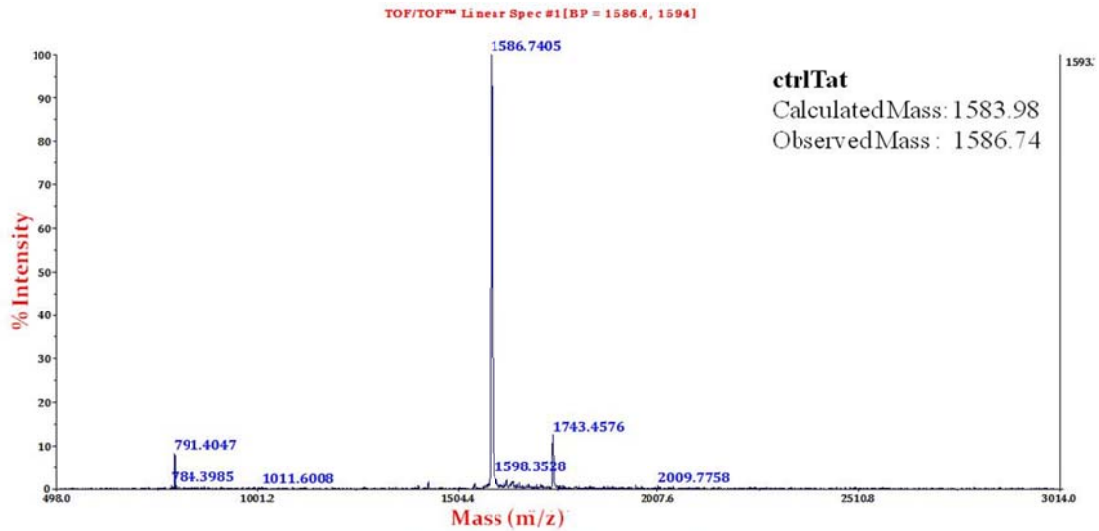
Compound and characterization	Page No.
RP-HPLC Chromatograms of Peptides	173 – 174
MALDI-TOF Spectra of Peptides	175 - 178

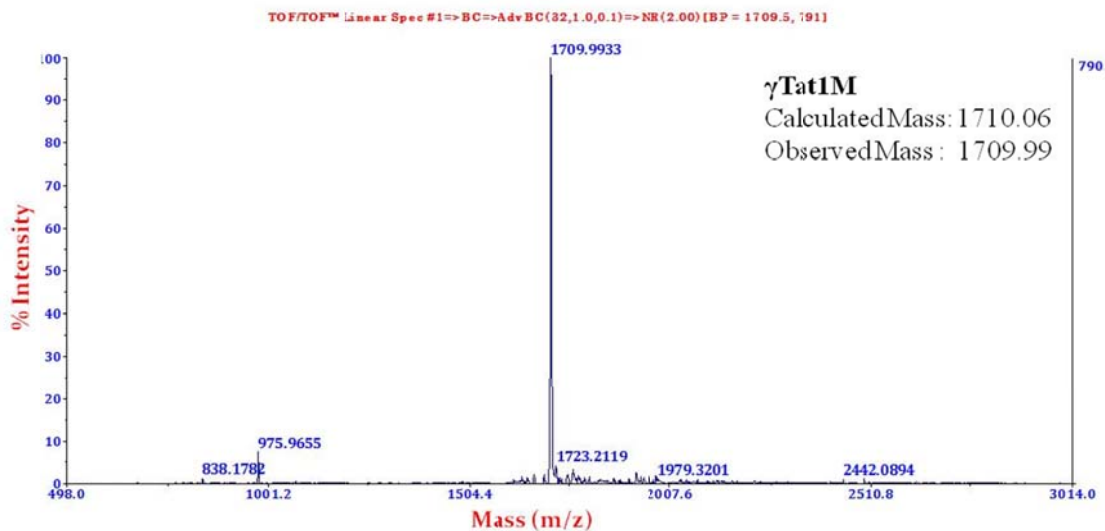
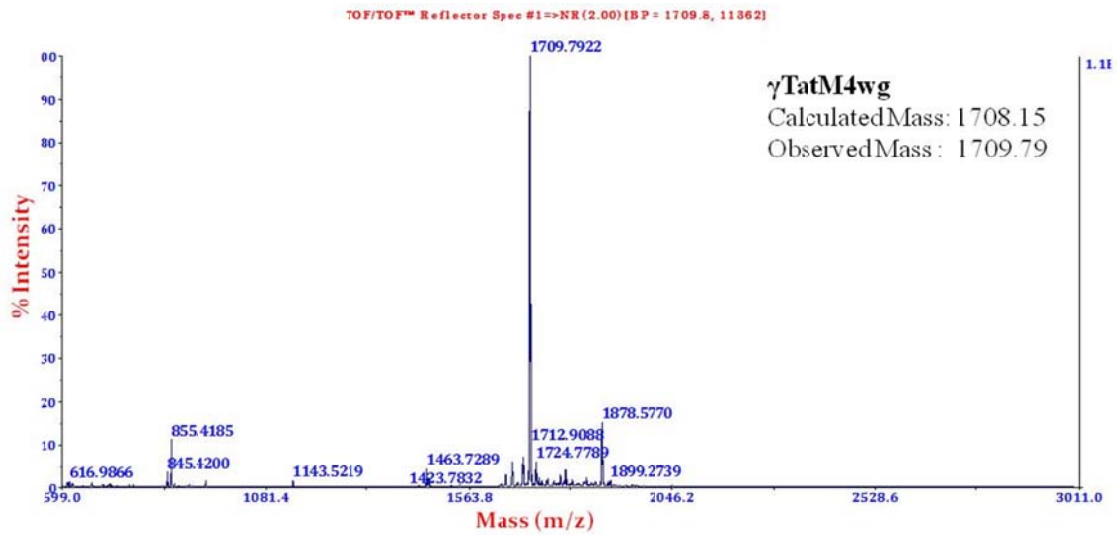
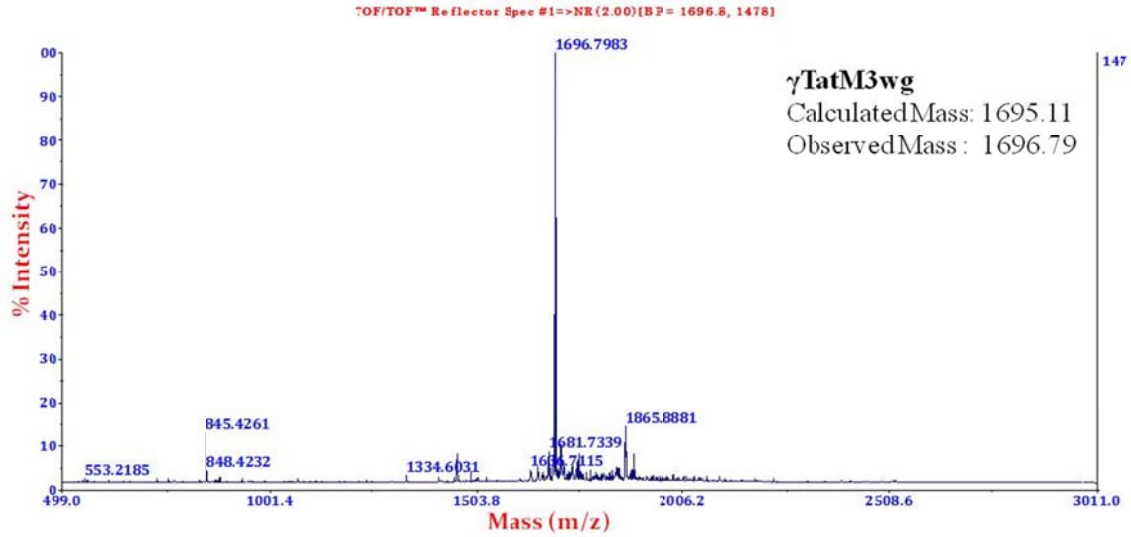
RP- HPLC chromatograms of peptides

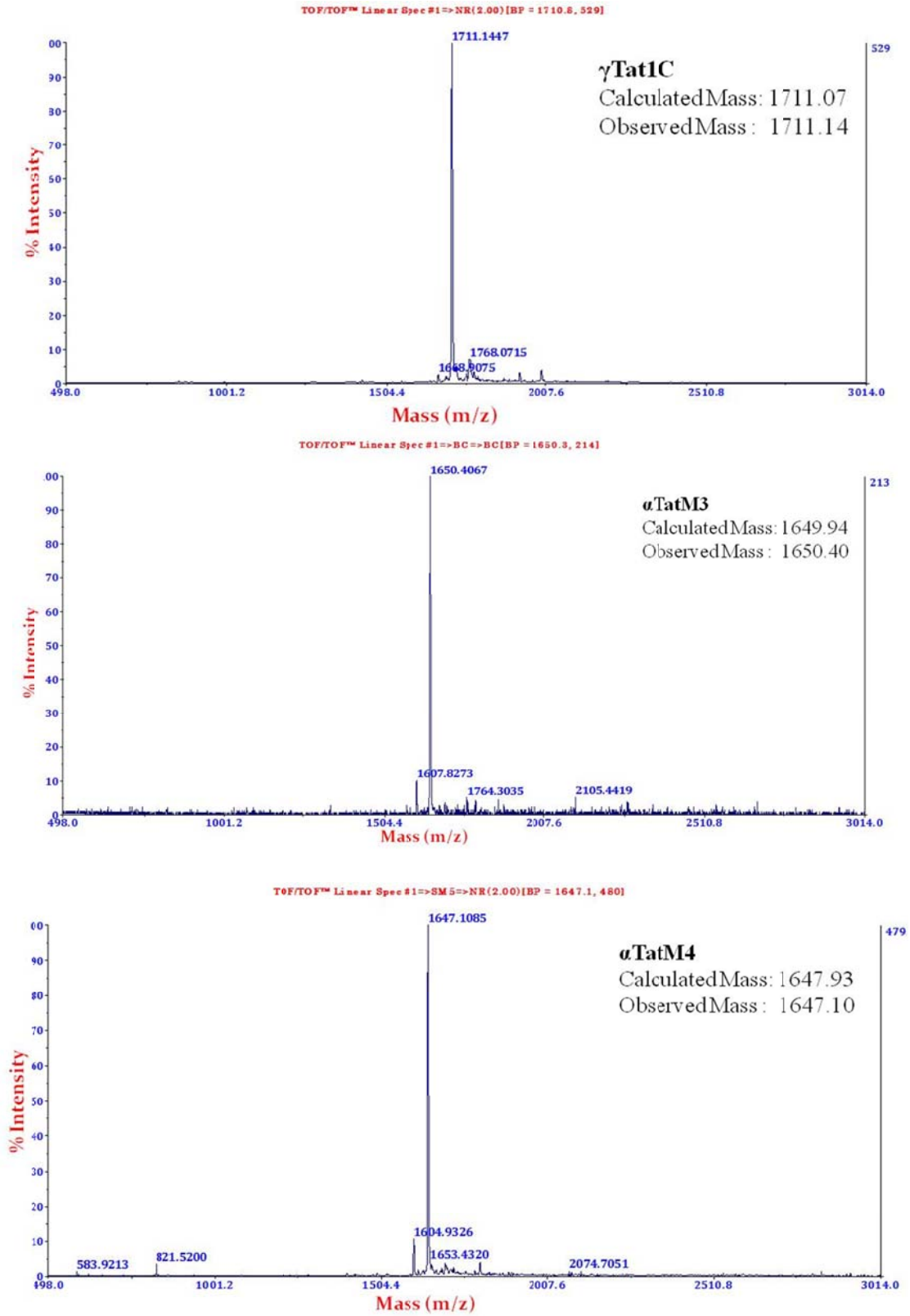


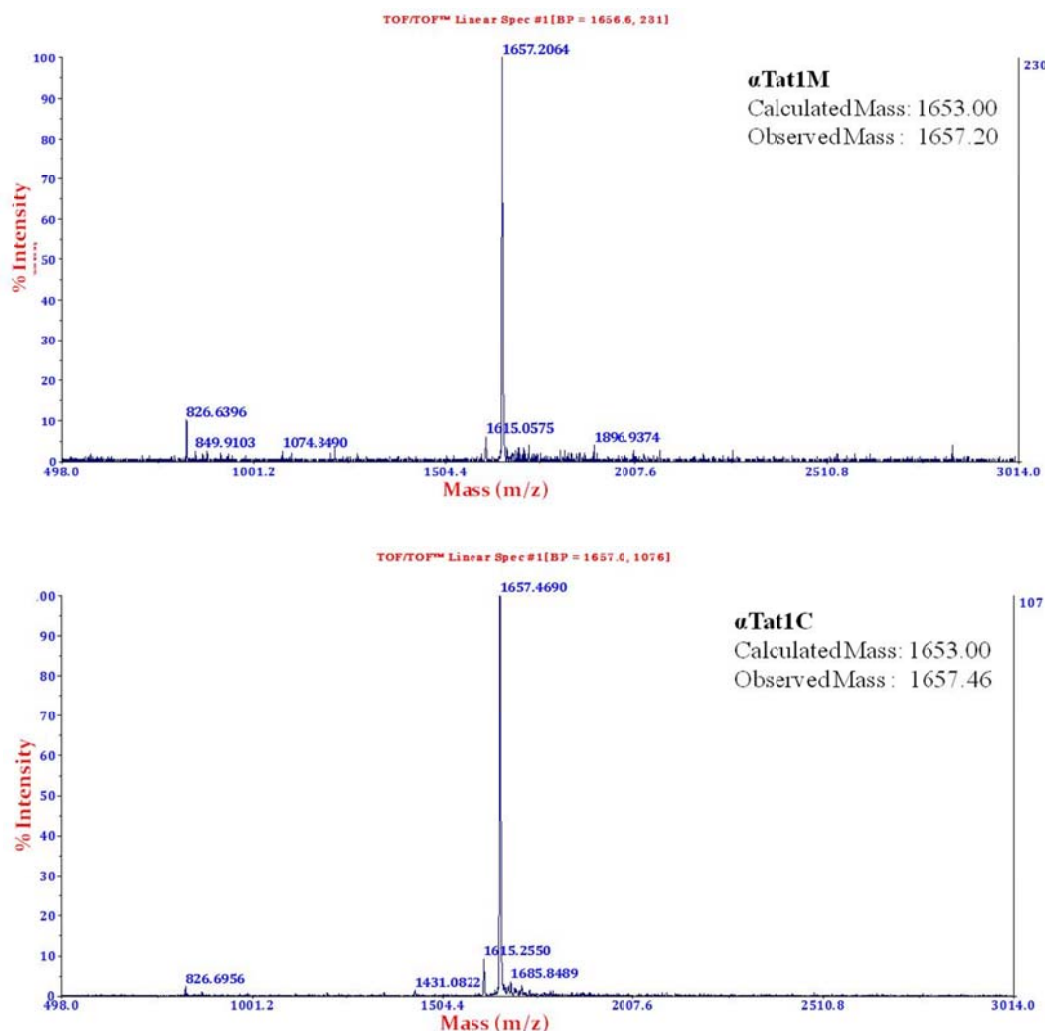


MALDI-TOF spectra of peptides









4.8 References

1. a) Herzog, I. M.; Fridman, M.; *Med. Chem. Commun.*, **2014**, *5*, 1014–1026. (b) Melo, M. N.; Ferre, R.; Castanho, M. A. R. B.; *Nat. Rev. Microbiol.*, **2009**, *7*, 245–250.
2. Wu, M.; Maier, E.; Benz, R.; Hancock, R. E.; *Biochemistry*. **1999**, *38*, 22, 7235–7242.
3. Friedrich, C.L.; Moyles, D.; Beveridge, T. J.; Hancock, R.E.; *Antimicrob Agents Chemother.*, **2000**, *44*, 8, 2086–2092.
4. Zhang, L.; Dhillon, P.; Yan, H.; Farmer, S.; Hancock, R.E.; *Antimicrob Agents Chemother.*, **2000**, *44*, 12, 3317–3321.
5. Hancock, R.E.; Sahl, H.G.; *Nat Biotechnol.*, **2006**, *24*, 12, 1551–1557.
6. Méndez-Samperio, P.; *Peptides*, **2008**, *29*, 10, 1836–1841.
7. Zasloff, M.; *Nature*, **2002**, *415*, 389–395.

8. Brogden, K. A.; *Nat. Rev. Microbiol.*, **2005**, *3*, 238–50.
9. Reddy, K.V.R.; Yedery, R.D.; Aranha, C.; *Int.J. Antimicrob. Agents*, **2004**, *24*, 536–547.
10. Brogden, K. A.; *Nat. Rev. Microbiol.*, **2005**, *3*, 238–50.
11. Yeaman, M. R.; Yount, N.Y.; *Pharmacol. Rev.*, **2003**, *55*, 27–55.
12. (a) Sharma, A.; Pohane, A. A.; Bansal, S.; Bajaj, A. Jain, V.; Srivastava, A.; *Chem. Eur. J.*, **2015**, *21*, 3540-3545. (b) Lee, J. K.; Park, S. C. Hahm, K. S.; Park, Y.; *Biomaterials*, **2014**, *35*, 1025-1039.(c) Winfred, S. B.; Meiyazagan, G.; Panda, J. J.; Nagendrababu, V.; Deivanayagam, K.; Chauhan, V.; Venkatraman, S.; *Eur. J. Dent.*, **2014**, *8*, 254-260 (d) Lim, K.; Saravanan, R. R. Y. R.; Basu, A.; Mishra, B.; Tambyah, P. A.; Ho, B.; Leong, S. S.; *ACS Appl. Mater. Interfaces*, **2013**, *5*, 6412–6422. (e) Hicks, R. P.; Abercrombie, J. J.; Wong, R. K.; Leung, K. P.; *Bioorg. Med. Chem.*, **2013**, *21*, 205–214. (f) Romani, A. A.; Baroni, M. C.; Taddei, S.; Ghidini, F.; Sansoni, P.; Caviranib, S.; Cabassib, C. S.; *J. Pept. Sci.*, **2013**, *19*, 554–565. (g) Stempel, N.; Strehmel, J.; Overhage, J. *Curr. Pharm. Des.*, **2015**, *21*, 67-84.(h) Pinto da Costa, J.; Cova, M.; Ferreira, R.; Vitorino, R.; *Appl. Microbiol. Biotechnol.*, **2015**, *99*, 2023–2040.
13. Patch, J. A.; Barron, A. E.; *Curr. Opin. Chem. Biol.*, **2002**, *6*, 872–877.
14. Nepal, M.; Thangamani, S.; Seleem, M. N.; Chmielewski, J.; *Org. Biomol.Chem.*, **2015**, *13*, 5930-5936.
15. Domalaon, R.; Yang, X.; O'Neil, J.; Zhanel, G. G.; Mookherjee, N.; Schweizer, F.; *Amino Acids*, **2014**, *46*, 2517-2530.
16. Gademann, K.; Hintermann, T.; Schreiber, J. V. *Curr. Med. Chem.*, **1999**, *6*, 905-925.
17. Cheng, R. P.; Gellman, S. H.; DeGrado, W. F.; *Chem. Rev.*, **2001**, *101*, 3219-3232.
18. Porter, E. A.; Weisblum, B.; Gellman, S. H.; *J. Am. Chem. Soc.*, **2002**, *124*, 7324-7330.
19. Simon, R. J.; Kania, R. S.; Zuckermann, R. N.; Huebner, V. D.; Jewell, D. A.; Banville, S.; Ng, S.; Wang, L.; Rosenberg, S.; Marlowe, C. K.; *Proc. Natl. Acad. Sci. U. S. A.*, **1992**, *89*, 9367–9371.
20. Li, X.; Wu, Y. D.; Yang, D.; *Acc. Chem. Res.*, **2008**, *41*, 1428–1438.
21. Horne, W. S.; Johnson, L. M.; Ketas, T. J.; Klasse, P. J.; Lu, M.; Moore, J. P.; Gellman, S. H.; *Proc. Natl. Acad. Sci. U. S. A.*, **2009**, *106*, 14751–14756.
22. Horne, W. S.; Gellman, S. H.; *Acc. Chem. Res.*, **2008**, *41*, 1399–1408.
23. Lee, H. J.; Song, J. W.; Choi, Y. S.; Park, H. M.; Lee, K. B.; *J. Am. Chem. Soc.*, **2002**, *124*, 11881–11893.

24. Graybill, T. L.; Ross, M. J.; Gauvin, B. R.; Gregory, B. S.; Harris, A. L.; Ator, M. A.; Rinker, J. M.; Dolle, R. E.; *Bioorg. Med. Chem. Lett.*, **1992**, *2*, 1375–1380.
25. Zhang, L.; Gallo, R. L., *Current Biology*, **2016**, *26*, R1–R21.
26. Wagstaff, K. M.; Jans, D. A.; *Curr. Med. Chem.*, **2006**, *13*, 1371–1387.
27. (a) Wadia, J. S.; Stan, R. V.; Dowdy, S. F.; *Nat. Med.* **2004**, *10*, 310–315. (b) Kameyama, S.; Horie, M.; Kikuchi, T.; Omura, T.; Takeuchi, T.; Nakase, I.; Sugiura, Y.; Futaki, S.; *Bioconjugate Chem.*, **2006**, *17*, 597–602.
28. (a) Chiu, Y. L.; Ali, A.; Chu, C. Y.; Cao, H.; Rana, T. M.; *Chem. Biol.*, **2004**, *11*, 1165–1175. (b) Tripathi, S.; Chaubey, B.; Barton, B. E.; Pandey, V. N.; *Virology*, **2007**, *363*, 91–103. (c) Liu, Z.; Li, M.; Cui, D.; Fei, J.; *J. Controlled Release*, **2005**, *102*, 699–710. (d) Rudolph, C.; Plank, C.; Lausier, J.; Schillinger, U.; Müller, R. H.; Rosenecker, J.; *J. Biol. Chem.*, **2003**, *278*, 11411–11418.
29. (a) Ruan, G.; Agrawal, A.; Marcus, A. I.; Nie, S.; *J. Am. Chem. Soc.*, **2007**, *129*, 14759–14766. (b) Kersemans, V.; Cornelissen, B.; *Pharmaceuticals*, **2010**, *3*, 600–620.
30. (a) Pan, L.; He, Q.; Liu, J.; Chen, Y.; Ma, M.; Zhang, L.; Shi, J.; *J. Am. Chem. Soc.*, **2012**, *134*, 5722–5725. (b) Nori, A.; Jensen, K. D.; Tijerina, M.; Kopečková, P.; Kopeček, J.; *Bioconjugate Chem.*, **2003**, *14*, 44–50. (c) Rao, K. S.; Reddy, M. K.; Horning, J. L.; Labhasetwar, V.; *Biomaterials*, **2008**, *29*, 4429–4438. (d) Al-Taei, S.; Penning, N. A.; J. C.; Futaki, S.; Simpson, T.; Takeuchi, I.; Nakase, A.; Jones, T.; *Bioconjugate Chem.*, **2006**, *17*, 90–100.
31. Vivès, E.; Brodin, P.; Lebleu, B.; *J. Biol. Chem.*, **1997**, *272*, 16010–16017.
32. Tünnemann, G.; Martin, R. M.; Haupt, S.; Patsch, C.; Edenhofer, F.; Cardoso, M. C.; *FASEB J.*, **2006**, *20*, 1775–84.
33. Zhao, M.; Weissleder, R.; *Med. Res. Rev.* **2004**, *24*, 1–12.
34. Demizu, Y.; Oba, M.; Okitsu, K.; Yamashita, H.; Misawa, T.; Tanaka, M.; Kurihara, M.; Gellman, S. H.; *Org. Biomol. Chem.*, **2015**, *13*, 5617–5620.
35. Tamilarasu, N.; Huq, I.; Rana, T. M.; *Bioorg. Med. Chem. Lett.*, **2001**, *11*, 505–507.
36. Rana, T. M.; Huq, I.; *US Patent 5843995*, **Dec. 1, 1998**.
37. Zhu, W. L.; Shin, S. Y.; *J. Pept. Sci.*, **2009**, *15*, 345–352.
38. Piantavigna, S.; McCubbin, G. A.; Boehnke, S. B.; Graham, L.; Spiccia, L.; Martin, L.; *Biochim. Biophys. Acta*, **2011**, *1808*, 1811–1817.

39. Bourré, L.; Giuntini, F.; Eggleston, I. M.; Mosse, C. A.; MacRobert, A. J.; Wilson, M.; *Photochem. Photobiol. Sci.*, **2010**, *9*, 1613–1620.
40. Jung, H. J.; Jeong, K.-S.; Lee, D. G.; *J. Microbiol. Biotechnol.*, **2008**, *18*, 990–996.
41. Wang, H.; Xu, K.; Liu, L.; Tan, J. P. K. Y.; Chen, Y.; Li, W.; Fan, Z.; Wei, J.; Sheng, Y.-Y.; Yang, L.; Li; *Biomaterials*, **2010**, *31*, 2874–2881.
42. Jung, H.; Park, Y.; Hahm, K.; Lee, D.; *Biochem. Biophys. Res. Commun.*, **2006**, *345*, 222-228.
43. Wiradharma, N.; Khoe, U.; Hauser, C. A. E.; Seow, S. V.; Zhang, S.; Yang, Y.-Y.; *Biomaterials*, **2011**, *32*, 2204-2212.
44. Alekshun, M. N.; Levy, S. B.; *Cell*, **2007**, *128*, 1037–1050.
45. Chongsiriwatana, N. P.; Patch, J. A.; Czyzewski, A. M.; Dohm, M. T.; Ivankin, A.; Gidalevitz, D.; Zuckermann, R. N.; Barron, A. E.; *Proc. Natl. Acad. Sci. U.S.A.*, **2008**, *105*, 2794–2799.
46. Loret, E. P.; Georgel, P.; Johnson Jr., W. C.; Ho, P. S.; *Proc. Natl. Acad. Sci. USA*, **1992**, *89*, 9734-9738.
47. Greenfield, N. J.; *Nat. Protocols*, **2007**, *1*, 2876 - 2890.
48. Su, X.; Zhou, X.; Tan, Z.; Zhou, C.; *Biopolymers*, **2017**, *107*, 23041.

1. **Govind Bhosle**, Moneesha Fernandes*(R-X-R)₄-motif peptides containing conformationally constrained cyclohexane-derived spacers: Effect on cellular uptake. [*ChemMedChem*, 2017, 12, 1743 – 1747.](#)
2. **Govind Bhosle**, Shalmali Kharche, Santosh Kumar, Durba Sengupta, Souvik Maiti* Moneesha Fernandes*. Superior HIV-1 TAR-Binders with Conformationally Constrained R52 Arginine Mimics in Tat (48-57) Peptide. [*ChemMedChem*, 2018, 13, 220 – 226.](#)
3. **Govind Bhosle**, Laxman Navale, Amar Yeware, Dhiman Sarkar, Moneesha Fernandes* “Antibacterial and anti-TB Tat-peptidomimetics with improved efficacy and half-life” Manuscript Accepted. [*European Journal of Medicinal Chemistry*, 2018, 152, 358–369](#)
4. Harsha Chilukuri, Yogesh M. Kolekar, **Govind Bhosle**, Rashmi K. Godbole, Rubina S. Kazi, Mahesh J. Kulkarni* and Moneesha Fernandes* N-(3-Aminoalkyl)proline derivatives with potent antiglycation activity. [*RSC Adv.*, 2015, 5, 77332.](#)
5. **Govind Bhosle**, Santosh Kumar, Souvik Maiti* Moneesha Fernandes*. Synthetic DNA-compacting peptides derived from basic region of HIV-1 TAT peptide. Manuscript under preparation.

(R-X-R)₄-Motif Peptides Containing Conformationally Constrained Cyclohexane-Derived Spacers: Effect on Cellular Uptake

Govind S. Bhosle^[a, b] and Moneesha Fernandes^{*[a, b]}

Arginine-rich peptides having the (R-X-R)_n motif are among the most effective cell-penetrating peptides (CPPs). Herein we report a several-fold increase in the efficacy of such CPPs if the linear flexible spacer (-X-) in the (R-X-R) motif is replaced by constrained cyclic 1,4-substituted-cyclohexane-derived spacers. Internalization of these oligomers in mammalian cell lines was found to be an energy-dependent process. Incorporation of these constrained, non-proteinogenic amino acid spacers in the CPPs is shown to enhance their proteolytic stability.

The therapeutic importance of a variety of drug candidates has been limited by their poor cell membrane permeability, resulting in the discovery of cell-penetrating peptides (CPPs). CPPs are short peptides which facilitate the transport of hydrophobic/hydrophilic small- or macro-molecules across the cell membranes of living cells.^[1] The CPPs such as proline-rich peptides,^[2] β-peptides^[3] and cationic amphiphilic polyproline helices^[4,5] have been shown to have good cell-penetrating abilities, possibly because of favorable backbone structure while interacting with the cell membrane. A significant number of most effective CPPs are cationic in nature and contain at least six amino acids such as lysine or arginine which are positively charged at physiological pH. It was demonstrated that the guanidine head-group of arginine in polyarginine peptides was the critical component for their membrane penetration efficiency.^[6,7] An optimum balance of hydrophilic-hydrophobic components together with the favorable spatial presentation of guanidine moieties to interact with functional groups on the cell membrane was found to be important to achieve efficient cell penetration. Synthetic polyarginines in which the arginine residues were spaced by alkyl chains (RX)_n of differing lengths showed enhanced cellular uptake relative to the polyarginines themselves.^[8] One of the most successful type of arginine-rich cell-penetrating peptide, is the (R-X-R)_n-motif peptides,^[9] where X is a non-natural amino acid, either 6-aminohexanoic acid (Ahx) or 3-aminopropanoic acid (β-alanine). Con-

jugates of such (R-X-R)₄-CPP with peptide nucleic acid (PNA) and phosphorodiamidate morpholino (PMO) oligomers are reported for splice correction^[10] and exon-skipping activity.^[11] Recently, it was reported that intracellular biological activity of PMO conjugated to (R-X-R)₄-peptide can be influenced by the spacing between the charges, hydrophobicity of the linker between the R residues and stereochemistry of the R units.^[12]

To improve the cell-penetrating ability of (R-X-R)₄-type peptides, we previously reported replacing the backbone amide linkages by carbamates, which resulted in improved cellular uptake and cargo delivery properties with decreased cytotoxicity.^[13] We also reported earlier that incorporation of five-membered pyrrolidine spacers (X') derived from proline in the (R-X'-R)₄-motif improved cell-penetrating ability of (α-ω)-peptides as molecular transporters.^[14] Five-membered rings are known to be conformationally more flexible relative to the six-membered rings. We now report the inclusion of a six-membered ring as a part of the spacer (X), where 6-aminohexanoic acid is replaced by its analogues containing a conformationally constrained cyclohexane ring. Specifically, we present our studies where *cis*- and *trans*-4-aminocyclohexanecarboxylic acid (X_{CHA} and X_{THA} respectively) and *cis*- and *trans*-4-aminocyclohexanecetic acid (X_{CHAA} and X_{THAA} respectively) are employed as spacers (X) in place of aminohexanoic acid (X_{HA}) (Figure 1). The rigidity and stereochemistry of the 6-membered ring structure in 4-aminocyclohexanecarboxylic acid and 4-aminocyclohexanecetic acid units would allow variation of the conformational constraint and backbone chirality in the peptide. Thus, the designed 4-aminocyclohexanecetic acid and 4-aminocyclohexanecarboxylic acid spacers (X) differ in stereochemistry at the C4 position, being derived from either the *cis* or *trans* configu-

[a] G. S. Bhosle, Dr. M. Fernandes
Organic Chemistry Division, CSIR – National Chemical Laboratory (CSIR-NCL), Dr. Homi Bhabha Road, Pune 411008(India)
E-mail: m.dcosta@ncl.res.in

[b] G. S. Bhosle, Dr. M. Fernandes
Academy of Scientific and Innovative Research, AcSIR, CSIR-NCL Campus, Pune(India)

Supporting information and the ORCID identification number(s) for the author(s) of this article can be found under:
<https://doi.org/10.1002/cmdc.201700498>.

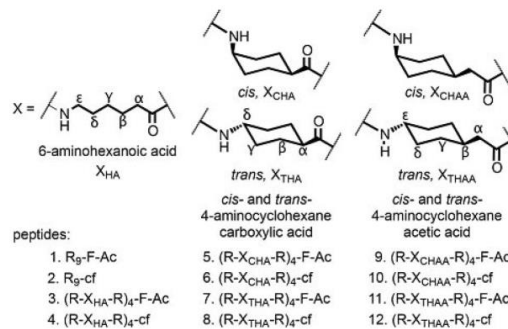


Figure 1. The (-X-) units in designed (R-X-R)₄-peptides.

Superior HIV-1 TAR Binders with Conformationally Constrained R52 Arginine Mimics in the Tat(48–57) Peptide

Govind S. Bhosle,^[a, d] Shalmali Kharche,^[b, d] Santosh Kumar,^[c] Durba Sengupta,^[b, d] Souvik Maiti,^{*[c, e]} and Moneesha Fernandes^{*[a, d]}

We report a 100-fold increase in binding affinity of the Tat(48–57) peptide to HIV-1 transcriptional activator-responsive element (TAR) RNA by replacing Arg52, an essential and critical residue for Tat's specific binding, with (2*S*,4*S*)-4-guanidinoproline. The resulting α Tat1M peptide is a far superior binder than γ Tat1M, a peptide containing another conformationally constrained arginine mimic, (2*S*,4*S*)-4-amino-*N*-(3-guanidinopropyl)proline, or even the control Tat peptide (CtrlTat) itself. Our observations are supported by circular dichroism (CD), isothermal titration calorimetry (ITC), gel electrophoresis and UV spectroscopy studies. Molecular dynamics simulations suggest increased interactions between the more compact α Tat1M and TAR RNA, relative to CtrlTat. The CD signature of the RNA itself remains largely unchanged upon binding of the peptides. The Tat mimetics further have better cell uptake properties than the control Tat peptide, thus increasing their potential application as specific TAR-binding molecules.

ture formed by the nascent transcript.^[2] Tat–TAR interactions are localized mainly to a trinucleotide pyrimidine bulge (residues U23–U25) and adjacent duplex region in TAR RNA,^[3] and the 11-amino acid basic region of Tat^[4] (residues 47–57, YGRKKRRQRRR; Figure 1). The disruption of this interaction is

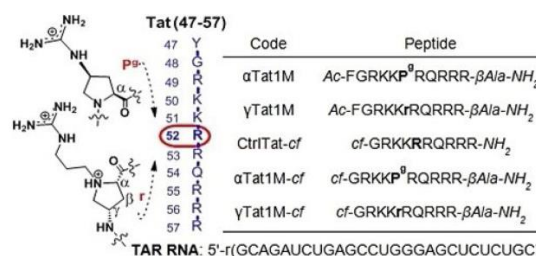


Figure 1. The Tat(47–57) peptide and proposed arginine mimics. Inset: Oligomers of the study. The residue at position 52 of the Tat peptide is indicated in boldface.

RNAs are known to play key roles in many biological processes and are considered key regulators of gene expression. They serve as the main genetic material for many viruses such as HIV, HCV, influenza, and flaviviruses. Therefore, molecules that can bind specifically to critical target RNA and disrupt its function are highly important in the efforts to control such retroviruses.^[1] Transcription of HIV-1 RNA requires the interaction of the virally encoded Tat protein with the transcriptional activator-responsive element (TAR), a bulged RNA stem–loop struc-

thus an area of much research toward the control of HIV-1. In this direction, a variety of ligands^[5] including peptides^[6] besides Tat, peptidomimetics,^[7] peptoids,^[8] and peptide nucleic acids^[9] have been reported. Backbone-modified Tat analogues including a β -peptide,^[10] oligocarbamate,^[11] oligourea,^[12] and various peptoid-based structures^[8] have been reported and preserve the side chains of the Tat(47–57) peptide, but vary (in spacing and/or chirality) in the relative positions of the functional groups. The success of these analogues in disrupting the Tat–TAR interaction underscores the importance of the cationic nature of the peptide and also the relative presentation of cationic groups in determining the binding affinity. In spite of these reports, there is still a pressing need for newer effective agents that can selectively and strongly bind TAR RNA. Although proteolytically stable peptide derivatives have been used previously to target TAR,^[10,13] linear peptide analogues were found to be highly flexible and to bind various RNAs, preventing sufficient activity in cells. Therefore, we focused our attention on conformationally pre-organized mimics of HIV-1 Tat. Arginine 52 (R52) has been shown to be essential for TAR binding,^[14] through possible bidentate hydrogen bonding with the two phosphate groups between residues A22–U23–C24, and also with the ribose 2'-OH groups, of the trinucleotide bulge region of TAR RNA. The presentation of the forked arginine guanidine group in the context of flanking cationic residues is

[a] G. S. Bhosle, Dr. M. Fernandes

Organic Chemistry Division, CSIR – National Chemical Laboratory (CSIR-NCL), Dr. Homi Bhabha Road, Pune 411008 (India)
E-mail: m.dcosta@ncl.res.in

[b] S. Kharche, Dr. D. Sengupta

Physical and Materials Chemistry Division, CSIR – National Chemical Laboratory (CSIR-NCL), Dr. Homi Bhabha Road, Pune 411008 (India)

[c] S. Kumar, Dr. S. Maiti

Structural Biology Unit, CSIR – Institute of Genomics and Integrative Biology (CSIR-IGIB), Delhi (India)
E-mail: souvik@igib.res.in

[d] G. S. Bhosle, S. Kharche, Dr. D. Sengupta, Dr. M. Fernandes

Academy of Scientific and Innovative Research (AcSIR), CSIR-NCL Campus, Pune (India)

[e] Dr. S. Maiti

Academy of Scientific and Innovative Research (AcSIR), CSIR-IGIB Campus, Delhi (India)

Supporting information and the ORCID identification number(s) for the author(s) of this article can be found under:
<https://doi.org/10.1002/cmdc.201700653>.



Contents lists available at ScienceDirect

European Journal of Medicinal Chemistry

journal homepage: <http://www.elsevier.com/locate/ejmech>

Research paper

Antibacterial and anti-TB tat-peptidomimetics with improved efficacy and half-life

Govind S. Bhosle^{a, b}, Laxman Nawale^b, Amar M. Yeware^{b, c}, Dhiman Sarkar^{b, c},
Moneesha Fernandes^{a, c, *}

^a Organic Chemistry Division, CSIR-National Chemical Laboratory (CSIR-NCL), Dr. Homi Bhabha Road, Pune, 411008, India

^b CombiChem-Bio Resource Center, Organic Chemistry Division, CSIR-National Chemical Laboratory (CSIR-NCL), Dr. Homi Bhabha Road, Pune, 411008, India

^c Academy of Scientific and Innovative Research (AcSIR), CSIR-NCL Campus, Pune, India



ARTICLE INFO

Article history:

Received 22 December 2017
Received in revised form
15 March 2018
Accepted 18 April 2018
Available online 30 April 2018

Keywords:

Non-natural amino acid
Tat-peptide
Anti-Bacterial
Anti-TB
Mycobacterium tuberculosis

ABSTRACT

Non-natural antimicrobial peptides are ideal as next-generation antibiotics because of their ability to circumvent the problems of drug resistance and *in vivo* instability. We report novel all- α - and α , γ -mixed Tat peptide analogues as potential antibacterial and anti-TB agents. These peptides have broad spectrum antibacterial activities against Gram-positive (MICs 0.61 ± 0.03 to $1.35 \pm 0.21 \mu\text{M}$ with the peptide γTatM4) and Gram-negative (MICs 0.71 ± 0.005 to $1.26 \pm 0.02 \mu\text{M}$ with γTatM4) bacteria and are also effective against active and dormant forms of *Mycobacterium tuberculosis*, including strains that are resistant to rifampicin and isoniazid. The introduction of the non-natural amino acids of the study in the Tat peptide analogues results in increased resistance to degradation by proteolysis, significantly increasing their half-life. The peptides appear to inhibit bacteria by a membrane disruption mechanism, and have only a low cytotoxic effect on mammalian cells.

© 2018 Elsevier Masson SAS. All rights reserved.

1. Introduction

Antimicrobial peptides (AMPs) act either by interacting with the cell membrane and causing lysis and ultimately cell death, or after penetrating the cell membrane, upon interaction with intracellular components [1], in contrast to conventional drugs that typically act through inhibition of metabolic processes. Such peptides thus offer an opportunity to overcome the problem of resistance development, which is increasingly being encountered, and that makes diseases such as those caused by *Mycobacterium tuberculosis* (Mtb) and other pathogenic bacteria difficult to treat. To improve the stability to enzymatic hydrolysis and to increase bioavailability, several synthetic, non-natural AMPs [2] and mimetics have been reported [3]. Many AMPs have a helical component that has been shown to be necessary for their antimicrobial activity. Among these, recently, Nepal et al. [4] described cationic and amphiphilic proline-rich polyproline type II (PPII) helices for effective cell penetration of macrophages that also exerted potent antibacterial

activity. PPII [5] and other helical peptides such as 12-helical β -peptides have been reported by several groups to have varying degrees of antimicrobial activities [6–8], including against some species that are resistant to common antibiotics such as vancomycin or penicillin [8]. Several other groups have reported peptoids [9], α -aminoxy-peptides [10], α/β -peptides [11,12], or azapeptides [13,14], as synthetic mimics of AMPs.

We chose to study the effect of non-natural amino acid surrogates on the antibacterial properties of the Tat (48–57) peptide. The basic translocating region (48–60) of the *trans*-activating transcriptional activator (TAT) peptide [15], derived from the human immunodeficiency virus 1 (HIV-1) tat protein is a positively charged peptide, rich in arginine, and is highly studied for cell penetration and delivery of a variety of cargo molecules [16–19]. The presence of several arginine residues, in addition to lysine residues, makes it particularly susceptible to the degradative action of enzymes, precluding its possible application in biological systems. Several reports of modifications in the Tat peptide have appeared in literature, where non-natural amino acids [20] as well as backbone linkages [21,22] have been explored in relation to cell penetration. They have, however, not been studied for antimicrobial activity. There have appeared few reports [23–28] of the antibacterial properties involving the cell-penetrating Tat peptide

* Corresponding author. Organic Chemistry Division, CSIR-National Chemical Laboratory (CSIR-NCL), Dr. Homi Bhabha Road, Pune, 411008, India.
E-mail address: mdcosta@ncl.res.in (M. Fernandes).

<https://doi.org/10.1016/j.ejmech.2018.04.039>
0223-5234/© 2018 Elsevier Masson SAS. All rights reserved.



Cite this: *RSC Adv.*, 2015, 5, 77332

N-(3-Aminoalkyl)proline derivatives with potent antiglycation activity†

Harsha Chilukuri,^{ab} Yogesh M. Kolekar,^a Govind S. Bhosle,^b Rashmi K. Godbole,^a Rubina S. Kazi,^a Mahesh J. Kulkarni^{*a} and Moneesha Fernandes^{*b}

The importance of amino acids in the therapy of conditions such as renal failure, neurological disorders and congenital defects has been documented. Some amino acids such as lysine and glycine have also been reported to have antiglycating activity. Herein we report the synthesis of a new series of *N*-(3-aminoalkyl)proline derivatives which are non-natural in nature. The compounds were unambiguously characterized by NMR, mass and IR spectroscopy. Their *in vitro* antiglycation activity was studied by circular dichroism and fluorescence spectrometry. The mechanism of action was also studied and found to take place by inhibition of Amadori product formation. The inhibition of AGE formation was further confirmed by western blot and LC-MS/MS analyses and the IC₅₀ values of the potent compounds were determined. Compounds containing hydroxyl substituents at C4 were found to have superior antiglycation properties than those containing azide substituents at the same position. The compounds were additionally found to possess good anti-oxidant properties, which could lead to further reduction in AGE formation. Moreover, the title compounds were found to have low cytotoxicity in mammalian cells, another important attribute. Thus, the title compounds represent a novel promising class of antiglycating agents.

Received 23rd June 2015
Accepted 4th September 2015

DOI: 10.1039/c5ra12148e

www.rsc.org/advances

Introduction

Advanced Glycation End products (AGEs) are formed due to non-enzymatic reactions between proteins and reducing sugars. They are involved in the pathogenesis of diabetes and its complications. Thus, reducing AGE levels¹ and inhibition of protein glycation is crucial in the prevention of the above complications. Some molecules such as aminoguanidine that reduce AGE levels, but have toxic side-effects have not been approved by the FDA, while other FDA-approved drugs have been shown to display anti-glycation activity^{1–3} in addition to their originally intended activities. These offer the possibility of repositioning these drugs for the treatment of diabetes and its complications. Reports from this laboratory have also been made for the use of *N*-(aminoalkyl)proline- and 4-hydroxy-*N*-(aminoalkyl)proline-derived compounds towards the synthesis of peptide nucleic acids⁶ and cell-penetrating oligomers,⁷ where

these compounds were used as analogues of amino acids such as lysine and arginine.^{7b} Since amino acids such as glycine and lysine have been reported to exert antiglycating activity,⁸ we surmised that the use of non-natural analogues such as the title compounds, would have advantages in terms of stability *in vivo*.

In this study, we report the synthesis and anti-glycation activity of selected *N*-(3-aminoalkyl)proline derivatives and their mode of action by various physicochemical assays such as circular dichroism (CD), fluorescence spectroscopy, MALDI-TOF and LC-MS/MS assays. We also show that these compounds are capable of exerting good anti-oxidant properties and display low cytotoxicity, thus enhancing their value as potential anti-glycation agents.

Results and discussion

Synthesis of title compounds

The title compounds were synthesized using a simple strategy outlined in Scheme 1. Accordingly, 4(*S*)-hydroxy-2(*R*)-proline methylester was *N*-alkylated by treating it with 3-((*tert*-butoxycarbonyl)amino)propyl methanesulfonate in CH₂Cl₂ in the presence of triethylamine to yield compound **1** which was subjected to acidolytic removal of the Boc protecting group to afford compound **2** in 62% yield. Compound **3** was obtained from **1** upon saponification with lithium hydroxide and subsequent purification by column chromatography on neutral alumina.

^aProteomics Facility, Division of Biochemical Sciences, CSIR-National Chemical Laboratory, Pune-411 008, India. E-mail: mj.kulkarni@ncl.res.in; Tel: +91 2025902541

^bOrganic Chemistry Division, CSIR-National Chemical Laboratory, Pune 411008, India. E-mail: m.dcosta@ncl.res.in; Tel: +91 2025902084

† Electronic supplementary information (ESI) available: NMR, mass spectra of **1–9**, mass spectra of glucose adducts with **4**, **6**, **8** & **9**, Orbitrap analysis, database search & PTM analysis, Ponceau staining of anti-AGE & anti-CML blots, AGE fluorescence spectra of glycated BSA treated with **1**, **3**, **5** & **7**. See DOI: 10.1039/c5ra12148e

Symposia Attended/ Poster Presentations

1. Attended **International Meeting on Chemical Biology (ICMB-2013)** Organized by IISER-Pune, 2013 Pune, India.
2. Poster presentation on "Synthetic DNA-compacting peptides derived from basic region of HIV-1 Tat peptide" at **International Symposium on Bioorganic Chemistry-10 (ISBOC-10)** organised by IISER Pune in 2015.
3. Poster presentation on "Conformationally Constrained Arginine Mimics in lieu of R52 in Tat(48-57) Peptide: Influence on Binding to HIV-1 TAR RNA" at **Peptide Engineering Meeting-7 (PEM-7)** organised by IISER Pune in 2016.
4. Poster presentation on " Tat peptide analogues with 4-amino-N-(3-aminopropyl)prolyl-derived lysine/arginine surrogates have promising antibacterial properties " **Organised by Chemical research society of India-North Bengal University, Siliguri in 2016.**
5. Poster presentation on " Tat peptide analogues with 4-amino-N-(3-aminopropyl)prolyl-derived lysine/arginine surrogates have promising antibacterial properties " **Organised by Chemical research society of India-CSIR National Chemical Laboratory, Pune in 2015.**

Erratum

Erratum

Erratum
